THE UNIVERSITY
of EDINBURGH

Biochemical characterisation of sugar beet pulp and its biotechnological product Curran®

Anne E. K. Bulling

Doctor of Philosophy - Cell and Molecular Biology

University of Edinburgh

2018

I. Declaration

This thesis has been composed by myself and the work, of which it is a record, has been carried out by myself. All sources of information have been specifically acknowledged by means of a reference.

2/11/2018

Anne E. K. Bulling, Edinburgh, 2018

I. Abstract

For the production of biotechnological materials, sustainable resources are required that do not compete with the food supply. Such a material is the cheap and plentiful sugar beet pulp (SBP), a cell-wall-rich by-product from the sugar industry. The long-term goal of this study is to improve effective waste management of SBP and its application as a carbohydrate-rich material.

I have characterised SBP and its derived biotechnological product, Curran®, by investigating the chemical composition, the constituent polysaccharides' molecular mass and the product's potential to interact with water. Curran® has valuable rheological properties and thus numerous potential industrial uses, for example as an additive in paints. Viscosity of Curran® is considered the most significant parameter to distinguish between high- and low-value products (high viscosity is usually regarded as being of higher value). Therefore, a wide range of different viscosity experimental Currans® (eC) were selected for this project.

I hypothesised that the composition, as well as polysaccharides' molecular mass, have a significant influence on viscosity. Results from this project showed that eC are a changed cell wall polymer network, comprising essentially all the cellulose, much of the hemicellulose but only low levels of pectins.

I further tested whether the molecular mass of hemicellulosic and pectic polysaccharides in eC affects viscosity of the product. All hemicelluloses and pectins in eC showed decreased molecular mass compared with the polysaccharides in SBP. In addition, high-viscosity eC contained the smallest pectic polysaccharides. This led to the conclusion that viscosity increases with decreasing molecular mass of the non-cellulosic polysaccharides.

I finally investigated the accessibility of hydroxyl (–OH) groups in the polysaccharide network of eC products and other carbohydrate samples. The –OH group availability is an important factor for the interaction of eC with other industrial ingredients. Hence, the availability of –OH groups was hypothesised to correlate with viscosity of the eC products. This work established an easy, but sensitive, method for the relative quantification of available –OH groups in different carbohydrate materials such as paper, xyloglucan, SBP and eC products. The method is based on the quantification of ^{3}H remaining bound to carbohydrate samples after removal of $^{3}H_2O$ by desiccation. The percentage of ^{3}H retained and hence availability of –OH groups in eC products

increased with increasing viscosity. Greater availability of –OH groups might increase the interaction of eC particles with each other and water molecules which leads to enhanced viscosity. Furthermore, the addition of these eC or Curran® products to paints may benefit the paint's properties (such as cracking resistance in hot or cold conditions).

The findings of this thesis contribute to an improved understanding of Curran's® rheological properties and may lead to an optimised production of Curran®. In future, this might inform strategies of adding Curran® to a wide range of products and thereby increase the use of "waste" for biobased materials.

II. Lay summary

For the production of chemicals and biotechnological materials, sustainable resources are required that do not compete with general food supply. Such a material is the cheap and plentiful sugar beet pulp (SBP), a plant cell-wall-rich “waste” product from the sugar industry. The aim of this study is to improve effective waste management of SBP and its application for the manufacture of valuable products.

This work characterised SBP and its derived biotechnological product, Curran®, a polysaccharide (carbohydrate) network. Curran® has valuable properties and thus numerous potential industrial uses, for example as a viscosity enhancer in paints.

I hypothesised that the composition of experimental Curran (eC), and the size of its polysaccharide molecules influence viscosity profoundly. During the production process of eC, polysaccharides in SBP are degraded to a certain extent and most pectins (a class of polysaccharides) are removed while the eC products become enriched in cellulose (another class of polysaccharide). In fact, the viscosity of eC decreased with the loss of mainly pectins. The size of non-cellulosic polysaccharides affects their ability to interact with each other and form a polysaccharide network. Compared with SBP, all tested polysaccharides in eC showed a significant decrease in size and decreased with increasing viscosity of the eC products.

This work also established an easy, but sensitive, relative quantification method to test the interaction of different carbohydrate samples (especially eC) with the water in which they are bathed. It is based on the quantification of radioactivity that remained bound to carbohydrate samples after incubation in radioactive water, and then removal of water by drying. This interaction was hypothesised to correlate with viscosity of the eC products because it can increase the binding of eC particles to each other and promote stronger polysaccharide networks (that then form higher viscosity products). The radioactivity retained, and hence the estimated interaction of eC products with water, was confirmed to increase with increasing viscosity.

III. Acknowledgements

I would like to give a great thank you to CelluComp Ltd. and the School of Biological Sciences who gave me the financial support for the past four years to successfully finish my PhD project.

Dr. E. Whale made a placement at CelluComp Ltd. possible for me and supported me throughout my PhD. I am very grateful to the whole team at CelluComp Ltd. for making my visits so enjoyable and productive.

I immensely appreciate the support from my supervisor Prof. S. C. Fry over the past four years, his help and guidance were invaluable for the completion of my thesis. He has greatly contributed in me becoming an independent scientist.

I will always cherish the four years I spent in the Fry lab and IMPS; to start and finish this PhD was the best decision of my career thus far. There are so many Fry-lab members and IMPS friends and colleagues that made my time really special and to thank all of them would exceed the confines of this chapter, but I would especially like to thank my dear Janice, who welcomed me to the lab like family and always has and had warm words for me; Lenka, who would always be very busy but take all the time needed to help me out. A special thank you goes to my current lab members whose support and love was immense, especially during the final months of handling my pregnancy and completion of my PhD: Amy, Dayan, Ninni, Klaus, Anzhou, Martina, Michael, Thurayya and Rifat: thank you all for your friendship and professional support!

I am grateful to Susanne, Amy, James and Anthony who proofread my thesis.

My family and friends in Germany have always looked out for me, and without their love I would not be the person that I am today or have been able to appreciate my life in Edinburgh as much as I did.

To my love Anthony: the last three years with you have been the best of my life! I am forever grateful for your immense love and support and I am looking forward to what the future holds for us three.

To my unborn son: I could not have completed my PhD before your birth without your help; you were the most supportive baby!

One more thing that I wanted to say: Supercalifragilisticexpialidocious!

IV. List of Abbreviations

AIR:	Alcohol-insoluble residue	hveC:	High viscosity experimental Currans
^{2}H MAS NMR:	^{2}H magic-angle-spinning NMR	HVPE:	High-voltage paper electrophoresis
^{2}H:	Deuterium	IP:	Isoprimeverose
^{3}H:	Tritium	K_{av}:	partition coefficient $K_{av} = V_i - V_0$
$^{3}H_2O$:	Tritium in water	LSC:	Liquid scintillation-counting
Ara:	L-arabinose	MAE:	Microwave assisted extraction
ASP:	Alkaline soluble polysaccharides	Man:	D-mannose
BAW:	Butan-1-ol, acetic acid and water	MCC:	Microcrystalline cellulose
CMC:	Carboxymethyl cellulose	MD:	Molecular dynamics
CPM:	Counts per minute	min:	Minute(s)
D_2O:	Deuterated water	MLG:	Mixed-linkage glucan
DP:	Degrees of polymerisation	MM:	Marker mixtures
dpm:	Disintegrations per minute	M_r:	Molecular mass
dps:	Disintegrations per second	MS:	Mass spectrometry
Dr.:	Driselase	NMR:	Nuclear magnetic resonance
eC:	Experimental Currans	o/n:	Overnight
EDTA:	Ethylenediaminetetraacetic acid	–OH groups:	Hydroxyl groups
EPyAW:	Ethyl acetate, pyridine, acetic acid and water	PC:	Paper chromatography
EPyW:	Ethyl acetate, pyridine and water	PCC:	Parenchymal cell cellulose
EtOH:	Ethanol	PLA:	Poly(lactic acid)
FT-IR:	Fourier transform infrared spectroscopy	PyAW:	Pyridine, acetic acid and 0.5% chlorobutanol in water

Fuc:	L-fucose
Gal:	D-galactose
GalA:	D-galacturonic acid
Glc:	D-glucose
GlcA:	D-glucuronic acid
GPC	Gas-liquid-chromatography
h:	Hour(s)
H_2O:	water
H_2O_2:	Hydrogen peroxide
H_2SO_4:	Sulfuric acid
Ha:	Hemicellulose a
Hb:	Hemicellulose b
HbP:	Hemicelluloses and pectins
HCl:	Hydrochloric acid
HOAc:	Acetic acid
HPLC:	High pressure liquid chromatography
R_F	= distance travelled by the compound/ distance moved by solvent
RG-I/ II:	Rhamnogalacturonan I and II
Rha:	L-rhamnose
Rib:	Ribose
RT:	Room temperature
SA:	Specific radioactivity
SBP:	Sugar beet pulp
SEM:	Standard error
SEPs:	Soluble extracellular polysaccharides
TFA:	Trifluoroacetic acid
TLC:	Thin-layer chromatography
V_0:	Void volume
V_i:	Included volume
vol:	Volumes
XET:	Xyloglucan endotransglucosylase
Xyl:	D-xylose
Xyl_2:	Xylobiose

V. Table of Contents

VI. List of tables

VII. List of figures

1 Introduction

1.1 Sugar beet (*Beta vulgaris* L.)

Beta vulgaris L. is an angiosperm plant in the order Caryophyllales, family Amaranthaceae (Dohm *et al.* 2014; Encyclopaedia Britannica 2015). It is an important agricultural crop as it provides the source of half the sugar consumed in the UK. In the UK, sugar beet is sown in March and grown in regions such as Yorkshire, Essex or the West Midlands. It is harvested from September to December when sugar content is highest in the roots (Hoffmann *et al.* 2005). Sugar beet produces only a negligible amount of starch in the roots and uses sucrose to store energy (Wen *et al.* 1988; Turesson *et al.* 2014). The harvest season 2017 yielded the highest ever recorded harvest of 83.4 t/ ha in the UK (105,000 ha growing area within Wales and England) (Fleming 2018). The average composition of a sugar beet root when harvested is: water 77.7%, sucrose 15.9–18.0%, pulp 5.5–7.0% (water-insolubles) and 0.9% ash, betaine, glucose (Glc) and fructose (Spagnuolo *et al.* 1997; Centre, F. A. O. I., Europe, E. and States 1999; Mouelhi *et al.* 2014; Liquid Energy Trading Company Swiss S.A. 2015). Sugar factories extract sucrose from the roots for sugar production, while molasses and pulp are mainly used as animal feed. Molasses, the syrup left after crystallisation of sugars, are very high in sucrose and additionally used to produce industrial alcohol, bioethanol, yeast, organic chemicals and even rum (Centre, F. A. O. I., Europe, E. and States 2009; Vučurović & Razmovski 2012).

SBP is a highly abundant by-product of the sugar beet industry (McCready 1966). The record harvest of 2017 in the UK resulted in 438,000 t of dry sugar beet pulp (SBP). For these large amounts of cellulosic by-product, a new valuable purpose must be found (Dinand *et al.* 1996).

1.2 Sugar beet pulp

Dried SBP consists of approximately 80% polysaccharides (Table 1) and is therefore a potential industrial material (CelluComp Ltd.; McCready 1966; Dinand *et al.* 1996; Kühnel *et al.* 2011). The energy and production costs to prepare SBP as animal feed have increased over the last years and thereby diminished the demand for SBP in that sector (Fishman *et al.* 2009).

Dinand *et al.* (1996) studied the raw composition of SBP and a product which they called parenchymal cell cellulose (PCC) derived from SBP. SBPs' carbohydrates are the primary cell walls from sugar beets and therefore the main point of interest in the study of SBP. Dinand *et al.* (1996) identified the main cell wall components cellulose, hemicellulose and pectin (Table 1). These three main classes of cell wall polymer made up 81% of the dry SBP while inorganics, proteins, lignin and fats were present in minor amounts (total 19%). SBP pectin showed a degree of methyl esterification of 70% (Fishman *et al.* 2009).

The exact composition can vary between different methods and publications (McCready 1966; Sidi Ali *et al.* 1984; Thibault & Rouau 1990; Hoffmann *et al.* 2005).

Table 1: Chemical composition (% dry weight) of sugar beet pulp.
Cellulose, hemicellulose, pectins and lignin are typical cell wall components (Dinand *et al*. (1996)).

Components	**% dry weight**
Cellulose	22
Hemicellulose	32
Pectins	27
Inorganics	8
Proteins	7
Lignin	2
Fats	2

Similar compositions were published by other authors and the high arabinose content (§1.3.2.2) in pectin, compared to other dicotyledons, was especially noted (McCready 1966; Ralet *et al.* 2009).

To date, multiple studies have been conducted that could lead to a wide range of applications for the highly abundant SBP: Three US patents from the 1980s deal with the exploitation of SBP for future applications. Weibel (1986, 1989) and Weibel & Myers (1990) invented a methodology to isolate cellulose and matrix polysaccharides from SBP. Beale *et al.* (1984) presented a non-caloric bulking agent that could replace high-caloric ingredients in food. Fibrex®, a sugar beet fibre additive, is such a product. It is currently produced by Nordic sugar in Sweden and shows promising health benefits (Nordic Sugar 2011, 2014). Buchholt *et al.* (2004) extracted and modified pectins from SBP. Drusch (2007) found that sugar beet pectin and Glc syrup could be used as a suitable material for the microencapsulation of fish oil. SBP may also find potential application in removing metal ions from aqueous solution (Dronnet *et al.*

1997; Gérente *et al.* 2000; Aksu & Işoğlu 2005; Pehlivan *et al.* 2008) or as a suitable material for bioethanol production (Zhao *et al.* 2014). In 2017 the European Biogas Association published their plan to build a plant for utilizing SBP as a sole source for biogas production (to increase the market for SBP and decrease logistical costs when coupled directly with a sugar factory). Arabinose (Ara), for use in the production of therapeutic ingredients (e.g. L-gluco-heptulose, can be extracted from SBP in a facility connected to a sugar factory (Cárdenas-Fernández *et al.* 2017). In Poland a project to utilise monosaccharides hydrolysed from waste sugar beet for the extraction of 5-hydroxymethylfurfural (a flavouring agent in food) was started (Tomaszewska *et al.* 2018).

CelluComp Ltd. is a material science company focussing on high performance products from sustainable materials like root vegetables. SBP as raw material is currently used by CelluComp Ltd. to produce Curran® which can be used as a performance enhancer and is mainly used in paints and coatings to date. Properties of coatings like hardness, flexibility and cracking resistance are enhanced by the addition of Curran® (CelluComp Ltd.). This material is related to the eC products studied in this work. To produce eC (§2.1) SBP is rehydrated in water and subjected to a hydrogen peroxide and sodium hypochlorite treatment.

1.3 The plant cell wall

As SBP — the raw material that is studied in this project — mainly consists of plant cell wall polymers (Table 1), the plant cell wall and specifically the sugar beet cell wall will be discussed in this chapter.

A cell wall gives stability and shape to a plant cell. Typically, plant cells have a primary cell wall and, in some cells, a secondary cell wall. The secondary cell wall is deposited after the cell has stopped growing. It usually consists of a thicker layer of polysaccharide (mainly cellulose (Figure 1)) than the primary cell wall and is sometimes heavily lignified. Most primary cell walls are thin and, most importantly, allow the cell to grow (Albersheim *et al.* 2010). Besides structural proteins and approximately 70% water, all primary cell walls contain the three classes of structural polysaccharides: cellulose, hemicelluloses and pectins (Albersheim *et al.* 2010; Fry *et al.* 2011).

Mechanical disruption and treatment with different solvents can separate the cell walls from the cytoplasm. Chemical and enzymic hydrolysis may be used to separate the

structural polymers from each other and digest them into smaller components such as monomers and dimers (Albersheim *et al.* 2010).

Because sugar beet is mainly composed of parenchymal tissue (lacking a secondary cell wall) (Dinand *et al.* 1996; Ralet *et al.* 2009), the structural polysaccharides of the primary cell wall will mainly be discussed in the following (§1.3.2).

1.3.1 The plant secondary cell wall

1.3.1.1 *Lignin*

The second most abundant polymer on earth is the phenolic lignin (after cellulose) and subject of great interest especially for industries trying to exploit lignocellulosic biomass to produce higher value materials. It is well known, that the presence of high amounts of lignin, in mainly secondary plant cell walls, leads to stability (called recalcitrance) towards degrading conditions such as acids and enzymes (Himmel *et al.* 2007). Lignin's natural role in the plant is to prevent water escaping from xylem vessels and guide water to the areas where it is needed in the plant. Lignin is highly abundant in woody tissue of trees (approximately 20–30% dry mass) (Heitner *et al.* 2010) but only present in minor quantities in sugar beet (McCready 1966; Wen *et al.* 1988; Dinand *et al.* 1996). Lignin is composed of three phenylpropane precursors, namely *p*-coumaryl alcohol, coniferyl alcohol and sinapyl alcohol that are combined in different ratios depending on the specific plant and plant tissue. Oxidative coupling of these monomers forms a growing, irregular, highly cross-linked polymer (Heitner *et al.* 2010; Heinze *et al.* 2018).

Lignin was not studied in this work as it was expected to only be present in minor quantities in SBP and negligible quantities in sodium hypochlorite-treated eC products (Wen *et al.* 1988).

1.3.2 The plant primary cell wall

Typical primary cell walls of dicots are composed of almost equal amounts of three types of polysaccharides: pectin (rich in galacturonic acid (GalA), galactose (Gal), Ara and rhamnose (Rha)); hemicelluloses (rich in glucose (Glc), Xyl and Man); and cellulose (composed of Glc residues).

1.3.2.1 *Cellulose*

The most stable and insoluble polymer in the cell wall is cellulose. The polymer's subunits are cellobiose, made of two Glc monomers positioned at 180° relative to each other. Cellobiose units form an unbranched polysaccharide of contiguous

β-1,4-linked glucopyranose residues (Figure 1). The cellulose chain may have different degrees of polymerisation; most common in plants it is crystalline (ordered) cellulose with amorphous (unordered) regions. Cellulose chains are arranged in microfibrils and embedded in a mesh of matrix polysaccharides (pectins and hemicelluloses) (Albersheim *et al.* 2010).

Intra- and inter-molecular hydrogen bonds are responsible for the stiffness and sheet-like structure of cellulose. They are formed between the hydroxyl groups (–OH groups) on Glc residues of the cellulose chains (Figure 1) (Kondo 2004; Heinze *et al.* 2018). Intramolecular hydrogen bonds cause relative stiffness and rigidity of the cellulose molecule; they are formed between the –OH of C(3) and the adjacent ether oxygen of the Glc residue, as well as between the –OH oxygen at C(6) and the adjacent OH at C(2). Intermolecular hydrogen bonds are formed between the OH of C(6) and the oxygen at C(3) on an adjacent cellulose chain (Heinze *et al.* 2018). The various H-bonds lead to versatile three-dimensional cellulose structures. Native cellulose is named cellulose I; it is crystalline and formed from parallel chains that are interconnected via H-bonds (Gardner & Blackwell 1974). The parallel and anti-parallel orientation of cellulose chains is determined by the position of the reducing and the non-reducing termini of each chain. For example, in the parallel orientation the reducing terminus of one chain is adjacent to the reducing termini of the neighbouring chains etc. This is reversed in the antiparallel orientation, where the reducing terminus of one chain is next to the non-reducing termini of neighbouring chains (Heinze *et al.* 2018).

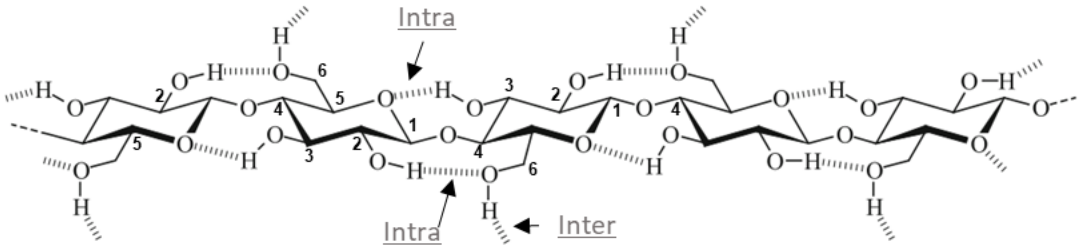

Figure 1: Chemical structure and hydrogen-bonding system of cellulose I (modified from Heinze *et al.* (2018)).
Some carbon atoms are numbered for easier understanding of the hydrogen-bonding system.

Two forms of cellulose I have been identified: Iα mostly prevalent in bacterial and algal cellulose, and Iβ which is the dominant type in land plants (Atalla & VanderHart

1984). The two forms differ in their combination of intramolecular H-bonds (Heinze *et al.* 2018).

Cellulose II can be obtained from cellulose I by mercerisation (for example by swelling in sodium hydroxide) and does not exist in nature. It is comprised of antiparallel cellulose chains that are extensively H-bonded (Stipanovic & Sarko 1976).

In the presented work, the native cellulose in SBP was subjected to two oxidising chemical treatments, which could have caused structural changes of the cellulose in the eC products. Oxidising treatments, depending on their severity, can cause many different modifications of cellulose (Rutherford *et al.* 1942). Oxidising agents typically attack

- the few (if any) aldehyde end groups and oxidise them into carboxyl groups;
- the primary alcohol groups can be oxidised to the carboxyl or aldehyde stage;
- the glycol group (2,3-dihydroxy group) which can be oxidised to the ketone, aldehyde or carboxyl stage.

Oxidation of cellulose (called oxycellulose) can result in scission of the chain (supported by viscosity studies) and lower molecular weight oxycellulose (Gilbert *et al.* 1984). H_2O_2, a widely used bleaching agent in industry, was shown to produce radicals that reduced the degree of polymerisation of cellulose and were able to transform it into oxycellulose (Zeronian & Inglesby 1995). Other cell wall polysaccharides also show susceptibility towards oxidising reagents such as H_2O_2; the results depend on the composition of the polysaccharide, the temperature and the pH of the environment (Miller 1986; Zeronian & Inglesby 1995). Sodium hypochlorite (the second oxidising reagent in the production of eC materials) together with H_2O_2 was shown to transform part of the –OH groups into carbonyl groups (aldehydes or ketones) without cutting the bond between carbon 2 and 3; this reaction was pH dependent (Diankova & Doneva 2009).

1.3.2.2 *Pectin*

Pectins in the primary plant cell wall play an important role in fruit ripening when it is fragmented leading to fruit softening (Wang *et al.* 2018). Three pectic domains were extracted from sugar beet roots with imidazole-HCl by Ishii and Matsunaga (2001): homogalacturonan and rhamnogalacturonan-I and –II (RG-I and RG-II) (Figure 2). Gel-permeation chromatography of the *endo*- and *exo*-polygalacturonase fragmented

pectin confirmed that RG-II was covalently linked within homogalacturonan chains (Ishii & Matsunaga 2001). In fact, pectic components are thought to be linked end-to-end by glycosidic bonds into a single polysaccharide (Fry 2011).

Homogalacturonans are made of anionic GalA and uncharged methyl α-D-galacturonate joined through 1-4 bonds (Fry 2011) (**Figure 4**).

The RG-I backbone is made up of repeating Rha and GalA residues. About half of the Rha residues have side chains attached that are rich in Gal and Ara (Fry 2011). Sugar beet pectin is rich in these so-called “hairy regions”, about 40% of the Rha residues are substituted at position 4 by neutral sugars, mainly arabinose-rich side chains (Oosterveld *et al.* 1996). In contrast, RG-II is a more complex polymer with a backbone of α-GalA residues and side chains (made of up to 12 different residues) attached to it. Five different side chains have been identified, called A-E. Four of them (A-D) are acidic but differ in their residue composition. Driselase, a cell wall degrading enzyme mixture (§2.4), is not successful in digesting RG-II and can therefore be used to isolate the RG-II domain (Fry 2000).

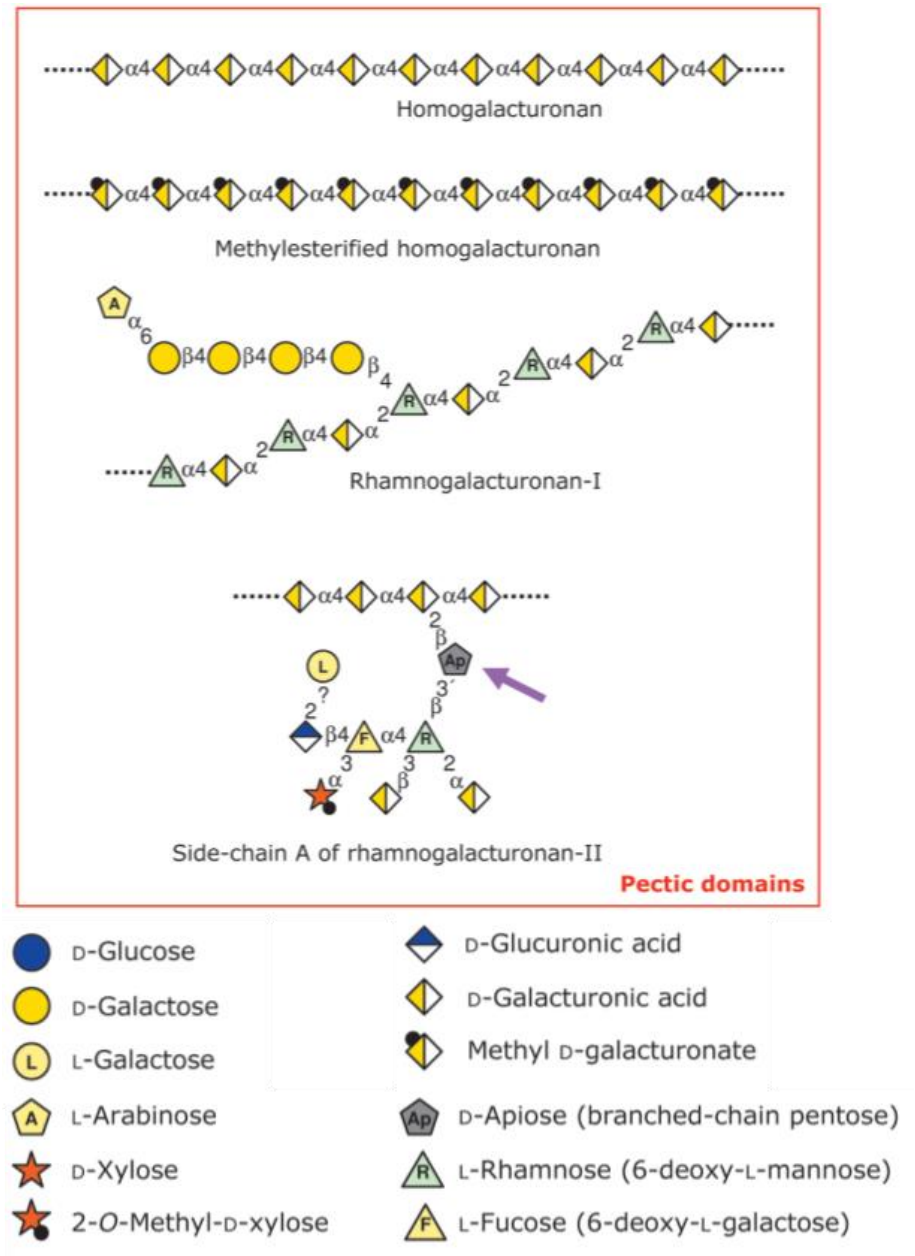

Figure 2: Representation of three different structures found in pectins of the primary cell walls in flowering plants (modified from Fry *et al.* (2011)).
The purple arrow points to the apiose residue which forms borate bridges in RG-II; only side chain A of RG-II is shown. (……=continuation of the polysaccharide backbone). Modified from Fry *et al.* (2011).

Sugar beet pectin does not gel as easily as citrus pectin does, probably owing to the high content of acetyl ester groups (Roboz and Van Hook, 1946; Michel *et al.*, 1985). Beet pectin was nonetheless used in jellies during the second world war in Germany (Roboz & Van Hook 1946), probably due to the good availability of sugar beets (and the lack of other sources). Furthermore SBP pectins have a low average molar mass (Ralet *et al.* 2009).

To efficiently extract pectin from SBP, heating or alkaline treatments can be used but this results in partial degradation of pectin molecules (Ralet *et al.* 2009).

1.3.2.3 *Hemicellulose*

The widely accepted tethering role for hemicelluloses in the primary cell wall describes their ability to form hydrogen-bonds (Roland *et al.* 1989) to cellulose and tether adjacent cellulose microfibrils (Fry 1989a). In recent years, this model has been questioned by several authors (§4.4). Xyloglucans, heteroxylans and mannans are hemicelluloses found in land plants (Figure 3). The concentration of typical hemicellulosic residues (i.e., Xyl, Man, non-cellulosic Glc and fucose (Fuc)) is usually very low in beet cell walls (Ralet *et al.* 2009).

Xyloglucans have a β- 1,4- Glc backbone with short side chains containing various combinations of Xyl, Gal, Fuc and Ara (Albersheim *et al.* 2010). Enzymic Driselase digestion yields the typical marker for xyloglucans, which is the disaccharide isoprimeverose (IP) (D -xylopyranosyl-α-(l-6)- D -glucose) (Fry 1989b, 2000).

After xyloglucan, xylan is the second most abundant hemicellulose in the primary cell walls of dicots. All xylans have a backbone of (1-4)-linked β-Xyl residues. Enzymic digestion by Driselase will give xylobiose plus Xyl as evidence of xylan in the sample (Fry 2000). Arabinoxylans have the same backbone of β-1,4-xylose residues, which are frequently substituted with side chains containing Xyl, Ara, GlcA and 4-O-methyl glucuronic acid residues. Dinand & Vignon (2001) found a (4-*O*-methyl-D-glucurono)-D-xylan attached to the microfibrils of a SBP-derived cellulose suspension in water.

Mannans can be found in the primary cell walls of dicots in low amounts. Their backbone is built from (1-4)-linked Man residues (sometimes interrupted by β-Glc residues) with or without α-Gal side chains.

Hemicelluloses (and pectins) can be extracted from primary plant cell walls by 6 M NaOH (Fry 2000). Extraction with 4 M NaOH demonstrated the presence of xyloglucans and mannans in beet (Oosterveld 1997).

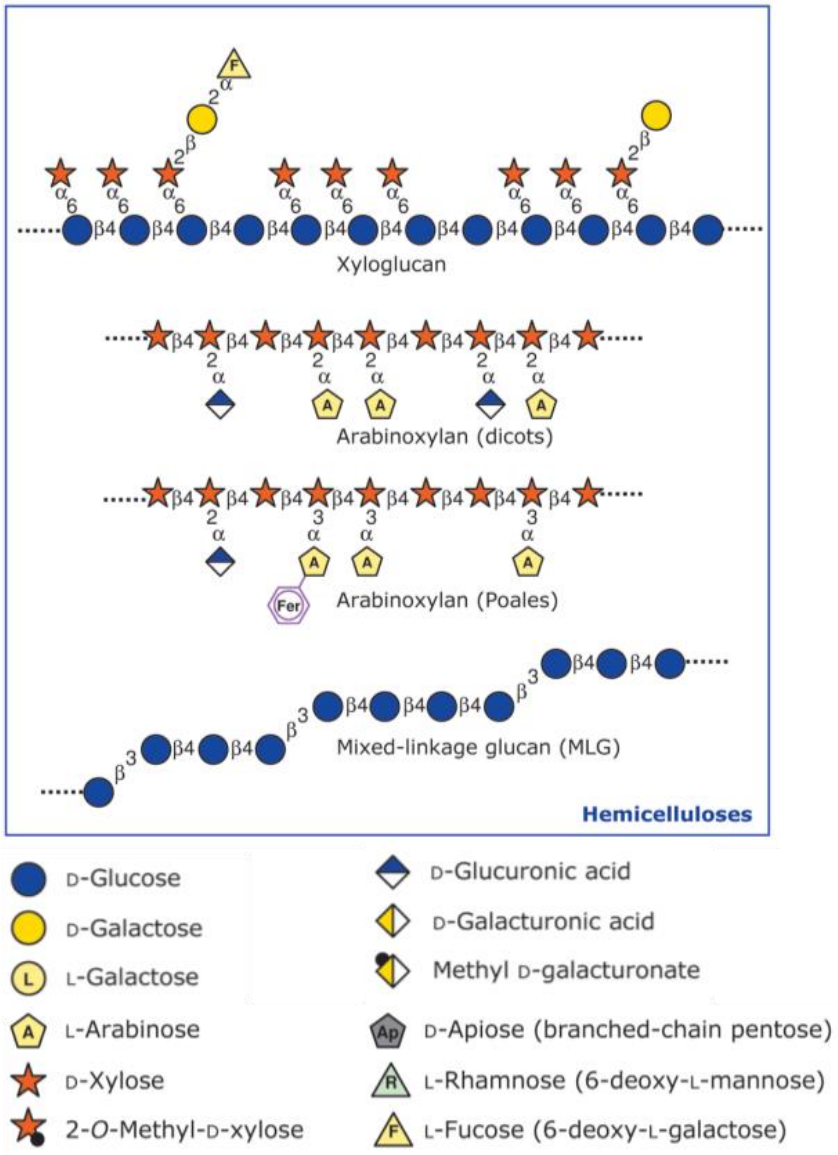

Figure 3: Representation of common hemicelluloses in flowering plants (modified from Fry *et al.* (2011)).
'Fer' is a ferulate (=4-hydroxy-3-methoxycinnamate) group esterified to O(5) of Ara of arabinoxylan in Poales. For details see Figure 2.

The molecular structure of the major monosaccharides forming cellulose, pectins and hemicelluloses is depicted in Figure 4.

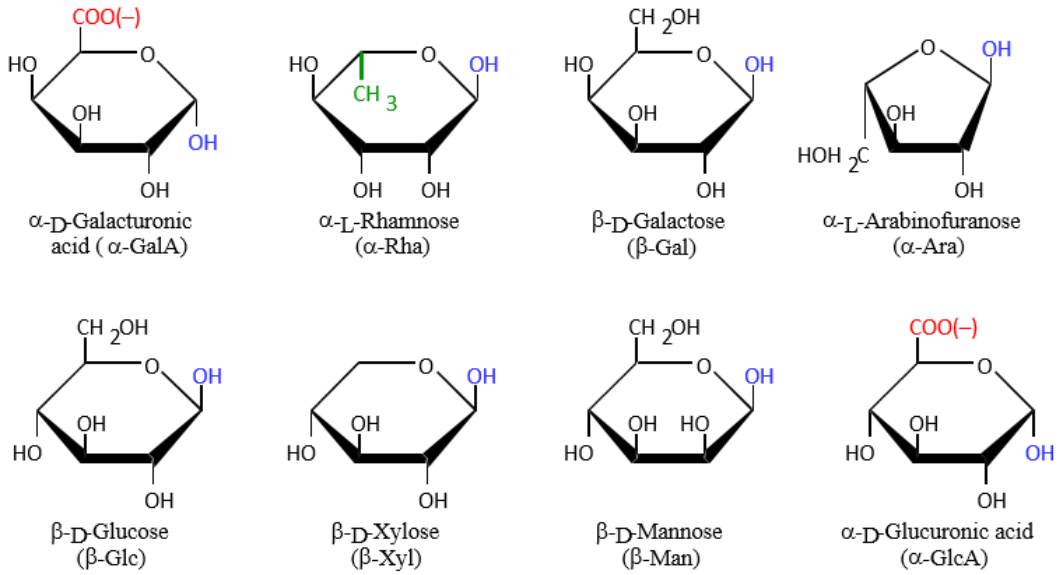

Figure 4: Eight monosaccharide building blocks (shown as Haworth formulae) of plant cell wall polysaccharides (modified from Fry *et al.* (2011)).
The eight most abundant monosaccharides of the primary cell wall. The top four are the major monosaccharides in pectins while the second row of monosaccharides are mostly present in hemicellulose; Glc is the only monomer in cellulose. The -OH group, coloured blue, will be lost from the structure when the sugar becomes incorporated into a polysaccharide, thereby becoming a residue. The free carboxy groups are marked in red and the hydrophobic (non-polar) group in green. The commonly used abbreviations for the sugars are given in parentheses under the names. (modified from Fry *et al.* (2011)).

1.4 Biocomposites

As the fossil resources for producing plastics and other materials are being used up, there is increasing demand of new alternatives from sustainable stocks. Suitable alternatives need to show a wide variety of different physical properties (Faruk *et al.* 2012). Agricultural by-products like corn stover, sugar cane bagasse or SBP are annually renewable, available in abundance and therefore cheap (Reddy & Yang 2005). Biocomposites are made of a matrix material with a reinforcement in which at least one component is derived from a biological origin (Fowler *et al.* 2006). Biocomposite's properties can be highly variable and hence their potential applications are unlimited. The high consumption of plastics generates a big demand for environmentally friendly plastics. Poly(lactic acid) (PLA) is a compostable 'green' polymer composite prepared from starch-rich crops. Food crops as a sole source for PLA are highly disadvantageous as it leads to competition with the food supply (Kawamoto 2007). PLA furthermore has a low softening temperature which reduces the range of applications (Mathew *et al.* 2006). Finkenstadt *et al.* (2008) made a PLA composite with SBP as a filler. Compared to pure PLA controls, an addition of 30%

dry weight SBP reduced the tensile strength and increased stiffness. The authors proposed that it could be used for packaging utensils and as light weight construction material (Finkenstadt *et al.* 2008). Biofibre-reinforced plastic composites find increasing acceptance in industrial applications (Faruk *et al.* 2012). Another group (Gårdebjer *et al.* 2015) analysed the water permeability in a PLA/microcrystalline cellulose–xyloglucan composite. They used PLA as a matrix and microcrystalline Avicel with pre-adsorbed tamarind xyloglucan as a filler. Xyloglucan hindered the cellulose microfibrils from aggregating due to steric stabilization of the absorbed xyloglucan. The composite's water permeability and mechanical properties were improved by the addition of xyloglucan, and it was suggested for use in biomedical applications or agriculture (Gårdebjer *et al.* 2015). Leitner *et al.* (2007) fragmented sugar beet cellulose into nanofibrils and produced strong cellulose sheets, which upon addition to a polymer matrix improved reinforcement properties. These studies prove the reinforcing and strengthening effect of SBP cellulose.

Curran®, produced from SBP, likewise shows great potential to be used in biocomposites in the future (CelluComp Ltd.). The use of vegetable particles in concrete has been subject to recent discussion in *The Times*. The research led by Professor Mohamed Saafi (from Lancaster university) constructed a cement nanocomposite material that included vegetable platelets produced by CelluComp Ltd.. They found significant improvement of the mechanical properties of concrete. Moreover, addition of platelet sheets to existing concrete increases its flexibility. Application of this concrete in the future will decrease CO_2 emission of the cement industry (Lancaster University 2018; Bridge 2018).

1.4.1 Introduction to experimental Curran

Curran® and eC (produced by CelluComp Ltd.) are biotechnological products from the cell walls of sugar beet and both were therefore expected to consist of polysaccharides and components from the plant cell wall.

Several patents (e.g. Weibel (1986) and Hepworth & Whale (2016)) and studies (e.g. Wen *et al.* (1988) and Dinand *et al.* (1996)) have been published that deal with products that are similar in many ways to eC products studied in this work.

In 2016 Hepworth & Whale published a patent (Hepworth & Whale 2016) about a cellulose-containing material that could be used in paint formulations or composites from herbaceous plants with a preferably low lignin content. The material showed

versatile applications as a strengthening agent and rheology modifier in water-based systems. The production process included hot hydrogen peroxide treatment that cleaved covalent bonds within the cell wall material and enabled the product to swell in water. After a pH drop of 2 units, peroxide was removed by washing and filtering. An optional bleaching step could be added before the material was pressed to solid contents of 20–50% dry weight for storage. The material was composed of 40–60% dry weight cellulose, preferably less than 2% hemicellulose and less than 10% pectin. Additionally, glycoproteins and extensin in a non-carbohydrate part of 20–50% were present. Viscosity of these shear-thinning fluids did not measurably change between pH 2 and 14. Hepworth & Whale were able to produce high-viscosity (2500–8000 centipoise (cP)) and low-viscosity material (10–1000 cP). The produced "cell-ghost" particles had a good water-holding capacity (90–99.5% (w/w) water) and were between 10 and 200 µm in size. Shear-thinning of high-viscosity cellulose-containing particles was especially good as this was useful for anti-settlement of pigments in paint cans while providing high shear rates for application of the paints to surfaces; low-viscosity particles were useful as strengthening agents and provided anti-cracking resistance to paint.

One example process described in the patent by Hepworth & Whale (2016) demonstrated the process of making high-viscosity cellulose particulate material from SBP (similar to the process described in this work §2.1). SBP pellets were washed in excess water, cooked for 3 h and uniformly dispensed. A hot peroxide reaction for 2 h caused a pH drop from around 5 to 3.5 and was followed by a bleaching treatment for 0.5 h. Between each reaction the material was washed free from the oxidising chemicals. The product was pressed, resuspended for viscosity measurement (1% dry weight) and resulted in 4600 cP.

Agoda-Tandjawa *et al.* (2010) likewise took dry SBP, but treated it with nitric acid (0.1 M, 30 min, 85°C) followed by sodium hydroxide (0.5 M, 30 min, 80°C) which resulted in almost pure cellulose (80% Glc per dry weight). The delaminated cellulose suspension (hydrolysis treatment combined with mechanical shearing and high-pressure blending) displayed a gel-like behaviour which did not flocculate or sediment.

Another viscosity enhancing product made from SBP, called PCC, was invented by Weibel (1986, 1989) and Weibel & Myers (1990) and studied intensely by Dinand *et al.* (1996, 1999). This work discusses the similarities to eC in §4.3.1.3.

1.4.2 Viscosity

To explain the valuable rheological properties of eC products, the specific terms used to describe viscosity need to be described. This chapter will explain these terms only very briefly.

A fluid's viscosity describes its resistance to flow and was measured in centipoise (cP) in this work (1 cP = 0.01 g/ cm/ s = 0.001 Pa·× s). In more technical terms, it is the ratio of the shear stress to the shear rate (viscosity = shear stress / shear rate). Application of a shear stress results in deformation of the fluid; the shear rate is the rate at which this deformation occurs. Shear thinning is observed when viscosity decreases with increasing shear stress (Schramm 1994; Viswanath *et al.* 2007). Shear-thinning fluids are sometimes also described as pseudoplastic when the fluid returns to its normal viscosity as soon as shear stress is removed. Shear stress, shear rate and other factors such as concentration, temperature and molecular mass of the solids can affect rheological properties (Toğrul & Arslan 2003a).

Toğrul & Arslan (2003a) prepared carboxymethyl cellulose (CMC) from SBP to find the relationship between temperature and concentration dependence of the viscosity. After they had extracted fat, protein, pectin, hemicelluloses and lignin from SBP, the CMC was dissolved in 37% HCl. CMC solutions were Newtonian in character: at higher concentrations the viscosity increased, at higher temperatures it decreased. The term "Newtonian" describes a linear relationship between shear stress and shear rate. Toğrul & Arslan (2003b) formulated an equation to describe the relationship of molecular mass to intrinsic viscosity. Intrinsic viscosity is the viscosity determined by the volume of a given polymer mass (dependence on solids). eC and Curran® are non-Newtonian, pseudoplastic fluids (non-linear relationship between shear stress and shear rate)

1.5 Availability of hydroxyl groups in a polymer network

The availability of –OH groups in cellulose has been studied for at least half a century but is still not fully understood and proves difficult to quantify. Rowland *et al.* (1969) determined the availability ratio of all three O-bonded H atoms in a Glc residue of cellulose (Figure 1) — O(2)H : O(3)H : O(6)H. They achieved this by reacting cellulose with 2-chloroethyldiethylamine and quantifying the distribution of 2-(diethylamino)ethyl substituents in the monosaccharides released from the

hydrolysed cellulose. By studying reactions of cellulose in solution and from reactions of disordered cellulose in heterogeneous systems, the ratio in perfectly crystalline microfibrillar cellulose is expected to be 1.0 : 0.0 : 0.5 and for perfectly amorphous cellulose 1 : 1 : 1 (Rowland *et al.* 1969). The O(3)H was found to be unreactive in highly crystalline cellulose due to strong intra-molecular hydrogen bonds with O(5) (Sarko & Muggli 1974).

In recent research, Lindh *et al.* (2016) applied heavy water (D_2O) to study site-selectivity of the exchange of the ^1H in the different HO groups of cellulose with the deuterium atoms (^2H). Through joint interpretation of ^2H magic-angle-spinning NMR (^2H MAS NMR), Fourier transform infrared spectroscopy (FT-IR) and molecular dynamics (MD) simulations, they determined that two out of three –OH groups were available for exchange. These tests were performed on commercially available highly crystalline microcrystalline cellulose (MCC) from cotton with fibril diameters of 7–9 nm. After the exchange had reached dynamic equilibrium in a heavy-water atmosphere they then vacuum dried the deuterated samples. ^2H MAS NMR spectra showed ^2H signals arising from exchanged deuterons in the –OH groups which were assigned to the O(2)^{2}H and the O(6)^{2}H groups. The intensity of the spectrum showed that the total amount of exchanged –OH groups in MCC was 23%, which made the authors conclude that 42% of all Glc residues were on the surface and not in a crystalline environment. It therefore followed that 23% H-exchange represented two out of three available –OH groups on the surface. FT-IR results also supported the observation that only the O(2)H and the O(6)H groups participated in exchange. These observations and conclusions were backed up by MD simulations showing that O(3)H exhibited as many hydrogen bonds to water molecules as the other two available groups, but donated its H only to O(5) (Lindh *et al.* 2016). This complemented the MD simulations done by Matthews *et al.* (2006) which suggested that the H-bond between O(3)H and O(5) is strong at the surface of cellulose fibrils.

Lindh *et al.* (2017) relied on the widely accepted model that cellulose chains form microfibrils that themselves aggregate into bigger bundles. This model has two –OH group exposing surfaces, the internal surface on microfibrils in one aggregate or the external surface of the aggregates. The latter might be exposed or bonded to other aggregates, matrix polysaccharides, air or water molecules. For re-dried deuterated MCC, Lindh *et al.* (2017) measured 1.0 % dry weight increase due to residual water and 0.4–0.5% due to the exchange of ^1H with ^2H. Within the experimental uncertainty,

they found that spectra arising from ^{2}HO groups in cellulose were insensitive to the removal of adsorbed water (Lindh *et al.* 2017). Adsorption sites for water in cellulose are –OH groups to which water molecules hydrogen-bond (Matthews *et al.* 2006). Lindh *et al.* (2017) additionally found two populations of water adsorbed in dried cellulose, one showing a significantly slower mobility than the other. They seemed to be spatially separated, the faster population becoming more mobile after increasing the relative humidity during exposure to $^{2}H_2O$, and possibly residing on the external surface. The slower population exhibited limited motion, possibly owing to entrapment at the internal surfaces inside the microfibril aggregates (Lindh *et al.* 2017).

The availability of –OH groups is important for the interaction of one material with another. eC's and Curran®'s ability to form a viscous suspension in water is a good indication of how much the polysaccharide network interacts with water. This work aims to use the radioisotope ^{3}H to establish an easy, low-tech method to semi-quantify –OH groups available for exchange with H_2O in eC and other carbohydrate materials.

1.6 Aim of the PhD project

This project investigates the utilisation of SBP in the production of a biotechnological, cellulose-enriched product called Curran®. The aim is to understand eC's composition and properties as a viscosity enhancer. This should be achieved by hydrolysis of the carbohydrate composition and analysis of eC's hemicelluloses and pectins molecular mass. It is hoped that this will lead to the improvement and optimisation of the Curran® production process. Furthermore, the accessibility of –OH groups in the polysaccharide network of eC products and other carbohydrate samples will be investigated. The –OH group accessibility is an important factor for the interaction of eC's cellulosic particles with other industrial ingredients. This work will establish an easy method for the quantification of available –OH groups in different carbohydrate materials and eC products.

2 Materials and Methods

Many of the methods described were modified from Fry (2000).

2.1 Production of experimental Curran and other samples

For the production of normally produced eC materials SBP starting materials were oxidised in H_2O_2 (optimal reaction up until a pH drop of 1-2 units), washed (with water) completely to remove all H_2O_2 and finally subjected to a second oxidising treatment with (sodium) hypochlorite before another complete wash with water. Normally produced eC materials B and B.B are identical in solid content and viscosity; the same applies to C and C.C. Hence, B, B.B, C, C.C, D, E and F are technical replicates of normally produced eC (from starting material A); the same applies to W and X (from starting material “like A”). From eC samples B, E and F (stored in grated form) new eC pastes (1% dry material) were prepared after a storage period of 6 month, resulting in B’, E’ and F’ respectively (technical replicates). A portion of normally produced eC X was drum dried (100% dry material) and named eC Z. Small alterations to the normal production process (named “changed production process”) led to different eC materials. For example, incomplete washing after optimal reaction in H_2O_2 and omitting of the hypochlorite treatment resulted in eC Y. Other eC materials (such as R and O (technical replicates, but from two different biological replicates)) were overreacted in H_2O_2 (pH drop greater than 1-2 units) but otherwise normally produced. Starting material G was only used for the production of high viscosity eC materials (technical replicates H, I, J and V). These got the optimal reaction in the two oxidising steps and were completely washed, but the concentrations of the oxidising chemicals were doubled. From the paste eC V (after storage for 4 month at 4°C) a 1% dry weight paste was produced and named eC V’.

All eC products (Figure 5) were produced at CelluComp Ltd. in Burntisland. All eC materials originated from sugar beet pulp which was pre-treated to yield SBP starting materials. SBP was powdered to yield starting materials A and “like A” while it was washed, frozen (for storage) cooked and blended to yield starting materials K and L. To produced starting material G, SBP was directly cooked and drained before

blending in fresh water, biocide was added for storage. The wet starting materials G, K and L had a solid content between 2.1 and 2.4% dry weight (determined with moisture analyser Kern (Frankfurt am Main, Germany) and Mettler Toledo (Columbus (OH), US)). SBP starting material A and “like A” were used as a dry powder (100% dry weight). The first oxidising reaction on the starting materials took place in H_2O_2 (a relatively brief “optimal reaction” until a pH drop of 1-2 units had occurred or “overreacted” until a pH drop of more than 2 units had occurred), after which the materials were completely water-washed (with some exceptions; Figure 5) to remove all unreacted H_2O_2 and to dilute out soluble acids. The second oxidising treatment was with sodium hypochlorite (with some exceptions), the product of which was likewise thoroughly water-washed (with some exceptions). High-viscosity experimental Currans (hveC) were produced with doubling the concentration of H_2O_2 and sodium hypochlorite. The viscosity of each eC and hveC product was measured with a viscometer (Brookfield Viscometer DV2T or DV-II Pro Extra (Toronto, Canada)) at 10 rpm for 5 min at a temperature of 20-21°C using the appropriate spindle (error +/- 200 cP). eC Materials were stored in grated or paste form (Table 2). All eC and SBP starting materials used in this work, are presented in Figure 5 to clearly differentiate between the different pre-treatments (of SBP) and production processes of the many eC materials.

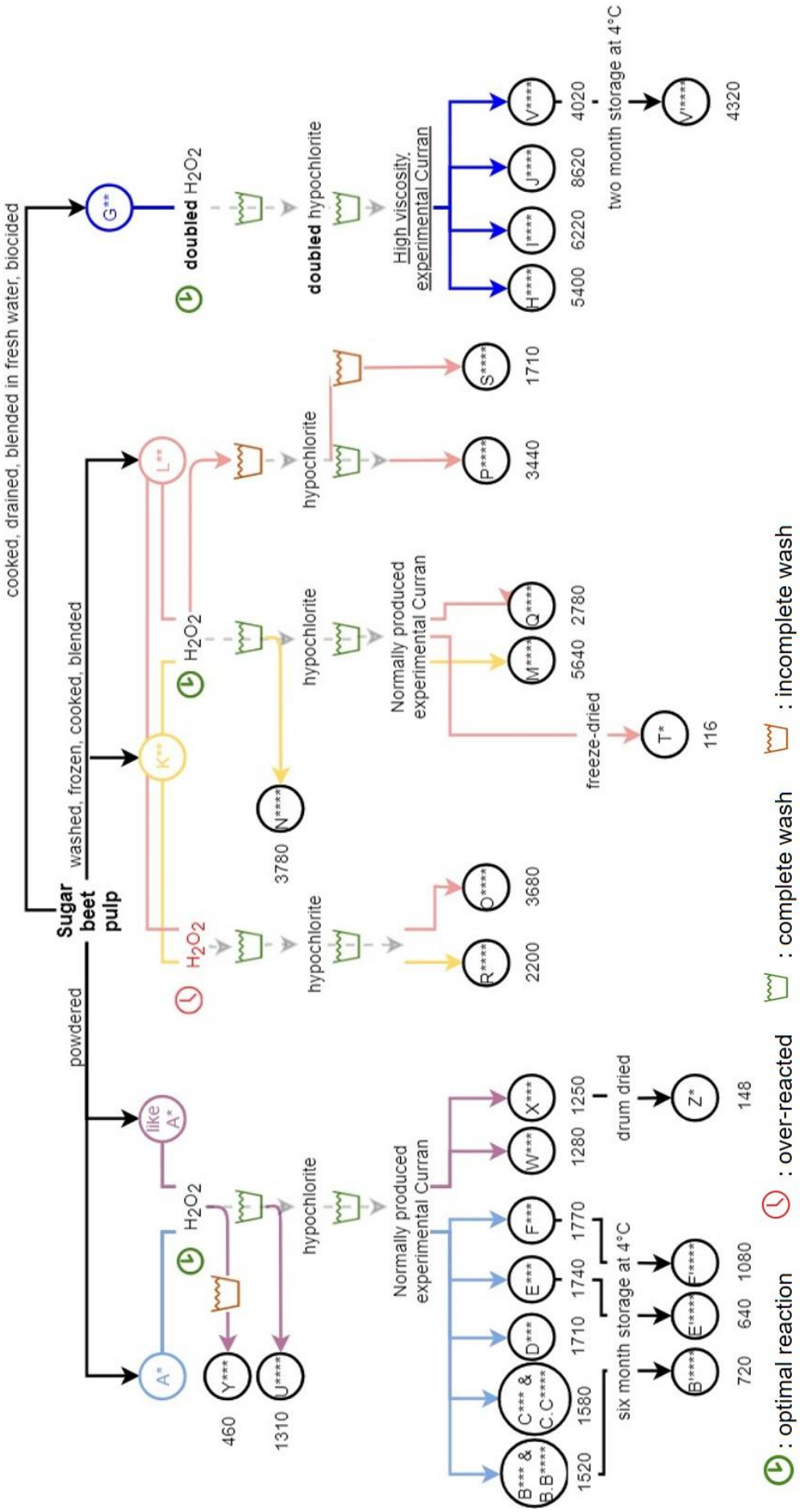
Sugar beet pulp
powdered
washed, frozen, cooked, blended
cooked, drained, blended in fresh water, biocided
A*
like A*
G**
K**
L**
H_2O_2
doubled H_2O_2
hypochlorite
doubled hypochlorite
Normally produced experimental Curran
High viscosity experimental Curran
freeze-dried
drum dried
six month storage at 4°C
two month storage at 4°C
Y***
460
J****
1310
B*** & B.B****
1520
C*** & C.C****
1580
D***
1710
E***
1740
F***
1770
B****
720
E****
640
F****
1080
W***
1280
X***
1250
Z*
148
R****
2200
O****
3680
N****
3780
M***
5640
Q****
2780
T*
116
P****
3440
S****
1710
H****
5400
I****
6220
J****
8620
V****
4020
V****
4320
: optimal reaction
: over-reacted
: complete wash
: incomplete wash
*: dry powder or sheet
**: slurry
***: grated
****: paste

Figure 5: (continued from the previous page) Experimental Curran production.
This diagram shows the step-by-step production of eC materials used in this work. All eC materials originated from sugar beet pulp which had been pre-treated to yield starting materials A, “like A”, K, L and G. In this study, the different pre-treatments yielded biological replicates of SBP (K and L are technical replicates of SBP starting material). Starting materials A, K. L and G all came from the same distributor; “like A” came from a different distributor of SBP. All eC materials are labelled with the respective viscosity in cP, additionally asterisks indicate the material consistency (see bottom of the diagram). For the production of normally produced eC materials, SBP starting materials were oxidised in H_2O_2 (“optimal reaction”), washed completely and finally subjected to a second oxidising treatment with hypochlorite before another complete wash. eC B, B.B, C, C.C, D, E and F are technical replicates of normally produced eC (from starting material A); W and X are technical replicates of each other (from starting material “like A”). From eC samples B, E and F (stored in grated form) new eC pastes (1% dry material) were prepared after a storage period of 6 month, resulting in B’, E’ and F’ respectively (technical replicates of each other). A portion of normally produced eC X was drum dried (100% dry material) and named eC Z. Small alterations to the normal production process (named “changed production process”, includes all eC materials that are not part of “normally produced eC” or “high-viscosity eC”) led to different eC materials. For example, incomplete washing after optimal reaction in H_2O_2 and omitting of the hypochlorite treatment resulted in eC Y. Other eC materials (such as R and O (technical replicates, but from two different biological replicates)) were overreacted in H_2O_2 but otherwise normally produced. Starting material G was only used for the production of high viscosity eC materials (technical replicates H, I, J and V). From the paste eC V (after storage for 4 month at 4°C) a 1% dry weight paste was produced and named eC V’.

The above diagram is summarised in Table 2.

Table 2: Sugar beet pulp and experimental Curran materials.
All viscosities were measured at CelluComp Ltd. in an aqueous suspension of 1% dry weight at 10 rpm for 5 min at 20–21°C. SBP starting materials are labelled in green; normally produced eC in blue; hveC in red; eC produced with a changed production process in yellow. The consistency of the materials is indicated by asterisks.

Material	Material description	Made from	% Dry weight of stock	Viscosity [cP]
A	Sugar beet pellet powder*		100.00	
B	Experimental Curran***	A	16.47	1520
B.B	Replicate of B****		17.54	1520
B’	Prepared from B, six months later****		1.06	720
C	Experimental Curran***		16.59	1580
C.C	Replicate of eC C****		18.49	1580
D	Experimental Curran***		19.86	1710
E	Experimental Curran***		17.51	1740
E’	Prepared from E, six months later****		0.91	640
F	Experimental Curran***		18.85	1770
F’	Prepared from F six months later****		1.01	1080
G	Sugar beet pellets (hydrated, cooked, washed, blended), biocide added**		2.38	
H	High viscosity experimental Curran****	G	1.27	5400
I	High viscosity experimental Curran****		1.30	6220
J	High viscosity experimental Curran****		1.30	8620

K	Sugar beet pellets (washed, frozen, cooked, blended)**		2.33	
L	Sugar beet pellets (washed, frozen, cooked, blended)**		2.12	
M	Experimental Curran****	K	1.00	5640
N	Experimental Curran, no sodium hypochlorite treatment****		1.00	3780
O	Experimental Curran, overreacted in H_2O_2****	L	1.00	3680
P	Experimental Curran, incompletely washed out H_2O_2****		1.00	3440
Q	Experimental Curran****		1.00	2780
R	Experimental Curran, overreacted in H_2O_2****	K	1.00	2200
S	Experimental Curran, incompletely washed out H_2O_2, sodium hypochlorite incompletely washed out****	L	1.00	1710
T	Experimental Curran freeze dried at -180°C*		100.00	116
U	experimental Curran, no sodium hypochlorite treatment****	A	3.40	1310
V	High viscosity experimental Curran****	G	2.67	4020
V'	Prepared from eC V two months later****	G	0.90	4320
W	experimental Curran from sugar beet pellet powder from a new distributor***	Like A	17.42	1280
X	experimental Curran from sugar beet pellet powder from a new distributor***	Like A	17.25	1250
Y	experimental Curran, incompletely washed out H_2O_2, no sodium hypochlorite treatment***	A	22.80	460
Z	experimental Curran X, drum dried*	eC X	100.00	148

cP: centipoise; *: dry powder or sheet; **: slurry; ***: grated; ****: paste

2.2 Preparation of alcohol-insoluble residue (AIR) and washed samples

To clean the sugar beet materials from contaminating free sugars, or other EtOH-soluble components, alcohol-insoluble residue (AIR) was prepared from materials K–S (Table 2) and used for multiple experiments. This procedure will wash out soluble contaminants and lipids (Albersheim *et al.* 2010). When it was suggested that EtOH might remove small carbohydrates in the materials that contribute to eCs' biochemical composition and viscosity, materials A–J were just washed with 0.5% (w/v) chlorobutanol and then directly used for all following experiments.

These AIR and washed materials were named "SBP preparations" and "eC preparations". It is important to differentiate between the starting materials (SBP or eC products) and these preparations.

A sample (Table 2) (of typically 2 g fresh weight) was blended with a hand-held blender in 70% EtOH (in the smallest volume possible, typically 90 ml per 2 g, to increase blending efficiency) for 1–10 min (depending on sample size and rigidity). The equipment was rinsed with 70% EtOH and the washings were added to the homogenate to give a solid content of ~2% dry weight. The suspension was rotated in 50-ml Falcon tubes or stired in a beaker for 10 min. The ethanolic supernatant was then replaced by the same volume of fresh 70% EtOH. This was left to rotate or stir for 1 h before EtOH was replaced again. This step was repeated twice more with washing times of 2 h and 12 h. The final ethanolic supernatants were analysed to check for free sugars by TLC in EPyAW (6:3:1:1) solvent and stained with thymol staining solution (§2.5) (for the common monosaccharides) and later discarded. After the 4th EtOH wash, the supernatant was replaced with acetone for 30 min to remove all EtOH. The acetone supernatant was removed (also checked on TLC) and the solid residue left to dry.

If the last washing step was not free of sugars (judged from TLC plates) another two washing steps (using EtOH and acetone) followed.

Dry AIR (100% dry weight) was used for some of the following experiments.

2.3 Acid-catalysed hydrolysis in trifluoroacetic acid

To analyse a carbohydrate sample (e.g. SBP) it was hydrolysed into its component monosaccharides. Acid hydrolysis by trifluoroacetic acid (TFA) breaks down the non-cellulosic polymers into neutral and acidic monosaccharides. TFA is volatile and is therefore easy to separate from the hydrolysis products.

Dry sample was mixed with 2 M TFA (1% dry weight) (e.g. 5 mg in 500 µl TFA) in tared screw-cap tubes. The tightly sealed tube was incubated at 120°C for 1 h in a heat block. After the sample had cooled it was spun (13000 rpm, 1 min) and the supernatant dried using a vacuum concentrator (Thermo Scientific SpeedVac) (only called SpeedVac hereafter) (it was taken care not to dry supernatants for longer than needed so they could easily be re-dissolved). Immediately after concentration, the dried supernatant was re-dissolved in 0.5% (w/v) chlorobutanol (to inhibit growth of contaminating organisms) to yield a known concentration according to the weight of the dry starting material. The TFA-resistant pellet was thoroughly washed with water

(3x 1 ml) and completely dried in the SpeedVac. In some cases it was further used for Driselase hydrolysis (§2.4), to determine the TFA-resistant residue or used in carbohydrate analysis (§2.8). The supernatant was analysed using TLC (§2.5).

2.4 Driselase hydrolysis

A complete hydrolysis of preparations from SBP and eC by Driselase will yield the components of the cellulosic and non-cellulosic polymers of the preparation. Driselase is a fungal enzyme mixture from Basidiomycetes sp.; it contains endo- and exo-enzymes that are highly active on the plant cell wall (manufacturers information; (Fry 2000)).

A 1% dry weight purified Driselase solution was prepared in PyAW (1:1:98) buffer. The dry preparation (§2.2) or fraction (§2.9) was added and left for incubation at 37°C in an incubator for three to five days. If time point samples were taken, the samples were spun down for 1 min at 13000 rpm in a minicentrifuge and a few µl of supernatant taken off before the tube was placed back for continued incubation.

To denature the enzymes 0.25x vol of 90% (v/v) formic acid was added. The mixture was spun for 1 min at 13000 rpm to seperate solids (i.e. residual AIR) from the supernatant. The supernatant was stored at -20°C or directly analysed using TLC (§2.5) or paper chromatography (§2.7). The Driselase-resistant pellet was washed three times with 1 ml de-ionised water and dried in the SpeedVac. It was sometimes used for total residual carbohydrate analysis (§2.8).

2.5 Thin-layer chromatography

By thin layer chromatography a mixture of compounds is separated. The stationary phase is a silica gel bound to a plastic plate. The mobile phase (solvent mixture) rises up the plate by capillary force and transports the compounds at different characteristic rates (R_f) relative to the solvent front. High R_f meaning further away from the origin. A compound's solubility in the solvent and the strength to adsorb to the adsorbent (e.g. silica gel) determines how far it will run on the TLC plate. Monosaccharides of the plant cell wall can be well seperated from one another by this method.

TLC silica gel 60 (20 x20 cm) plates (from Merck) were baked at 120°C for 15 min

prior to use to decrease cracking of the silica gel during staining. The samples were loaded 2 cm from the bottom and 1 cm from the sides of the plate. Samples of 2.5 µl were applied in streaks or drops on a 8 mm pencil line to the plate. The spacing between the samples was 2 -4 mm.

Different marker mixtures where prepared (each with a different combination of sugars) and 2 µg of each marker loaded to the plate. Sometimes dilution series of markers from 0.06 - 8 µg were used for quantification of the sample components (§2.5.2). If more than 2.5 µl had to be applied to a TLC as one sample, the first loading was dried (sometimes with a hairdryer for faster drying) and then followed by the second loading. Some samples where applied in different concentrations for better quantification of the separated components to avoid overload or too little sample.

The dry plate was placed in a glass tank containing 100 ml of the mobile phase. The TLC plates may bend during the run, so sticky tape was used to secure it to the glass walls. A glass lid closed the tank and Vaseline was used to provide an airtight seal. When the solvent was about 1 cm from the end of the plate, the TLC plate was taken out to dry. All TLC plates in this work were run in EPyAW (6:3:1:1) twice for 2.5–3 h. When the plates were completely dry they were ready for staining in thymol.

2.5.1 Thymol staining

A thymol staining solution was prepared (or kept in a light-tight bottle and not more than two weeks old) to stain reducing sugars on TLC plates. EtOH (99% (v/v) purity) was carefully mixed with H_2SO_4 to get a final H_2SO_4 concentration of 5% (v/v) (it gets hot when mixed) before thymol was added (0.5% (w/v)) and stired until dissolved. Usually 600 ml were prepared. The plates were dipped at an even pace into the solution, the back of the plastic plate thoroughly wiped and the plates left to dry (for at least 20 min) in the fume hood. For the colour reaction, TLC plates were baked at 105°C for 5–10 min (can be up to 30 min if needed). For documentation purposes, plates were scaned and the pictures brightness and contrast adjusted (using Adobe Photoshop software). Scaning settings of the EPSON GT-15000 scanner were as follows:

Image type: 24-bit colour
Backlight correction: High
Histogram adjustment: Input: 55 100 245

		Output: 5	–	245
Image adjustment:	Brightness: 0		Contrast: 0	Saturation: 5
Colour balance:	0	0	0	
Tone correction: linear				

The original pictures were analaysed for quantification of the sugar components when needed (§2.5.2).

2.5.2 Quantification of the components on Thin layer chromatography plates released by hydrolysis

The results of a TLC can be quantitatively analysed using the Photoshop software. The results give a good estimation of how much of each measured component is present in the hydrolysed samples.

The original scanned picture of TLC plates was opened in Photoshop for analysis. The “elipse tool” was chosen, because it fits best around the coloured spots on the TLC. One elipse (note width and height) was chosen for each marker component. The same elipse was chosen to measure the mean pixel values of the respective components in the samples by placing it exactly over the spot to be measured. The measurement was done by choosing the tab “image –histogram –channel –green” (because green gives the lowest mean). The “Photoshop mean” was taken for each spot individually. Appropriate negative controls were also measured to identify the mean value of the background. Gradients of the marker components were used to generate a function with the Sigma plot 12.5 software or Graph pad prism 6. The “Hyperbola double rectangular, 4 parameters” (Equation 1) applied by Sigma plot usually fitted best to all the data points of one gradient. In the respective report generated by Sigma plot, the parameters (a–d) of the function were given. The equation was solved towards x and further used to calculate the amount of each component in the samples.

Equation 1: Hyperbola double rectangular, 4 parameters (Sigma plot 12.5).
Adapted from Sigma plot 12.5. y: Photoshop mean difference; x: µg component loaded on TLC plates; a–d: parameters from the function given by Sigma plot.

$$y = \left(\frac{a * x}{b + x}\right) + \left(\frac{c * x}{d + x}\right)$$

The difference between the “Photoshop mean” of each sample spot and the mean

value of the negative control was used as y in the respective function (Photoshop mean differences). The result (x) is the amount of component in µg on the TLC plate (usually per 50 µg or 100 µg initial starting material). The results were often presented in a stacked column graph (amount of each component/ 100 µg hydrolysed sample).

2.6 Gel-permeation chromatography

To analyse the molecular mass of a given sample it is useful to separate its polysaccharides according to their relative molecular mass (Mr). There are several commercially available gel chromatography columns and stationary phases with a wide fractionation range. The fractionation range for dextrans (in kDa) was used to decide which stationary phase to use in the following experiments. In this project, Sepharose CL-6B (fractionation range for dextrans 10–1,000 kDa) and Sephacryl S-200 (1–80 kDa) were chosen.

Polysaccharides above the fractionation range elute early from the column in the void volume (V_0) whereas small molecules under the size limit elute late in the included volume (V_i) (Fry 2000). To mark V_0 and V_i, radioactively labelled molecules were used. These markers are only needed in quantitatively minor amounts and are thus not detected in a carbohydrate assay (§2.8) or on a TLC plate (§2.5) used to quantify the carbohydrates in the sample. Tritium labelled SEPs (soluble extracellular polysaccharides) from maize (hereafter called [^{3}H]SEPs) were used to mark the high molecular mass cut-off (V_0) and carbon-14 labelled Glc (hereafter called [^{14}C]Glc) was used as a low molecular mass marker (for V_i). The markers were used to determine the K_{av} and eventually used to calculate the relative molecular mass (M_r) of the polysaccharides in the sample.

For every column chromatography it is crucial to have a well packed column, meaning the stationary phase should not contain any air bubbles that would distort the run. The gel resin was mixed with the elution buffer (PyAW, 1:1:23 (v/v/v)) and carefully filled into the glass column. To ensure that the packed column wasn't damaged the column was never allowed to run dry. An aqueous sample of max. 4% column volume (including 1% dry weight hemicellulose plus pectin fraction (HbP); §2.9) was applied to the column by mixing it with the first cm of gel resin. It was given time to settle down and run into the resin. At that point a sufficient volume (about 10 ml) of elution buffer was applied onto the resin and the collection of eluted fractions was started using a

fraction collector. 1.5 column volumes were collected over 6-8 h in 2 ml fractions. The dripping speed was adjusted in advance by changing the vertical distance between column and elution buffer and by changing the size of the tubing attached to the end of the column. After all fractions were collected the column was washed with 5 column volumes of elution buffer. The fractions were further used for scintillation counting (§2.11), Driselase hydrolysis (§2.4) and TFA hydrolysis (§2.3).

The relative molecular mass range was tested for the HbP fractions (§2.9) to study molecular mass differences between the most prevalent non-cellulosic polysaccharides in eC preparations.

2.6.1 Sepharose CL-6B column chromatography

Sepharose CL-6B consists of a bead-formed agarose-based gel filtration resin and 6% crosslinked agarose gel (6B) (manufacturer's data). [^{3}H]SEPs had a K_{av} of 0 and [^{14}C]Glc a K_{av} of 1.

The glass column was filled with Sepharose CL-6B agarose gel up to a length of 45.4 cm with a total volume of 81.1 ml.

The M_r (Equation 2) was calculated from the K_{av} values using the following formula taken from Steele *et al.* (2001).

Equation 2: Linear relationship between K_{av} and logM_r (Steele *et al.* 2001).

$$K_{av} = -0.369(logM_r) + 2.238$$

Steele *et al.* calibrated a Sepharose CL-6B column using carbohydrates of known molecular mass between 0.342–40,000 Da and found a linear relationship between K_{av} and logM_r for a range of 2.3–1162 kDa (K_{av} 0–1).

2.6.2 Sephacryl S-200 to separate polysaccharides in experimental Curran 'hemicellulose plus pectin' fractions

A second column was chosen to study the polysaccharides in the eC HbP fractions as the fractionation range of the CL-6B column was not narrow enough to determine significant differences between the eC preparations. The matrix of Sephacryl resins is a cross-linked copolymer of allyl dextran and N,N'-methylene bisacrylamide. It is suitable for dextrans of 1–80 kDa. (manufacture's data). The radioactive markers [^{3}H]SEPs and [^{14}C]Glc have K_{av} values of 0.08 and 1 respectively.

The glass column was filled with the resin up to a length of 66 cm with a total volume of 116.5 ml.

The relative molecular mass (Equation 3) was calculated from the K_{av} values using the fractionation range of the Sephacryl S-200 column for dextrans (log(1000)=K_{av} 0; log(80,000)= K_{av} 1). Assuming a linear relationship between K_{av} and logM_r resulted in the following formula.

Equation 3: Linear relationship between K_{av} and logM_r for the Sephacryl S-200 column.

$$K_{av} = -0.526(logM_r) + 2.576$$

2.7 Paper chromatography for separation of xylobiose and mannose

This method was used to estimate the quantities of xylobiose and mannose in Driselase digested size-fractionated samples (§2.4 and §2.6.2) (these two compounds were indistinguishable on TLC (§2.5)). For this purpose, 500–600 µl of three pooled column chromatography (§2.6) eluted fractions were dried with the SpeedVac and redissolved in 10 µl Driselase in buffer. The mixes were digested for three days at 37°C in a shaking incubator and acidified to stop the enzyme digestion. The acidified digested samples were applied to Whatman paper (No. 20) (57 cm in length and up to 45 cm in width) and a marker gradient of Man and Xyl_2 was applied onto the same paper. The dry chromatograms were run in BAW (12:3:5 (v/v/v)) for 18 h, dried o/n, followed by EPyW (8:2:1 (v/v/v)) for 5-5 ½ days (separates Man and Xyl_2 well from other components). The silver nitrate stain (§2.7.1) proved to be more sensitive towards the low concentrations of Xyl_2 and Man than the Wilsons dip (Fry 2000) and was therefore the chosen method for staining. With the help of a light table and by referring to the sugar gradient the amounts of Xyl_2 and Man were estimated to determine the ratio in the Man/Xyl_2 spot previously quantified from TLC plates. The paper chromatograms were not suitable for quantification by Photoshop as the background was too inconsistent.

2.7.1 Silver nitrate staining to detect all sugars and sugar-like molecules on paper

Paper chromatography (§2.7) was used to separate the components in eC HbP Driselase-digested and size-fractionated. By applying a gradient of known

compounds and concentrations the quantity of each separated component could be estimated.

Dried paper chromatograms were dipped through solutions A-C with drying periods of 15 min between each dip. Solution A (5 mM $AgNO_3$ in acetone, with minimal H_2O added to redissolve precipitated $AgNO_3$) was used once and the excess added back into the bottle (light sensitive stain, so only a dim light was used during the entire staining procedure). Dipping through solution B (0.125 mM NaOH in 96% (v/v) EtOH) was done three times to increase the staining of low amounts of compounds. The final dip through solution C (10% $Na_2S_2O_3$ in H_2O) made the paper very fragile and was therefore done with great care before transferring the wet paper directly into a running water bath for at least 2 h. The washed chromatograms were dried on a flat clean surface. Silver nitrate-stained papers can be kept for a long time without decolourizing.

2.8 Total (residual) carbohydrate determination

2.8.1 The anthrone assay for total hexoses

For determination of total (residual) carbohydrate in each sample, the anthrone assay is suitable. It yields a coloured product from free and polymer-bound (soluble and insoluble) hexoses.

Dry samples and controls (e.g. paper) were dissolved at 0.2% dry weight in H_2SO_4/ water (2:1, (v/v)) at RT for 1 h on a roller. The solutions were then diluted with 4 volumes of water, giving a final H_2SO_4 concentration of 13.3% (v/v), ready to use for the assay. Samples that were already aqueous solutions were suitably diluted in water. Anthrone reagent (0.2% dry weight in concentrated H_2SO_4) was freshly prepared, kept in the dark and used before a colour change occurred, usually within three days. Sample supernatant (50 µl) was transferred into a 96-well microtitre plate (PCR wells) or a flat-bottom well plate (resistant to 100°C) and each sample mixed with 100 µl anthrone reagent (the mixture got warm and needed to be mixed thoroughly). Before incubation the plate was closed tightly with sticky aluminium foil. The oven was used to incubate the samples for 5 min at 100°C. After cooling, 120 µl was transferred into a flat-bottom 96-well plate and the absorption at 595 nm was read using a microtitre plate reader (the measurement had to be done within 30 min after the reaction was stopped as the colour changes over time).

A Glc-gradient (0–1 mg/ ml) was assayed in duplicate or triplicate to generate a standard curve.

2.8.2 Saeman hydrolysis for total carbohydrates

Just like the anthrone method, the Saeman method was modified from Fry (2000) but it was established by Saeman (1945). It yields the total hydrolysis of cellulosic and non-cellulosic plant cell wall carbohydrates into monomers which can then be analysed by TLC (§2.5). α-Cellulose and Ha fractions (§2.9) from preparations A–J were used in this method. Freeze-dried eC fractions and controls (Whatman paper No.1) were weighed into Sarstedt tubes (4 mg ± 0.2 mg dry weight) and 80 µl of 72% (w/w) H_2SO_4 was added for shaking at room temperature for 1–2 h until all solids dissolved completely (visibly). To the slightly brown solutions 1680 µl de-ionised water was added in the fume hood (this diluted H_2SO_4 to 3.2 % (w/w)). The samples were mixed well and incubated at 120°C for 1 h. The hot tubes were cooled on ice and 4 µl 1% (w/v) bromophenol blue (pH indicator) were mixed with each sample. Next, ~6.5 ml of ~0.18 M $Ba(OH)_2$ (prepared in de-ionised water with excess (undissolved) $BaCO_3$) were added gradually in small doses with thorough mixing in between the additions. This changed the pH and a colour change from yellow to blue was observed; addition of $Ba(OH)_2$ was stopped just before the samples turned blue. If too much $Ba(OH)_2$ was added (colour changed to blue) a few µl of 72% H_2SO_4 were added to return to yellow. All samples were rotated on the wheel overnight. The next day, 160–320 mg of $BaCO_3$ were added to each sample and thoroughly mixed to complete neutralization (solutions turned light blue). Again, samples were rotated for 7–10 h before they were centrifuged at 3000 g for 15 min (to precipitate the solids $BaSO_4$ and $BaCO_3$). The supernatants were stored overnight at -20°C and thawed before a second centrifugation (3000 g for 15 min) to remove all traces of solids. The still blue supernatants (~ 8 ml) were acidified with 5–20 µl of glacial acetic acid until a colour change to yellow was observed. All samples were stored at -80°C and freeze-dried (blue freeze-dried material). For analysis via TLC, pellets were dissolved in 150 µl de-ionised water (intense violet solutions) (25–28 µg initial dry weight/ µl). A portion of the sample (50–70 µg initial dry weight) was applied to TLC plates besides dilutions of 2–2.8 µg per initial dry weight. TLC plates were run in EPyAW (6:3:1:1) for 2 × 2.5 h and stained with thymol. The hydrolysed products on the TLC plates were quantified by Photoshop (§2.5.2).

2.9 Polysaccharide extraction with sodium hydroxide

Hemicelluloses and pectins can be extracted by strong alkali from a cell wall sample. NaOH breaks ester-bonds and might partially act as a chaotropic agent bringing hemicelluloses and pectins into solution. Upon acidification, a sub-group of hemicelluloses (hemicellulose a (Ha)) precipitate while hemicelluloses b plus pectins (HbP) stay soluble (Fry 2000).

AIR, washed preparations and Ha fractions of samples H and J were treated with 6 M NaOH (Edelmann & Fry 1992) (containing 1% (w/v) $NaBH_4$, a reducing agent to inhibit degradation of the polysaccharides) for 16-18 h in a shaking incubator at 37°C. After incubation the samples were centrifuged (10–30 min, 5000 g) and the supernatant (Ha and HbP) separated from the residue (α-cellulose). The supernatant was centrifuged again for 20 min at 5000 g to sediment any possible solids before acidification with 0.5 vol. of 100% acetic acid. For complete precipitation of Ha, the samples were left standing overnight at RT and centrifuged again to watch for further precipitation. Ha was rinsed in plenty of water and freeze dried.

The acidified supernatant contained HbP and was dialysed against running tap water for 5 days or against de-ionised water (5 vol. of the sample volume) overnight and then for 4 days against running tap water. Possible precipitates were added to Ha and the HbP fraction was also freeze-dried.

The residue after extraction of hemicelluloses and pectins was washed with water (three times with 50 ml) and finally with 40 ml of 1% (v/v) acetic acid. The water washes were pooled (“washings”) and acidified (pH ≤7) before dialysis. Both washes and the α-cellulose residue were freeze dried (adapted from Fry (2000) and O’Rourke *et al.* (2015)).

2.9.1 Quantification of carbohydrate losses during NaOH extraction

The extraction of Ha, HbP and α-cellulose from cell wall samples led to material loss for some samples. To account for this loss the three washing steps of Ha and α-cellulose were collected and freeze dried (without prior dialysis). The outside dialysis liquid (dialysate), for the first dialysis step in de-ionised water of HbP fractions, was also freeze dried (dialysis was finished in running tap water). These freeze-dried washes and dialysates were tested for total carbohydrate with the anthrone assay (§2.8.1).

2.10 Quantitative analysis of the hydrogen exchange between polysaccharides and tritiated water

A novel methodology for study of the accessible –OH groups on microfibril surfaces in Curran® and other cellulose samples was established in this work. This potentially reveals the extent to which cellulose can bind other industrial ingredients, and further characterises the polysaccharide samples' properties. Tritiated water can naturally exchange H atoms with the –OH groups of polysaccharides, resulting in radioactive polysaccharides. This process can be exploited to quantify accessible –OH groups by measuring the bound radioactivity after removal of the water.

Experiments were conducted using radioactive H (tritium, ^{3}H) in water ($^{3}H_2O$).

The methodology was subjected to a lot of changes before the final method (explained in the following steps) was established:

1. Approximately 10 mg dry weight per sample (except for xyloglucan where only 1–2 mg dry weight was used) were dispensed into flat-bottom glass scintillation vials (three samples per experiment and one water control with 0.65 µl H_2O).
2. To all four vials exactly 20 µl $^{3}H_2O$ (with 0.5% (w/v) chlorobutanol (volatile antimicrobial agent) was added.
3. Vials were caped tightly for incubation at RT on a shaker for 0.5 h. Next, the vials were opened and quickly transferred into a prepared glass desiccator (Figure 6). An empty glass vial was added as a background control. For some experiments the desiccator was connected via a $^{3}H_2O$ trap to the pump (to prevent $^{3}H_2O$ contamination of the pump).

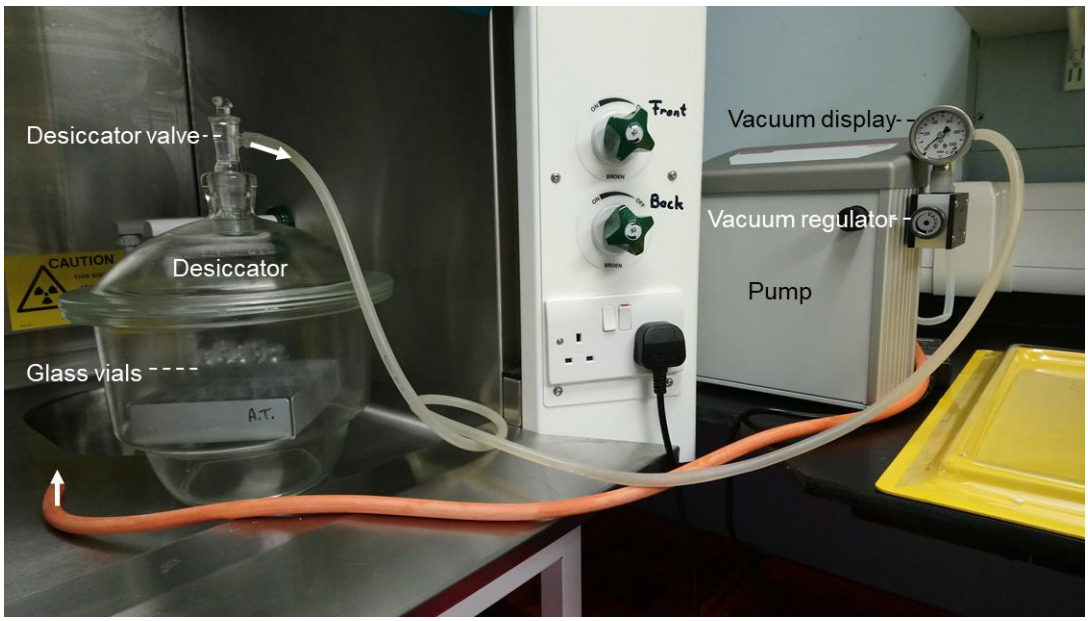

Figure 6: Experimental setup without a ^3H_2O trap to dry tritiated samples.
A metal tray with open glass vials (four tritiated samples and one empty vial) was added to the glass desiccator. The lid was slid on quickly (grease facilitated the airtight fit) and the valve (connected to the pump via a clear plastic tube) was opened. The outlet of the pump was connected to an orange plastic tube leading the exhaust into the fume hood. After starting the pump to establish a vacuum in the desiccator the flow could be adjusted with help of the vacuum regulator. A maximum vacuum of <5 mbar was established for 8 h.

4. A pump (Diaphragm pump MPC 095 Z Welch by Gardner Denver (Ilmenau, Germany)) was connected to the desiccator to create a vacuum of <5 mbar to dry the samples for 8 ±0.08 h. A tube attached to the outlet of the pump led the exhaust of ^3H_2O-contaminated air into the fume hood. Samples were dried to completion (checked for visually by looking at the dried ^3H_2O control).
5. After drying, the desiccator valve was closed, the pump switched off, the clear tubing detached from the desiccator valve and the valve opened. Immediately after releasing the vacuum to the desiccator, 500 µl 3 M NaOH was added to the dried samples within 45–60 seconds and they were capped tightly.
6. Samples were left to swell in NaOH with strong agitation (on a shaker) for 14–18 h). Suspensions were acidified by addition of 500 µl 35% HOAc (final pH between 5 and 7). They were then mixed with 10x vol. of ‘OptiPhase Hisafe 3’ scintillation fluid (Perkin Elmer, Waltham, USA) and rotated for at least 5 h before being assayed in the scintillation-counter (§2.11).

The first §2.10.1 of the following sub-chapters explains the method used to prepare all carbohydrate samples that were tested. All other sub-chapters (§2.10.2–2.10.5)

will introduce the experiments that were done to establish this new methodology; the chapters refer to the different steps 1–6 that were just introduced.

2.10.1 Sample preparation

eC products were provided by CelluComp in the form of pastes (1.0–3.4% dry weight), grated shavings (16.5–22.8% dry weight) or dried sheets (details see Table 2). Only eC products B', E', F' and V' could be directly used in the experiments. The preparation of the other samples for the following experiments included grinding the product with mortar and pestle in water (containing 0.5% (w/v) chlorobutanol) to achieve a uniform suspension. These suspensions, with a dry weight content of 0.9–2.9% (w/v) (except eC W suspension with a solid content of 7.6% w/v), were easily transferable with a spatula into the sample container.

The following lists the carbohydrate controls that were tested:

- Glc
- Whatman paper No. 1 (GE healthcare (Chicago, IL, US)) (from hereon called paper)
- 'Avicel' cellulose (called Avicel hereafter)
- microcrystalline cellulose (MCC) (90-µm) (Acros Organics, part of Fisher Scientific (Hampton, NH, US))
- 'never-dried cellulose' (hardwood dissolving pulp, provided as a gift for research) (moisture content 27.3 ±1.0% (mean ±SD) confirmed by Ninni Nuorti)
    - 'never-dried cellulose' dried at 180°C in the oven for 27 h (called 'dried cellulose' hereafter)
- Tamarind xyloglucan (provided as a gift to the lab)
- SBP A (powder) and SBP G slurry (provided directly from CelluComp Ltd.)

From Glc, Avicel and MCC a solution and two suspensions of 10% dry weight in water (with 0.5% (w/v) chlorobutanol) were prepared respectively. Xyloglucan powder was wetted with a few drops of EtOH before addition of water (with 0.5% (w/v) chlorobutanol), the mixture was then stirred constantly and boiled for 30 min to achieve a uniform 1% dry weight solution. No suspension or solution was prepared from paper, SBP A powder, 'never-dried cellulose' and 'dried cellulose'. They were directly weighed into vials and mixed with 0.65 ml water (including 0.5% (w/v) chlorobutanol) (solid content in the experiments 1.1–3.2%).

2.10.2 Containers and materials (refer to step 1)

The following lists the containers and materials tested and used for drying of the different samples (they are listed in order of replacement):

- 1.5-ml plastic tubes (used inside the SpeedVac)
- Whatman glass fibre paper of grade GF/A–GF/C (Maidstone, UK) pinned (with metal pins) onto an aluminium covered polystyrene disk.
- Plastic scintillation vials
- Glass scintillation vials fitted with plastic caps with cork and aluminium lining.
- Wheaton liquid scintillation vials (glass) with polypropylene caps (lined with polyethylene foam) from Sigma (St. Louis (MO), US).

2.10.2.1 *Desiccants*

Four different desiccants were added individually to the desiccator to improve the efficiency of drying. They were eventually all excluded from the desiccator.

- Molecular sieve rods, ~1.6 mm (Merck, Darmstadt, Germany)
- Magnesium perchlorate ($Mg(ClO_4)_2$, 223.2 g/mol) anhydrous (Alfa Aesar (Haverhill, (MA) US): The minimal amount of magnesium perchlorate to react with 1 g H_2O is 6.2 g $Mg(ClO_4)_2$; to take up 0.33 g H_2O, 2.05 g $Mg(ClO_4)_2$ are needed. In the experiments ten times more desiccant was used, so 20.5 g was added in a glass vial.
- Calcium oxide (CaO, 56.08 g/mol) (Alfa Aesar (Haverhill, (MA) US): 3.12 g CaO/ g H_2O, so 1.03 g CaO are minimally needed for 0.33 g H_2O, thus ten times more led to the use of 10.3 g CaO.
- Phosphorus pentoxide (P_4O_{10}, 283.9 g/mol) (Sigma Aldrich (St. Louis, (MO) US): 2.63 g H_3PO_4/ g H_2O, to take up 0.33 g H_2O, 0.87 g P_4O_{10} are necessary, so 8.7 g phosphorus pentoxide was added in a glass vial.

In experiments conducted with a ^3H_2O trap, a glass vessel filled with an excess amount of silica rods was placed between the pump and desiccator.

2.10.1 The solid concentrations added to the desiccator changed (refers to step 1)

The volume of ^3H_2O (and H_2O added to “cold” controls) as well as the amounts of solids added to the desiccator at a time varied for the pre-experiments conducted. The amount of water that was added to the paper controls was increased from 100 µl up to 650 µl (in the final established method). This was done to ensure that the ratio

of water to solids was similar in all samples tested. Additionally, the number of samples was varied, which also influenced the total amount of solids and the volume of water present in the drying device.

The final experiments were done with mostly equal amounts of solids and water volume: The water content in the desiccator connected to a ^3H_2O trap was 2.40 g ±0.093 g (errors present SEM); without the trap 2.29 g ±0.082 g. Experiments done with a ^3H_2O trap used 37.9 mg ±4.1 mg solids and without the trap 35.2 mg ±2.1 mg. Thus, on average 11.7–12.7 mg solids per sample were present.

2.10.2 The amount of radioactivity added to the desiccator (refer to step 2)

About 20 kBq ^3H_2O were added to each sample in the pre-experiments before the final methodology was established. In the experiments dried with a ^3H_2O trap, 16.0 kBq ^3H_2O was added to each sample. Samples in experiments dried without a ^3H_2O trap were incubated with 14.1, 16, 23.8 or 103.8 kBq/ sample; all samples dried at the same time were given equal amounts of ^3H_2O.

2.10.3 Incubation time in ^3H_2O (refer to step 3)

After adding ^3H_2O to samples, several time courses were performed to ensure complete exchange of H between ^3H_2O and samples. For each incubation time course the samples were shaken vigorously on a shaker before drying.

2.10.4 Drying time course (refers to step 4)

To estimate the correct amount of time needed to dry all samples from free water, different time courses were completed on paper, Glc, MCC, water and eC B samples. All samples were placed in the desiccator and vials were then removed after different times. Alternatively, samples were dried for different length of time without interrupting the drying process.

2.10.5 Drying devices (refers to steps 3–5)

A SpeedVac was used to dry the first samples. As this system proved to be inadequate a glass desiccator attached to a vacuum pump was chosen for drying. The Genevac CVP 100 pump (Ipswitch, UK) (20 years old) was not able to continuously maintain a strong vacuum and switched off after a few hours due to overheating. The replacement Diaphragm pump MPC 095 Z from Welch by Gardner (Denver, Ilmenau, Germany) was able to maintain a vacuum of <5 mbar for several hours (at least 48 h); this pump was used for all major experiments and the final experiments testing eC samples and carbohydrate controls.

2.10.5.1 *Grease (refers to step 3)*

To keep an airtight seal between the glass parts of the desiccator two types of grease were tested, commercial Vaseline (Unilever, Rotterdam, Netherlands) and high vacuum grease (Dow Corning®, Midland (MI), US). The high vacuum grease was most effective in keeping an airtight seal and enabling quick opening of the desiccator.

2.11 Liquid scintillation-counting to measure radioactivity quantitatively

Liquid scintillation-counting (LSC) was used to quantify the radioactivity of the markers used for the gel-permeation chromatography (§2.6) and radioactive samples after exchange with tritiated water (§2.10).

From each column chromatography fraction to be tested 0.2–0.5 ml was transferred into a scintillation vial and mixed with 10 vol. of 'OptiPhase Hisafe 3' scintillation fluid (Perkin Elmer, Waltham, USA).

Radioactivity in the scintillation vials (column eluted samples and tritiated samples) was measured with a scintillation counter (LS 5000 CE (Beckman (Brea, (CA) US) using the settings in Table 3. All data was transferred into an excel sheet and analysed.

Table 3: Different programs and their settings for the Scintillation counter.

Program settings	Column chromatography	Tritiated samples
Preset time [min]	8	6
H number	Yes	Yes
Sample repeats	2	2
Data calc	CPM	CPM
Printer	STD	STD
SCR	No	No
Replicates	1	1
Count Blank	No	No
RS232	Off	Off
RCM	Yes	Yes
Multiplier	1.000000	1.000000
Vial size	Maxi	Maxi
Isotope 1	^{3}H	^{3}H
%Error	1.00	1.00
BKG. Sub	0	0
Half life	No	Yes
Isotope 2	^{14}C	
%Error	0.0	
BKG. Sub	0	
Half life	No	

H number: counting efficiency; CPM: counts per minute; SCR: sample channels ratio; RS232: print format; RCM: sample channels ratio; BKG. Sub: background rate

2.12 Viscosity measurements using gravitational force in pipette-type viscometer

Viscosity of four hveC (§2.1) were tested with a simple low-tech method. hveC product V was diluted to 1.3% (w/w) dry weight paste, samples H–J were provided as 1.3% dry weight pastes. A 5-ml Greiner plastic pipette (Kremsmünster, Austria) with a diameter of 0.7 cm (whole tube) was used for all measurements at 21–23°C (RT). The pipette was filled with 5 ml sample, the pipette filler was detached, and the time measured that the sample took to flow from 0 to 1 ml and 2.6 to 3.6 ml respectively (this was repeated thrice). Before each new testing, the pipette was washed thoroughly with de-ionised water. CelluComp Ltd.s' viscosity measurements (with a Brookfield viscometer) were compared to the results.

3 Results

3.1 Changes in the production process of experimental Curran can decrease or increase viscosity of the products

All materials were produced at CelluComp Ltd. (Burntisland). They were grouped into four categories (for further details see Table 2):

- SBP: (A, G, K and L) starting material for the different batches
- Normally produced eC (B–F, M, Q, W and X)
- hveC (H–J and V)
- changed production process eC (N–P, R–U, Y and Z)

Viscosity was one of the main parameters to distinguish the eC products from each other in this work.

SBP was the starting material for all eCs: SBP A was prepared by milling (producing smaller particles) whereas it was washed, cooked and blended to make SBP starting materials G, K and L. Washing and cooking removed soil and protein from the materials. The production process of eC included an H_2O_2 treatment followed by sodium hypochlorite treatment (leading to normally produced eC). Both oxidising chemical reactions were stopped by washing the products in excess water.

eC W and X were produced from SBP powder from a new distributor (like A but not separately studied), they were the lowest viscosity materials among the normally produced eC products directly produced from SBP powder (eC B–F, W and X). This indicates that the new distributor provided a less suitable starting material. Three normally produced eCs (B', E' and F') were prepared from eC B, E and F respectively, after these products had been stored in the fridge for up to 6 months in grated form. This storage led to a decrease in viscosity as only 37–61% of the original viscosity could be recovered (Table 2). No decrease was observed for hveC V' (prepared from eC V paste after two months storage). This could have been due to the shorter storage period, storage as a paste (not grated) or the production into a hveC (instead of normally produced eC).

eC B–F were normally produced from SBP powder A and were of a narrow viscosity range (1520–1770 cP) in contrast to the four hveCs which were of much higher viscosity (4020–8620 cP) and produced from SBP G with an increased concentration of oxidising chemicals.

eC M, N and R were made in one batch from SBP K; the normally produced eC M (5640 cP) was of higher viscosity than eC N (no sodium hypochlorite treatment, 3780 cP) and eC R (overreacted in H_2O_2, 2200 cP). This suggests that overreaction in H_2O_2 led to a greater reduction in viscosity than no sodium hypochlorite treatment (which also led to reduced viscosity). Another eC batch comprised eC O–P and S (from starting material SBP L). Normally produced eC Q in this batch was of lower viscosity (2780 cP) (compared to the first batch eC M) and did not possess the highest viscosity in the batch as was expected. Unexpectedly, the slightly overreacted eC O and the incompletely washed from H_2O_2 eC P, were of higher viscosity than eC Q. This disagreed with the previous observation that normal reaction in H_2O_2 and sodium hypochlorite treatment were leading to increased viscosity. The viscosity of eC S (1710 cP), which was incompletely washed free of H_2O_2 and sodium hypochlorite, was expectedly lower than the normal eC Q product (lowest viscosity in this batch.

Drying led to the biggest observed reduction in viscosity as eC T (116 cP, freeze dried (original viscosity unknown)) and eC Z (148 cP, drum dried (original viscosity of starting material eC X was 1250 cP) both showed the lowest viscosities amongst all eC.

For the production of high viscosity products, these results show that it was beneficial to increase the concentration of oxidising chemicals used (as done for the hveC samples), do both chemical treatments (H_2O_2 and sodium hypochlorite) and wash the products thoroughly from each.

In the lab, preparations from all SBP starting materials and eC products were made (§2.2) and used in most of the following experiments (except for §3.8).

3.2 Material loss during preparation of α-cellulose, hemicellulose b plus pectins, and hemicellulose a

A more detailed analysis of all SBP and eC preparations was achieved by splitting them into three–four different fractions (§2.9). Unexpectantly, after fractionation only part of the starting material was recovered.

From the first set of material (SBP K, L and eC M–S) AIR was prepared and freeze dried. A different preparation procedure was applied to the second set of SBP A, G and eC B–J: they were washed (in 0.5% (w/v) chlorobutanol in water) to remove the

biocide but no other carbohydrates that may contribute to viscosity. All these AIR and washed preparations were subjected to 6 M NaOH and the gained fractions acid hydrolysed (Figure 7).

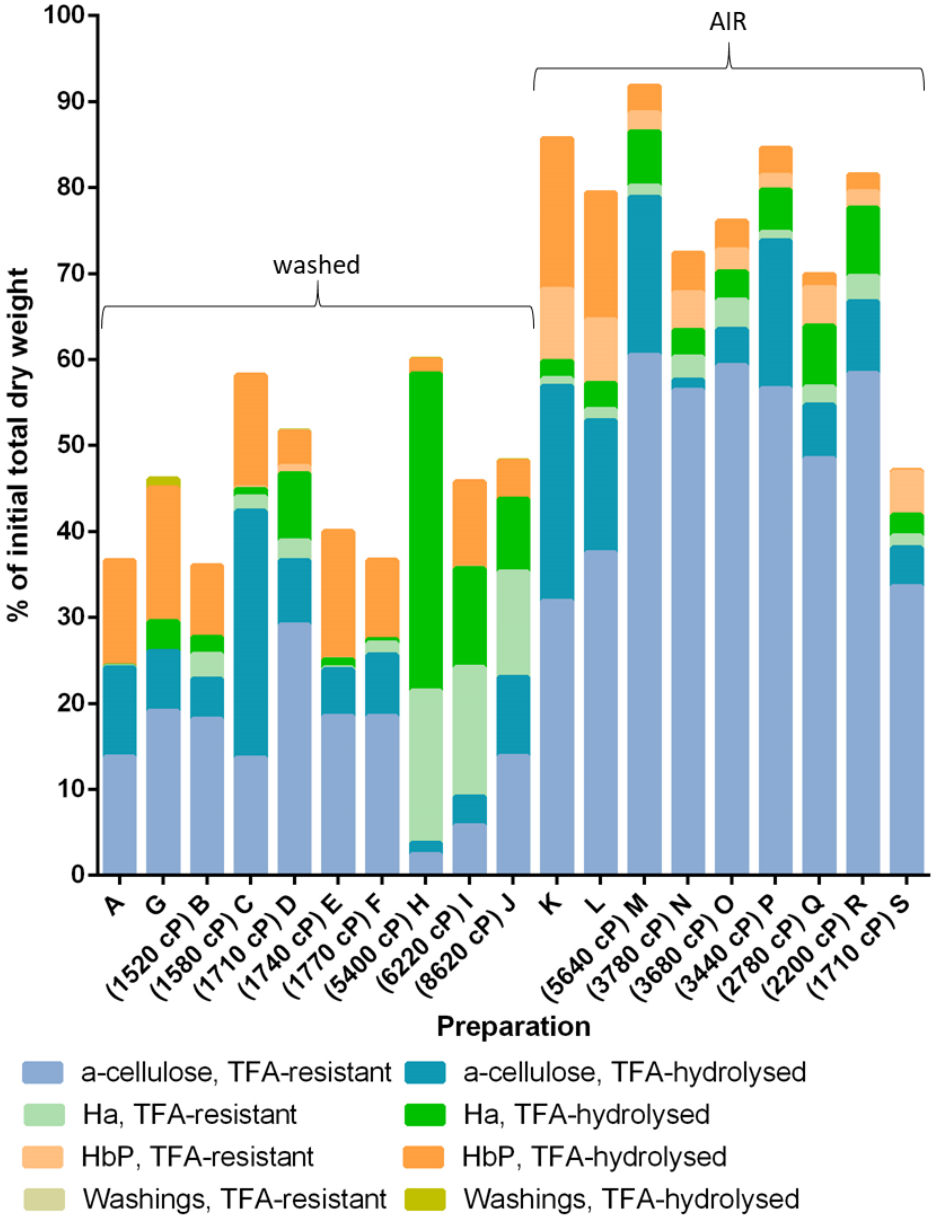

Figure 7: Recovery of hot TFA-soluble and -insoluble material from four fractions of each SBP and experimental Curran preparation.
Preparations A, G, K and L were produced from SBP material, B–J and M–S from eC (viscosity of eC given in cP). α-Cellulose, HbP and Ha were fractionated from all preparations. The α-cellulose residue from washed preparations A–J was additionally washed with water and acetic acid (fractions combined into 'Washings'). All fractions were hydrolysed in hot TFA leading to a soluble portion ('TFA-hydrolysed') and an insoluble one ('TFA-resistant'). The dry weight of the TFA-resistant portion and the difference between fraction and the TFA-resistant portion (leading to the dry weight for the TFA-hydrolysed portion) were recorded.

The proportion of each fraction that was (or became) TFA-soluble and TFA-resistant was presented in Figure 7. Not all starting material from the AIR or washed preparations was recovered after extraction of the fractions. From AIR preparations (K–S) 48–92% of initial total dry weight was recovered and from washed preparations A–J only 37–61% could be recovered. The preparation of AIR seemed to have increased the percentage of polysaccharides that could be fractionated. Alcohol soluble components such as lipids and amino acids (from degraded proteins) were removed by preparation of AIR from SBP material and eC products. TFA-resistant α-cellulose (light blue) presented the biggest difference between the two sets (2–29% of initial total dry weight for A–J but 32%–61% for K–S). Especially from preparation D the α-cellulose fraction solubilized by TFA (dark blue) was bigger than the TFA-resistant residue, in all other preparations α-cellulose was mostly TFA-resistant. In contrast to all other eC, the hveC preparations H–J were composed of a big portion of Ha, and a quantitatively minor (or equal) portion of α-cellulose and HbP (TFA-hydrolysed plus TFA-resistant). HbP fractions (which were soluble in 6 M NaOH) were mostly TFA-hydrolysable: almost no TFA-resistant HbP fraction was found in the washed preparations which contrasts with TFA-hydrolysed and -resistant HbP from AIR preparations. The weight of the washings (TFA-hydrolysed and -resistant) was negligible (0–1% of initial total dry weight). SBP preparations, A, G, K and L, were poor in Ha but richest in HbP fractions.

The big proportion of Ha extracted from hveC preparations was studied further in §3.6, whereas the loss of material was investigated in §3.3.

3.3 Through NaOH extraction carbohydrate material is lost in washes and dialysate

During fractionation of eC and SBP preparations (§2.9) material loss was observed (§3.2). To track the weight loss, I chose five representative preparations (eC B, D, H, I and SBP G) (weight loss between 72% and 39% after fractionation (not the same preparations as shown in Figure 7) (data not shown)) and tested the washes and dialysates (the outside dialysis liquid) for total carbohydrate content (§2.9.1). Indeed, some carbohydrate could be detected in this preliminary experiment, but it only made a quantitatively minor proportion of the total weight loss.

The following washes and dialysates were analysed (from three consecutive 6 M NaOH changes resulting in three sub-fractions of Ha and HbP):

- Washes of Ha (sub-fractions 1+2 and 3) with H_2O (washes termed 'Ha_{1-2}' and 'Ha_3' respectively)
- Washes of α-cellulose
    - With H_2O ('α-cellulose H_2O')
    - Subsequent wash with acetic acid ('α-cellulose HOAc')
- First dialysate of HbP (sub-fractions 1+2 and 3) in de-ionised water ('HbP_{1-2}' and 'HbP_3')

The α-cellulose H_2O wash was turbid (for some preparations) and alkaline (pH 14 due to the high NaOH concentration). The subsequent acetic acid wash resulted in clear solutions with pH 3.0–3.5. After extraction with NaOH, washing and dialysis remove sodium acetate (formed upon acidification of NaOH with acetic acid) from the fractions. This salt was therefore found in high quantities in washes and especially the HbP dialysates (white freeze-dried powder).

For pre-testing, an aqueous solution of washes and dialysate from SBP G was subjected to TLC (250 µg freeze-dried material, result not shown) but no carbohydrates (coloured spots on TLC) could be detected after staining with thymol.

To quantify any carbohydrates in these washes and dialysates I therefore tested with the anthrone carbohydrate assay (§2.8.1) (Figure 8). As Glc was the main component found in TFA-hydrolysed Ha and α-cellulose fractions (Figure 10 and Figure 12), a Glc gradient in sodium acetate (0.15 g/ ml) was used to quantify Glc equivalents. This concentration was chosen because higher salt concentrations resulted in precipitation after the heating step. The Glc gradient in sodium acetate showed the same absorbances as a Glc gradient in de-ionised water. The colour of the solutions did not change due to the presence of salt. Freeze-dried dialysates and washes were dissolved in a known volume of de-ionised water to be used in the test. They contained sodium acetate as well as other components (likely to be carbohydrates washed or solubilized out of the fractions) in unknown ratios; therefore, the exact amounts of salt and carbohydrate used in each test were unknown. Some samples had to be tested repeatedly and diluted further with de-ionised water (e.g. HbP dialysates) as some precipitate was found after heating at 100°C. These samples might have contained higher amounts of sodium acetate which precipitated only upon

heating. The concentration of solids in the freeze-dried material in the anthrone assays ranged from 0.005 to 0.404 g/ ml; the HbP dialysates were among the lowest concentrations.

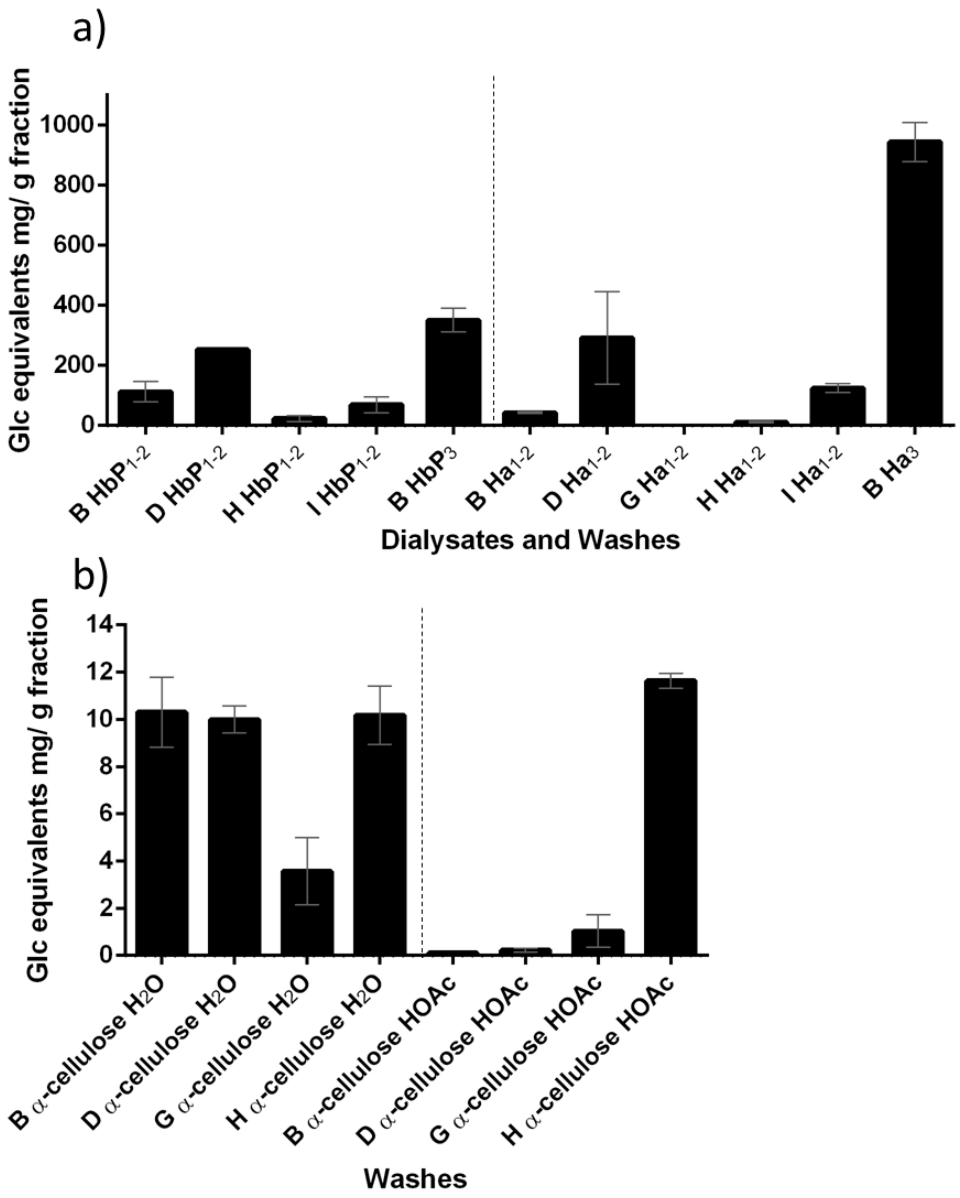

Figure 8: Carbohydrates detected in washes and dialysate of fractions from sugar beet pulp and experimental Curran preparations.
The anthrone assay for total carbohydrate quantification was performed on (a) washes of Ha ($Ha_{1\text{-}2}$ and Ha_3) and the dialysate of HbP fractions ($HbP_{1\text{-}2}$ and HbP_3); (b) washes of α-cellulose (washed in H_2O and dilute HOAc). As the identity of the carbohydrate was unknown, Glc was used as a standard and the data expressed in Glc equivalents. The error bars represent SEM; most samples were tested with N=3 with exceptions: D $HbP_{1\text{-}2}$ (N=1), B α-cellulose HOAc (N=1), D, G and H α-cellulose H_2O (N=2). The assay could not be performed on Hb_3 from D, G and H nor from Ha_3 D, G, H and I as no measurable dry weight of these fractions were obtained; absorbance measured for I Hb_3 dialysate and I α-cellulose H_2O wash were too high and were not repeated.

The anthrone assay estimated between 23 mg Glc equivalents/ g HbP (H HbP_{1-2}) up to 351 mg/g HbP (B HbP_3) in the dialysates. The very high concentration of Glc equivalents in D HbP_{1-2} and B HbP_3 (the only HbP_3 fraction produced and tested) was unexpected. They reveal a carbohydrate loss of up to 35% Glc equivalents from these HbP fractions. The carbohydrates found in the dialysates could have resulted from degradation of polysaccharides in the original products from CelluComp Ltd., in the preparations or by NaOH into low molecular mass carbohydrates (<12,000 Da which can escape the dialysis sac).

Similar results were obtained for Ha washes amongst which B Ha_3 held the highest concentration of Glc equivalents found amongst all tested samples. Carbohydrates in Ha fraction washes could result from insufficient centrifugation of Ha in water or residual HbP (in the acidified NaOH supernatant). It is unlikely that water solubilised carbohydrates in Ha that had not already been solubilised by 6 M NaOH.

Only low concentrations of Glc equivalents were present in α-cellulose washes (0–12 mg Glc equivalents/ g α-cellulose). As explained for Ha fractions, H_2O and HOAc were not expected to solubilise carbohydrates from α-cellulose; therefore, it is more likely that low concentrations of HbP and Ha solubilised by NaOH were found in α-cellulose washes.

To my knowledge, a carbohydrate analysis of salt-rich samples like mine has not yet been attempted. It should be noted that the presented data can only be considered preliminary results: the identity of the measured carbohydrates was unknown (probably a mixture of components) and a Glc standard can therefore not express the exact concentration of carbohydrates present. The identity could be revealed by TFA hydrolysis coupled with TLC, but TLC alone failed to show any carbohydrates (possibly due to salt interference with the TLC run). As stated above, the range of solid concentrations in the assay was large and their salt or carbohydrates ratios were unknown. Much higher salt concentrations (compared to carbohydrate in the test) could lead to carbohydrate concentrations under the detection limit of the assay so the sample dry weight used in the tests needs to be chosen carefully preferably tested in multiple concentrations). Although the absorbances for Glc in sodium acetate were comparable to those in de-ionised water, higher concentrations of salt might have a

different effect on absorbance. This may well be tested by measuring the absorbance of Glc in different concentrations of sodium acetate.

The data presented are very surprising as some results indicate a very high proportion of carbohydrate that was lost in the washes and dialysate (e.g. 94% of all B Ha_3 carbohydrates were lost in the wash). This would explain a very low yield of those fractions (Figure 7). These results cannot directly be correlated to the losses observed during the extraction of the fractions where the weight of the fractions was measured (not the concentration of Glc). But if the Glc equivalents recovered in the washes and dialysate could directly be added to the total weight of the fractions they would only account for 0.04–4.51% of the preparations initial total dry weight. The weight loss from these five preparations would hence still range from 35% to 71% (data not presented).

3.4 TFA destroys monosaccharides

The following experiment (Table 4) showed that hot TFA was partially able to destroy monosaccharides (commonly found in eC and SBP preparations).

Table 4: Monosaccharides destroyed by TFA.
Eight common cell wall monosaccharides were treated with TFA under conditions used for hydrolysis of polysaccharides (§2.3); supernatants were applied to TLC plates, run in the solvent EPyAW (6:3:1:1) for 2 × 2.5 h and stained with thymol. Components were quantified from TLC plates by Photoshop. The percentage of the monosaccharide remaining (in relation to the non-hydrolysed monosaccharide) is given (N=3).

	GalA	**GlcA**	**Gal**	**Glc**	**Man**	**Ara**	**Xyl**	**Rha**
remaining %	82.5	45.5	94.8	94.3	93.5	88.7	86.5	78.6
SEM %	2.5	0.9	1.8	1.4	1.8	1.4	1.7	3.6

Over 50% GlcA monomer was destroyed by TFA but only a quantitatively minor portion of all other monosaccharides (82.5–94.8% remained). It is known, that GlcA can be lactonized by acid (Zhang *et al.* 2007) and as GlcA was not identified from any SBP or eC preparations (§3.5 and §3.7, neither after TFA or Driselase digestion), it can be considered negligible for quantification of preparations in this work.

3.5 Experimental Currans are enriched in cellulose

This chapter shows that all eC preparations were enriched in cellulose (around 90% of dry weight) and contained less pectic components than the SBP preparations.

eC is a biotechnological product from the cell walls of sugar beet and was therefore expected to consist of polysaccharides and components from the plant cell wall. These were studied in §3.5.1 and §3.5.2 by acid hydrolysis (§2.3) and total carbohydrate assays (§2.8). Two sets of preparations were studied: the first set comprised eC preparations M–S (from starting materials SBP K and L) produced in different production processes (§2.1; §3.5.1). The second set comprised preparations of normally produced eC B–F (from SBP A) and hveC H–J (from SBP G) (§3.5.2).

3.5.1 Changes to the production process of normally produced experimental Curran result in composition variations

This chapter focuses on the carbohydrate composition of the first set of eC preparations which varied in viscosity and production processes. It was shown that the composition of SBP, rich in cellulose and pectic components, is changed in eC products to rich in cellulose, poor in pectic components but enriched in Xyl and non-cellulosic Glc (typically hemicellulosic origin). Furthermore, with decreasing viscosity of eC the components Ara, Gal, GalA and Rha (typical pectic components) in preparations were decreasing too.

The following list of SBP and eC products only mentions the changes to the production process for normally produced eC and does not inform about the whole production process (§2.1). It lists the eC in order of decreasing viscosity:

- SBP K (starting material for eC M, N and R)
- SBP L (starting material for eC O, P, Q and S)
- eC M (5640 cP)
- eC N (no sodium hypochlorite treatment, 3780 cP)
- eC O (slightly overreacted in H_2O_2, 3680 cP)
- eC P (H_2O_2 incompletely washed out, 3440 cP)
- eC Q (2780 cP)
- eC R (overreacted in H_2O_2, 2200 cP)
- eC S (H_2O_2 incompletely washed out, sodium hypochlorite incompletely washed out, 1710 cP)

All viscosities quoted above are for blended suspensions at 1% dry weight. From TFA hydrolysis (§2.3) of the AIR preparation (§2.2) it became clear that starting material SBP showed very high quantities of Ara, Gal, Rha and GalA whereas these components were greatly reduced in eC preparations (Figure 9).

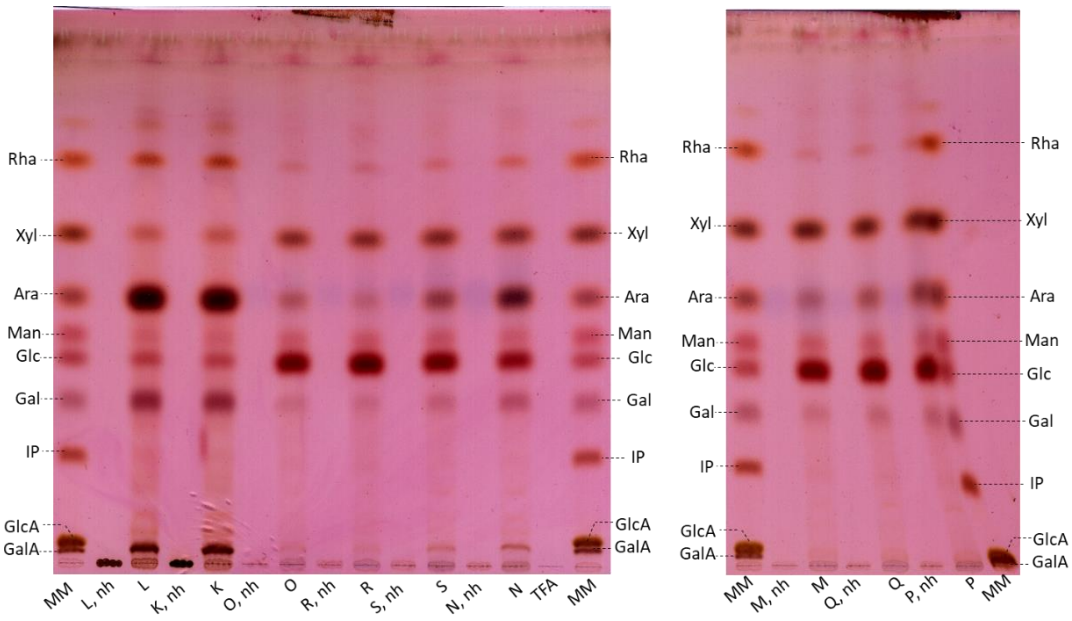

Figure 9: Monomeric composition of SBP (K and L) and experimental Curran (M–S) AIR. AIR preparations of SBP (K and L) and eC M–S were hydrolysed in 2 M TFA for 1 h at 120°C. Non-hydrolysed (nh) samples were taken before heating. All supernatants were applied to TLC plates, run in the solvent EPyAW (6:3:1:1) for 2 × 2.5 h and stained with thymol. MM: marker mixture. Preparations from eC Q and P did not run in a straight line and were therefore reapplied onto another TLC plate (Figure 10).

Acid hydrolysis of AIR combined with TLC (Figure 9) allowed for a quick analysis of the monomers present in matrix polysaccharides. Non-hydrolysed (nh) samples were free from reducing sugars (verifying the successful preparation of AIR from all SBPs and eC materials). The two SBP preparations L and K upon TFA hydrolysis showed to be rich in Ara, GalA, Gal, Rha, besides only little Glc and Xyl (compared to the eC preparations). As the eC products were produced in different processes (see list above) I paid closer attention to which changes may have led to which altered composition.

Quantities of Man did not seem to be influenced by changes in the production processes, as it was only present in minor quantities in all preparations. In the normally produced eC M and Q (Figure 9 and Figure 10) GalA was missing and the amounts of Gal, Ara and Rha were greatly reduced whereas M and Q were enriched in Glc and Xyl (compared to the starting materials K and L). Overreaction in H_2O_2 (eC O and R) did not cause a detectable difference in composition (compared to normally produced eC M and Q). eC P was treated normally with H_2O_2 but then incompletely washed before sodium hypochlorite treatment, eC S was additionally incompletely washed after sodium hypochlorite treatment. Both preparations contained more Ara than normally produced eC M and Q; eC S additionally contained little amounts of

GalA. The latter observation pointing towards further removal of GalA from SBP by sodium hypochlorite treatment. The non-bleached eC N preparation was richest in Ara, GalA, Gal and Rha among all eC. This confirmed that sodium hypochlorite was responsible for further removal of GalA as well as Ara, Gal and Rha from SBP during the production process.

For more details about the eC composition Ha, HbP and α-cellulose fractions (§2.9) from all preparations were hydrolysed by TFA (Figure 10–Figure 13).

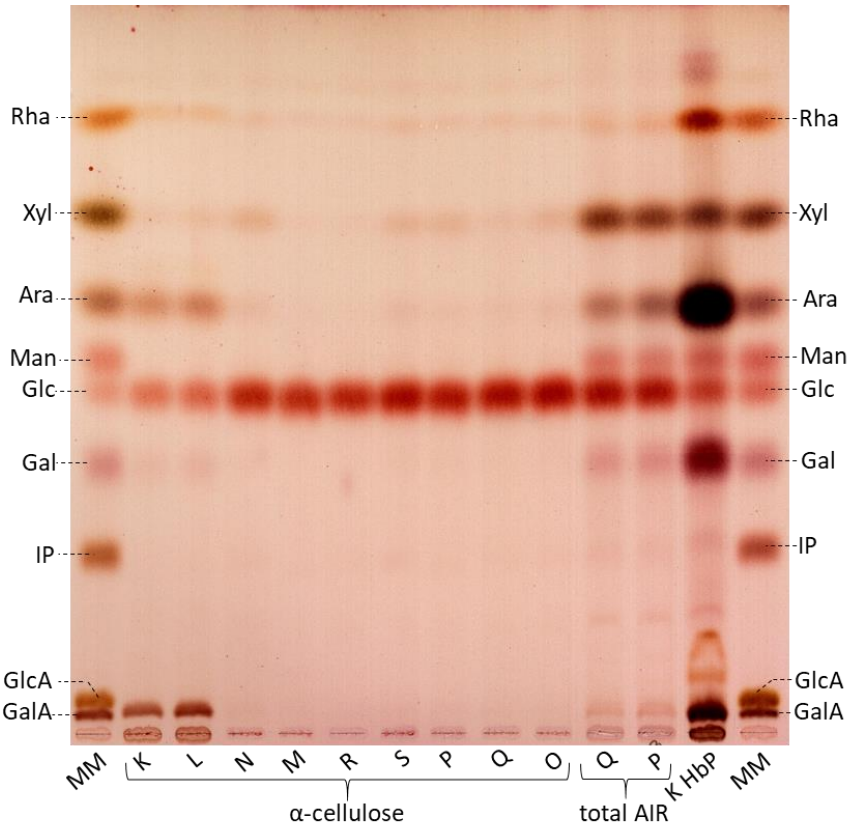

Figure 10: TFA-hydrolysed composition of AIR and fractions from SBP (K and L) and experimental Currans (M–S).
α-cellulose and HbP were prepared from AIR of SBP K–S and subjected to TFA hydrolysis for 1 h at 120°C. Additionally, TFA hydrolysis was applied to total AIR of eC Q and P and the TFA-hydrolysates applied onto the TLC plate. Further details as in Figure 9.

The hydrolysis products of α-cellulose from SBP K and L preparations contained GalA, Glc and Ara beside very little Gal, Xyl and Rha. All eC α-cellulose fractions were almost exclusively composed of Glc with traces of Xyl. Some of the Glc may have resulted from the partial hydrolysis of cellulose (confirmed by personal communication from Martina Pičmanová). In the non-bleached eC N preparation Ara, Xyl and Rha were found. As cellulose is mostly non-TFA-hydrolysable (Figure 7), it was expected that most of it would remain insoluble in TFA. Indeed, most of the α-cellulose was found in the TFA-residue (Figure 7).

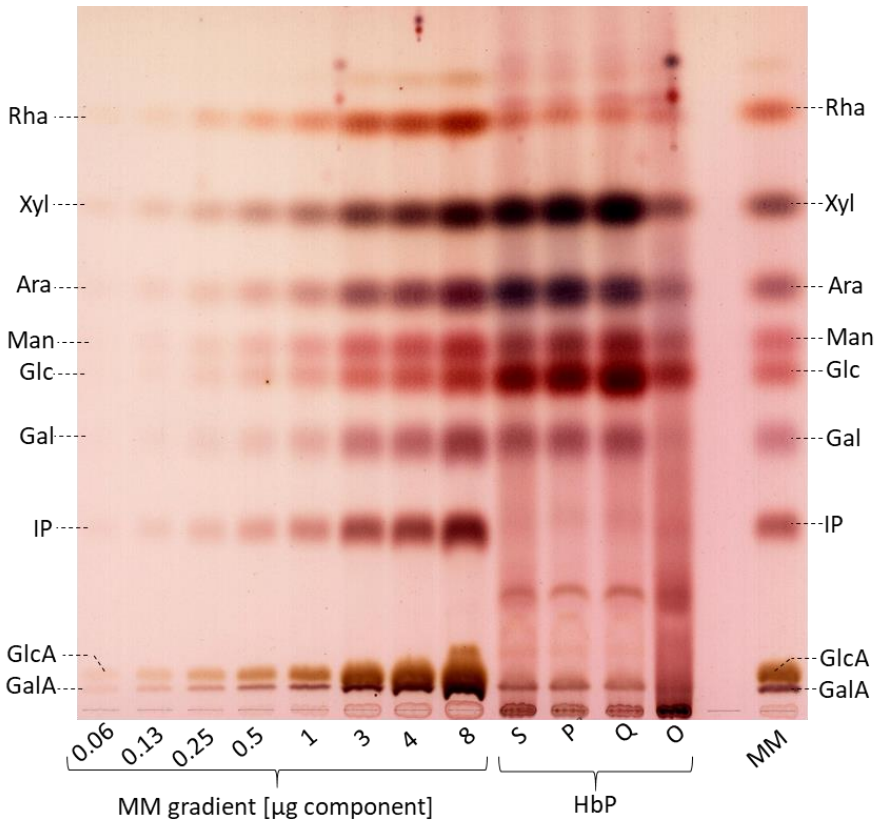

Figure 11: Composition of hemicellulose b plus pectins from experimental Curran preparations O–Q and S.
HbP was prepared from AIR of eC O–Q and S and TFA hydrolysed for 1 h at 120°C. a marker mixture (MM) was applied as a gradient from 0.06–8 µg per component. Further details as in Figure 9.

The marker mixture gradient was used as a standard for quantification of the samples from TLC plates by Photoshop. TFA hydrolysis products of HbP eC O on the TLC plates (Figure 11 and Figure 13) were streaked, hence new fractions from preparation eC O were hydrolysed and quantified (TLC not shown). All hydrolysis products of HbP fractions (Figure 10–Figure 12) contained components that were present in higher quantities than the highest marker gradient (e.g. Glc and Xyl); for quantification purposes they were therefore diluted 1:10 (Figure 13).

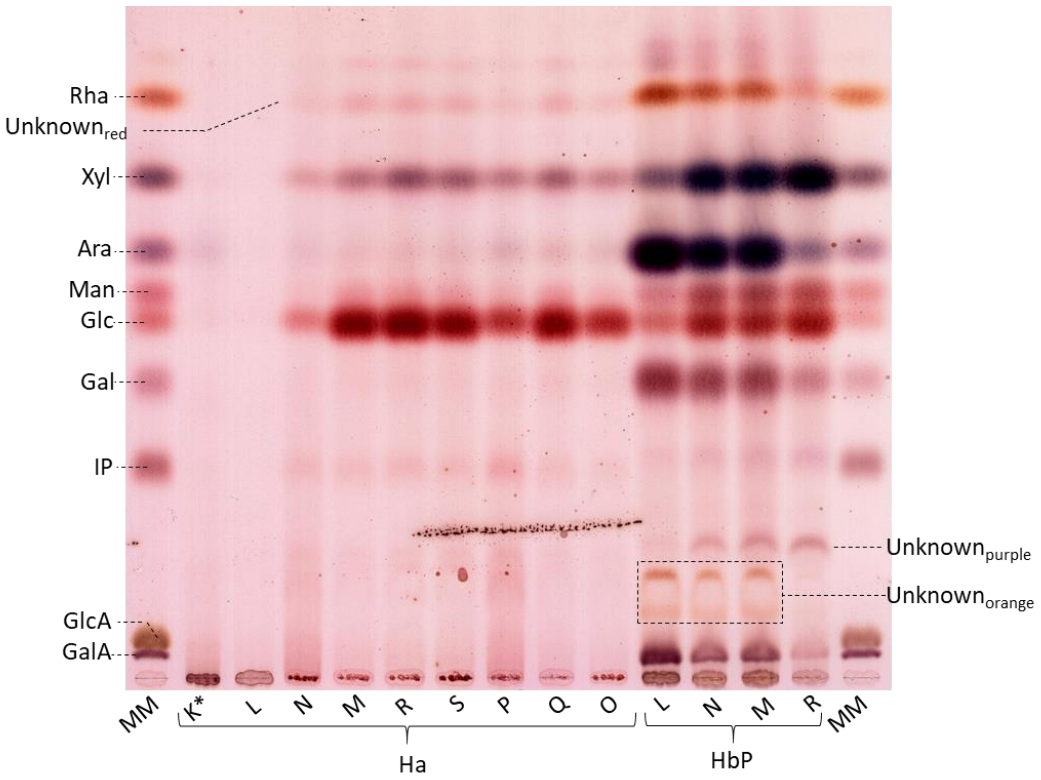

Figure 12: TFA-hydrolysed composition of hemicellulose a and hemicellulose b plus pectins from SBP (K and L) and experimental Curran (M–S) preparations.
Ha and HbP were prepared from AIR and TFA hydrolysed for 1 h at 120°C. *: only ½ the amount compared to the other samples was applied to the TLC plate. Further details as in Figure 9.

All HbP and Ha samples (spread over three TLC plates, Figure 10–Figure 12) showed one or two components with higher R_f than Rha that stained red/brown. These unknown hydrolysis products were not studied in this work. Additionally, two more unknowns, unknown$_{orange}$ and unknown$_{purple}$, were identified in HbP fractions. These were quantified but only made up a quantitatively minor portion of the preparation (Figure 16). HbP of SBP K (Figure 10) and L (Figure 12) contained both unknowns but unknown$_{purple}$ only in minute quantities. In contrast, all eC preparations contained more unknown$_{purple}$ and less unknown$_{orange}$ than SBP HbP, leading to the conclusion that the presence of these components was connected to the process of eC production. Unknonwn$_{purple}$ could be connected to the enrichment of Xyl and Glc in eC preparations whereas unknown$_{orange}$ might relate to the removal of typical pectic components.

A red staining component with an identical R_f to Rha was found on the TLC plate in Ha fractions. It was not possible to separate this from Rha and was therefore quantified together with Rha (named Rhamnose/ unknown$_{red}$) for all fractions (as it

could not be ruled out that it wasn't also part of the Rha spot in HbP or α-cellulose). For SBP K and L the dry weight of the Ha fraction was quantitatively minor (Figure 7) but K showed traces of Ara and Xyl. Ha from SBP L did not show any TFA-hydrolysable components. The major portion of all Ha fractions was not TFA-hydrolysable (most material remained as a residue after TFA hydrolysis). All Ha fractions from eC preparations contained Glc, Xyl, little Ara, Man, Rha/unknown$_{red}$ and another red staining component with the same R_f as the IP marker component. Another component with the same R_f was also found in undiluted HbP hydrolysis products (stained purple). Both components were named unknown$_{red2}$ and unknown$_{purple2}$ respectively and quantified from the second sample set in §3.5.2. Ha of eC N (no sodium hypochlorite treatment during production) was different from the other eC samples as it contained a smear and less of the afore mentioned components. eC preparations M, Q, R and S contained about the same amounts of Glc, Ara, Xyl and the unknown hydrolysis products.

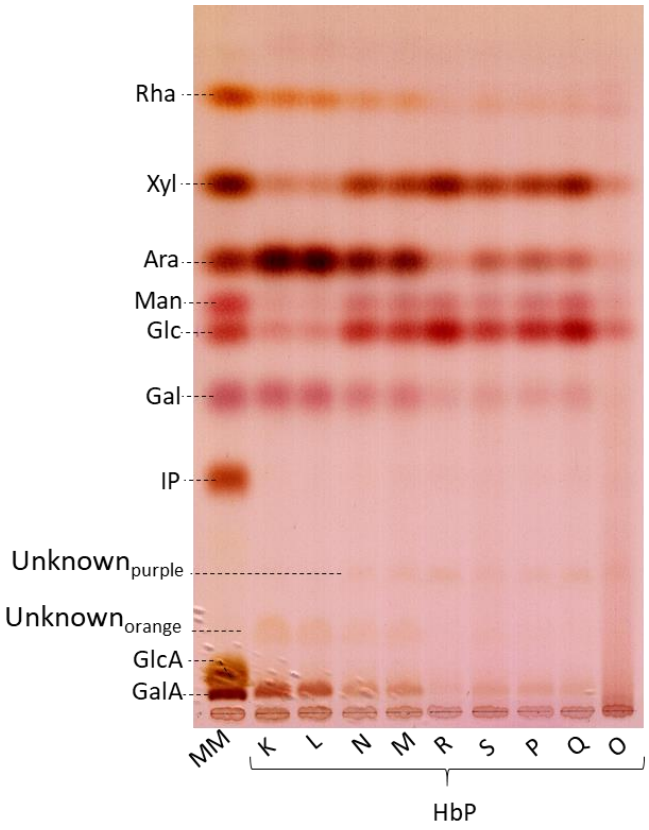

Figure 13: Composition of hemicellulose b plus pectins from SBP (K and L) and experimental Curran (M–S) hydrolysed by TFA.
HbP was prepared from AIR of K–S and TFA hydrolysed for 1 h at 120°C. Hydrolysis products were applied to TLC plates in a 1:10 dilution (for quantification purposes). Further details as in Figure 9.

SBP K and L HbP were richest in Ara; additionally, they also contained more GalA, $unknown_{orange}$, Gal and Rha/$unknown_{red}$ compared to all HbP fractions from eC. Only little Glc, Man and Xyl were hydrolysed from SBP HbP. All eC HbP fractions were enriched in Glc, Man, Xyl and $unknown_{purple}$ while GalA and Rha/$unknown_{red}$ were only minor constituents (confirming that $unknown_{orange}$ may be connected to the presence of GalA, Gal, Ara and Rha). HbP from preparations of eC O–S did not differ much in composition, only eC R and Q were richer in Xyl and Glc but contained less Ara (especially R) (eC R was overreacted in H_2O_2 during the production process). Sodium hypochlorite treatment did not cause a notable difference to the composition of the HbP fraction as the composition of HbP from eC M and N was almost identical, both contained more Ara, Gal, GalA and Rha than eC O–S.

All TFA-resistant residues (Figure 7) (very little from HbP) were analysed by the anthrone assay (§2.8.1) for Glc (commonly from cellulose in plant cell wall samples). For easier visualisation of the TLC results and the anthrone assay the quantified components were presented in Figure 14 and Figure 15.

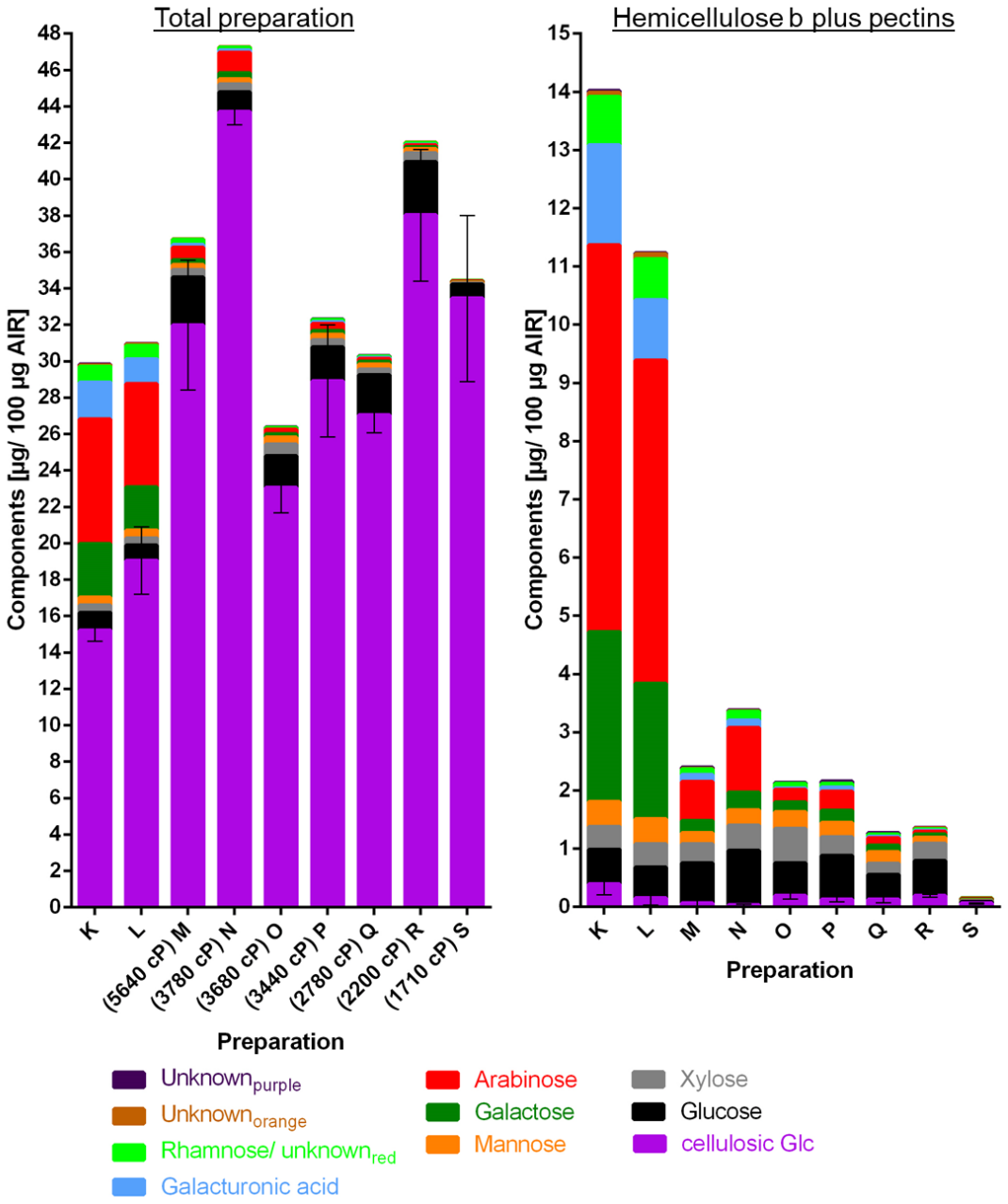

Figure 14: Quantified components in hydrolysed preparations and the hemicellulose plus pectin fraction of SBP (K and L) and experimental Currans (M–S).
The top left graph shows the composition of the total preparation (summary of all quantified components in HbP, Ha and α-cellulose) (viscosity in cP).The TLC plates (Figure 11–Figure 13), with TFA-hydrolysed fractions from preparations of SBP (L and K) and eC M–S, were quantified by Photoshop. Anthrone assays were performed on the TFA-resistant residues to quantify cellulosic Glc; error bars represent SEM, N=3. Nine components were identified, and their quantities are presented per 100µg dry weight initial preparation. eC M–S are in order of decreasing viscosity (5640–1710 cP).

Several observations could be made after analysing the total carbohydrate composition in SBP and eC preparations. Total AIR from SBP (K and L preparations) was composed of ~30 µg/ 100 µg AIR and so ~70% of the total dry
weight was unaccounted for by carbohydrate analysis. Among the eC preparations the unaccountable weight loss ranged from 52 µg (eC R preparation) up to 70 µg (eC O preparation). This phenomenon was examined in §3.2 and §3.3.

Focusing solely on the carbohydrate composition of the total AIR (ignoring the lost weight) I found that SBP samples are composed of about 50% cellulosic Glc per dry weight measured, while the TFA hydrolysable components were mainly Ara, Gal, GalA and Rha (mainly pectic components). When SBP was processed into eC the total AIR carbohydrate composition became enriched in cellulosic Glc besides ~10% of non-cellulosic components (mainly Glc).

Most non-cellulosic components were largely extracted in the HbP fraction (Figure 14). The quantities of Ara, Gal, GalA and Rha greatly reduced in the process of making eC from SBP. HbP from eC preparations was TFA-hydrolysed primarily into Glc, Xyl and Ara with only very little cellulosic Glc in the TFA-resistant residue.

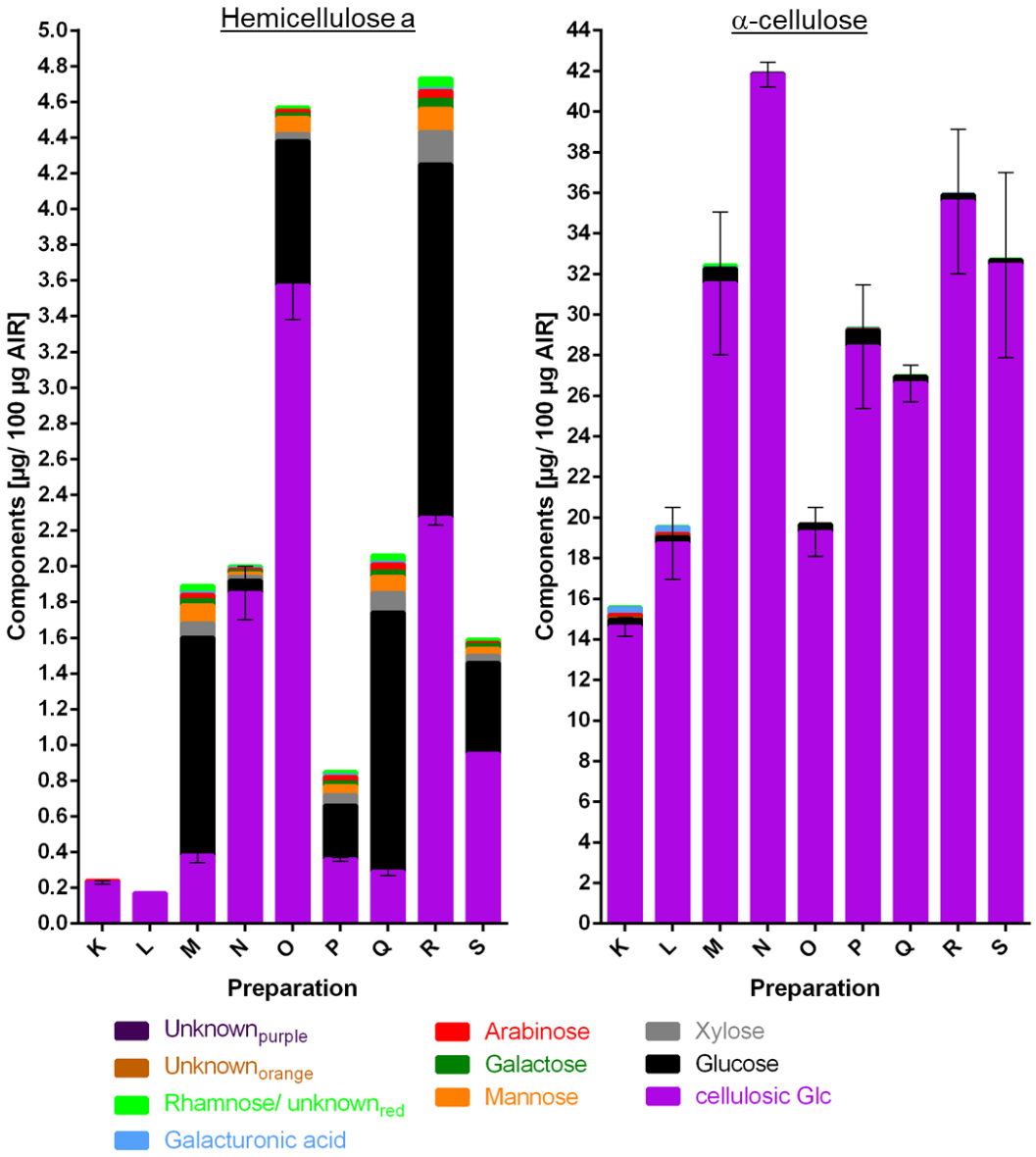

Figure 15: Quantified components in hydrolysed fractions of SBP (K and L) and experimental Currans (M–S).
The two graphs show the composition per 100 µg AIR that were identified from the hemicellulose a and the α-cellulose fractions. For further details see Figure 14.

SBP Ha fractions (Figure 15) were almost exclusively cellulosic Glc. Likewise, most Ha fractions from eC samples were rich in cellulosic Glc (48–93 µg/ 100 µg AIR), besides mostly TFA-hydrolysed Glc (see eC preparations N–P, R and S). Unlike these eC preparations both Ha fractions from normally produced eC M and Q were richest in TFA-hydrolysed Glc (~60%). α-Cellulose fractions from all eC preparations were almost exclusively composed of cellulosic Glc, this made the major portion of the total AIR samples (Figure 14).

The non-cellulosic components from the total preparation were grouped together in Figure 16, to show that some components in the eC preparations decrease with decreasing viscosity of the eC product.

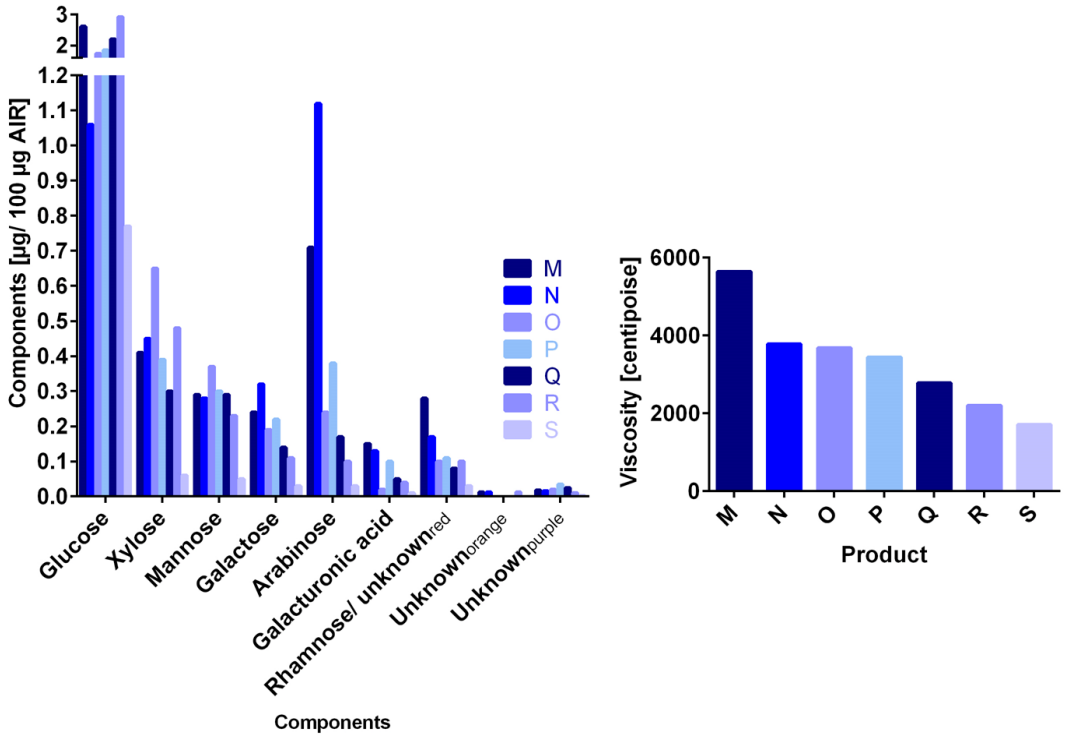

Figure 16: Detailed TFA-hydrolysed carbohydrate composition from experimental Curran preparations in order of decreasing viscosity.
The TFA-hydrolysed components in total AIR from eC M–S preparations were quantified (Figure 14). The graph on the right shows the eC products in order of decreasing viscosity. eC M and Q are coloured the same as they represent technical replicates of the same production process. eC O and R were both overreacted in H_2O_2.

Components such as GalA, Rha/unknown$_{red}$, Gal and Ara showed a decreasing trend with decreasing viscosity (with 1–2 outliers among the preparations). Ara was decreasing at a steeper rate than GalA, Rha/unknonwn$_{red}$ and Gal. Moreover, the rate at which viscosity decreased (the right graph of Figure 16) was steep between eC M and N products (almost 2000 cP difference), but relatively flat between eC N to S. It should be remembered that these eC products were prepared in different production processes and these latter observations may therefore not just be connected to a decrease in viscosity but also to the changed production process.

In summary, AIR from eC M–S was mainly composed of cellulosic Glc from α-cellulose fractions. The major part of all non-cellulosic components was extracted

in the HbP fractions of eC which were rich in Glc and Xyl (especially from eC O–S preparations) and/or Ara and Man (e.g. in eC M–P). SBP was mostly composed of cellulosic Glc and pectic components such as Ara, Gal, GalA and Rha. Among all preparations tested I found unaccountable weight loss from 52–70% AIR dry weight. Various eC preparations showed that decreasing viscosity was correlated with decreasing amounts of GalA, Rha, Gal and Ara. Hence, the removal of these typical pectic components from eC products might have a negative influence on viscosity. Nonetheless, the rate at which the single components were decreasing was not equal to the rate at which viscosity decreased; therefore, there are more factors that influence viscosity than the carbohydrate composition alone.

3.5.2 Increasing the concentration of hydrogen peroxide and sodium hypochlorite in the production process leads to a decrease of non-cellulosic components

This chapter reveals that normally produced eC preparations contain more non-cellulosic components than the hveC preparations suggesting an increase in viscosity with further removal of pectins and hemicelluloses. Additionally, components indicating the presence of xylan and xyloglucan were detected in eC preparations.

Just like the first set of preparations (A–J) also the second set of preparations comprised SBP and eCs (all normally produced). In addition, hveC were part of the eC preparations (for details see Table 2):

- SBP powder A (starting material for B–F)
- SBP G (starting material for H–J)
- eC B, 1520 cP
- eC C, 1580 cP
- eC D, 1710 cP
- eC E, 1740 cP
- eC F, 1770 cP
- hveC H, 5400 cP
- hveC I, 6220 cP
- hveC J, 8620 cP

All viscosities quoted above are for blended suspensions at 1% (dry weight). As in §3.5.1, all preparations were split into α-cellulose, Ha and HbP fractions (§2.9). Additionally, the acetic acid wash of the α-cellulose fraction was tested. All four

fractions (including the wash) and the total preparation were TFA hydrolysed (§2.3) and the hydrolysis products quantified from TLC plates (§2.5). Figure 49–Figure 59 show the TLC plates and are available in the appendix (§6.2). The total components identified in these preparations are summarised in §3.5.2.2.

The anthrone method (§2.8.1) was used to determine the total hexoses in the TFA-resistant residues. As an alternative, the Saeman method was used on the complete α-cellulose and Ha fractions. This resulted in different estimates of total Glc, discussed in §3.5.2.1.

3.5.2.1 *Saeman hydrolysis and anthrone assay result in different estimates of total glucose*

Quantification of the residual insoluble carbohydrates after TFA hydrolysis in Ha and α-cellulose fractions was done by the anthrone assay. This gave the total 'cellulosic' hexoses present in the preparations which were quantified as Glc. In the process of solubilising α-cellulose and Ha fractions in sulfuric acid, coloured solutions (different intensities) were generated (even before the addition of the anthrone reagent) which caused different colorimetric measurements between the samples as they were all based on the same blank value. This was undesirable as it probably impacted the total quantity of Glc estimated for each fraction. To improve these results, the Saeman method, was performed on the total Ha and α-cellulose fractions (§2.8.2). This needed to be done without prior TFA hydrolysis of the fractions as it was shown to result in difficult and incomplete solubilisation of the samples (personal communication from Ninni Nuorti and Martina Pičmanová). Therefore, non-cellulosic components such as Xyl and Ara were detected with the Saeman method besides the total Glc). The dry fractions (fluffy light material) were easily dissolved in the Saeman method.

The Saeman hydrolysis of α-cellulose fractions from all preparations led to the production of Glc as the main component (TLC plates, Figure 44–Figure 47). The preparations from SBP A and G additionally contained Xyl, Ara and some unknown components. These unknowns were:

- two components that stained red (after thymol staining) and showed a similar R_f to cellobiose (C_2) and cellotriose (C_3) respectively.
- One component that stained identically to GalA (but did not show identical R_f)

- The component unknonwn$_{red}$, (colour red and same R_f as Rha; previously observed after TFA hydrolysis).

All hydrolysis products from α-cellulose fractions and paper contained Xyl and the three red-staining unknowns in addition to mainly Glc. Dilutions of these samples showed only Glc, except for α-cellulose from SBP A and G which additionally contained GalA (not detected in the un-diluted samples but showing the same colour as the unknown component staining like GalA). Due to unknown reasons, GalA seems to have shown a different R_f in the concentrated samples but was identified as GalA after dilution of the samples. Glc spots were quantified by Photoshop (quantities of other components were considered negligible) (Figure 17).

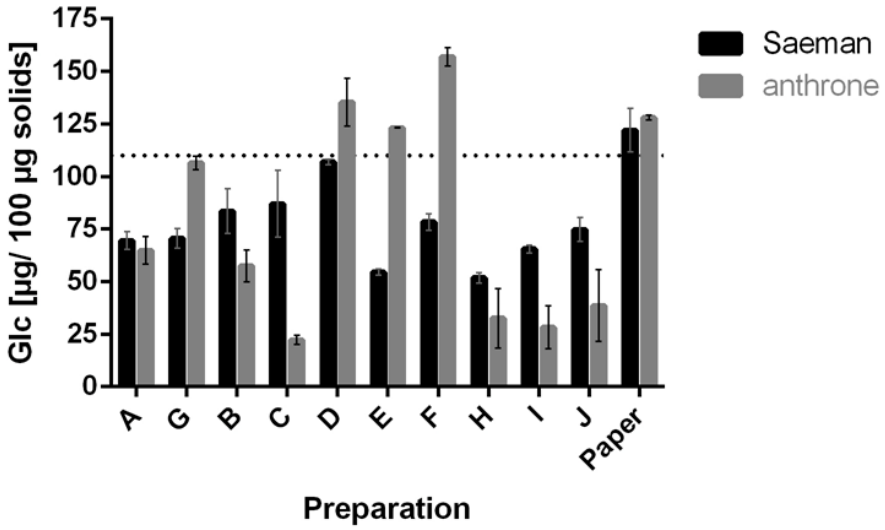

Figure 17: Glucose released by the anthrone and the Saeman methods from α-cellulose fractions and paper.
α-Cellulose fractions from preparations A–J were assayed by the anthrone (§2.8.1) and the Saeman method (§2.8.2); paper served as a control. The anthrone assay was performed on TFA-resistant α-cellulose fractions. Saeman-hydrolysis products of α-cellulose fractions were diluted 1:25 and applied to TLC plates which were quantified by Photoshop for Glc (some dilutions are shown in Figure 46 and Figure 47). A dotted line represents the expected value (110µg Glc) for the hydrolysis of 100 µg cellulose. Error bars represent SEM with N=3.

From the hydrolysis of 100 µg cellulose 110 µg Glc were expected; this is due to the change in molecular mass from a Glc-residue in cellulose to monomeric Glc. From 100 µg paper 122 µg (Saeman) and 128 µg Glc (anthrone) was produced. Glc quantified by the anthrone assay was significantly ($P<0.0001$) higher than the expected concentration, meaning the anthrone assay overestimated Glc from paper and possibly also from α-cellulose fractions. Glc released from paper by Saeman

hydrolysis was not significantly different (P=0.3125) and judged to be more suitable to estimate the amount of Glc released from paper and fractions.

Differences between the two anthrone and Saeman results were expected due to the additional TFA-hydrolysable Glc in α-cellulose and Ha fractions in the Saeman assays (missing from the anthrone assayed fractions). Only a few of the fractions (α-cellulose from A, B, C, H, I and J) contained higher amounts of Glc according to the Saeman analysis compared to the anthrone quantified Glc. This may have been due to overestimation of Glc by the anthrone assay. The anthrone assay clearly overestimated the quantity of Glc in fractions from preparations D–F (125–158 µg Glc/ 100 µg dry weight α-cellulose) but quantified very little Glc in fractions from eC H–J. Nonetheless, part of the Glc quantified by the anthrone assay would have resulted from TFA-hydrolysable Glc in the fractions. The preparation from eC C (Figure 7), showed a high percentage of TFA-hydrolysable α-cellulose, consequently a high concentration of Glc quantified by the anthrone assay was expected. In agreement with this, the amount of Glc estimated by the Saeman method in α-cellulose from eC C was a lot higher than what was estimated by the anthrone assay. α-Cellulose fractions from eC H–J had very high standard errors for the anthrone assayed Glc. Furthermore, the anthrone method quantified between 22 and 157 µg Glc / 100 µg α-cellulose but the range and concentration for the Saeman method was minor (52–107 µg Glc/ 100 µg α-cellulose).

Saeman hydrolysis of the Ha fractions from preparations B–H and paper resulted in less Glc than expected. This was combined with the presence of more (and higher quantities) of unknown products in the paper control as well as the Ha fractions (Figure 18).

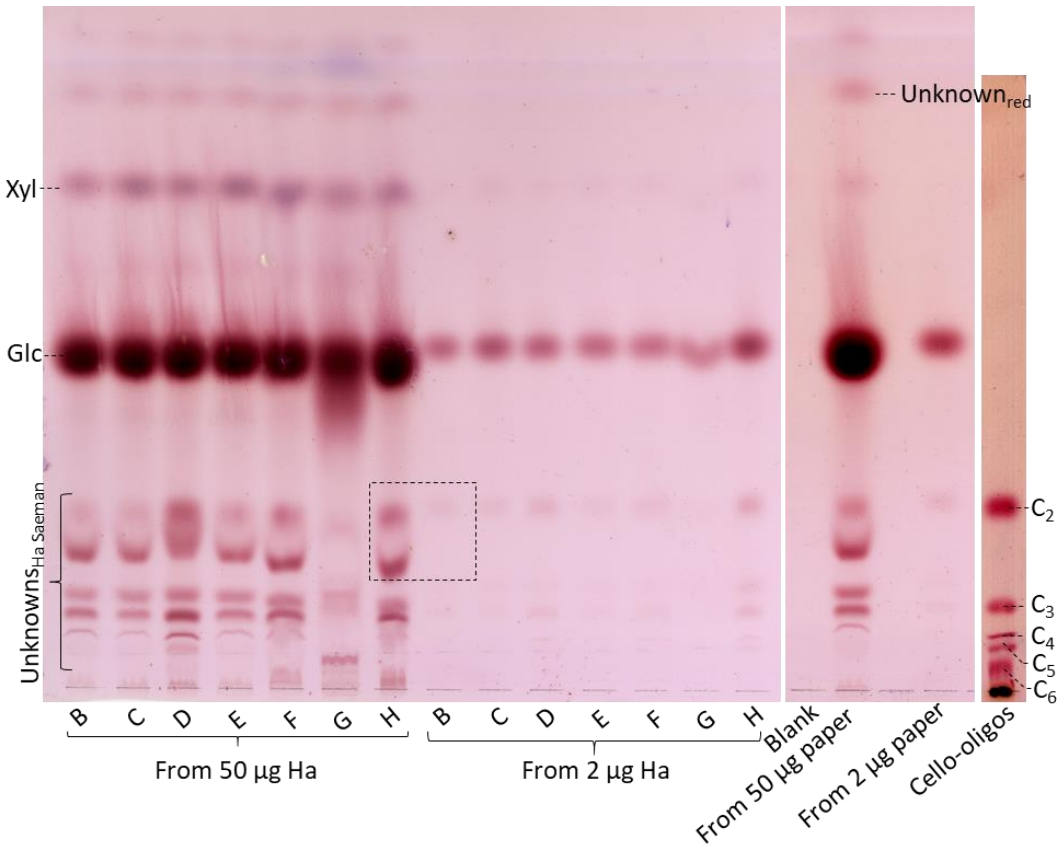

Figure 18: Saeman hydrolysis of hemicellulose a and paper into glucose and unknowns.
Ha fractions from preparations B–H were hydrolysed by the Saeman method, applied to TLC plates, run in the solvent EPyAW (6:3:1:1) for 2 × 2.5 h and stained with thymol (§2.8.2). Cellulose oligomers ('Cello-oligos' C_2 to C_6) were applied as a marker mixture of different degrees of polymerization of Glc. Unknown components were grouped into 'unknowns$_{Ha\ Saeman}$'; the component with the highest R_f is indicated in a rectangle. The Saeman method was not performed on Ha fractions from preparations A, I and J as there was not enough material extracted.

Saeman hydrolysis of Ha fractions and paper led to a group of unknown red-staining components with low R_f values (grouped into 'Unknowns$_{Ha\ Saeman}$'). Most of these unknown components were not produced from the first Saeman hydrolysis presented earlier (TLC plate Figure 44); in contrast, this second Saeman hydrolysis resulted in an (irreproducible) artefact (confirmed by personal communication from Ninni Nuorti, Klaus Herburger and Martina Pičmanová). Unknowns$_{Ha\ Saeman}$ might be intermediate products of cellulose degradation e.g. cellobiose (C_2) and cellotriose (C_3). The components found in Saeman hydrolysates from 2 µg Ha (the diluted hydrolysates) only show traces of some unknowns$_{Ha\ Saeman}$. The unknown component with the highest R_f (marked with a rectangle in Figure 18) seems to be split into two bands (from 50 µg Ha) and only shows up as one band in 2 µg Ha.

Glc, Xyl, Man and Ara were hydrolysed from Ha by TFA (Figure 50 and Figure 51) and the Saeman method. Glc (cellulosic and non-cellulosic) and $unknowns_{Ha\ Saeman}$ were quantified. The $unknowns_{Ha\ Saeman}$ formed a minor portion of the total (results of all single quantified components in Ha Saeman hydrolysates in Figure 48). The total components quantified (combination of Glc and the $unknowns_{Ha\ Saeman}$) are compared to the anthrone method results (Figure 19).

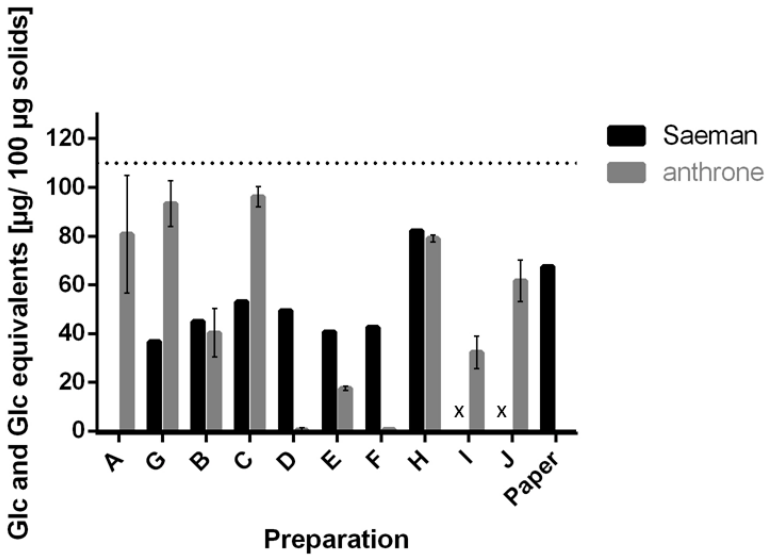

Figure 19: Glucose equivalents released by the anthrone and the Saeman methods in hemicellulose a and paper.
Ha fractions from preparations B–H were assayed by the anthrone (§2.8.1) and the Saeman method (coupled with TLC for quantification by Photoshop) (§2.8.2). Error bars represent SEM, N=1 for anthrone assays. N=1 for Saeman method results as there was not enough material for replicates. Data from the Saeman method presents Glc equivalents from '$unknowns_{Ha\ Saeman}$' plus Glc quantified from Ha fractions. Further details see Figure 18.

Only 64 µg Glc and 4 µg Glc equivalents (in $unknowns_{Ha\ Saeman}$) were generated from 100 µg paper by the Saeman method (Figure 48) (the total accounting for 68 µg components/ 100 µg dry paper (Figure 19). It can be speculated that a full hydrolysis of the $unknowns_{Ha\ Saeman}$ would have resulted in 46 µg Glc/ 100 µg (an ~11 fold increase of Glc equivalents to Glc) (total of 110 µg Glc from the hydrolysis of 100 µg cellulose). Paper was only hydrolysed to 58%. This would suggest that also the Ha fractions were not fully hydrolysed: they contained 40 µg Glc/ 100 µg Ha (e.g. Ha from eC G and F) up to 85 µg/ 100 µg Ha (from eC H) beside 2.7–11.2 µg Glc equivalents/ 100 µg Ha in $unknowns_{Ha\ Saeman}$ (Figure 48).

The anthrone method again resulted in inconsistent results with big error bars and a wide range (1–97 µg Glc/ 100 µg Ha).

None of the two carbohydrate assays resulted in simple to interpret quantifications: the anthrone assay was performed on coloured solutions (different intensities between the samples) prior to addition of the anthrone reagent, overestimation of Glc and moreover resulted in high standard errors. The Saeman hydrolysis was not reproducible (the second time) and resulted in good quantification of Glc in α-cellulose but underestimated Glc in Ha fractions.

3.5.2.2 *Total hydrolysis of preparations and fractions from SBP and experimental Curran A–J*

For an overview of the total monosaccharide composition, the second set of preparations (from SBP A and G, eC B–J) was hydrolysed with (Figure 21) and without (Figure 20) prior fractionation and the products were analysed by TLC and Photoshop quantification. Unexpectedly, this revealed differences between the total carbohydrate compositions from fractionated and non-fractionated preparations (details in this chapter) but both confirmed the enrichment in cellulose and the reduced concentration of non-cellulosic components in all eC preparations (compared with starting materials SBP A and G). Pectic components were even further reduced in hveC preparations than in normally produced eC preparations, which again (as in §3.5.1) hints towards greater viscosity with decreasing concentration of pectic components.

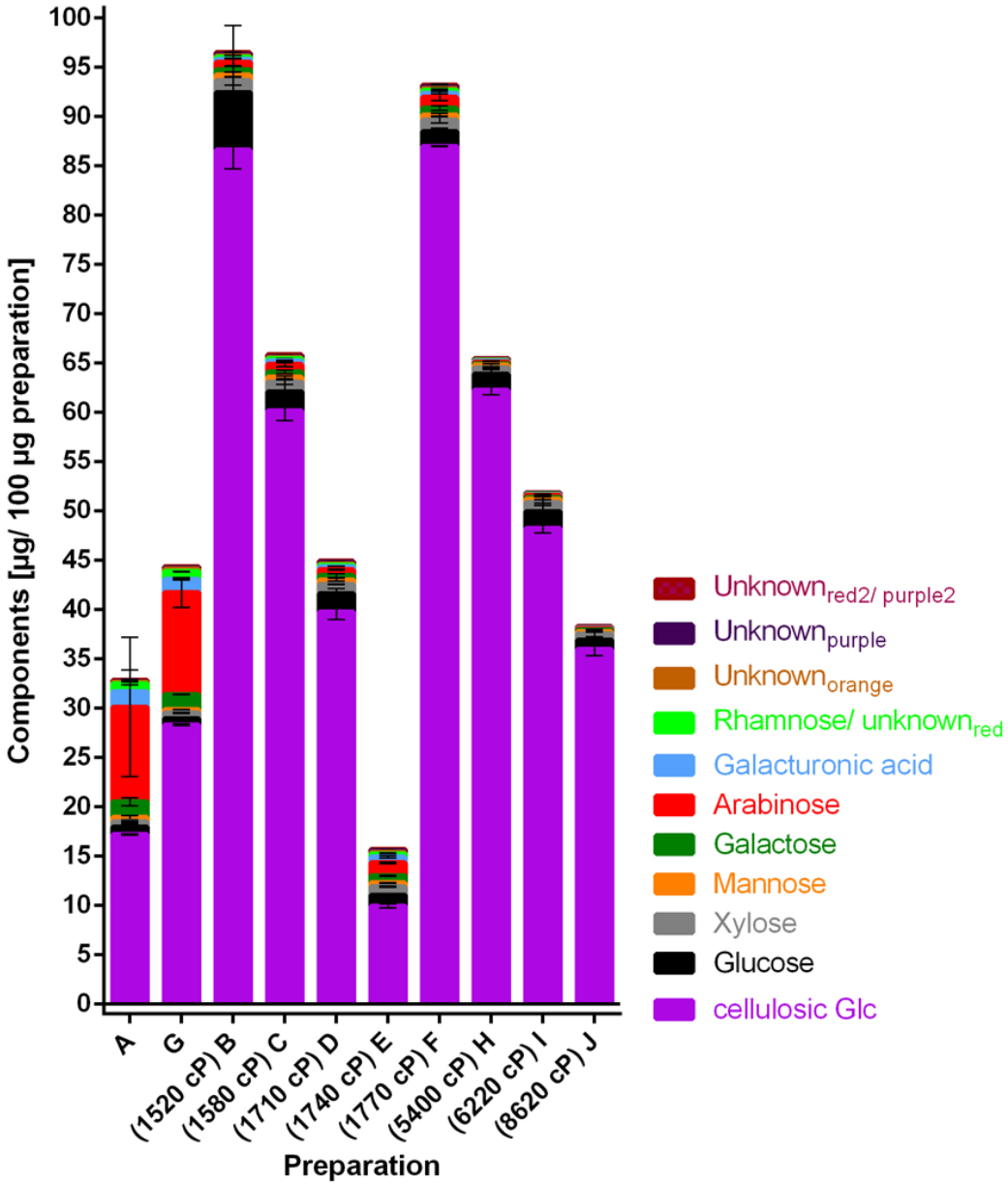

Figure 20: Quantified components in hydrolysed total SBP and experimental Curran (including high viscosity experimental Curran) preparations.
The TLC plates (Figure 53, Figure 56–Figure 58), with TFA-hydrolysed duplicates of preparations from SBP (A and G) and eC B–J, were quantified by Photoshop. Cellulosic Glc (purple bars) was quantified by the anthrone assay (N=6). eC B–J are in order of increasing viscosity (1520–8620 cP).

As observed in §3.5.1, the hydrolysis of SBP and eC preparations into TFA-hydrolysable components and cellulosic Glc could not account for the total weight of the initial preparation. Provided that SBP and eC preparations are mainly composed of polysaccharides (§1.2) the weight loss ranged from 0 (eC B) to 83 (eC E) µg/ 100 µg washed preparation. As stated in §3.5.2.1, 100 µg cellulose should

result in 110 µg Glc therefore even 0 µg/ 100 µg preparation indicates weight loss. This might point towards non-carbohydrate parts in washed preparations or overestimated solid contents. The observed carbohydrate composition of SBP A and G preparations only made up 38 µg and 46 µg/ 100 µg of the total washed preparation respectively. The major component of SBP was cellulosic Glc (up to 28 µg) and Ara was the major non-cellulosic component (these results confirm the carbohydrate composition of SBP K and L (§3.5.1; Figure 14)). If the cellulosic Glc was determined correctly, perhaps the cellulose in SBP G was more accessible to hydrolysis than powdered SBP A.

As was also seen earlier, cellulosic Glc made up the major portion of carbohydrates in the eC preparations while all non-cellulosic components only made an addition of up to 10 µg of 100 µg washed preparation (eC B, richest in non-cellulosic components) (Figure 60). In the non-cellulosic polysaccharides in eC preparations, Glc and Xyl were the major components quantified on TLC plates (identical to most eC M–S preparations in the first set (Figure 14)). Furthermore, more Ara, Gal, GalA and Rha were found in preparations from eC E and F (compared to other normally produced eC B–D). The quantities of Glc, Xyl, Man and the unknowns were each measured to be similar among eC B–F preparations. hveC preparations showed little reduced quantities of Xyl while pectic components were reduced much more. In conclusion, non-cellulosic Glc and Xyl were the major non-cellulosic components in all eC preparations, the composition of B–F was similar (E and F were richer in pectic components) and hveC preparations were the poorest in pectic components.

Fractionation of the total preparation revealed a different but overall similar composition. The composition resulting from hydrolysis of the fractions from SBP and eC B–J preparations was summarised by adding up the quantified components from TFA hydrolysis and Saeman hydrolysis (or anthrone hydrolysis for Ha A, I and J). As the Saeman method was performed on the whole α-cellulose and Ha fractions it hydrolysed the ‘non-cellulosic’ as well as the’ cellulosic’ Glc in those fractions, therefore TFA-released Glc in Ha and α-cellulose was not added to the composition (Figure 21). The acetic acid wash of α-cellulose only contained traces of Man and the $\text{Unknown}_{\text{purple2/red2}}$ (TLC in Figure 57) and made up a negligible part of the total components (therefore not listed by itself in Figure 21). Carbohydrates solubilized in this washing step were also found in O’Rourke *et al.* (2015).

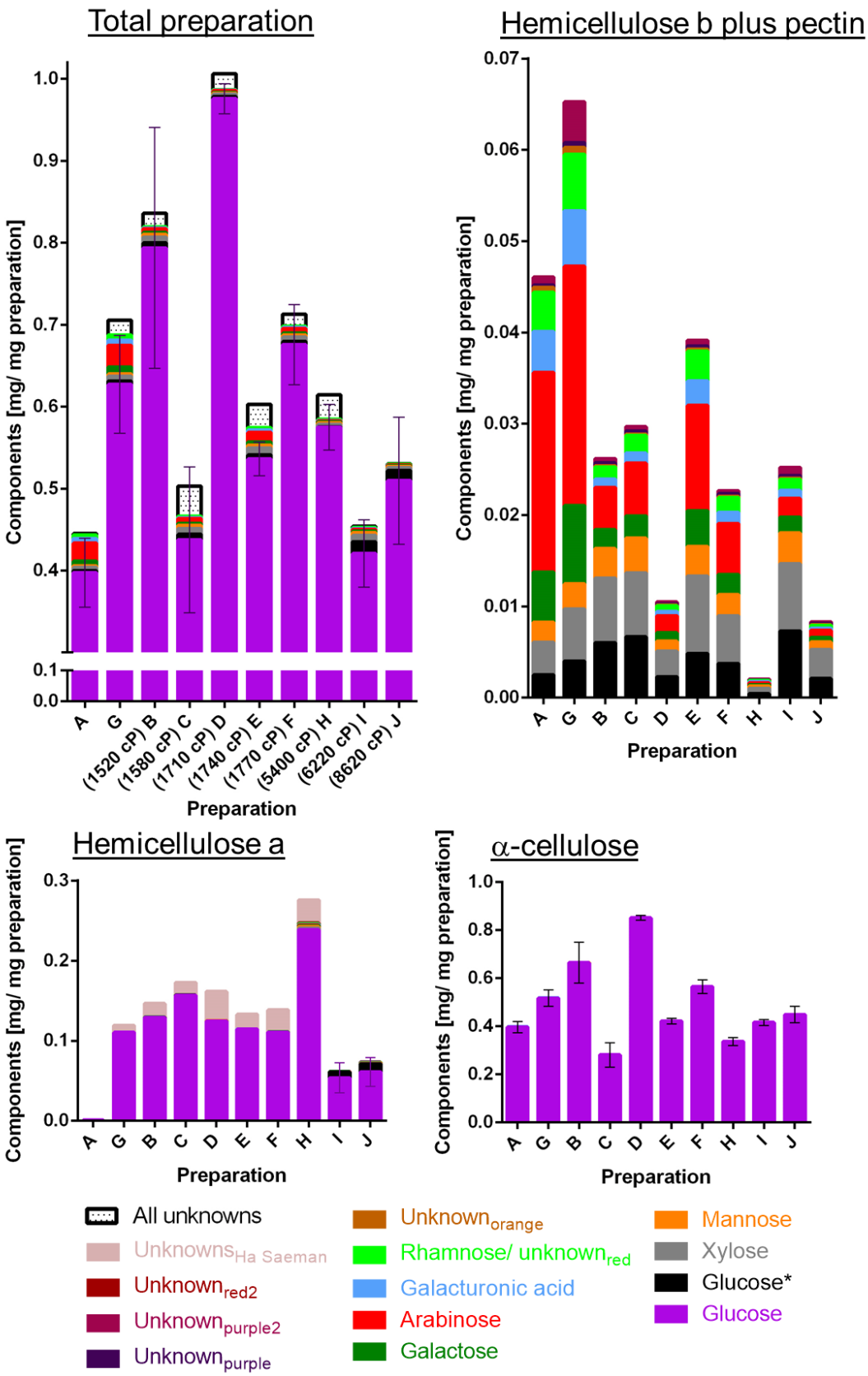

Figure 21: Components quantified in fractions from SBP and experimental Curran (including high viscosity experimental Curran) preparations (continued on the next page).

(caption continued from Figure 21). The TLC plates (Figure 49–Figure 57), with TFA-hydrolysed fractions from preparations of SBP (A and G) and eC B–J, were quantified by Photoshop. Glucose* (black bars) was quantified from TFA-hydrolysed HbP and some Ha fractions. $Unknown_{orange}$, $Unknown_{purple}$ and $Unknown_{purple2}$ were found in TFA-hydrolysed HbP; $unknown_{red2}$ was hydrolysed from Ha by TFA. Saeman hydrolysis was performed on α-cellulose and Ha to quantify Glc (cellulosic and non-cellulosic Glc) (purple bars) and $Unknowns_{Ha\ Saeman}$: error bars represent SD, N=3 for α-cellulose and N=1 for Ha. Ha from preparations A, I and J was quantified by the anthrone assay (N=3). Several components were identified, and their concentrations presented per mg total dry preparation. Preparations eC B–J are in order of increasing viscosity (1520–8620 cP). The top left graph shows the total preparation (viscosity in cP) (summary of all quantified components in HbP, Ha, HOAc wash and α-cellulose) with a collection of all unknown components (except for $unknown_{red}$ which was quantified together with Rha).

Once more, only 0.45–1.01 mg/ mg preparation was recovered (out of ~1.10 mg expected yield) (total preparation, top left in Figure 21) and all preparations were mainly composed of Glc (~90% of the total preparation, primarily in the α-cellulose fraction, §3.5.2.1) quantified after the Saeman or anthrone analysis.

Only a quantitatively minor amount of Ha was extracted from SBP A preparation (Figure 7), which only yielded a minimal quantity of cellulosic Glc (0.0008 mg/ mg preparation). Ha from SBP G and normally produced eC B–F preparations contributed 0.11–0.16 mg Glc per mg preparation. Ha from hveC I and J preparations contributed less cellulosic Glc (0.06 mg/ mg preparation) to the total. The Ha fraction from hveC H showed a surprisingly high concentration of 0.24 mg Glc/ mg preparation. It was unexpected to find this four-fold difference amongst the three Ha fractions from hveC preparations; this might be due to:

- the different methods used for analysis of Glc (§3.5.2.1).
- the possibility that α-cellulosic material was carried over into the Ha fraction from hveC H during extraction (discussed in §3.6).

Non-cellulosic components were again mostly present in the HbP fraction (Figure 21, top right); compared to all other HbP fractions, HbP from eC D, H and J were poor in total quantified components. As discussed in §3.2 the HbP fractions from these three preparations were quantitatively minor. I found different compositions between the three hveC HbP fractions. More precisely, only a very low quantity of components was detected in the HbP fraction of hveC H (0.002 mg total components/ mg preparation), compared to 0.009 mg in hveC J and 0.025 mg total components/ mg preparation in hveC I.

The weight loss after fractionation did not match the loss observed after hydrolysis of the total washed preparation (Figure 20). Nevertheless, the carbohydrate compositions were similar; all preparations were rich in α-cellulosic or TFA-resistant Glc and SBP preparations contained most non-cellulosic components such as Ara (found in HbP).

All eC preparations tested (washed and AIR; B–J and M–S) were mainly enriched in cellulosic Glc and greatly reduced (compared to all SBP preparations) in their pectic components such as Ara, Gal, GalA and Rha (Figure 20 and Figure 21).

3.6 Hemicellulose a fractions from high viscosity experimental Currans were rich in cellulosic glucose

hveC Preparations were unusually rich in their Ha proportion (Figure 7) which was worthy of further investigation.

Ha was soluble in NaOH (§2.9) but precipitated upon acidification which is how it can be separated from HbP and the NaOH-insoluble α-cellulose fraction. Nevertheless, Ha (from eC and hveC preparations) was shown to mainly consist of cellulosic Glc (§3.5.2.2). As shown in this chapter, the general procedure of separating Ha from α-cellulose and HbP was inadequate on the hveC preparations as all three fractions were re-extracted from Ha fractions.

Like all other Ha from eC preparations, those from the hveC preparations were only partially soluble by TFA hydrolysis and the monosaccharides observed were mostly Glc (with little Xyl) (discussed in §3.5.2; Figure 51). The TFA-resistant residue was hydrolysed by the Saeman method into Glc (and unknowns) (discussed further in §3.5.2.1; Figure 19) meaning that Ha was mainly composed of carbohydrates containing ‘cellulosic’ Glc.

Ha fractions from hveC preparations H and J were subjected to a second NaOH treatment (§2.9) to test if all could be resolubilised. This experiment resulted in three sub-fractions (Figure 22).

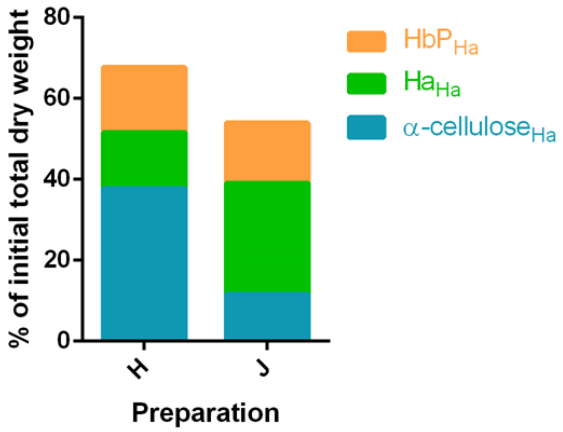

Figure 22: Polysaccharide sub-fractions from hemicellulose a of two high viscosity experimental Curran preparations.
Ha fractions (from hveC preparations of H and J) were subjected to 6 M NaOH extraction. The α-cellulose$_{Ha}$ sub-fraction was not soluble in NaOH, Ha$_{Ha}$ was soluble and precipitated upon acidification and HbP$_{Ha}$ was soluble but staying in solution on neutralisation. The weight of all dry sub-fractions was recorded.

The previously NaOH-soluble Ha fractions from preparations J and H could not be fully resolubilised in NaOH (38% and 12% α-cellulose$_{Ha}$ respectively). The main portion of starting Ha from preparation H was α-cellulose$_{Ha}$ while Ha$_{Ha}$ was the main sub-fraction in preparation J (28% initial total dry weight). Part of the initial Ha fraction was not recovered (31–45%); it might have been lost in the washing steps (of α-cellulose$_{Ha}$ and Ha$_{Ha}$) or during dialysis of HbP$_{Ha}$ (discussed in §3.3). HbP$_{Ha}$ (15–16%) was also extracted showing that a quantitatively minor portion was solubilised by this extraction and/or residual soluble material wasn't washed away in the previous washing steps of Ha.

These results showed that Ha extracted from hveC preparations was a mixture of NaOH-soluble and -insoluble material and unlike most Ha fractions extracted from other plant materials. The Ha fraction for eC preparations generally contained little hemicellulose and mostly cellulose-like polysaccharides.

3.7 Molecular mass of SBP polysaccharides changes during the production of experimental Curran

From most eC and SBP preparations only a quantitatively minor amount of Ha and a bigger fraction of HbP was extracted. HbP contained most non-cellulosic

polysaccharides and it was therefore interesting to study the molecular mass of matrix polysaccharides in SBP and eC preparations. This was expected to lead to a possible correlation of molecular mass of hemicelluloses plus pectins and viscosity in eC products. Indeed, it was observed that the molecular mass of hemicelluloses and pectins decreased during the production process of eC, furthermore some polysaccharides seemed to be especially targeted. hveC preparations showed the lowest M_r polysaccharides detected amongst eC preparations.

3.7.1 Polysaccharides from differently produced experimental Currans separated by column chromatography on Sepharose CL-6B

A fraction of HbP was extracted from AIR of SBP and eC preparations (§2.9) to be separated by molecular mass on a column packed with Sepharose CL-6B for gel-permeation chromatography (§2.6). A comparison of preparations L, M, N, R and S revealed that SBP (L) HbP contains bigger polysaccharides, which were then partially broken into smaller molecules in the process of making eC products (TLC plates in Figure 23–Figure 25 and Figure 61–Figure 67).

The eCs chosen were different in viscosity and production process. The following list only mentions the changes to the production process for eC (more details on the whole process §2.1). It also gives information about the viscosity of eCs:

- SBP L
- eC M (5640 cP)
- eC N (no sodium hypochlorite treatment, 3780 cP)
- eC R (overreacted in H_2O_2, 2200 cP)
- eC S (incompletely washed from H_2O_2 and sodium hypochlorite, 1710 cP)

The following Figure 23 shows the result for HbP from SBP L.

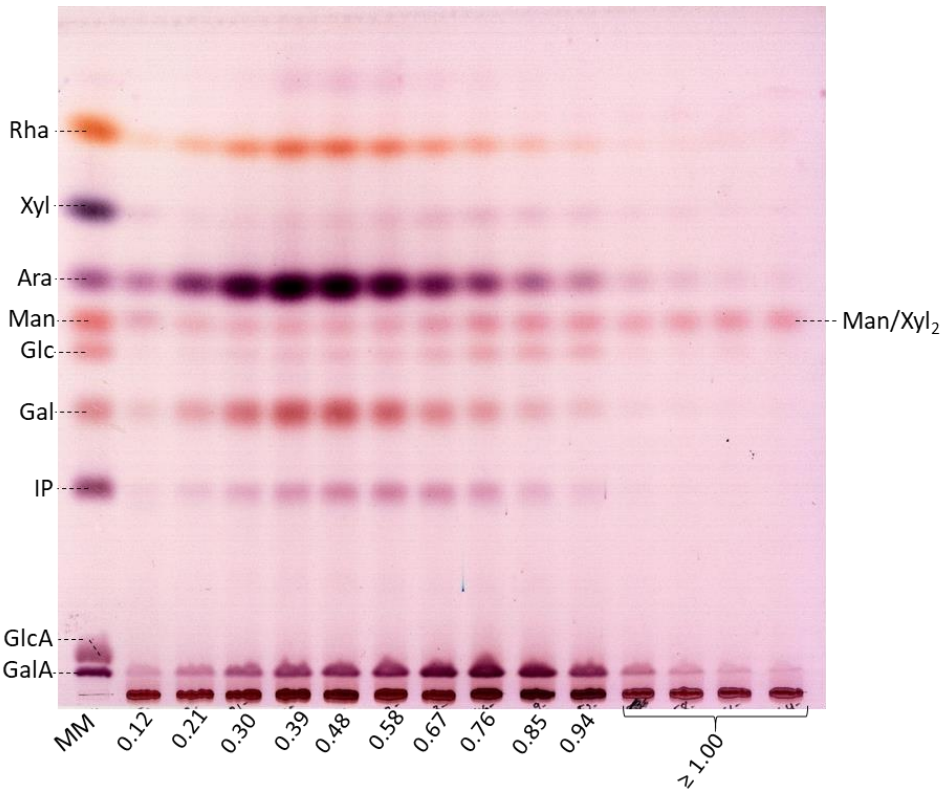

Figure 23: Composition of the hemicellulose b plus pectin fraction from SBP L separated by molecular mass on Sepharose CL-6B and Driselase-digested.
SBP L HbP was size-fractionationed on Sepharose CL-6B, three column fractions were pooled for Driselase digestion and the supernatants applied to a TLC plate. This plate was run in the solvent EPyAW (6:3:1:1) for 2 × 2.5 h and stained with thymol. Each lane was labelled with the pool's respective median K_{av} value. MM: marker mixture. Radioactive markers for K_{av} 1 and K_{av} 0 were used to calibrate the column (§2.6.1).

Figure 23 shows the Driselase digestion products of SBP L HbP size-fractionated by gel-permeation chromatography. High levels of Ara, Gal, GalA and Rha residues were found, among which Ara, Rha and Gal residues showed the same elution profile (mainly 0.30–0.58 K_{av}). GalA containing-polysaccharides were smaller and mainly eluting 0.67–0.85 K_{av}. A low amount of Man was detected in all fractions which was also found in the Driselase-only control (the latter was subtracted from all quantified Man in the pooled fractions). A quantitatively minor amount of Man was still attributable to HbP from SBP itself. IP was mostly present in polysaccharides eluting with a K_{av} of 0.48–0.76.

As described in §2.5.2, I quantified all components and the amounts were presented per mg HbP fraction (Figure 24).

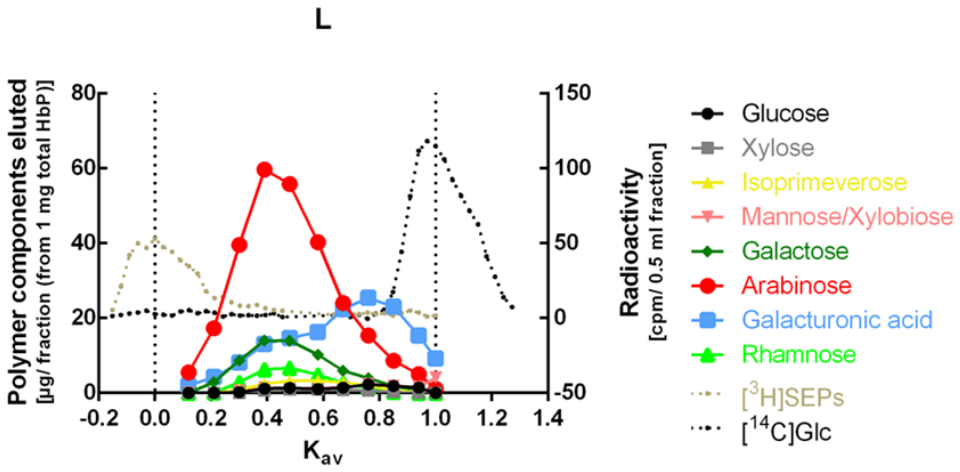

Figure 24: Quantified components in CL-6B size-fractionated, Driselase-digested hemicellulose b plus pectins from SBP L.
The TLC plate (Figure 23) with the size-fractionated, Driselase-digested SBP L HbP was quantified by Photoshop. Nine polymer components were identified, and their elution profiles are shown according to the pools' respective median K_{av} value. Man and Xyl_2 were quantified together. Radioactive markers—[^{3}H]SEPs and [^{14}C]Glc—mark the V_0 (K_{av} 0) and the V_i (K_{av} 1) respectively.

The quantified data confirmed the results observed in Figure 23. In SBP L, Ara was clearly the major component in the HbP extract, most of the Ara-containing polysaccharides together with Rha and Gal eluted around K_{av} 0.4. The smallest polysaccharides mainly eluted around K_{av} 0.8: they contained GalA in large quantities, Man/Xyl_2 and Glc in minor quantities (the last two are not distinguishable from the baseline in Figure 24). In this TLC solvent, the disaccharide Xyl_2 (stained purple) shows the same R_f as Man (stained red), these components can therefore not be separated in this TLC system and are consequently quantified together. In the SBP L preparation the quantified Man/Xyl_2 component was red (no hint for purple Xyl_2, still it might have been present in minor quantities).

This elution profile for the components changed when SPB was processed into eC as can be seen in Figure 25 and Figure 26, which show the results for HbP from preparation eC N.

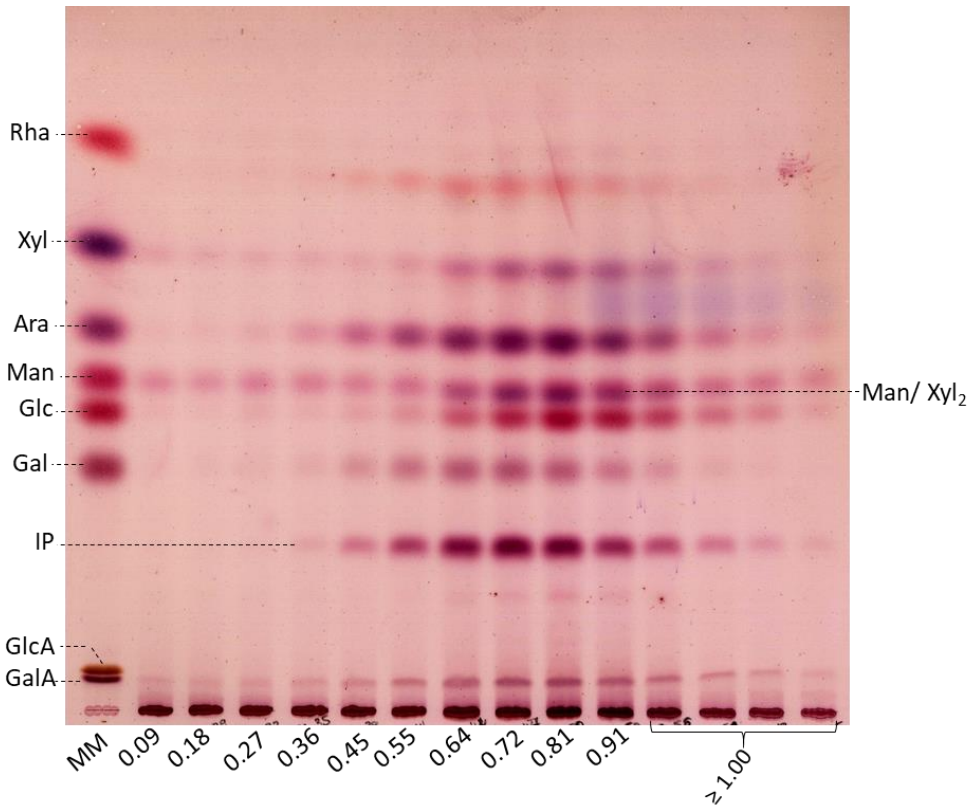

Figure 25: Composition of hemicelluloses plus pectins from preparation experimental Curran N separated by molecular mass and Driselase-digested.
eC N HbP was treated like HbP from SBP L; further details as in Figure 23.

On the Sepharose column CL-6B the main components in eC N HbP elute later than the ones found in SBP L. Again, the major component was Ara but IP, Glc, Man/Xyl_2 were also found in high quantities. In contrast to SBP, eC N clearly contained Xyl_2 (stained purple) in addition to Man (stained red/pink). Gal and GalA quantities were reduced (compared to SBP L).

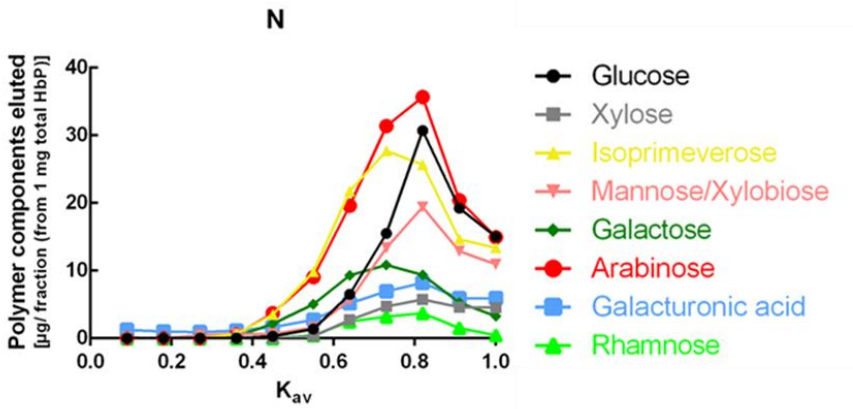

Figure 26: Quantified components in size-fractionated, Driselase-digested hemicelluloes plus pectin fraction from experimental Curran N preparation.
The TLC plate (Figure 25) with the size-fractionated Driselase-digested HbP from eC N (after the run on Sepharose CL-6B) was quantified by Photoshop. Further details as in Figure 24.

In eC N HbP an overall shift of the polysaccharides in the HbP fraction towards higher K_{av} (smaller molecules) could be observed (compared to the starting material SBP L). The HbP fraction of eC N was mainly composed of Ara, Glc, IP and Man/Xyl_2, whereas the starting material SBP L contained a lot more Ara, GalA, Rha and Gal (typical pectic components).

The results found for HbP fractions from eC M, R and S are accessible in the appendix (§6.3). They showed an elution profile similar to that seen for HbP from eC N.

For better comparison between the eC HbP fractions, the quantified polymer components eluted were converted into cumulative components eluted (from 1 mg HbP) and cumulative percentage eluted (Figure 27). With the K_{av} data and the published fractionation range of Sepharose CL-6B (product information provided by Sigma Aldrich), the respective relative molecular mass (kDa) was calculated (§2.6.1) and plotted instead of the K_{av} (as it gives more absolute information about the polysaccharides in the sample).

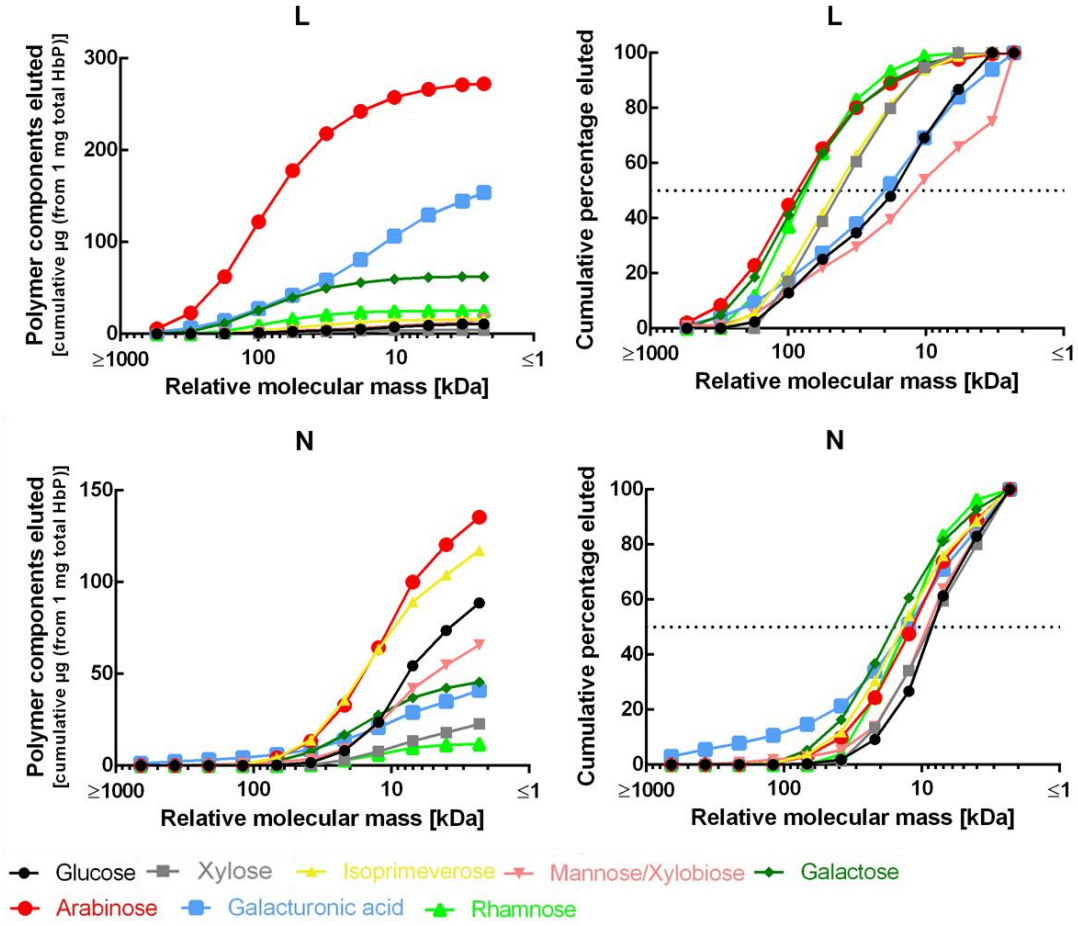

Figure 27: Cumulative amounts and percentages of hemicellulose plus pectin fraction from SBP L and experimental Curran N eluted from Sepharose CL-6B size-fractionated and Driselase-digested.
The results displayed in Figure 24 and Figure 26 were converted into cumulative components eluted (left-hand side) and cumulative percentage eluted (right-hand side). The K_{av} was converted into the relative molecular mass. A dotted line in the 'cumulative percentage eluted' graphs indicates the median relative molecular mass.

The two graphs on the left-hand side of Figure 27 show the cumulative polymer components eluted; large differences between the total amounts of components from 1 mg HbP between SBP L and eC N can be seen. The total weight of the HbP fraction applied to the column could not be accounted for, possibly due to incomplete quantification from TLC by Photoshop. The cumulative percentage graphs on the right make it easier to compare all relative molecular masses of the polymers in one sample to each other. I used the median relative molecular mass (relative molecular mass at 50% eluted) (median M_r) to compare the different sizes of the polysaccharides among all components eluted and between different HbP fractions. It was again apparent that most polymers in SBP L are bigger than polymers in the eC HbP fractions (here only eC N was shown). The components in SBP HbP seem to be grouped into the biggest polymers containing Ara, Gal and Rha (median M_r ~80 kDa) followed by IP and Xyl

(~45 kDa). The smallest polysaccharides in SBP HbP (median M_r 12–21 kDa) contain GalA, Glc and Man/Xyl_2. In contrast to these quite distinct groups, polymers in HbP from eC (irrespective of their different production procedures) elute very close to each other (median M_r 8–16 kDa) as can be easily seen in Figure 28.

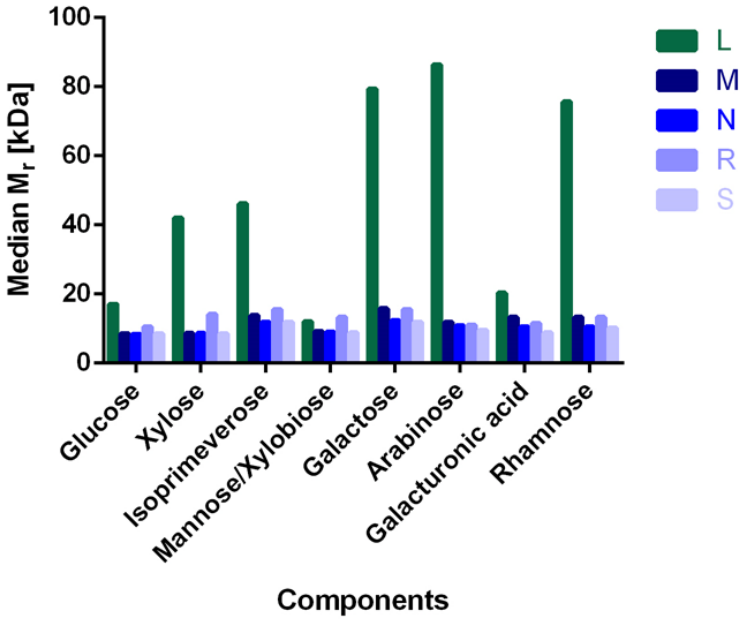

Figure 28: Median relative molecular mass for components in hemicellulose plus pectin from SBP L and the experimental Curran size-fractionated on Sepharose CL-6B and Driselase-digested.
The M_r (in kDa) was read of the graphs in Figure 66. SBP L is in green, eC M–S are in blue.

The fractionation range for dextrans on Sepharose CL-6B was 10–10^3 kDa (product information provided by Sigma Aldrich). Judging from the results obtained in this chapter, this seemed to be too high to find differences between the polymers in HbP of eC preparations. All later column chromatography experiments were therefore done with a column packed with Sephacryl S-200 (fractionation range for dextrans 1–80 kDa (product information provided by Sigma Aldrich)), described in §3.7.2.

3.7.2 Column chromatography on Sephacryl S-200 to separate polysaccharides in experimental Curran preparations (including high viscosity experimental Currans)

As the Sephacryl S-200 column has a more suitable fractionation range than the Sepharose CL-6B, this experiment was designed to find significant differences between the polysaccharide's molecular mass in HbP from different eC preparations. A new set of eC and SBP preparations A–J (plus SBP preparation K (technical

replicate of L) as a reference to the previous column chromatography) were chosen for this experiment to find molecular mass differences among hemicelluloses and pectins from both production processes (normal and higher concentrations of oxidising chemicals):

- SBP K
- SBP powder A and A.2 (technical replicates)
- SBP G
- eC B, 1520 cP
- eC C, 1580 cP
- eC D, 1710 cP
- eC E, 1740 cP
- eC F, 1770 cP
- hveC H, 5400 cP
- hveC I, 6220 cP
- hveC J, 8620 cP

A new stock of [3H]SEPs was purified and resulted in a peak on Sephacryl S-200 at K_{av} 0.08 (slightly higher than the SEPs on Sepharose CL-6B; §3.7.1).

As already described earlier Xyl_2 and Man had the same R_f value and were therefore not separated in the EPyAW TLC system (§2.5). This problem was solved using paper chromatography with BAW (12:3:5) followed by EPyW (8:2:1) as the solvent system (§2.7) in the following experiment.

HbP from SBP A preparation was eluted in duplicate from the S-200 column and resulted in slightly different elution profiles for Ara (§6.4; Figure 80). The first elution resulted in two overlapping peaks for Ara while the second resulted in only one peak. Two peaks were also seen for the Ara elution profile of HbP from SBP K eluted from the S-200 column. This suggested that there were two populations of Ara-containing polymers in the HbP from SBP which were very close in molecular mass. The second elution of HbP from A (A.2) and the run of HbP from SBP G did not result in two Ara peaks which might have resulted from pooling eluted column fractions from the Driselase digestion in threes. A closer analysis of the single fractions might have resulted in two Ara peaks.

All other components in the HbP of SBP K, A, A.2 and G show very similar elution profiles (Figure 80). Size-fractionated HbP from eC B showed elution profiles for all

components were very similar to HbP from eC C and D while HbP from eC E and F were quite distinct. The hveC fractions differed from the eC fractions but were similar to each other. For simplicity, only size-fractionated HbP from SBP A.2, G, and eC B, E, F and hveC J preparations were chosen as representatives in Figure 29.

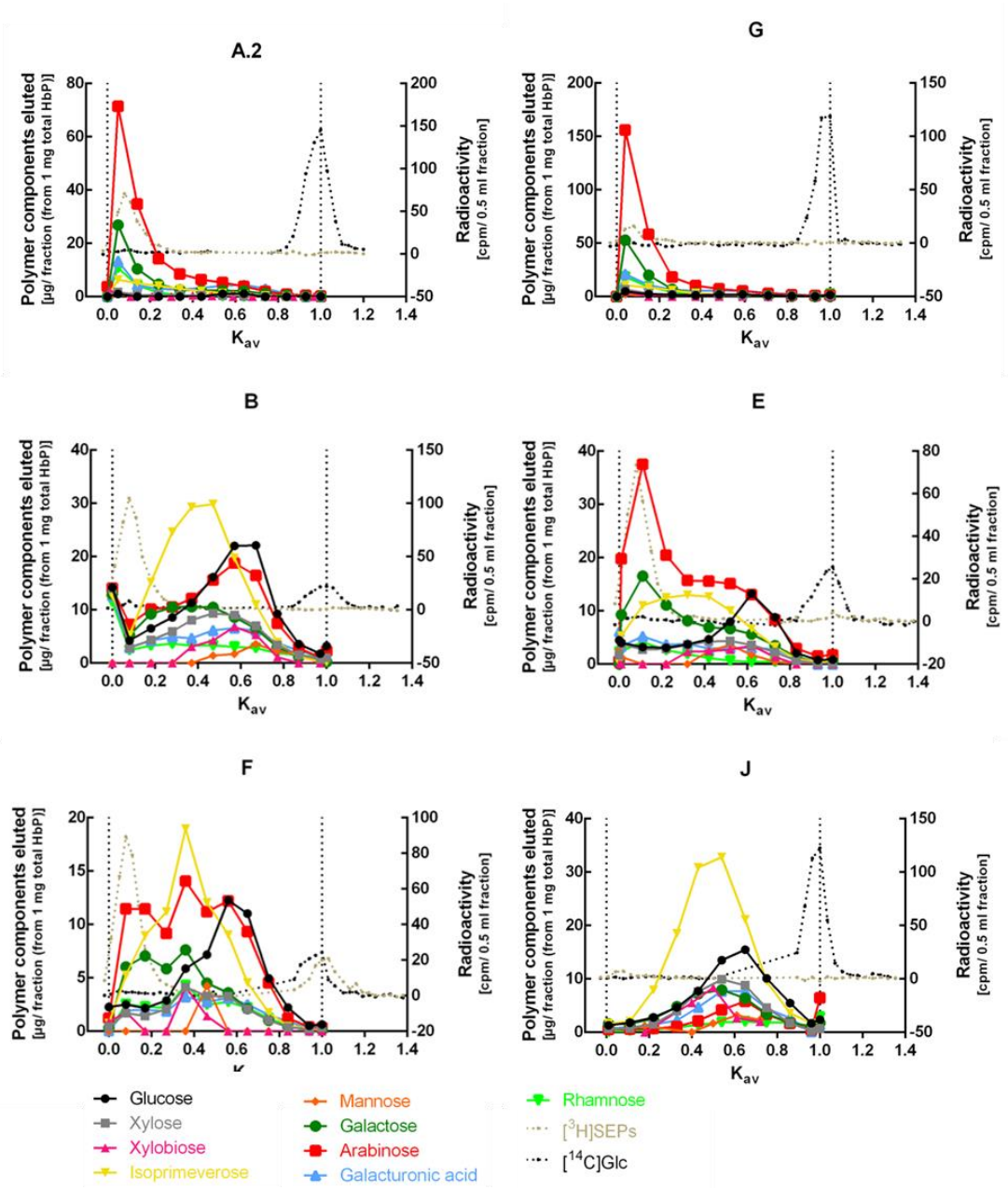

Figure 29: Quantified components in hemicellulose plus pectin from SBP and experimental Curran preparations size-fractionated on Sephacryl S-200 and Driselase-digested.
Size-fractionated HbP from SBP A.2 and G (the two top graphs), eC B, E, F and hveC J. The TLC plates (§6.4) with the Driselase-digested HbP fractions (after the run on Sephacryl S-200) were quantified by Photoshop. For the quantification of Xyl_2 and Man the same Driselase digests were applied to paper chromatograms for PC (results not shown). Nine polymer components were quantified and their elution profiles are shown according to the pools' respective median K_{av} value. Radioactive markers—[^{3}H]SEPs and [^{14}C]Glc—mark K_{av} 0.08 and K_{av} 1 respectively and are measured in cpm/ 0.5 ml fraction.

Major components in the HbP from SBP were again confirmed to be Ara, Gal, GalA and Rha followed by IP. All polysaccharides mainly eluted close to the V_0 of the column (around K_{av} 0.04) and were close to the top end of the fractionation range for

dextrans of 80 kDa. In the production process of eC (including hveCs) the HbP polysaccharides in SBP, all get partially fragmented to smaller sizes (as can be seen in all four eC elution profiles presented in Figure 29). Polysaccharides in HbP from eC B (comparable to eC C and D, Figure 80) eluted mainly around K_{av} 0.4–0.7; IP being the main component in HbP from eC B followed by Glc and Ara. HbP from eC E and F contained more and bigger polysaccharides rich in Ara and Gal eluting around K_{av} 0.1 (and 0.4 for the second peak in eC F). Additionally, these HbP fractions were also enriched in IP (eluting later K_{av} 0.2–0.4). Glc- and Xyl-containing polysaccharides showed a similar elution profile in all eC HbPs with K_{av} 0.6–0.7 and 0.5–0.6 (0.4 for eC F) respectively. Pectic components Gal, Ara, GalA and Rha were eluting together in the column fractions. A general comparison of all components in HbP from eC B, E, F and J showed a range of K_{av} 0.4–0.7, except for eC E (additional major peaks at K_{av} 0.1).

As described in §2.6.2, I used the K_{av} values and the fractionation range of the column to calculate the relative molecular mass of the polymers in HbP. Additionally, I generated the cumulative µg eluted graphs (§6.4; Figure 81) and percentage eluted graphs (making the total of each single component 100%) (Figure 82). In this chapter, only the percentage eluted graphs are presented for size-fractionated HbP from A.2, G, B, E, F and J (Figure 30) to give the reader an overview of the most important differences.

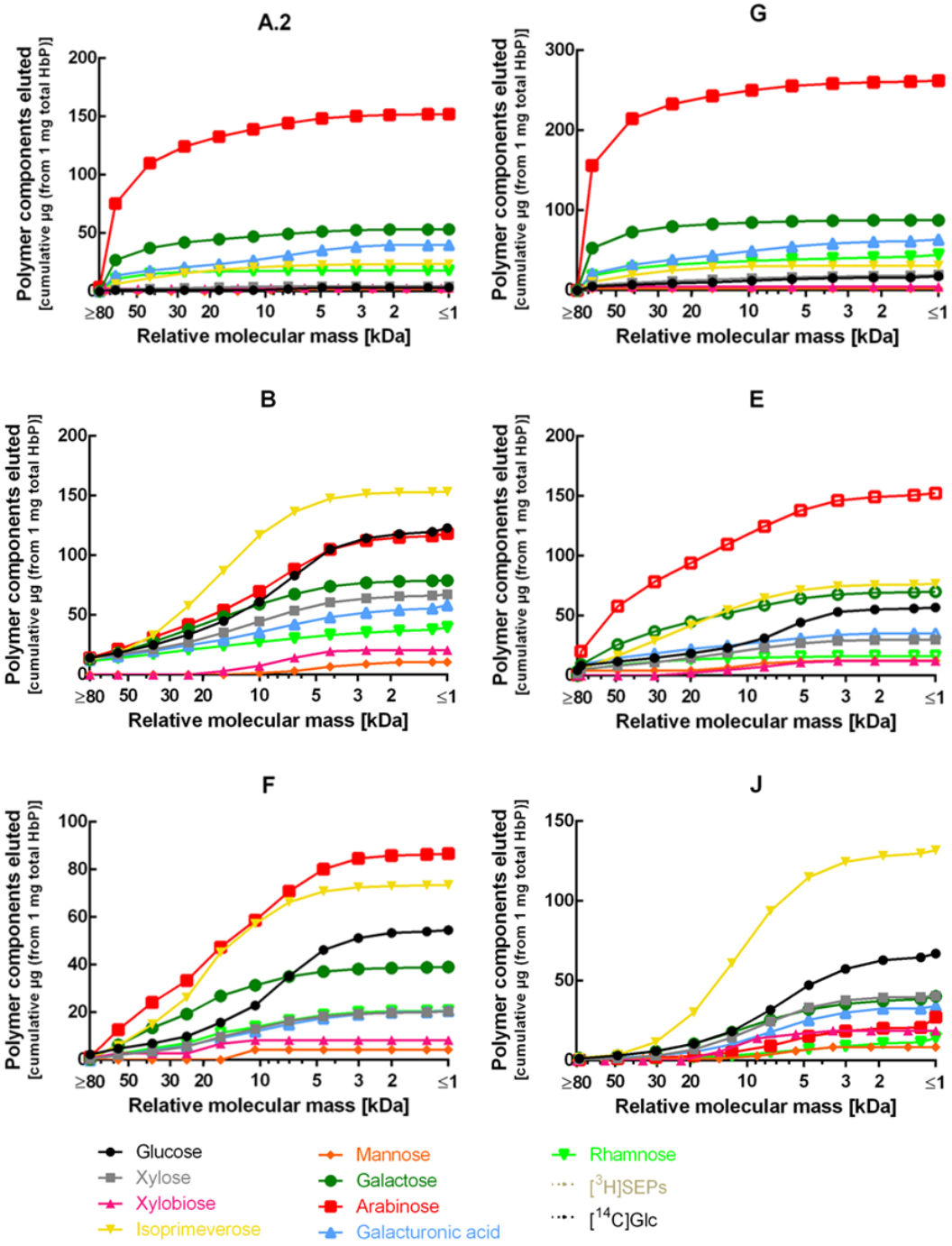

Figure 30: Cumulative percentage eluted of hemicellulose plus pectin components from SBP and experimental Currans size-fractionated on Sephacryl S-200 and Driselase-digested. The results displayed in Figure 29 were converted into cumulative percentage eluted. Further details as in Figure 27.

The graphs show the relative molecular mass (M_r) for the polymers in the three pooled column fractions. As seen before, the major portion of all components eluted early in HbP from SBP starting materials A.2 and G and were thus of high molecular mass.

All components in the eC HbP column fractions eluted later and were therefore of lower molecular mass with a wider size-range.

In Figure 31, I chose to present the data for all HbP fractions from A–J grouped by single polymer components as this can aid in detecting the similarities and differences among the samples.

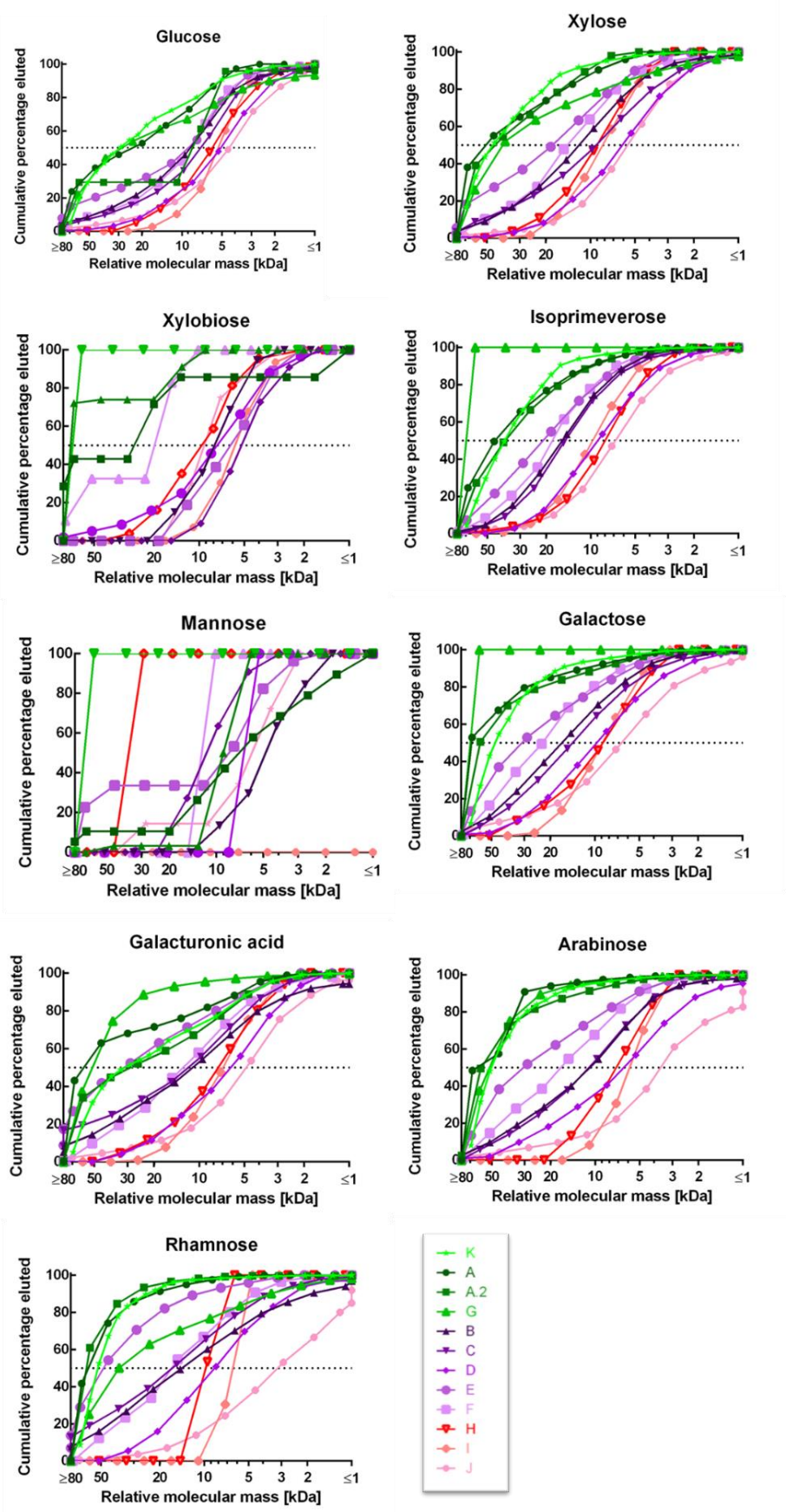
Glucose
Xylose
Xylobiose
Isoprimeverose
Mannose
Galactose
Galacturonic acid
Arabinose
Rhamnose
Cumulative percentage eluted
Relative molecular mass [kDa]
≥80 50 30 20 10 5 3 2 ≤1
0 20 40 60 80 100
K
A
A.2
G
B
C
D
E
F
H
I
J

Figure 31: (continued from previous page) Cumulative percentages eluted for polymer components in hemicellulose plus pectin from SBP and experimental Currans size-fractionated on Sephacryl S-200 and Driselase-digested.
The results displayed in Figure 82 were rearranged to present the data for the single polymer components in all size-fractionated HbP. Further details as in Figure 27.

By comparing the polymer components analysed in size-fractionated HbP from SBP and eC side by side (Figure 31) it became apparent that all SBP HbP fractions (K, A, A.2 and G) were mostly similar in their relative molecular mass. Across the whole fractionation range they demonstrated the highest relative molecular mass (23–70 kDa) compared to HbP from eC preparations. These results were comparable to the results obtained from the previous HbP size-fractionated on Sepharose CL-6B (§3.7.1). Exceptions were Xyl_2 and Man which showed unusual elution profiles (Figure 31). These components were quantified by combining paper chromatography and TLC of the Driselase digested pooled fractions. As shown in Figure 29 only very quantitatively minor amounts of these two hemicellulosic components (no Man in HbP from hveC I) were detected (confirmed by prior TFA hydrolysis of the total HbP fraction, §3.5.2.2). Simultaneously the paper chromatography method might not have been sensitive enough to detect low amounts of these components in every size-fractionated and Driselase-digested HbP pool. The paper chromatograms did not allow for quantification by Photoshop as the background was too irregular and resulted in false positive and negative results. The quantification could therefore only be done by eye and the minimum amount to be quantified was 2 µg. Xyl_2 and Man spots that contained <2 µg were considered to not contain any (as those were not distinguishable from the background). Only bigger differences were consequently detected and may have resulted in poor resolution of the elution profiles for Man and Xyl_2. The presented data could therefore only be considered a rough estimation of the total quantities.

The median M_r of HbP polysaccharides from eC B–F were 5–32 kDa, whereas polysaccharides from hveC H–J were smaller (3–10 kDa). It was notable that components such as Ara, Gal, GalA and Rha in HbP from eC E and F were among the biggest polysaccharides in the eC group; between HbP from eC B–D the median M_r range was only 6–17 kDa for those components. In the previous experiments, fractionated on Sepharose CL-6B (§3.7.1), HbP from eC M, N, R and S showed polysaccharides of similar sizes (8–16 kDa) (although only eC M was produced with the same process as eC products B – F while production processes for N, R and S were changed; §2.1).

While there are clear differences between polysaccharide sizes in HbP from eC, there was no clear-cut correlation between increasing viscosity and increasing or decreasing relative molecular mass; nevertheless, some trends were apparent. Firstly, size-fractionated HbP from eC E and F (viscosities of 1770 and 1740 cP) contained the biggest HbP polysaccharides among all eCs. Secondly, HbP from hveC were the smallest polymers found among all HbP tested (hveC J possessing the highest viscosity and the smallest polysaccharides). Both statements lead to the hypothesis that viscosity increases with decreasing molecular mass of hemicelluloses and pectins.

For further analysis I presented the median M_r of all polymer components in HbP from preparations A–H side by side (Figure 32).

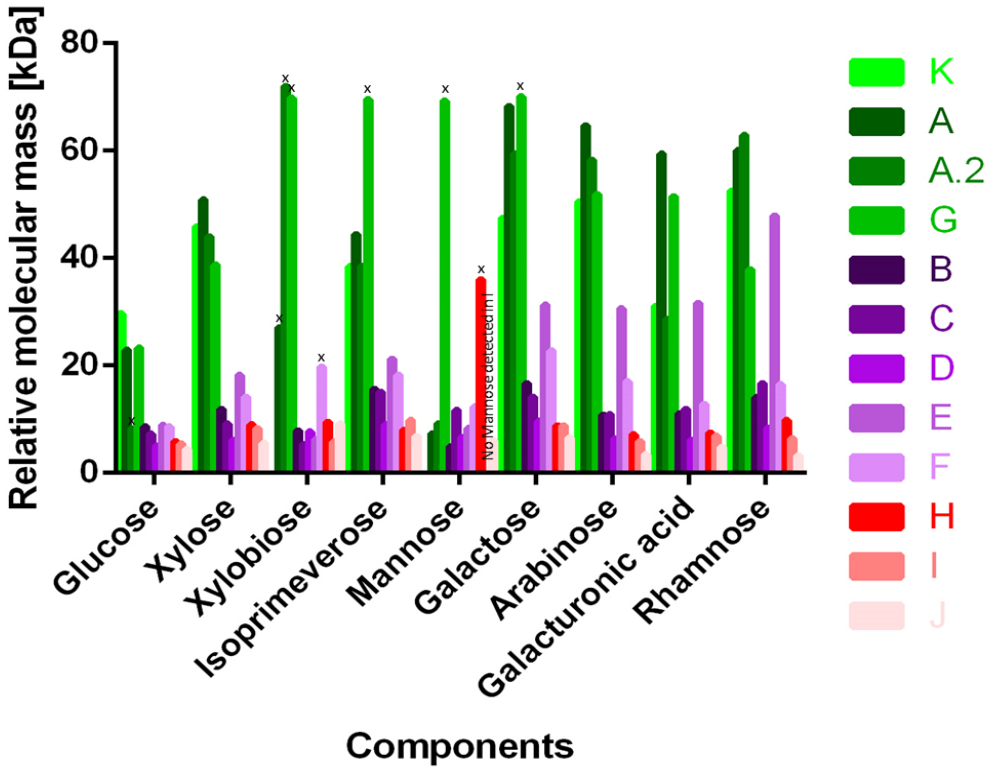

Figure 32: Median M_r of components in HbP from SBP and experimental Currans size-fractionated on Sephacryl S 200 and Driselase-digested.
eC products B-F (purple bars) were of similar viscosity (1520–1770 cP); hveC products (red and pink bars) 5400–8620 cP. An x above some bars was used to mark data that showed an unusual elution profile as seen in Figure 31.

On the first glance, it was easy to see that SBP (K, A, A.2 and G) HbP polysaccharides were of higher median M_r than all eC HbP polysaccharides. The only exception to this was Man which showed unusual elution profiles (Figure 31). Data marked with an x was excluded from the succeeding statistical analysis as it was clearly different from

the other comparable samples. Excluded samples were: Glc in HbP from A.2; Xyl_2 from eC F (all SBP HbP profiles were also quite unusual but still included to enable a comparison); IP in SBP G; Man (all elution profiles were unusual but only HbP from G and H were excluded; this left only HbP from hveC J in the hveC group and no standard error could be calculated) and GalA in HbP from SBP G.

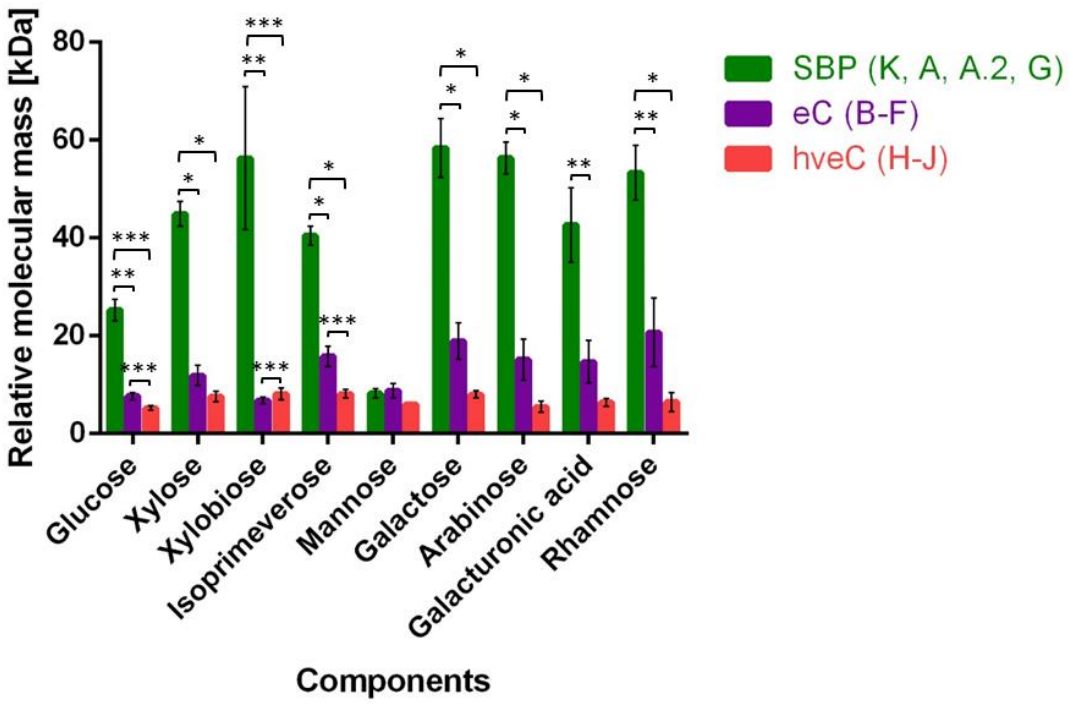

Figure 33: Median relative molecular mass of Driselase-generated components in hemicellulose plus pectin from SBP, eC and hveC size-fractionated Sephacryl S-200 fractions. The error bars represent SEM; N varies between 1 and 5 and was listed in Table 5. Statistically significant differences in the t-test were marked with asterisks.
*: P=<0.001; **: P= =<0.01; ***: P=≤0.05

This summary of the grouped mean median M_r confirmed that SBP HbP were significantly bigger than all HbP in eC and hveC. Man-containing SBP polymers seemed exceptionally small which might have been the result of insufficient quantification as discussed before. There are only few significant differences between the two groups eC and hveC. Only IP- and Glc-containing polysaccharides in eC HbP were significantly bigger than the same HbP polysaccharides in hveC. Even though polymers containing the other seven components did not show statistical differences, the average median M_r in HbP from eC was higher than in hveC HbP. The statistical analysis and the trends observed supported the hypothesis that viscosity increased with smaller hemicellulosic and pectic polysaccharides. Xylans might be an exception to this as the data for Xyl_2 suggested that xylans in eC were smaller than xylans in

hveC. Considering that Xyl and Xyl_2 were both Driselase digestion products from xylans it was surprising that they did not show the same median M_r. Xyl was the more reliable marker for xylan in this project as it was more reliably quantified.

Table 5 :Mean median relative molecular mass of hemicellulose plus pectin polysaccharides from SBP, experimental Currans and high viscosity experimental Currans.
This is the data visualised in Figure 33. Some data was excluded from the statistical analysis as they showed unusual elution profiles (cumulative percentage eluted). Excluded samples were: Glc components in HbP from A.2; Xyl2 from eC F; IP in SBP G; Man from SBP G and hveC H and GalA in HbP from SBP G.

	Mean median Mr of HbP polymers from preparations								
Driselase generated components	**SBP K, A, A.2, G**			**eC B-F**			**hveC H-J**		
	Mean	SEM	N	Mean	SEM	N	Mean	SEM	N
Glucose	25.3	2.2	3	7.7	0.7	5	5.2	0.4	3
Xylose	44.9	2.5	4	11.9	2.1	5	7.6	1.0	3
Xylobiose	56.3	14.6	3	6.8	0.6	4	8.2	1.2	3
Isoprimeverose	40.5	2.0	3	15.8	2.0	5	8.2	0.9	3
Mannose	8.3	0.9	2	8.8	1.4	5	6.0	0.0	1
Galactose	58.4	6.0	3	18.9	3.7	5	8.1	0.7	3
Arabinose	56.4	3.3	4	15.1	4.2	5	5.5	1.1	3
Galacturonic acid	42.7	7.6	4	14.7	4.4	5	6.4	0.8	3
Rhamnose	53.4	5.6	4	20.7	7.0	5	6.5	1.9	3

With the help of Figure 33 and the summary of the mean median relative molecular mass data in Table 5, I confirmed that the biggest polysaccharides found in HbP fractions were those containing Gal, Ara and Rha in SBP. All polysaccharides decreased in size during the production processes of eC (median M_r 5 – 32 kDa in HbP from eC) and even further in HbP from hveC (3 – 10 kDa) (excluding the data for Xyl_2 and Man). Xyl_2 and Man were successfully separated by paper chromatography, but the method for quantification was not sensitive enough to get satisfactory data.

The results obtained for both gel-permeation chromatography columns were comparable: eC B–F and M products were produced with the same production process and they showed a viscosity of 1520 – 1770 cP and 5640 cP respectively. No clear differences between their HbP polysaccharide compositions could be found, although eC M was of higher viscosity compared to eC B–F. eC N, R and S products were not produced using the normal production protocol (Table 2) but were either incompletely washed or did not get the sodium hypochlorite treatment. According to the data presented, these changes did not influence eCs' polysaccharide molecular mass. Finally, hveCs contained smaller hemicelluloses and pectins than all other eCs. All results summarised here would suggest that viscosity increased with decreasing

molecular mass of hemicelluloses and especially pectins (and the removal of the latter (§3.5)).

3.8 Water and polysaccharide samples exchange hydrogen atoms (H-exchange of polysaccharides with ^3H_2O)

The availability of –OH groups is important for the interaction of one material with another. eCs' viscosity in water is a good indication of how much their cellulosic networks interact with water. This work aimed to establish an easy method to semi-quantify –OH groups available for exchange with H_2O in eC and other carbohydrate materials. The proposed method (§2.10) is based on quantification of radioactivity (^3H) remaining bound to carbohydrate samples after removal of ^3H_2O by desiccation. To achieve this, several pre-experiments were conducted: time courses for drying and incubation (penetration of ^3H_2O into the sample) (§2.10.3 and §2.10.4), addition of different desiccants during drying (§2.10.2.1), adjustment of water and solid contents inside the desiccator (§2.10.1), changes of materials (§2.10.2) and drying devices (§2.10.5) and controlled exposure to atmosphere.

If not otherwise stated, the following step was done to all samples that had just been dried from ^3H_2O (or H_2O in the case of "cold" non-radioactive controls) and is therefore not stated again: An excess of water (1 ml) (or 3 M NaOH (0.5 ml) in the case of the later experiments) was added to the dried samples to stop exchange with atmospheric water vapour and for overnight swelling (in a sealed vial to avoid exchange with atmospheric H_2O). This excess volume for swelling was a crucial step to re-exchange bound ^3H back into solution and the scintillation fluid for full quantification of the samples' radioactivity. NaOH was then acidified with 0.5 ml 35% (v/v) HOAc. To all samples in acidified NaOH or water ten volumes of scintillation fluid were added and mixed for minimally 5 h before radioactivity was measured in a scintillation counter (§2.11).

The method that was finally established is described in §2.10. Here, I will first present (§3.8.2–§3.8.5) the steps that led to that method. The final method was then used (§3.8.6.2 and §3.8.6.3) to measure the availability –OH groups in eC products and carbohydrate controls.

3.8.1 Summary of the exchange of hydrogens between –OH groups of carbohydrate samples and ^3H_2O

This work established a sensitive method to semi-quantify exchangeable hydrogens in –OH groups of carbohydrate controls and eC samples. Incubation of carbohydrate samples with ^3H_2O resulted in an almost instantaneous exchange of ^3H from ^3H_2O with H atoms from samples (§3.8.2). Incubation time was therefore set to 0.5 h. Radioactivity remaining bound to dry samples decreased the longer they were dried in the desiccator (§3.8.3). This was independent of the material and especially observed for eC samples (§3.8.6) (which are known to retain residual water even after drying at 80°C). Several materials that additionally interfered and lowered radioactivity (such as plastic scintillation vials and desiccants) were excluded from the desiccator (§3.8.4). Four different desiccants were tested but none proved to be beneficial to the drying process. Exposure to the atmosphere critically and rapidly lowered the measured radioactivity in previously dried samples and was kept at a constant minimum of 45–60 seconds (§3.8.5). This was achieved by replacing Vaseline grease with high vacuum grease which enabled me to open the desiccator quickly. “Cold” carbohydrate samples dried together with “hot” samples became radioactive by exchanging H atoms with ^3H from the (thin) atmosphere inside the desiccator. Nevertheless, ‘”hot” paper ended up with slightly more radioactivity than “cold” paper (Figure 35), showing that the direct contact with liquid ^3H_2O had led to higher remaining bound radioactivity. NaOH swelled eC samples reasonably well and was used instead of water to bring the ^3H out of the polysaccharides while stopping exposure to atmospheric water vapour after drying. Drying with a ^3H_2O trap resulted in higher remaining bound radioactivity (‘% ^3H retained’) than without a trap (§3.8.6.2). The highest percentage ^3H retained after drying off ^3H_2O was found for xyloglucan (180–239% of the ^3H expected to be retained by a theoretical xyloglucan sample of the same weight (§3.8.6.1)). SBP resulted in 91–158% of the ^3H expected to be retained by a theoretical cellulose sample of the same dry weight (higher percentages due to drying with a ^3H_2O trap). Increasing percentages of ^3H retained in eC samples was related to increasing viscosity (significant data from samples dried with a ^3H_2O trap) (§3.8.6.3). hveC samples resulted in the highest percentages of ^3H retained and hence the highest number of available –OH groups among all eC samples; the percentage of ^3H retained was as high as the one found for ‘never-dried cellulose’. Normally produced eC samples showed similar availability of –OH groups to SBP. This proves that the availability of –OH groups is not simply increased due to the

action of oxidising chemicals on SBP during the production of eC. In fact, it requires increased concentrations (§2.1) of oxidising chemicals to achieve higher availability of –OH groups and increased viscosity.

The established protocol to semi-quantify the available –OH groups was sensitive to changes in drying time, exposure to atmosphere after drying as well as to changes in quantities of water, solids and radioactivity in the desiccator. Additionally, drying with or without a $^{3}H_2O$ trap influenced the percentage ^{3}H retained. All these influencing factors will in the future need to be studied further to establish a method for measurement of the absolute number of available –OH groups and exchanged H atoms. However, the established method in this work is an initial step towards this goal and can already be used to compare the relative availability of –OH groups in the same material.

3.8.2 The exchange of cellulosic oxygen-bonded H atoms with $^{3}H_2O$ is instantaneous but radioactivity is transferred through the atmosphere in the desiccator

For complete exchange between ^{3}H from $^{3}H_2O$ and the O-bonded H atoms of carbohydrate samples the optimal incubation time had to be determined. The incubation time courses conducted led to the conclusion that the exchange was practically instantaneous.

Carbohydrate samples in water, such as Whatman paper No.1 (henceforth called paper), Glc and MCC (in 110 µl water) were mixed with 20 kBq $^{3}H_2O$ (“hot”). “Cold” controls were mixed with the same volume of H_2O instead of $^{3}H_2O$. The samples were left for incubation at room temperature for different time periods (0–32 h) and fully dried together in a SpeedVac. The radioactivity remaining bound to the dry carbohydrate samples was measured and found to be independent of the incubation time (data not shown). The results also revealed that “cold” samples (dried together with “hot” samples) became radioactive during the drying process. The experiment displayed an instant exchange of ^{3}H from $^{3}H_2O$ and the H atoms in the “cold” and “hot” carbohydrate samples. This indicated that ^{3}H was transferred from “hot” to “cold” samples through the atmosphere inside the SpeedVac. After drying, the SpeedVac was found to be contaminated with ^{3}H and had to be cleaned to remove all traces of radioactivity. The SpeedVac was consequently deemed to be unsuitable for drying of radioactive $^{3}H_2O$ samples.

A new drying device was found by attaching a glass desiccator to a Genevac CVP 100 pump (§2.10). The glass desiccator contained an excess of molecular sieve rods (desiccant, §2.10.2.1) in the bottom of the desiccator and a ceramic stage (between samples and desiccant) and was greased with Vaseline (for an airtight seal). This desiccator-pump drying system also resulted in transfer of radioactivity from "hot" to "cold" samples (Glc, paper, Avicel and MCC) dried at the same time (data not shown). A second incubation time course experiment confirmed the instant exchange of H atoms between ^3H_2O and all carbohydrate samples. Furthermore, it showed highest radioactivity remaining bound to dried Glc (compared with MCC, Avicel, and paper) (data not shown). Glc samples never fully dried but formed a syrup-like film (meaning the water was not fully removed and some ^3H_2O would still be present). Indeed, dried Glc solutions were 17.4 ±1.1% heavier than what was expected from completely dry Glc. It could be expected that radioactivity of dried Glc increases by the same percentage.

As longer incubation with ^3H_2O did not influence radioactivity remaining bound to the dry samples, a constant incubation period of carbohydrate plus ^3H_2O of 0.5 h prior to drying was chosen for all following experiments (unless otherwise stated).

3.8.3 Prolonged drying led to a gradual loss of remaining bound radioactivity from dry samples

A drying time course of paper, Glc and MCC samples (3.5–24 h, the drying process being interrupted briefly to take out the respective samples) showed a loss of radioactivity from all dry carbohydrate samples over time (data not shown). To find the source of this loss, a new drying approach was tested in which ^3H_2O or H_2O was applied to glass fibre papers (non-carbohydrate) and paper pinned onto an aluminium covered polystyrene disk without touching each other. After successfully drying the samples from ^3H_2O or H_2O, both "hot" and "cold" paper still possessed radioactivity while the glass fibre papers only showed background radioactivity (data not shown). This proved that glass fibre papers were suitable as an almost inert surface for removing ^3H_2O from carbohydrate samples. The Genevac CVP 100 pump broke after these drying experiments and was replaced with the Diaphragm pump MPC 095 Z. A drying time course of 2–48 h with the new pump was done on "hot" samples (Glc, MCC and ^3H_2O each on separate glass fibre papers) and "cold" paper in the same desiccator. The ^3H_2O glass fibre controls only showed the expected background radioactivity after only 2 h drying (constant for 48 h). However, all carbohydrate

samples lost more radioactivity the longer they were dried (data not shown). The loss upon drying could not be prevented through any adjustment to the experiment; it was therefore considered an unwelcome (but constant) side-effect of the method.

3.8.4 Materials and vials added to the desiccator bind and might release ^3H_2O or H_2O

Drying carbohydrate samples (e.g. MCC) on flat glass fibre papers proved difficult as some dried powdered material was lost during release of the vacuum and transfer of the filters into plastic scintillation vials. Glass fibre papers were therefore replaced with plastic scintillation vials, whose plastic itself proved to retain a higher background radioactivity (100-200 cpm). Replacing plastic vials with glass scintillation vials resulted in a much lower background reading (28–44 cpm).

Drying paper, MCC and Glc in glass scintillation vials did not yield reproducible results and it was proposed that the molecular sieve rods, added to the bottom of the desiccator, could potentially adsorb or release ^3H_2O. This would thereby lead to an increased amount of available H atoms and reduce the specific radioactivity of the ^3H atoms. Molecular sieve rods were consequently not used in the desiccator. The experiments performed without a desiccant did not lead to reproducible results either (data not shown) and radioactivity of dried samples still decreased upon longer drying. Hence, more inert desiccants were tested (§2.10.2.1) (data not shown): drying in the presence of phosphorus pentoxide resulted in slightly higher radioactivity (than without a desiccant) of the dried carbohydrate samples whereas calcium oxide was comparable to drying without a desiccant. Another drying time course without desiccant (24–48 h) resulted in lower radioactivity for Glc (than what was observed earlier) upon longer drying but higher radioactivity for MCC and paper. This was unexpected and not reproducible. The lids of the glass scintillation vials were made of hard plastic, with an aluminium foil and cork liner which proved difficult to decontaminate (producing high and varied background radioactivity (data not shown)). They were eventually replaced with glass liquid scintillation vials with polypropylene caps (lined with polyethylene foam). These were easy to clean and produced rather consistent radioactivity backgrounds.

To remove as many sources of additional interfering H atoms as possible, most following experiments were conducted without desiccants (unless otherwise stated). Moreover, the porcelain stage was taken out of the desiccator and old glass scintillation vials were replaced with new ones (plus new lids).

To understand why replicated experiments produced irreproducible results, I next tested the interaction of atmosphere with radioactive samples.

3.8.5 Exposure to the atmosphere caused rapid loss of radioactivity from dry samples

Glc and paper incubated with ^3H_2O were fully dried and then exposed to atmosphere for different periods of time. This experiment (Figure 34) demonstrated that the exposure to atmosphere caused a substantial decrease in radioactivity of dried tritiated paper and Glc.

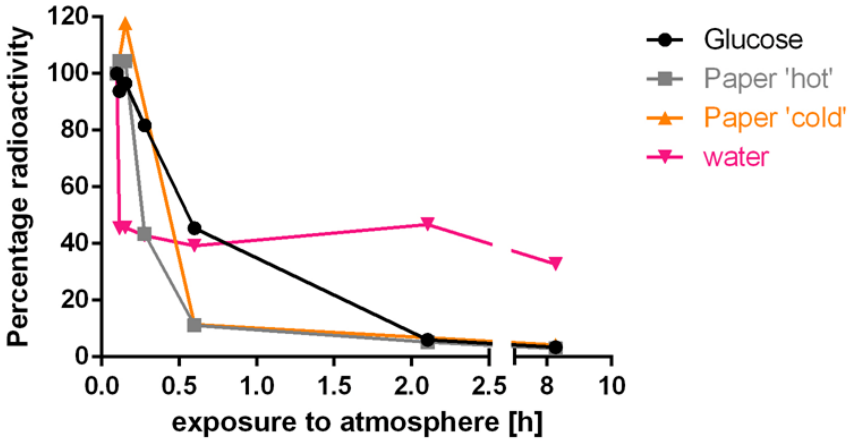

Figure 34: Loss of ^3H during exposure of dried radioactive samples to the atmosphere.
Glc, paper and an empty glass vial ('water') were incubated with 20 kBq ^3H_2O for 0.5 h (H_2O was added to 'paper cold' instead of ^3H_2O). All samples were dried for 48 h together in a glass desiccator connected to a vacuum pump. Dry samples were then exposed to the atmosphere, for different periods of time (0.1–8.3 h). Exposure was stopped by the addition of water to each sample and the vial was tightly sealed. Radioactivity was measured and recorded as a percentage of the initial radioactivity measured at 0.1 h: Glc 56900 cpm/ 10 mg Glc, 'paper hot' 5960 cpm/ 10 mg paper, 'paper cold' 5410 cpm/ 10 mg paper and water 71 cpm/ vial.

The highest radioactivity was measured after 0.1 h (with one outlier for paper "cold" at 0.15 h). Six minutes (0.1 h) was the time it took to release the vacuum, open the desiccator and add water to the samples. All samples lost radioactivity the longer they were exposed to atmosphere. The water control (glass scintillation vials dried from ^3H_2O) lost 58% of their initial low radioactivity (little higher than background radioactivity) after 0.6 h but then displayed almost constant background radioactivity. Radioactivity of "hot" and "cold" paper as well as the loss thereof were almost identical (after 0.6 h both had decreased to 11%). Glc in contrast to paper retained 46% of its initial radioactivity after 0.6 h exposure to atmosphere; all samples could only hold 3–8% of the initial radioactivity after 8.3 h exposure to atmosphere (papers and water were then only showing background radioactivity). In repeat experiments it was

possible to further minimise exposure to the atmosphere to 2–4 min instead of 6 min between releasing the vacuum and getting the samples into the ‘quenching’ water. Nonetheless, the radioactivity measurements were not reproducible (i.e. the radioactivity measured for paper dried for the same amount of time in one experiment was only 200 cpm/ 10 mg and in the next 6000 cpm/ 10 mg).

The results demonstrated that ^{3}H was not tightly bound to the dried carbohydrate samples and could readily re-exchange with H atoms in the atmosphere leading to high loss of radioactivity. This process was highly dependent on the time that samples were exposed to the atmosphere (the first minutes or seconds being of major importance) and the drying time. I found that keeping the time of exposure to the atmosphere minimal and approximately constant (3–5 min), after a drying period of 4, 8 or 16 h, did not prevent the loss of radioactivity (Figure 35). Under the newly introduced conditions (no porcelain stage, new glass scintillation vials and controlled exposure to atmosphere), three desiccants were again tested to dry “hot” paper.

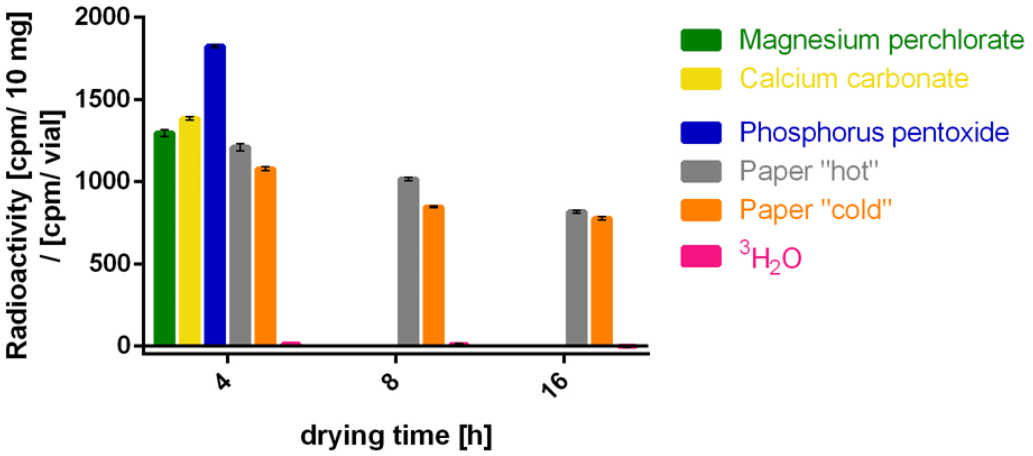

Figure 35: Drying time course of paper and $^{3}H_2O$ with and without desiccant.
Radioactivity is given in cpm/ 10 mg dried paper and in cpm/ vial for the dried $^{3}H_2O$ control (pink bars). $^{3}H_2O$, “hot” and “cold” paper were dried for 4, 8 and 16 h without desiccant; after drying, the exposure to atmosphere was stopped within 3–5 min by the addition of 1 ml water (this was the time required to open the desiccator lid and “quench” the samples in 1 ml water). Green, yellow and blue bars represent “Hot” papers that were individually dried with one desiccant for 4 h, after which the exposure to atmosphere was stopped within 1–3 min. The desiccants used were magnesium perchlorate, calcium oxide and phosphorus pentoxide respectively. Error bars present SEM, N=3.

The $^{3}H_2O$ control in the glass vial showed background radioactivity and was fully dry after 4, 8 and 16 h so it was expected that all paper samples had also dried sufficiently

(with and without desiccant). “Hot” paper was slightly but significantly higher in the remaining radioactivity (P values 0.0001–0.0337) than “cold” paper samples when dried without a desiccant. Moreover “cold” and “hot” paper samples showed significant decrease in radioactivity the longer they were dried. All three desiccants and no desiccant resulted in significantly different radioactivity remaining bound to “hot” paper (P values 0.0001–0.0466). Drying with phosphorus pentoxide resulted in “hot” papers with much higher radioactivity than the other two desiccants or no desiccant. To test why this happened, the drying experiments with desiccants need to be repeated (including different amounts of desiccant in the desiccator). Overall, radioactivity of “hot” paper dried for 4 h (with and without desiccant) was between 1210 and 1825 cpm/ 10 mg paper. This was much lower than what was measured earlier (5960 cpm/ 10 mg paper, Figure 34) but in contrast to that earlier high radioactivity, these lower radioactivity results were reproducible and therefore verifiable.

After drying “hot” paper for 4 h with and without one of the three desiccants, the paper samples were quickly (to prevent long atmospheric exposure of the desiccants) replaced with “cold” dry paper which was then dried for 2 h. This was done to test whether the three desiccants or the desiccator itself could release $^{3}H_2O$ which could then be picked up by “cold” dry paper. Indeed, “cold” dry paper became slightly radioactive with and without a ‘used’ desiccant in the desiccator (49–199 cpm/ 10 mg paper). Thus, ‘used’ desiccants, and even to some extent a recently ‘used’ desiccator, evidently harboured ^{3}H, some of which could subsequently be released (presumably as $^{3}H_2O$ vapour) and re-adsorbed by previously non-radioactive paper. No desiccant, phosphorus pentoxide and magnesium perchlorate all resulted in low radioactivity (49–61 cpm/ 10 mg paper). The significantly higher radioactivity was measured for “cold” paper dried with calcium oxide (199 cpm/ 10 mg paper, $P < 0.0001$). This was undesired and as the use of desiccants did not clearly benefit the drying process, they were excluded from the desiccator for all following experiments.

Exposure of the samples to the atmosphere needed to be further reduced as it posed a high potential for losing radioactivity from dried samples. Henceforth, Vaseline was replaced with high vacuum grease which enabled me to open the desiccator quicker and limit the exposure of samples to the atmosphere to a maximum of 60 seconds. As expected, this replacement resulted in higher retention of radioactivity when hot

papers were dried without desiccant (“hot” paper 1473 cpm/ 10 mg paper) than measured before.

A second approach to measure interaction of atmospheric water vapour with dry paper was to test the weight gain of “cold” dry paper when re-exposed to the atmosphere (Figure 36).

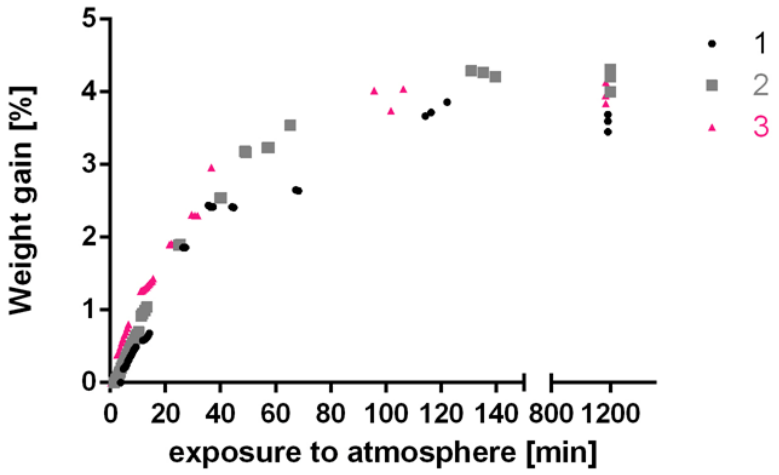

Figure 36: Recorded weight gain of dried paper when re-exposed to the atmosphere.
Dry papers (samples 1, 2 and 3, each approximately 140 mg as received from the supplier) were re-dried thoroughly in the desiccator for 4 h and then re-exposed to the atmosphere for 0–1200 min. The weight change was recorded during exposure to atmosphere; it is expressed as weight gain in % of the initial dry weight.

The weight gain of the dried papers was not recorded during the first minute after opening the desiccator, so the initial dry weight was recorded after 1 min of exposure to atmosphere. During the first 10 min weight increase followed a linear trend but saturated over time and plateaued after 140 min. This experiment confirmed that dried paper quickly interacts with the atmosphere, which especially the first minutes (or seconds) could significantly influence the results.

The experimental method established up to this point was thus:

1. Three carbohydrate samples (most often paper) exposed to 20 kBq $^{3}H_2O$; one $^{3}H_2O$ control and one empty scintillation vial were individually incubated in sealed vials for 0.5 h;
2. All five vials were then dried (together) in a glass desiccator (greased with high vacuum grease to seal off air leaks) connected to a strong vacuum pump for a variable time (2–16 h);

3. exposure to atmosphere (45–60 seconds) was stopped by the addition of 1 ml water.

Radioactivity of carbohydrate samples still decreased with increasing drying time in step (2). When the drying time and the exposure to atmosphere was kept approximately constant the radioactivity results were reproducible.

Most experiments so far had been done with paper as carbohydrate samples. The next experiments were therefore performed with eC suspensions to optimise the methodology for analysis of eC products.

3.8.6 viscosity increases with increasing –OH group availability in experimental Currans

eC products were provided by CelluComp Ltd. in the form of pastes, grated shavings or dried sheets (details see Table 2 and §2.10.1). The products were ground with water into uniform suspensions. A uniform suspension was not accomplished for eC T and Z, which were provided as dried sheets. Although the dry weight content of the original eC products was reported by CelluComp Ltd. (and could therefore be used to calculate solid concentrations of eC suspensions), a portion of each suspension was freeze-dried or dried on a moisture analyser to independently determine the solid content. Solid contents were therefore determined by three different methods and the results were presented in §3.8.6.4.

The following list gives an overview of the eC products tested by the ^3H_2O method and their viscosities (details in Table 2). They are sorted into three groups which differ in production processes, the last group (named ‘changed production process eC’) briefly refers to the changes that were done to the normal production process (§2.1).

- Normally produced eC products (640–1770 cP) (in order of increasing viscosity)
    - eC E’ (product of E after 6 month storage), 640 cP
    - eC B’ (product of B after 6 month storage), 720 cP
    - eC F’ (product of F after 6 month storage), 1080 cP
    - eC X (from SBP from a new distributor), 1250 cP
    - eC W (from SBP from a new distributor), 1280 cP
    - eC B and B.B, 1520 cP
    - eC C and C.C, 1580 cP
    - eC D, 1710 cP

    - eC E, 1740 cP
    - eC F, 1770 cP
- hveC: produced with increased concentrations of H_2O_2 and sodium hypochlorite (5400–8620 cP)
    - hveC V, 4020 cP
    - hveC V', 4320 cP
    - hveC H, 5400 cP
    - hveC I, 6220 cP
    - hveC J, 8620 cP
- changed production process eC (116–1280 cP)
    - eC T (freeze-dried), 116 cP
    - eC U (no sodium hypochlorite treatment), 1310 cP
    - eC Y (incompletely washed from H_2O_2, no sodium hypochlorite treatment), 460 cP
    - eC Z (drum-dried), 143 cP

Approximately 10 mg dry weight (from samples and controls) was used in each experiment (the exact dry weight was recorded for each sample). They were incubated in different volumes of ^3H_2O (also recorded per sample). All suspensions in ^3H_2O (approximately 550 mg fresh weight) were uniformly dispersed on the flat bottom (approximately 4.5 cm^2) of tared glass scintillation vials. They dried into a thin, rigid film in the desiccator. After drying, 500 µl of 3 M NaOH was added to swell samples in a sealed vial overnight and 500 µl of 35 % HOAc slightly acidified these samples. The swollen eC samples then formed a flexible, gel-like film. To each acidified sample ten volumes of scintillation fluid were added and rotated for 5–8 h before measuring radioactivity in a scintillation counter.

To verify if the established methodology was effective to test the availability of –OH groups in eC samples, the optimal incubation and drying time had to be investigated.

eC B suspensions were incubated with ^3H_2O for 0.5, 0.75 or 1 h and dried for 6.7 h. The different incubation times did not lead to significant differences in radioactivity (data not shown). As it had been determined previously for paper, MCC and Glc, the exchange of H atoms between ^3H_2O and eC samples was practically instantaneous.

Tritiated eC B samples were continuously dried (without interruption) for 4–17 h and again longer drying resulted in a decrease of radioactivity. All samples appeared fully

dry after 4 h and radioactivity of eC B decreased upon longer drying at a linear rate (data not shown). A drying time of 8 h was chosen for all the following experiments. It is possible that eC samples did not fully dry even after 17 h and might hold on to residual ^3H_2O. This possibility was even more likely, as eC that was dried at 80°C still contained approximately 10% residual water (personal communication from CelluComp Ltd.). For the purpose of the current work, it is assumed that even if ^3H_2O was still present in the samples it would be similar to all other eC samples and lead to comparable results.

Increasing the number of samples in the desiccator three-fold (and thereby the amount of carbohydrate and water) led to incomplete drying within 8 h. The number of samples, amounts of solids and water were henceforth kept to three samples of standard size, one ^3H_2O control and one empty vial (for background radioactivity).

These latter experiments again confirmed how sensitive the method was to changes of the chosen drying period and the amount of water or solids in the desiccator at a time. Great care was taken to ensure that water and solid concentrations, the drying period and the exposure to atmosphere after drying were kept relatively constant throughout the experiments.

Two experiments were set up to test a wide range of controls and eC samples:

Experiments with a ^3H_2O trap: The desiccator was connected to the pump via a glass vessel filled with the desiccant molecular sieve rods; this was done in an attempt to prevent possible contamination of the pump with condensed ^3H_2O.

Experiments without a ^3H_2O trap: The ^3H_2O trap was removed from these repeat experiments in case the desiccant could potentially release ^3H_2O back to the samples in the desiccator, even though that would be against the direction of the pump flow. Only normally produced eC (without B, W and X) and hveC samples were included in this experiment besides all controls.

The total water content in the desiccator connected to a ^3H_2O trap was approximately 2.4 g and without the trap 2.3 g. Typically, this comprised 0.55–0.65 g ^3H_2O in each of the three eC samples (less for some controls) plus 0.65 g ^3H_2O in the ^3H_2O blank. The carbohydrate dry weight inside the desiccator was also kept constant: with a ^3H_2O trap approximately 37.9 mg and without the trap 35.2 mg dry weight. Thus, on average 11.7–12.7 mg solids per sample (three different samples) were present in

the desiccator. To all three samples dried together, the same concentration of radioactive stock ^3H_2O was added which led to different specific radioactivities (SA) as the amount of water in each sample was not constant. I added 16.0 kBq ^3H_2O to each sample dried with a ^3H_2O trap. Samples in experiments dried without a ^3H_2O trap were incubated with 14.4–103.8 kBq.

A suspension of SBP G (approximately 12 mg solids; the exact mass of each sample was recorded) in a total of approximately 0.60 g water was incubated with three different SA (0.23 (three replicates), 0.35 and 1.97 kBq/mmol H) and showed that, as expected, radioactivity retained within the carbohydrate increased with increasing SA of ^3H_2O (Figure 37).

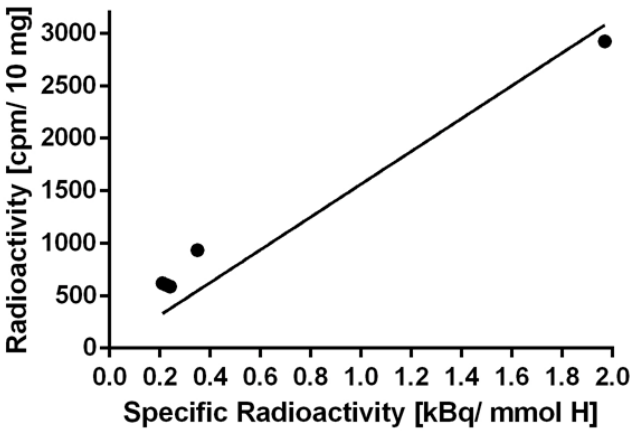

Figure 37: Relationship between radioactivity retained in dried SBP G and the specific radioactivity of ^3H_2O added for incubation.
SBP G (approximately 12 mg solids; the exact mass of each sample was recorded) was incubated in a total of~ 0.60 g ^3H_2O with three different SA for 0.5 h and then dried for 8 h in a desiccator connected to a vacuum pump (without a trap). The linear regression line can be described as: Radioactivity [cpm/10 mg] = 1564 × kBq/ mmol H.

Radioactivity retained in the dried SBP G increased linearly with the SA of the ^3H_2O (calculated based on the total water content per sample, i.e. that in the eC suspension plus that in the added ^3H_2O) in which the SBP was incubated. Other dried samples also increased in retained radioactivity after incubation with higher SA of ^3H_2O (data not shown), but these were only tested with two different SA and few replicates.

Due to the dependence of retained radioactivity on the SA of ^3H_2O incubated with each sample, all subsequent results are presented as a percentage (called percentage ^3H retained): the measured radioactivity of the retained ^3H/ the ^3H expected to be retained in each sample (§3.8.6.1).

3.8.6.1 *Calculating and the availability of –OH groups and the expected ^{3}H retained by each carbohydrate sample*

The exact number of available –OH groups present in all these carbohydrate samples was unknown except for the monomer Glc. The expected radioactivity of 10 mg Glc after incubation in 14.1 kBq $^{3}H_2O$ of a total volume 120 µl (SA of 1.050 kBq/mmol H in $^{3}H_2O$) was 0.286 kBq (detailed calculations in Box 1). It is therefore predicted that, incubated in the same SA, 10 mg cellulose (possessing two exchangeable H atoms per Glc residue (§1.5)) results in approximately 0.130 kBq, dextran (three exchangeable H atoms per Glc residue) in 0.193 kBq and xyloglucan (2.625 exchangeable H atoms per residue) in 0.181 kBq. Analysis of SBP and eC preparations (§3.5) revealed that cellulose was the major carbohydrate in these samples mixed with some hemicelluloses and pectins; the true number of available –OH groups was hence unknown. For simplification, SBP and eC are therefore considered to have the same number of accessible –OH groups as cellulose and would also result in 0.130 kBq. For controls (paper, never-dried cellulose, dried cellulose, MCC and Avicel) the same radioactivity was predicted (due to the lack of further information and for simplification).

Box 1: How the ^3H expected to be retained in glucose, cellulose and xyloglucan from 14 kBq ^3H_2O can be calculated.

The expected radioactivity bound by 10 mg Glc when incubated with, for example, 120 µl ^3H_2O containing 14 kBq was calculated as follows: 10 mg Glc contains 0.0556 mmol Glc (molecular weight 180), and each Glc molecule possesses five –OH groups, all available for exchange with ^3H_2O. Hence, 10 mg Glc contain 0.2777 mmol exchangeable (O-bonded) H atoms. The other seven H atoms of Glc ($C_6H_{12}O_6$) are C-bonded and cannot exchange with those of H_2O. A total volume of 120 µl ^3H_2O (equal to 120 mg as the SA of the water was too low for the ^3H to considerably change its density, assumed to be 1.000 mg/µl) corresponds to 6.667 mmol H_2O (or 13.3333 mmol H atoms, all exchangeable). Hence, the SA of the H atoms in the ^3H_2O used in this example was 14 kBq/ 13.333 mmol H = 1.050 kBq/ mmol H. The total exchangeable H in 120 mg H_2O (13.3333 mmol H) plus 10 mg Glc (0.2777 mmol H) was thus 13.6111 mmol exchangeable H. The ^3H atoms are assumed to have distributed themselves between the water and the glucose indiscriminately, therefore making 0.2777 mmol H in Glc/13.6111 mmol total H = 2.041% of the ^3H in Glc. Thus, the predicted ^3H remaining bonded (in the form of –O^{3}H groups) to the 10 mg Glc after drying was 2.04% of the initial 14 kBq, or 0.286 kBq.

There are some differences for calculating the expected radioactivity bound by 10 mg cellulose when incubated with the same SA. Cellulose is a polysaccharide of Glc residues (§1.3.2.1); two of the five O atoms that would have been –OH groups in a free Glc molecule are tied up participating in glycosidic bonds in cellulose, and hence do not have H atoms attached. The contribution of the free –OH group at C-4 of the non-reducing terminus and C-1 of the reducing terminus of the polysaccharide is negligible; for simplification, the calculation will therefore regard the cellulose in 10 mg as a single molecule with no termini. Furthermore, one OH group per cellulosic Glc residue was reported to be unavailable for exchange (Lindh *et al.* 2016); therefore only two H atoms per cellulosic Glc residue (molecular weight 162) were expected to exchange with ^3H from ^3H_2O. The calculation therefore is: 0.1235 mmol H exchangeable in cellulose/ 13.4568 mmol H total = 0.917% of the initial 14 kBq, or 0.130 kBq as a maximum theoretical value. However, some of the cellulosic Glc residues are predicted to be buried within the semi-crystalline microfibril and therefore to possess no exchangeable H atoms; therefore, the amount of bound ^3H may be well below 0.130 kBq, and this is open to experimental testing by the method developed here.

For tamarind xyloglucan (§1.3.2.3) the average repeat unit composition was assumed to be 4 Glc, 3 Xyl and 1 Gal residue. Hexoses are expected to have three and pentoses two available –OH groups, this leads to an average of 2.625 exchangeable H atoms per residue. With the average molecular weight for xyloglucan (150.75) and the SA of 1.050 kBq/ mmol H the maximum expected bound radioactivity was determined to be 0.181 kBq for xyloglucan.

For each tested sample the expected ^{3}H exchanged (maximally exchangeable H atoms in each sample) and the measured ^{3}H retained were individually calculated (§6.5). The following gives an example calculation:

SBP A, 0.0106 g dry weight in 0.670 g $^{3}H_2O$ incubated with 103.8 kBq, dried without a $^{3}H_2O$ trap resulted in 3406 cpm (counted with an efficiency factor of 0.30): 0.0106 g dry weight/ (0.162 g/ mmol Glc residue) = 0.0654 mmol Glc residue (each with two available –OH groups) = 0.1309 mmol H in dry weight. 0.670 g $^{3}H_2O$/ (0.018 g/mmol H_2O) = 37.2222 mmol $^{3}H_2O$ (each with 2 available –OH groups) = 74.4444 mmol H in $^{3}H_2O$. 0.1309 mmol H in Glc/ 74.4444 mmol H in H_2O= 0.0018 (or 0.18%) of 103.8 kBq= 0.1825 kBq expected ^{3}H retained. For this sample 3406 cpm was measured (with an efficiency factor of 0.30) = 11353 dpm= 189.2 dps= 0.1892 kBq measured ^{3}H retained. The final calculation of (0.1825 kBq expected ^{3}H exchanged/ 0.1892 kBq measured ^{3}H retained) × 100% resulted in 103% ^{3}H retained in this specific SBP A sample.

3.8.6.2 *Measuring carbohydrate controls with the method developed here*

Glc, MCC, Avicel, xyloglucan, paper, SBP A and SBP G were carbohydrate controls included in experiments with and without a $^{3}H_2O$ trap (Figure 38). “Dried cellulose” and “never-dried cellulose” were only included in experiments without a $^{3}H_2O$ trap.

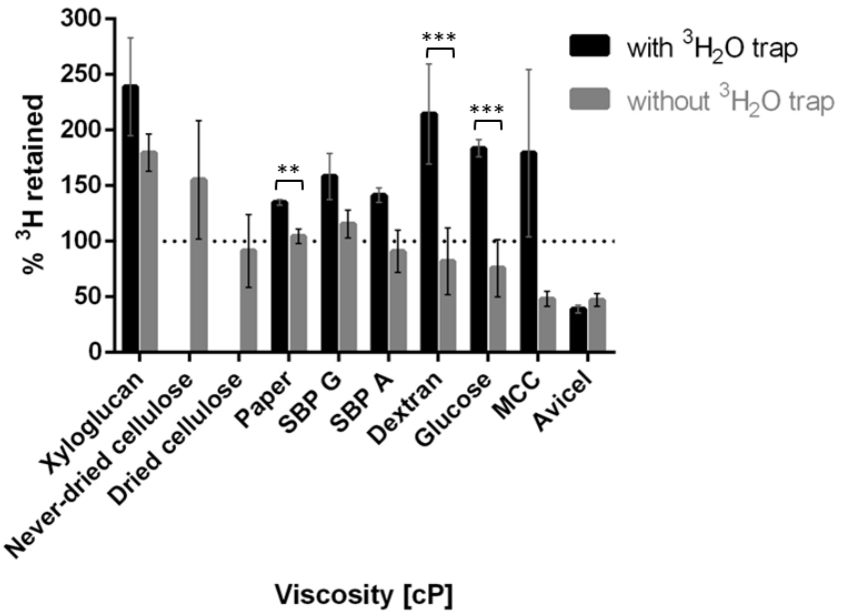

Figure 38: Percentage of the ^{3}H retained in each carbohydrate sample that was incubated with $^{3}H_2O$ and dried.
Different carbohydrate samples were incubated with $^{3}H_2O$ and dried for 8 h in a desiccator connected to a vacuum pump (with or without a $^{3}H_2O$ trap). The line at 100% represents the expected ^{3}H exchanged per sample (allowance being made for the different samples' numbers of expected ^{3}H exchanged). Error bars present SEM and N=3–5 (for details see §6.5). Some statistically significant differences in the t-test between samples dried with and without a $^{3}H_2O$ trap are marked with asterisks: **: P=<0.01; ***: P≤0.05.

These two drying experiments, dried with or without a $^{3}H_2O$ trap, resulted in significantly higher percentages of H retained for paper, dextran and Glc dried with a $^{3}H_2O$ trap. Avicel and MCC yielded 39–48% ^{3}H retained, except for MCC dried with a $^{3}H_2O$ trap (significantly higher, 179%) (this was unexpected, and no explanation can be provided at the time). Furthermore, higher percentages than expected were especially obtained for controls dried with a $^{3}H_2O$ trap. This might have resulted from $^{3}H_2O$ being released from the desiccant back into the desiccator (albeit against the pump flow). Another possible explanation would be that samples were insufficiently dried from $^{3}H_2O$. As seen before, Glc samples did not dry into a dry power but a syrup which still contained $^{3}H_2O$. Moreover, the maximum expected radioactivity (100%) for all cellulosic controls can only approximate the percentage of ^{3}H that can potentially be bound to these cellulose samples tested here. All tested samples (dried with and without a $^{3}H_2O$ trap) were additionally likely to lose some remaining bound radioactivity during the drying process inside the desiccator and upon exchange with the atmosphere while the desiccator was being opened, as observed in earlier experiments. Hence, the obtained results in both experiments resulted from a mixture

of influencing factors and are therefore only an approximation of the true number of H atoms that can be exchanged in each material. Nonetheless, most results, after drying controls without a ^3H_2O trap, were close to 100% ("dried cellulose", paper and SBP) or lower. Lower than 100% was expected for cellulosic materials that contained shielded or buried –OH groups (Box 1).

Xyloglucan showed 180–239% ^3H retained. This big discrepancy from 100% was not surprising, as it likely resulted from the assumptions and simplified calculations made. As xyloglucan in water is a viscous solution the drying process might have been insufficient to remove all ^3H_2O and the measured percentage hence resulted from exchanged H atoms and ^3H_2O retained.

Standard errors were rather high for some of the samples and should be reduced by increasing the sample size. Big error bars for experiments without a ^3H_2O trap may have been caused by the highly varied background radioactivity found for samples incubated with different specific radioactivities of ^3H_2O. The dried ^3H_2O and empty vial controls (dried with a ^3H_2O trap) showed radioactivity of 59.9 ±3.59 cpm and 41.6 ±1.98 cpm per vial respectively (the expected background radioactivity). However, the mean background radioactivity of empty vials in experiments without a ^3H_2O trap was doubled (75.9 ±9.83 cpm per vial) and ranged from 31 to 219 cpm per vial. This could not be explained thus far, but it underlines the sensitivity of the established method.

All the mentioned factors influencing the percentage of ^3H retained in a sample need to be considered when analysing eC samples and SBP controls. SBP resulted in 142–158% after drying with a trap but 91–116% without the trap; the results were similar to paper and dried cellulose. eC Samples were expected to show higher percentages if the polymer network was made more accessible during the production process and allowed for more interaction (and exchange) with water.

3.8.6.3 *The viscosity of experimental Curran increases with greater availability of –OH groups*

The percentage of ^3H retained in eC samples also showed dependence on drying with or without a ^3H_2O trap (Figure 39).

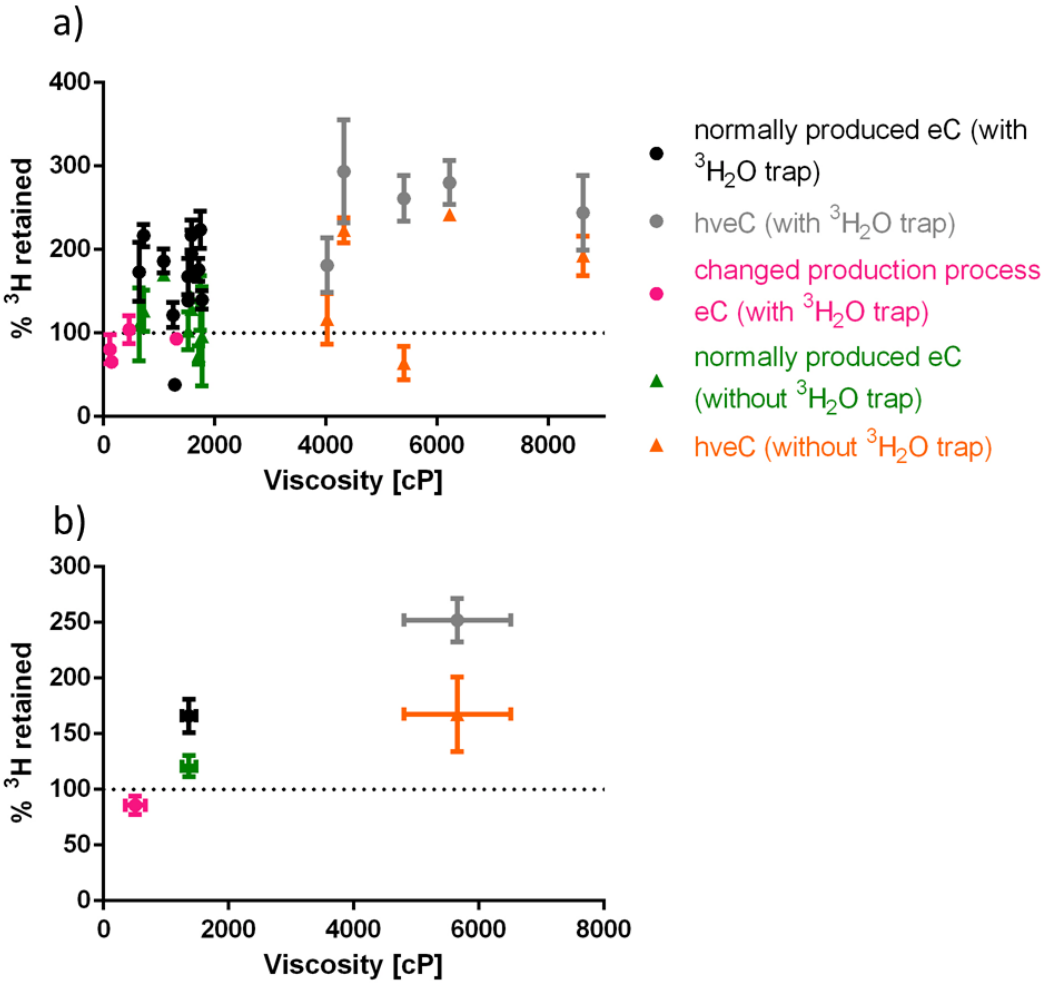

Figure 39: Percentage ^3H retained in each experimental Curran sample.
eC Samples used in the two drying experiments were: normally produced eC (black and green), hveC (grey and orange) and changed production process eC (pink). All samples were incubated with ^3H_2O and dried for 8 h. One experimental setup included a ^3H_2O trap (data marked in black, grey and pink); for the other experiments the trap was removed and most of the normally produced eC and hveC samples (green and orange) were tested again. (a) Measurements taken for each sample; as a visual reference 100% (expected radioactivity bound by the same dry weight of theoretical cellulose) is shown as a line. Error bars represent SEM, N=2–5 (for details see §6.5). (b) The mean percentage (H exchanged) and viscosity of each group dried with or without a ^3H_2O trap are presented. Error bars represent SEM, N=4–12 sample means.

Figure 39a portrays the percentage of ^3H retained that was calculated for each sample dried with and without a ^3H_2O trap. With each samples' mean the same was calculated for each of the five groups (Figure 39b) (normally produced eC, hveC (both dried with and without a ^3H_2O trap) and 'changed production process eC' dried with a ^3H_2O trap). Drying with a ^3H_2O trap generally led to a higher percentage ^3H retained compared to samples dried without a ^3H_2O trap (as already observed for controls, Figure 38). This was also mirrored by the means calculated for each group: Normally produced eC

dried with a ^3H_2O trap retained significantly higher ^3H percentages than eC dried without a ^3H_2O trap (P value 0.029). hveC Were not significantly different after drying with or without a ^3H_2O trap. Most interesting was that, when dried with a ^3H_2O trap, the percentage ^3H retained for the group 'changed production process eC' was significantly lower than for normally produced eC (P 0.010) which was itself significantly lower than for hveC (P 0.006). This leads to the prediction that the number of available and exchanged H atoms in an eC product increases with increasing viscosity of the product. The same trend was also observed between normally produced eC and hveC dried without a ^3H_2O trap, but the difference was not significant (P 0.113).

The percentage ^3H retained in hveC samples, after drying without a trap, was comparable to never-dried cellulose (Figure 38, second highest control sample). When dried with a trap, it was higher than dextran (second highest control sample here). In contrast to the hveC samples, all normally produced eC showed similar exchange of H atoms to SBP; eC produced with changed production processes led to percentages lower than then ones found for SBP. This proves that the availability of –OH groups is not simply increased due to the action of oxidising chemicals on SBP during the production of eC. In fact, it requires increased concentrations (§2.1) of oxidising chemicals to achieve higher availability of –OH groups and increased viscosity.

Detailed results for each sample among the five groups can be found in Figure 40.

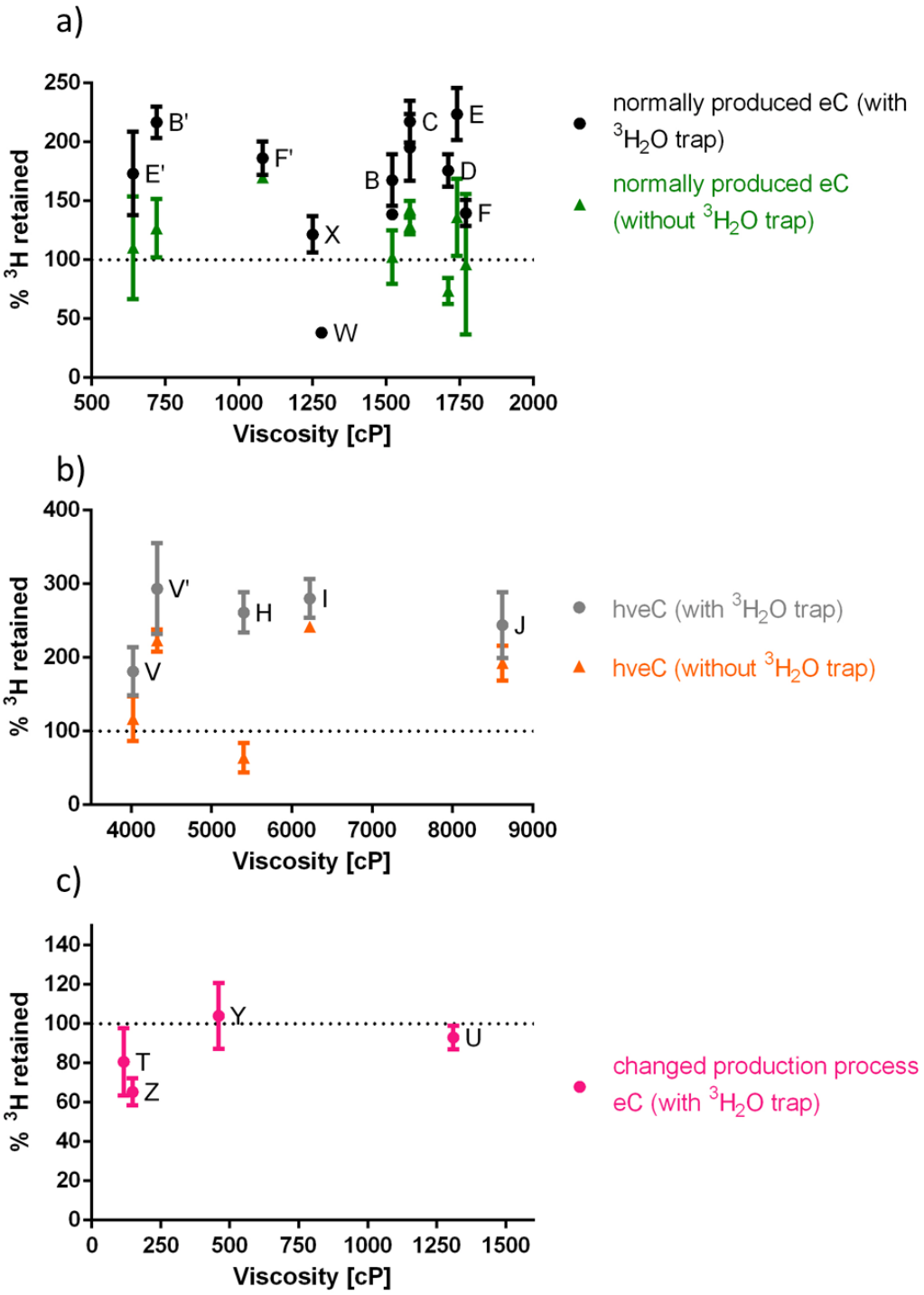

Figure 40: Percentage ^3H retained in each experimental Curran sample incubated with ^3H_2O and dried with and without a ^3H_2O trap.
(a) ^3H retained in normally produced eC; eC B, W and X were not tested without a ^3H_2O trap. Both viscosity replicates (eC B and B.B) and (eC C and C.C) were marked by 'B' and 'C' respectively. (b) ^3H retained in hveC samples. (c) ^3H retained in changed production process eC and dried with a ^3H_2O trap. Error bars represent SEM, N=2–5 (§6.5).

The detailed presentation of the single samples confirmed that drying with a ^3H_2O trap most often resulted in higher percentage ^3H retained than drying without a ^3H_2O trap; the difference between eC B', C, D and H samples was significant (P 0.033, 0.018, 0.005 and 0.001 respectively). The observed differences between the two drying methods did not follow a recognisable pattern (also observed for some controls; Figure 38). Hence, the reasons for these differences cannot be fully explained.

The four samples B', E', F' and V', produced from their respective eC products after a storage period of up to six months, were not all higher or lower than the starting eC product. Only V' was significantly higher in percentage ^3H retained than V (after drying without a trap (P 0.038)) (additionally viscosity of V' was unexpectantly 300 cP higher than the starting material V (might have been caused by non-uniform blending or an unintended higher solid concentration during viscosity measurement). The number of available H atoms for exchange did not seem to correlate with the decreased viscosity introduced after storage of the eC product.

Two normally produced eC (W and X) were products from SBP from a different distributor; these two were low in viscosity (only higher than the replicates of the products that had been stored for six months) and low in their percentage ^3H retained. This observation indicates again that the origin of SBP has an influence on the products viscosity.

3.8.6.4 *The solid content was determined in different ways— resulting in different measurements*

The original SBP and eC samples were provided by CelluComp Ltd. in pastes, powder, dried sheets, and grated form with specific dry weight contents so the solid concentration of sample suspensions could be calculated. Additionally, I determined solid concentrations by freeze-drying and measurement on a moisture analyser (Figure 41).

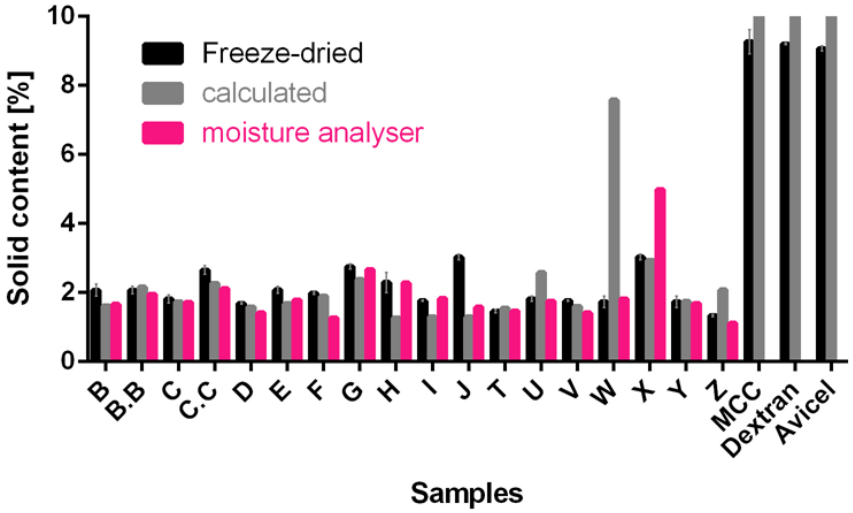

Figure 41: Solid contents of experimental Currans and controls determined by three methods. The solid content of eC suspensions was calculated with help of the dry weight contents of eC products (declared by CelluComp Ltd., grey). Subsequently I freeze-dried (black) or baked (in a moisture analyser; pink) portions of the eC suspensions. MCC, Avicel and dextran were prepared as 10 % dry weight samples based on the 'dry' samples as received from the suppliers. Freeze-dried samples are shown with the SEM and N=3.

All three methods to determine the solid content resulted in similar results with some exceptions. The moisture analyser determined a much higher solid content for eC X (5.0%) than the calculated and freeze-dried results. The solid determinations with the moisture analyser were conducted two weeks after freeze-drying, during this period eC X might have unintentionally lost water through evaporation which led to the big differences in solid content. The calculated solid content was highest in the case of eC U, W and Z which could also have been the result of partial drying-out between the production and measurement of the solid content in the lab. For future experiments, sample suspensions should be prepared from new eC products and their solid content analysed just before measuring the availability of –OH groups. For calculation of the percentage of ^{3}H exchanged (Figure 38–Figure 40), the solid contents measured by the moisture analyser were taken.

If some eC products or eC suspensions partially dried during storage, this could have led to a change in the products' viscosity (dependent on solid content). Regrettably not enough sample material was left for a second viscosity measurement with the Brookfield viscometer; therefore, a simple viscosity measurement with a pipette-type viscometer (§2.12) (needing significantly less material) was conducted on hveC products (§3.8.6.5).

3.8.6.5 *Viscosity of high viscosity experimental Currans could have changed over time*

Long storage was reported to lead to decreasing viscosity (§3.1). Changes in the solid content (Figure 41) due to partial evaporation of water were suspected to have the same effect. A simple fast method was used to measure viscosity of four hveC samples (Figure 42).

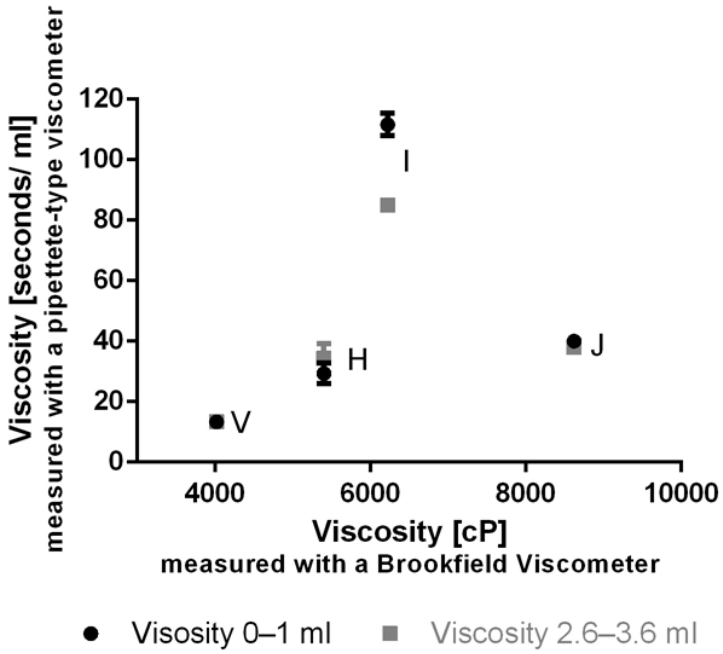

Figure 42: Viscosity measured for four high viscosity experimental Currans.
A 0.7-cm-diameter (5-ml) plastic pipette was filled with 5 ml eC paste (1.3% dry weight) and the time that it took to flow through the pipette was measured. Measurements were taken between two points on the pipette (0–1 ml and 2.6–3.6 ml); they are plotted according to the eC products' viscosity in cP (determined with a Brookfield viscometer). Error bars represent SEM, N=3.

The two measurements taken with the pipette-type viscometer for each hveC paste overlap, except for the significantly different results for hveC I (viscosity 6220 cP). hveC I Showed the highest viscosity when measured with a pipette-type viscometer, although it did not possess the highest viscosity determined with the Brookfield viscometer. Viscosity as measured by the two methods were expected to directly relate but viscosity measured with the pipette-type viscometer did not always increase with viscosity measured with the Brookfield viscometer. For the –OH group exchange experiments (§3.8.6.3), results were related to the viscosity measurements determined with the Brookfield viscometer on the fresh eC products at CelluComp Ltd..

4 Discussion

4.1 Overview and conclusion

This work successfully characterised SBP and its biotechnological product eC. SBP is made of primary cell wall polysaccharides: cellulose, hemicellulose and pectin (§4.2). Compared with other dicotyledons, sugar beet is poor in hemicellulose (e.g. Dinand *et al.* (1996)) (§4.2.1.2), very rich in pectins (§4.2.1.1) (e.g. Thibault *et al.* (1994)) and especially high in the typical pectic component Ara. SBP analysed in this work led to similar compositions compared to the published compositions (Figure 43). The production process of eC led to products that were enriched in cellulose but deprived of most pectins (§4.3). Xyloglucan was the major non-cellulosic polysaccharide identified (§4.3.1.2). Additionally, the contentious role of xyloglucan as a tether between cellulose microfibrils is discussed (§4.4). Complete quantification of eC and SBP preparations was not fully achieved, hence the different routes of material loss observed in this work (§4.6) were debated. The optimal production process (§4.3.1) identified in this work for normally produced eC products involved hydrogen peroxide treatment, followed by sodium hypochlorite (with extensive washing between these two oxidising chemical treatments). hveC Products were higher in viscosity owing to increased concentrations of oxidising chemicals used in the production process, which reduced the quantity of pectins even further (§4.3.1.2) (compared with normally produced eC). The relative molecular mass (§4.5) of hemicelluloses and pectins was decreased during the production of eC and was found to decrease even further during treatments that led to eC preparations with increased viscosity. Furthermore, hveC products contained the smallest matrix polysaccharides and possibly smaller cellulose molecules than normally produced eC (§4.3.1.3). A sensitive method (§4.7) for relative quantification of accessible –OH groups in different carbohydrate samples was established in this work. It led to the conclusion that viscosity increased with increasing availability of –OH groups in eC products.

In conclusion, the treatment of SBP with oxidising agents leads to cellulose-enriched eC products. Most pectins are removed from the final product, and the residual pectins are fragmented. Nonetheless, viscosity of eC products benefits from higher quantities of residual pectins. Xyloglucans, the major matrix polysaccharides in eC products, are likewise fragmented into smaller molecules but their quantities do not correlate with increasing or decreasing viscosity. Elevated concentrations of the oxidising chemicals hydrogen peroxide and sodium hypochlorite in the production of eC, raise the

viscosity. This is perhaps caused by the chemicals action on further decreasing the molecular mass of matrix polysaccharides, and possibly cellulose. At the same time, with elevated concentrations of the oxidising chemicals, the interaction of eC products with water molecules increases which is likely to be caused by greater availability of –OH groups in the polysaccharides.

This improved understanding of eC can be used to advance and upgrade the production process of commercial Curran®. In future, the optimised process might inform strategies of adding Curran® to a wider range of products and thereby drive further use of “waste”, such as SBP, for biobased materials.

4.2 Sugar beet pulp

4.2.1 SBP composition

For over six decades SBP has been studied for use as an inexpensive, abundant polysaccharide source. SBP is lignin-poor (Michel *et al.* 1988; Dinand *et al.* 1999) and therefore recalcitrance towards hydrolysis is low, making it a good starting material for industrial processes. Many studies have found that SBP is mainly composed of carbohydrates (75–80% of the pulps total dry weight) (Wen *et al.* 1988; Vučurović & Razmovski 2012)) of which 22–24% of total carbohydrate is cellulose microfibrils, 30–32% hemicelluloses, 25–27% pectin (Dinand *et al.* 1996; Vučurović & Razmovski 2012). Wen *et al.* (1988), found residual moisture (6% of the total dry weight of pulp), ash (12.2%), protein (5.8%) and crude fat (1.2%) in addition to the major carbohydrate portion. Toğrul & Arslan (2003a) found less ash (3.7% per dry weight) but more protein (8.9%). High ash was often found to be due to soil contamination (Wen *et al.* 1988). Similar compositions were found by other groups (e.g.Dinand *et al.* (1996); Ralet *et al.* (2009)).

For simplification, I calculated the mean of the monosaccharide compositions published for eight SBP materials (Guillon & Thibault 1989; Renard *et al.* 1997; Spagnuolo *et al.* 1997; Oosterveld 1997; Dinand *et al.* 1999; Fares *et al.* 2001; Reddad *et al.* 2002) to compare it to SBP preparations used in this work (Figure 43).

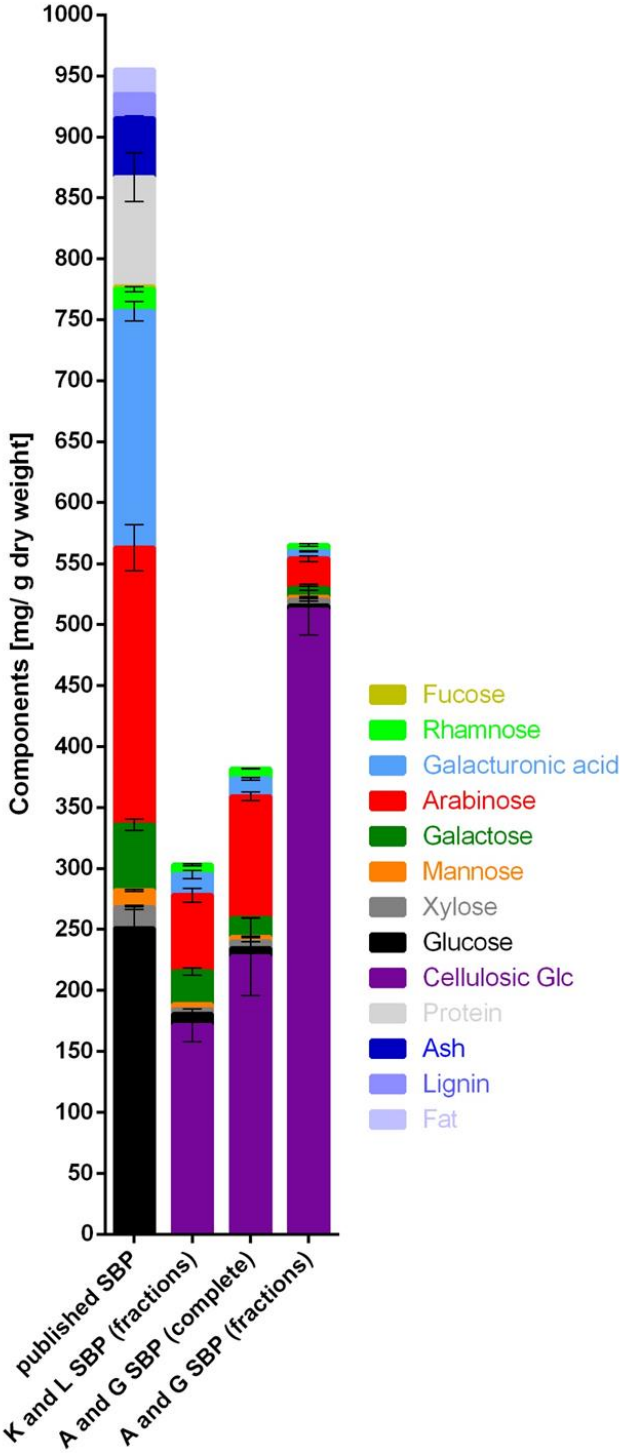

Figure 43: Carbohydrate compositions of SBP from this work and published studies.
Data for eight SBP samples were taken from seven studies (Guillon & Thibault 1989; Renard *et al.* 1997; Spagnuolo *et al.* 1997; Oosterveld 1997; Dinand *et al.* 1999; Fares *et al.* 2001; Reddad *et al.* 2002). Glc in the published composition represents cellulosic as well as non-cellulosic Glc. SBP preparations in this work, were analysed for 'cellulosic' (purple) and 'non-cellulosic' Glc (black). SBP A, G, K and L preparations were fractionated into α-cellulose, HbP and Ha which were also analysed for total carbohydrates ('K and L SBP (fractions)' and 'A and G SBP (fractions)'). Error bars represent SEM. 'Published SBP':N=8, except for: Fuc and protein (N=2), lignin and fat (N=1). This work: N=2, except for cellulosic Glc: K and L SBP (N=4), A and G SBP (N=6).

The published mean carbohydrate composition of SBP was mainly Glc ('cellulosic' plus 'non-cellulosic' origin) (251 mg/ g dry weight), Ara (227 mg) and GalA (194 mg). This was completed by Gal (54 mg) and quantitatively minor amounts of Xyl, Man, Rha and Fuc (together 51 mg). Fuc (2 mg/dry weight) was only quantified for two of the eight published compositions and not detected in SBP analysed in this work. Fuc is a minor component of mainly xyloglucan and can be released by TFA hydrolysis (Fry 2000). In the solvent system used for TLC in this work, Fuc R_f is almost identical to that of Xyl (O'Rourke *et al.* 2015) and as Xyl was found in abundance especially in eC preparations, this may have prevented the detection of the minor component Fuc. About 20% of the cited composition was made up of non-carbohydrate components such as protein, ash, lignin and crude fat (these components were not studied in this work). Except for the powdered SBP A, the three SBP preparations G, K and L were pre-treated (§2.1) in the following way: washed (to remove soil particles and residual sucrose), cooked (probably denatured proteins) and blended. The production of AIR from SBP K and L would then additionally have removed most lipids and low-M_r components. This should have led to an enriched polysaccharide composition with no or minimal fat, sugar and ash content. The composition found in this work could not account for the total dry weight of SBP however. As seen in result chapters §3.2 and §3.3 material was lost through extraction, dialysis and washing (discussed in §4.6).

The average compositions (Figure 43) of SBP A and G preparations (complete) and SBP K and L (fractions of the preparations) are similar to each other and 300–400 mg/ g dry weight was identified as carbohydrate material. 'Cellulosic' Glc (171–228 mg/ g dry weight, hydrolysed from cellulose) was identified as the major component of SBP (comparable to about 250 mg, as found in the cited publications). More cellulose was quantified from slurry SBP G than from powdered SBP A (§3.5.2.2), which might indicate that it was more accessible in the softer, bigger particles then in the smaller, harder powder particles. A general observation in this work was that hydrated solids were easier to hydrolyse than dry, lumpy residues. As the particle size of materials in this work was not determined, the effect of hydration and particle size cannot be sufficiently evaluated. A recent publication by Huang, Li, *et al.* (2018) demonstrated that decreasing particle size of SBP increased the surface properties and could therefore increase accessibility and hydrolysis of polysaccharides by acids.

With the assumption that the published SBP compositions reflect the true composition for SBP used in this work, the components hydrolysed from the matrix polymers in

SBP here have been underestimated and cellulose was overestimated (further details in §4.6). This is further discussed in the following §4.2.1.

4.2.1 Composition of SBP fractions

Fractions from SBP preparations were extracted by 6 M NaOH (§3.5). Pectins and hemicelluloses were part of the HbP fraction, which was mainly composed of Ara, followed by Gal and GalA, followed by Rha/unknown$_{red}$ and minor quantities of Glc, Xyl and Man (and unknowns). The HbP fraction isolated from SBP was the highest yield (in weight) among all HbP fractions from preparations A–S (Figure 7). The minor Ha fraction and the major α-cellulose fraction from all preparations were mainly composed of 'cellulosic' Glc.

Besides the fact that more carbohydrate material could be recovered from AIR preparations than from washed preparations (Figure 7, discussed in §4.6), additionally, SBP A and G preparations that had been split into fractions contained almost twice the amount of 'cellulosic' Glc compared to 'cellulosic' Glc measured in TFA-resistant residues from complete preparations (Figure 43). On the one hand, TFA hydrolysis of complete preparations and fractions led to TFA-resistant residues that were hard particles and difficult to dissolve in the subsequent carbohydrate assays, therefore possibly leading to incomplete hydrolysis and analysis of cellulosic Glc. On the other hand, α-cellulose and Ha from SBP A and G preparations were analysed by a different carbohydrate assay (the Saeman method (§2.8.2) instead of the anthrone method) which may have resulted in an overestimation of total carbohydrates in SBP A and G preparations (although the observations discussed in §4.6 do not support this argument).

Many published studies (e.g. Wen *et al.* (1988); Dinand *et al.* (1996); Oosterveld (1997) and Fares *et al.* (2001)) describe the polysaccharide composition of SBP after fractionating SBP into different fractions containing pectins, hemicelluloses and cellulose for the study of their composition and possible applications in industry.

4.2.1.1 *Pectins in SBP*

Most commonly, the industrial source of pectin is citrus fruit and apple waste for the main application as a gelling agent. SBP has long been identified as a source of large amounts of pectin but its poor gelling properties (due to acetyl ester groups (Pippen *et al.* 1950)) and low viscosity make it an unsuitable gelling agent. Nevertheless,

oxidative cross-linking of pectin from SBP with hydrogen peroxide/peroxidase increased the extracts' viscosity and led to formation of a gel (Oosterveld 1997).

Pectins are generally defined as plant polysaccharides rich in GalA residues (Fry 2011). More than one third of sugar beet AIR was solubilized by Fares *et al.* (2001) during pectin extraction. The composition of pectin extracted by citric acid (pH 2, for 2 h at 80°C) was found to be almost identical to the composition of commercial sugar beet pectin and EDTA-extracted pectin: about 60% GalA, 10% Ara and 8% Gal with only minor amounts of Rha, Glc, Xyl and Man (Wen *et al.* 1988; Agoda-Tandjawa *et al.* 2012; Ma *et al.* 2013). In another study, pectin extracted with EDTA contained pectin with a higher amount of Ara (~30%) (Wen *et al.* 1988). Other neutral sugars may have been generated in low amounts by degradation of hemicellulosic material (Ralet *et al.* 2009; Ma *et al.* 2013). Ralet *et al.* (2009) noticed that the amount of pectin and especially Ara in SBP were exceptionally high compared to other dicotyledons. Several studies found as much Ara as GalA (about 200 mg/g dry weight in SBP and AIR from sugar beet roots) (Thibault *et al.* 1994; Guillon *et al.* 1998; Levigne *et al.* 2002; Reddad *et al.* 2002) which is in contrast to the above-mentioned (published) mean composition (Figure 43). It is important to notice that different extraction methods can lead to different compositions of pectic extracts.

I would expect to find similar compositions in the pectin of the HbP fractions from SBP in this work. As discussed in §4.6, the quantification conducted after TFA hydrolysis by Photoshop in this work may not present the true composition of the preparations and fractions. In HbP fractions, GalA only made 9–12% and Rha 6–9% of the total HbP from SBP. If the ratio GalA/ Rha is correct, and Rha mainly originates from RG-I, the results suggest a high proportion of RG-I and very little homogalacturonan. Oosterveld *et al.* (1996) and Ma *et al.* (2013) concluded that the main domains in SBP pectin were homogalacturonan and RG-I. They also suggested arabinan and arabinogalactan-rich side chains in hairy regions of RG-I. The high percentage of Ara in HbP fractions from SBP preparations (38–48% dry weight) and Gal (13–21%) equally suggests the presence of hairy regions in RG-I, rich in arabinan and arabinogalactan side chains (assuming most Ara and Gal result from pectic polysaccharides).

4.2.1.2 *Hemicelluloses*

Typical hemicellulosic components were only found in quantitatively minor amounts (13–19% of the total HbP fraction from SBP preparations): non-cellulosic Glc 5–6%; Xyl 3% in samples K and L but ~8% in A and G; Man 3–4%. This agrees well with the previously cited studies (Figure 43). In the quantitatively minor Ha fraction, mainly 'cellulosic' Glc (usually found in α-cellulose) was found. This work used 6 M NaOH (overnight at 37°C shaking; §2.9) as it was shown to be optimal for extraction of hemicelluloses (Edelmann & Fry 1992).

The investigation by Fishman *et al.* (2009) assessed alkaline extractable polysaccharides from SBP. Mild acid and microwave-assisted extraction (MAE) were used to remove pectin from SBP. The residue was then subjected to mild alkali (0.15 M NaOH) treatment after which the resulting supernatant and residue were both subjected to concentrated alkali (12.5 M NaOH (pH 11.5), 0.335 uls 30% H_2O_2) under different MAE conditions (5–30 min, 80–105°C and pressure of 30–90 psi). Their hydrolysates were named alkaline soluble polysaccharides (ASP) I and II respectively. Both ASPs (extracted under all conditions) showed lower degrees of methyl esterification (due to the removal of pectin), neutral sugar content and GalA content (most GalA was removed with pectin) than total SBP and pectin. The recovery of dry weight (per pectin-free SBP starting material) of ASP II was about twice that of ASP I, meaning most weight was present in the fraction extracted with high alkali. Among the different MAE fractions of both ASPs, the components found were mostly Ara (38–54% dry weight), Rha (11–23%), Gal (8–29%) and GalA (typically ~10%). Glc, Fuc and Xyl were mostly extracted in the pectic extract. I find this quite unexpected as pectins (containing mostly Rha and GalA) are usually extracted using milder conditions than the hemicellulosic polysaccharides (containing Xyl and non-cellulosic Glc).

A different approach was used to extract hemicellulose from AIR from Moroccan beets that were harvested early and late in the harvesting season. Fares *et al.* (2001) gained 12% AIR dry weight for hemicellulose extracted with 1 M NaOH, the concentration was then increased to 4 M NaOH and resulted in an additional 5% (all done at 4°C). The final washing fraction (thorough washing in pH 7) was composed of mostly Ara and uronic acids (only 2% AIR dry weight). The NaOH fractions were rich in Ara (due to incomplete removal in the prior pectin extraction), followed by Xyl > Glc> uronic acids> Man and Gal> Rha and Fuc. The ratios of Fuc/Xyl/Gal/Glc suggested the

presence of heteroxylans in addition to xyloglucans (confirmed by ion-exchange chromatography) (Fares *et al.* 2001).

In this work, monosaccharide ratios in HbP might be difficult to judge or rely on as hemicellulose and pectins were extracted together and Fuc was not detected at all. The ratio of Xyl/non-cellulosic Glc in the HbP fractions was between 1.0 and 1.5 for SBP preparations A and G (meaning more Xyl than Glc), only 0.7 for SBP L and K HbP. The preparation of AIR from SBP L and K might have led to removal of small Xyl-containing carbohydrates such as partially degraded xylan. The calculated ratios suggest that xyloglucan and xylan were present in SBP (or just xyloglucan in K and L). Driselase digestion of SBP HbP (Figure 65 and Figure 81) supports this, as some IP but little or no Xyl_2 were detected. Xyloglucan in SBP, only present in low amounts, is heavily substituted with side-chains (three out of four Glc residues, resulting in a ratio of Xyl/Glc of 0.75) (Oosterveld 1997). This was also found for xyloglucan from apples (Vincken *et al.* 1996) or sycamore cell cultures (Bauer *et al.* 1973). It leads to the conclusion that SBP preparations with a higher Xyl/Glc ratio contain additional xylan (as was found in SBP A and G).

The only study found to describe Ha and hemicellulose b (Hb) fractions from SBP was done by Wen *et al.* in 1988. Their optimised method was starting with milled SBP filtered through a 60-mesh wire screen and freed of pectins by treatment at 85°C EDTA (pH 7.5) followed by pectinase digestion. Hemicellulose was then extracted in 2.5 M NaOH at 25°C and the remaining residue delignified in sodium chlorite (pH 4.2–4.7, 75°C for 1 h). The pulp contained 80% dry weight nonstarch polysaccharides; of this, crude hemicelluloses made 25.7% and cellulose (after delignification) 26.1% (cellulose was enriched in Glc but still contained approximately 28% matrix polysaccharide components). Total carbohydrate was quantified by the phenol sulfuric acid assay. The ash-free Ha fraction made up 8.4% dry weight of the total carbohydrates in SBP and Hb 5.9% (Wen *et al.* 1988). These numbers cannot be compared to the yields obtained in this study as the extraction procedures differed. Furthermore, almost no Ha was extracted from SBP preparations in this work. Wen *et al.* (1988) found EDTA-soluble polysaccharides were rich in uronic acid (55% of organic matter of SBP) and Ara (34%). Most Rha was only isolated in Ha and Hb suggesting the presence of RG-I. Ha was rich in Xyl (23%), Man (22%) and Glc (21%); this was very unlike the ‘cellulosic’ Glc rich Ha fraction found in my work. Hb in contrast (Wen *et al.* 1988) contained Ara (22%), Gal (17%) and Glc (26%). As Gal and Ara

were previously suggested to mostly be part of RG-I the Hb fraction in Wen *et al.* (1988) may contain some arabinan and arabinogalactan side chains (previously attached to RG-I). They found a ratio of Ara/Xyl of 1:1.7 for Ha and 1:0.6 for Hb (this difference was believed to contribute to the differences in water solubility of Ha and Hb) (Wen *et al.* 1988).

Summarizing the results for SBP, in comparison to published compositions, the recent findings from this work seem to have underestimated the amount of matrix polysaccharides in SBP preparations. Cellulose was the major polysaccharide found in SBP and might have been overestimated although this could not be confirmed. Homogalacturonan and RG-I hairy regions and Ara-rich side chains were found in the HbP fractions from SBP. Quantitatively minor amounts of xylan and larger amounts of xyloglucan were present too.

4.2.2 Cellulose in SBP

The cellulosic residue of SBP was not studied in detail in this work. It was shown to consist of cellulosic Glc (partially hydrolysed by TFA but mainly resisting TFA, and released by the anthrone assay and the Saeman hydrolysis) (§3.5) with residual pectic components (Figure 9). The molecular mass or structure of SBP cellulose was not studied further. Parenchymal cell walls of sugar beet were found to contain cellulose IV_1 (instead of the classical native cellulose I, §1.3.2.1) which was thought to be the consequence of the small diameter of the cellulose microfibrils (2-3 nm) (Dinand *et al.* 1999). Later studies rejected this cellulose structure and showed that IV_1 was a less ordered form of cellulose Iβ (Wada *et al.* 2004).

The cellulosic residue after extraction of pectins and hemicelluloses with 4 M NaOH (at 4°C) was 46% of dry AIR rich in Glc with residual Man and uronic acids (Fares *et al.* 2001).

As sugar beet cell walls contained very little xyloglucan, xylan or mannan, Renard & Jarvis (1999) concluded that most of the cellulose microfibril surface area must be bare. Hence the commonly accepted assumption that hemicelluloses coat microfibrils could not be the only or major mechanism responsible for preventing aggregation of cellulose within the beet cell wall. The ‘commonly accepted assumption’ is describing the role of xyloglucan forming a tether between cellulose microfibrils (Fry 1989b). As a tether, xyloglucans prevent the collapse of microfibrils onto one another and at the same time stabilise the structure. Previously cited studies (Figure 43) detected around

30% per total SBP dry weight hemicelluloses so the role and quantity of hemicellulose remains unclear.

4.3 Experimental Curran

Curran® is a novel biotechnological product from the abundant but low-value SBP. Addition of Curran® to paints and coatings can give them several beneficial properties, such as higher cracking resistance (in hot or cold conditions), increased biodegradability (it can replace volatile organic compounds) and especially stable viscosity. These benefits justify extensive analysis of experimental variants (eC) of this high-value product.

4.3.1 The production process greatly influences the viscosity of experimental Curran products

§3.1 presents the changes in viscosity that are caused by varying the production process of eC.

Even though the composition of SBP was found not to change much over the last decades or during one harvest season (§4.2) the results presented in this work show that the source of SBP can make a difference to the final viscosity of the products. Among the normally produced eC products were eC W and X, produced from SBP provided by a new distributor. They were of lowest viscosity among all normally produced eC. As the composition of the products and SBP starting material was not studied in this work, this observation can only suggest but not prove that SBP from the new distributor and its eC products were different in composition to the other SBP materials studied in this work.

eC B–F represent normally produced eC samples (1520–1770 cP) from SBP powder A and show that the production process is reproducible within a narrow viscosity range. Previously, normally produced eC M and Q were produced from SBP K and L and of higher viscosity, 5640 cP and 2780 cP respectively. These different viscosities may direct towards two different assumptions: that products from washed and cooked SBP (such as K and L) are higher in viscosity than products from SBP powder; or that small differences in the normal production process (such as slightly different concentrations of solids or oxidising chemicals) can lead to higher or lower viscosity products. As discussed by Huang, Li, *et al.* (2018) decreasing particle size of SBP increased the extraction yield, which contrasts with the assumption made. The increase in yield was due to increased surface area and water binding capacity of the

particles (Huang, Dou, *et al.* 2018). To study the influence of particle size and hydration of SBP particles on eC production, more eC replicates from SBP K and L would be needed.

In contrast to the five replicates of normally produced eC products B–F, the four hveC products (eC H–J and V) were produced with increased oxidising chemical concentrations (§2.1) and are of much higher viscosity (4020–8620 cP).

Hydrogen peroxide reduced the concentration of pectin in eC and increased the concentration of hemicelluloses (xyloglucan specifically) and cellulose in the eC products (§3.5.1). It is known that H_2O_2 can oxidise cell wall polysaccharides (including cellulose) (§ 1.3.2.1) (Rutherford *et al.* 1942; Gilbert *et al.* 1984) by either depolymerising the chain or modifying the groups (e.g. primary alcohol group). Miller (1986) studied the effect of H_2O_2 (concentrations of up to 10 mM) on isolated cell wall polysaccharides and found that pectin and xylan were most susceptible compared to arabionogalactan or polygalacturonic acid. With longer incubation times the release of reducing groups increased and the molecular weight decreased (Miller 1986). Sodium hypochlorite, as a second treatment, led to further removal of pectins. Both chemical treatments used in succession increased the viscosity of the final eC products (§3.1); whereas overreaction (as well as underreaction, data not shown) of SBP in hydrogen peroxide and omitting the sodium hypochlorite treatment both led to reduced viscosity of eC products. Increasing the concentration of oxidising chemicals for both treatments led to a further increase in viscosity. Incomplete washing after the hydrogen peroxide treatment and sodium hypochlorite expectedly led to a reduction in viscosity. Hepworth & Whale (2016) investigated and patented a comparable production process for viscosity enhancers from plant material and stated that the longer the reaction in hydrogen peroxide progressed, the lower the pH of their peroxide-plant material mixture. Higher viscosity materials were generally produced with a shorter reaction time and a pH drop of 1–2 units (Hepworth & Whale 2016). These statements concur with the findings from this work, as the reaction time was longer for the hydrogen peroxide-overreacted eC product (e.g. eC R (2200 cP)) and the pH drop greater than 1–2 units which was observed for normally produced eC products (e.g. eC M (5640 cP)). I add that sodium hypochlorite (possibly removing more pectins), as a second treatment, and full removal of both oxidising chemicals increase viscosity further which is a desirable trait for industry.

Complete drying of optimally produced eC products (eC T and Z) to a thin sheet (before resuspension in water with help of a blender for viscosity measurement) caused a drastic decrease in viscosity; with viscosities of 116 and 148 cP they were the lowest viscosity eC products. eC Z was produced from normally produced eC X with a viscosity of 1250 cP. A well-known process, called hornification, describes this reduced viscosity outcome: dried chemical pulp fibres can never regain their original water-swollen state when resuspended in water (Minor 1994) and therefore cellulose-rich eC could not return to its original viscosity. This is due to a physical change where additional hydrogen bonds are formed that remain after rewetting (Laivins & Scallan 1993).

Agoda-Tandjawa *et al.* (2010) produced dry cellulose microfibrils from SBP (after extraction of most pectins and hemicelluloses) leaving a product rich in Glc (80% dry weight; determined through gas–liquid chromatography after polysaccharide hydrolysis by 2 M H_2SO_4 at 100 °C for 2 h). TEM micrographs showed that native cellulose fibres were bundled and clustered, whereas, after extraction of the matrix polysaccharides and mechanical shearing, they appeared delaminated and entangled. The cellulose-rich blended product formed a uniform suspension in water which did not sediment or flocculate (this property and other similar products are discussed in §4.3.1.3). Delaminated cellulose suspensions displayed a gel-like behaviour (the structure was independent of the solid concentration) (Agoda-Tandjawa *et al.* 2010). This is comparable to the creamy viscous suspensions that eC products form in water. As was observed for freeze-dried eC, freeze-drying led to a loss of the viscoelastic properties (Agoda-Tandjawa *et al.* 2010) due to strong aggregation of microfibrils via hydrogen bonds (Laivins & Scallan 1993). Pressing too led to decreased viscosity of the resuspended eC product (probably also owing to newly formed H-bonds) although to a less drastic extend than complete drying: eC products B', E' and F' were prepared from three normally produced pressed and grated eC products with solid contents of 16.5–18.5%. B, E and F showed original viscosities of 1520–1770 cP (fresh after pressing and re-hydration for viscosity measurement) and were stored at 4°C for six months prior to the production of B', E' and F'. Viscosity measurements revealed that all these three eC products had lost 37–61% of their original viscosity (owing to the long storage in its pressed grated form).

Thawed cellulose microfibril suspensions showed shear-thinning behaviour (§1.4.2) with large decrease in viscosity over increasing shear rate (Agoda-Tandjawa *et al.* 2010). Thawed eC products flocculated but could be re-suspended to form a stable viscous suspension, albeit decreased viscosity (data not shown). Negative charges on microfibril surfaces, due to residual GalA (causing electrostatic repulsion), probably increased the organisation plus the stability of the cellulose microfibril system (Agoda-Tandjawa *et al.* 2010). GalA was extracted in minor quantities from eC products and found (together with Xyl and possibly Glc) to be tightly associated with cellulose (6 M NaOH did not remove all of these residues, §6.2; Figure 49). Viscoelastic behaviour increases with increasing salt concentration, probably due to the added Ca^{2+} ions screening the electrostatic repulsion between microfibrils (Agoda-Tandjawa *et al.* 2010). Change of the pH (4.5–9.0) did not vary viscoelastic properties (Agoda-Tandjawa *et al.* 2010). Hepworth & Whale (2016) found stable suspensions at an even greater pH range (2–14). Owing to the shear-thinning behaviour observed for the aqueous suspensions, the products generated and studied by Weibel (1986), Dinand *et al.* (1999), Agoda-Tandjawa *et al.* (2010) and Hepworth & Whale (2016) can be considered classical pseudoplastic materials (Agoda-Tandjawa *et al.* 2010). Similar observations were made for eC products: the cellulose enriched material (with residual pectins and hemicelluloses; discussed in detail in §4.3.1.2) formed a stable viscous suspension in water. eC can be considered a non-Newtonian (§1.4.2) (non-linear relationship between shear stress and shear rate), pseudoplastic fluid with shear-thinning properties.

To conclude this chapter, which focussed on the production process of eC products, first, the origin (distributor) of SBP starting material can possibly influence the viscosity of the eC products. Second, SBP powder or washed and cooked SBP are both suitable starting materials to produce eC. Third, the optimal production procedure for normal eC products is a short reaction time in hydrogen peroxide (with a pH drop of 1–2 units), subsequent sodium hypochlorite treatment and full removal of all oxidising chemicals by washing. Higher viscosity products can be produced by increasing the concentration of oxidising chemicals in both treatments. Pressing, for storage purposes, and drying decreases the products' viscosity probably due to microfibril aggregation. Fourth, eC products are formed from a cellulose-rich polysaccharide network with residual hemicelluloses but few pectins. These non-cellulosic components and especially GalA in residual pectins, were found to stabilise the viscous suspensions by causing electrostatic repulsion between microfibrils and

preventing them from aggregating (Agoda-Tandjawa *et al.* 2010). eC products can be described as non-Newtonian pseudoplastic fluids with shear-thinning properties.

4.3.1.1 *Alternative processing of SBP into experimental Curran*

As an alternative to the chemical treatments of SBP to produced eC certain enzymes and enzyme combinations could be used. These may result in more environmentally friendly processes but would also need to be evaluated from an economic point. Spagnuolo *et al.* (1997) aimed to find the optimal enzymatic hydrolysis conditions (single enzymes and combinations) for SBP into soluble sugars. Pectinolytic enzymes (including the enzyme mixture Viscozyme), all mainly showing polygalacturonase activity, were successful in hydrolysing parts of SBP singularly. Major sugars solubilised were Ara and GalA while Glc was only released to a small extent (Spagnuolo *et al.* 1997). These components probably resulted from the degradation of pectins which are highly abundant in SBP (§1.3.2.2). Binary combinations of cellulase–hemicellulase and cellulase–pectinase were more successful than the single enzymes (combinations of enzymes hydrolysed much more than the sum of the single enzymes). Pectinolytic enzymes improved the access of cellulases by removing sterically hindering pectins. The combination of cellulolytic, hemicellulolytic and pectinolytic enzymes were most successful and led to almost complete saccharification of SBP (compared to acid hydrolysis) (Spagnuolo *et al.* 1997). For the application of this knowledge for eC (and Curran®) production, enzyme combinations of hemicellulase-pectinase could be used to remove matrix polysaccharides from SBP but leave the cellulose network intact. Adding cellulases could alter the cellulose network beneficially. Changing the ratios of these enzymes may optimise the polysaccharide composition of the resulting product and its viscosity.

4.3.1.2 *Viscosity and composition of experimental Curran correlate to a certain extent*

This chapter focuses on the carbohydrate composition of eC products and their correlation to viscosity.

All eC preparations tested for carbohydrate composition (§3.5) (B–F, H–J and M–S) were enriched in cellulose (~90% of the total carbohydrate composition), contained little hemicellulose (typical components found were ‘non-cellulosic’ Glc, Xyl, Xyl_2 and IP (only traces of Man)) and even less pectin (minor quantities of typical pectic

components such as Ara, GalA, Gal and Rha). hveC Preparations (§3.5.2.2) were poorer in pectins and possibly hemicelluloses than the normally produced eC B–F.

Even though the matrix polysaccharides only make a quantitatively minor portion of the total components in eC preparations (e.g. Figure 60), their quantities show correlations to the products viscosity. eC Products (M–S with viscosities 1710–5640 cP) were produced with different processes and the polysaccharide analysis showed that the quantity of each typical pectic component decreased with decreasing viscosity (§3.5.1, Figure 16). This trend was again found among normally produced eC (B–F, 1520–1770 cP) (§3.5.2.2, Figure 21): the highest quantities of pectins were found in eC E and F (but they were only slightly higher in viscosity than the other three normally produced eC in the set). The rate of decreasing viscosity was not comparable to the rate of decreasing quantities of pectic components, hence pectins cannot be the only factor influencing viscosity. This was also reflected by hveC preparations which contained the least quantity of pectins but were made from the highest viscosity products. I conclude that pectins are beneficial to normally produced eC viscosity but are not a major influence on viscosity as the highest viscosity products contained the least number of pectins. Other components did not show a correlation to viscosity. 'Non-cellulosic' Glc, Xyl and IP (predominantly found in hemicelluloses such as xylan and xyloglucan) presented the major portion of matrix polysaccharides in all eC preparations. Interestingly, the proportions of Xyl to 'non-cellulosic' Glc and IP among normally produced eC and hveC did not differ much (Figure 80). This agrees with some of the discoveries by Dinand & Vignon (2001) who isolated (4-O-methyl-α- D-glucurono)-β- D-xylan from a cellulose-enriched suspension purified from SBP (named PCC). This hemicellulose aided electrostatic repulsion of charged entities (such as cellulose microfibrils) and thereby enabled stable PCC suspensions (Dinand & Vignon 2001). This complements the findings by Agoda-Tandjawa *et al.* (2010) that attributed this role to GalA attached to cellulose microfibrils (discussed in §4.3.1). All preparations (including SBP) on Driselase digestion yielded more IP (digestion product from xyloglucan) than Xyl_2 plus Xyl (products from xylan) (except for hveC H HbP). The ratio of xyloglucan/xylan was not found to be influenced by the production process of eC, nor did it corelate with viscosity of the eC products. In all eC samples very little GalA, much higher concentration of xyloglucan and lower concentrations of xylan were detected (Figure 29). Xyloglucan is therefore regarded to also play a role in viscosity of eC and may prevent aggregation of cellulose microfibrils. This might be caused by the ability of xyloglucan to form hydrogen bonds

to the surface of cellulose microfibrils (Hayashi *et al.* 1987) which are proposed to tether them (Fry 1989b). This widely accepted model has been challenged by other studies (discussed in more detail in §4.4). Xyloglucan and cellulose are considered to interact via hydrogen bonding, even though the connection in an in vitro generated xyloglucan/cellulose composite was broken under relatively mild alkaline conditions (0.71 M KOH, below 30°C, 3 h) (Hayashi & Maclachlan 1984). Moreover, carboxymethylcellulose and xyloglucan interact to form higher molecular mass complexes and the viscosity of carboxymethylcellulose increases with increasing concentration of xyloglucan (Hayashi *et al.* 1987). Even though, carboxymethylcellulose and an in vitro generated xyloglucan/cellulose composite are expected to be quite different from the native cellulose eC products, the interaction of xyloglucan with cellulose (the two major polysaccharides identified in eC products) may greatly contribute to its viscosity. Chanliaud *et al.* (2004) also studied cellulose/xyloglucan composites (produced by *Acetobacter aceti* ssp. *xylinum* in culture) and found that removal of xyloglucan tethers led to increased stiffness, decreased viscoelasticity and equal or greater extensibility (Whitney *et al.* 1999; Chanliaud *et al.* 2004). This further underlines the recently made conclusion that the viscosity of eC products benefits from tethering xyloglucan between cellulose microfibrils.

In summary, eC preparations were enriched in cellulose (approximately 90% of the total carbohydrate composition) with little hemicellulose and even less pectin. hveC Preparations contained even less pectin but approximately the same quantity of hemicelluloses. Among normally produced eC its pectins were identified to have a beneficial influence on eC's viscosity (the higher the amounts of pectin the higher the viscosity; §3.5.1 and §3.5.2.2). Other studies showed that xylan (Dinand & Vignon 2001) and GalA (Agoda-Tandjawa *et al.* 2010) were responsible for electrostatic repulsion of cellulose microfibrils and thereby prevent microfibril aggregation in eC-like products. Xyloglucan has been identified (Hayashi & Maclachlan 1984; Hayashi *et al.* 1987; Chanliaud *et al.* 2004) to play a critical role in viscosity by hydrogen bonding to cellulose microfibrils.

4.3.1.3 *Experimental Curran compared to the viscosity enhancer parenchymal cell cellulose*

Viscosity and factors influencing viscosity have been studied for a long time; factors such as aggregation and non-spherical particle shape are known to influence viscosity

(common knowledge, stated in Kraemer & Natta, 1931). Staudinger (1930) (and later articles) found that for linear high-molecular-weight polymers such as cellulose and rubber, viscosity was proportional to the molecular mass (discussed in more detail in §4.5). Kar & Arslan (1999) state that viscosity of apple pectin is a measure of molecular mass and the higher the molecular mass, the higher its viscosity. Moreover, viscosity depends not only on the molecular mass but also on the solid concentration and temperature of fluid (§1.4.2).

Although Curran® is a relatively new product, SBP as a starting material for production of viscosity enhancers had been studied for the last three decades. It is therefore surprising, given the good rheological properties and the abundance of the inexpensive SBP, that it has not been used for commercial application, as a rheology modifier, earlier.

Weibel (1986, 1989) and Weibel & Myers (1990) invented PCC produced from SBP and Dinand *et al.* (1996, 1999) characterised and studied it intensely. The following discussion gives a detailed comparison of PCC and eC products as they are equivalent in several aspects. PCC was produced with a similar production process to eC: SBP was uniformly dispersed in 0.5 M NaOH for 2 h at 80°C, filtered and washed to remove solubilised polysaccharides and inorganic material. It was subsequently bleached in sodium chlorite to remove most residual lignin and proteins. From 20 g dry weight SBP Dinand *et al.* (1996) received 4 g dry weight PCC with the following composition: cellulose 88% dry weight, hemicelluloses 7%, pectins 3%, inorganics 2% (Dinand *et al.* 1996). Acid hydrolysis (2 M TFA, 100°C, 1 h) of PCC resulted in 71% Glc, 2% Man, 1% Gal, 5% Xyl, 1% Ara, no Rha and 2% uronic acid (Dinand *et al.* 1999). The carbohydrate composition of PCC is remarkably similar to the composition of normally produced eC reported by me (§3.5.2.2). Likewise, eC preparations were mainly composed of Glc (around 90%) and, among the non-cellulosic components, Xyl (approximately 2%) and possibly ‘non-cellulosic’ Glc (2–6%) (TFA-hydrolysed eC preparations; Figure 20) were most abundant. It is likely that the component described as ‘non-cellulosic’ Glc (found in higher quantities than expected) was actually derived from partial TFA hydrolysis of cellulose and matrix polysaccharides alike. Martina Pičmanová found evidence for partial cellulose hydrolysis when she obtained Glc after TFA treatment of filter paper, Avicel or NaOH-treated filter paper (personal communication from Martina Pičmanová). As the α-cellulose present in eC preparations presents highly processed cellulose (treated

with hydrogen peroxide, sodium hypochlorite and extracted with 6 M NaOH) it is likely to have been partially TFA-hydrolysed.

Although cellulose is the major carbohydrate found in eC preparations, it is poorly understood (to the effect of polymerisation, molecular mass and crystallinity) compared to the more intensely studied hemicellulose and pectin fractions. Agoda-Tandjawa *et al.* (2010) hydrolysed SBP with 2 M H_2SO_4 at 100°C for 2 h but found incomplete hydrolysis because the acid could not access all glucosidic bonds in the glucan chains of cellulose. This was probably due to native cellulose containing amorphous (disordered) and crystalline (ordered) regions (Rowland & Roberts 1972) which show different accessibility to hydrolysis. The two chemical treatments used in the production process of eC are likely to change the cellulose structure of SBP; it might have changed native crystalline cellulose regions into amorphous regions making cellulose more accessible to acids (such as TFA). The cellulose structure of SBP and eC was not studied in this work but restructuring of cellulose in the products could have led to differences between the quantification of cellulose (by TFA and total carbohydrate assays) in SBP and eC. Differences in the production processes of eC could produce further differences in their cellulose structure.

As shown in §3.5, cellulose from eC preparations was found in both α-cellulose and Ha. It was unexpected to find cellulosic Glc in Ha as 6 M NaOH is not known to solubilise cellulose. It was suggested that very fine particles or small cellulose fragments (too small to see with the naked eye) were carried over into the Ha fraction (§3.6), resulting in insufficient separation of cellulose and the NaOH supernatant. The Ha fraction might be a good indicator for the molecular mass of cellulose molecules from the different eC preparations: SBP gave very little or no measurable Ha dry weight which was especially abundant in hveC preparations (compared to more minor fractions from all other eC preparations) (Figure 7). The native cellulose in SBP (with other polysaccharides attached) was possibly broken up into a network of smaller connected polysaccharides, while most matrix polysaccharides were removed during eC production at CelluComp Ltd.. Hydrogen peroxide and sodium hypochlorite might have loosened the microfibril structure and fragmented some cellulose chains into smaller molecules. Diankova & Doneva (2009) used H_2O_2 and sodium hypochlorite on textile dressings which resulted in transformation of the –OH groups into carbonyl groups without cutting the bond between carbon 2 and 3. Furthermore, Davidson (1938) was able to show that treatment with H_2O_2 did not always lead to lower

molecular weight but to instability of the oxycellulose towards alkali (without scission of the chain). The two oxidising treatments on the SBP starting material resulted in a loose network with high capacity to bind water and form viscous suspensions. It was eventually broken up by NaOH which solubilised matrix polysaccharides and potentially small cellulosic molecules (that precipitated upon acidification as Ha).

The composition of the hveC preparations H–J differed strongly in the quantity of each fraction (Figure 7): the quantitatively minor the α-cellulose fraction was, the bigger was the Ha fraction (and vice versa). I showed that the common procedure to separate preparations into the fractions was insufficient in splitting Ha from residual HbP and especially α-cellulose (§3.6). This relationship was clearly related to the composition of the two fractions: α-cellulose as well as Ha from hveC and normally produced eC were mostly composed of 'cellulosic' Glc (§3.5.2). On top of the previous discussion, the increased concentrations of oxidising chemicals during the production process apparently led to further fragmentation of cellulose than what was observed for normally produced eC.

This action of NaOH being able to solubilise cellulose fragments was also observed and studied by Dinand *et al.* (1999). Subjecting sodium chlorite-treated PCC to 2.5 M NaOH (and higher concentrations) caused crystalline modification of the native cellulose into cellulose II (§1.3.2.1), the microfibril structure disappeared and the sample had a gel-like appearance with loosely bound small round particles (microscopic studies) (Dinand *et al.* 1999). Besides, in water dispersed PCC formed thin, hard translucent films upon drying which were difficult to rehydrate and adhered strongly to polar surfaces (Weibel 1989). Dried eC products equally formed dry, hard and brittle films. Upon incubation with 3 M NaOH these turned into a gel-like, flexible, thin translucent film (§3.8.6.3). NaOH caused intra-crystalline swelling of the microfibrils and subsequent washing released (and partially solubilised (Takahashi & Shimazaki 1995)) cellulose chains that intermingled with one another and produced a gel-like cellulose II structure (Dinand *et al.* 1999). eC preparations were treated with 6 M NaOH which probably led to even greater swelling of microfibrils, release and solubilisation of even smaller cellulose chains that then did not sediment together with the α-cellulose fraction. Dinand *et al.* (1999) moreover discovered that the average viscometric degree of polymerisation of cellulose (DP_v) in PCC was not different from the parenchymal tissue found in SBP (DP_v 1000). It signified that the polymer chains in SBP cellulose were not degraded into smaller chains by the alkali and sodium

chlorite treatments performed for production of PCC. This cannot be directly related to eC products, but it offers the possibility that only upon NaOH treatment for extraction of the fractions eC cellulose was broken into smaller chains. Although H_2O_2 is known to fragment cellulose

Dry PCC consisted of spherical to oblong flattened “cells-ghosts” (20–200 µm diameter) of parenchyma from SBP, in which microfibrils were arranged in a random interwoven network. Disintegration of PCC in water (by blending) resulted in cells that were completely disrupted, showing individual and bundled microfibrils (Dinand *et al.* 1996). This contributed to PCC forming a stable homogeneous suspension in water (1.2% dry weight) (Weibel 1989). This hydrocolloid suspension possessed shear thinning properties together with pseudoplasticity due to liquid crystalline domains that broke upon stirring but reassembled into larger ones upon resting (Weibel 1989; Dinand *et al.* 1999). These PCC suspensions did not sediment or flocculate due to the presence of residual pectins. TFA treatment (1.8 M) allowed the microfibrils to aggregate due to the removal of residual pectins and hemicelluloses. Treatment with 3 M NaOH caused formation of cellulose II (Dinand *et al.* 1996, 1999). TFA and NaOH treatment equally removed residual pectins and hemicelluloses from eC preparations; among these removed components, pectic components contributed very little mass in contrast to the hemicellulosic components Xyl and Glc (e.g. Figure 9) or IP. PCC were durable to shear and not affected by extremes of temperature, salts or pH, which made PCC suitable to be employed for rheology control and as a viscosity and water loss control agent in well drilling (Weibel 1989). The authors further suggested PCC’s general application as a thickening, suspending, binding and coating agent (Weibel & Myers 1990; Dinand *et al.* 1996). The properties of PCC are strikingly similar to the properties of eC products which could hence be used as thickening agents not only in paints and coatings but also in the food industry, for healthcare products or in drilling fluids.

This chapter presents clear similarities between PCC (invented by Weibel (1986)) and the eC products. Both are suitable for multiple applications as thickening, suspending or binding agents and could be used by several industries. Both products are composed of native SBP cellulose (shown to easily disintegrate into soluble and insoluble fragments by NaOH) with residual pectins and hemicelluloses that, upon dispensation in water, stabilise the viscous, non-flocculating suspension.

4.3.1.4 *Unknown components in hydrolysed SBP and eC preparations*

Unknown components in this work were found after TFA hydrolysis of α-cellulose, Ha and HbP fractions from all SBP and eC preparations (§3.5). Another set of unknowns was also produced by Saeman hydrolysis of Ha fractions or paper (§3.5.2.1). Attempts made to identify and characterise some of these components (such as paper chromatography and high voltage paper electrophoresis of enzyme hydrolysis products) were unsuccessful (data not shown).

The most interesting unknowns were named $unknown_{orange}$ and $unknown_{pruple}$ and repeatedly observed after TFA hydrolysis of HbP fractions (Figure 12): although hot 2 M TFA was used for complete hydrolysis of the carbohydrate samples into monomers, it may have led to the production of disaccharides such as aldobiouronic acids (a uronic acid residue connected to a neutral sugar). $Unkown_{orange}$ (it was orange on thymol-stained TLC plates, just like Rha) was associated with the presence of pectic components and could be the disaccharide GalA-(1,2)-Rha from the incomplete hydrolysis of RG-I (Komalavilas & Mort 1986). The $unknown_{purple}$ (stained purple like Xyl with thymol) was tied in with the presence of hemicellulosic components (highest quantities found in eC preparations) and could be the product GlcA-(1,2)-Xyl of glucuronoxylan ((Fry 2000).

$Unknown_{red}$ showed the same R_f as Rha (but stained red) and was hence quantified together with Rha. It was often released together with Glc from cellulosic samples such as α-cellulose, Ha and even paper. It might therefore be an unusual hydrolysis product from Glc-containing polysaccharides.

4.4 Xyloglucan— does it form a tether between cellulose microfibrils?

Xyloglucan in eC products was suggested to play a major role in stabilising the cellulose microfibrils to form a stable viscous suspension. Currently, the tethering model (Fry 1989b) describing the tethering of xyloglucan coating cellulose microfibrils, is widely accepted as a major determinant of wall extensibility (Park & Cosgrove 2015). Hepworth & Bruce (2004) and other studies challenge this model, as it seems too tight to be compatible with some primary cell walls' high extensibility and flexibility (Hepworth & Bruce (2004) noticed unexpectantly high flexibility of onion epidermal cell walls). First, the molecular mass of xyloglucan was measured by different groups in different materials which found very different chain length. Estimation by gel

permeation chromatography (the commonly used method) is influenced by the extraction method used for xyloglucan, aggregation of the molecules and conformation and interaction with the column matrix. Typically, columns are calibrated with dextrans which have different conformational behaviour which could introduce overestimation of the molecular mass (therefore it needs to be regarded as relative data) (Park & Cosgrove 2015). Second, multiangle laser light scattering might provide better molecular mass estimation. This was done for tamarind xyloglucan estimated with GPC, coupled to multiangle laser, and also revealed that the coil shaped xyloglucan was much stiffer than dextran (Muller *et al.* 2011). The tethering model assumes that xyloglucan has a fully extended conformation and is present in sufficient amounts to coat most accessible cellulose surfaces (Park & Cosgrove 2015). Other studies found evidence that support the coil form of native xyloglucan (Hayashi 1989; Pauly *et al.* 1999). Third, Park & Cosgrove (2015) additionally note that commercial tamarind xyloglucan and the forms of cellulose used for most studies (Hayashi & Maclachlan 1984; Hayashi *et al.* 1987) differ from natural primary cell walls which might impact the applicability of those results on understanding xyloglucan/cellulose networks in native cell walls. A common assumption is that cellulose microfibrils are not in contact with each other directly. Contradicting the tethering model are results obtained through solid-state NMR showing that little of the cellulose microfibril surface is in contact with xyloglucan (Bootten *et al.* (2004) found 8%). Dick-Pérez *et al.* (2011) described the interaction of cellulose with Rha and GalA but not with xyloglucan. The research done by Dick-Pérez *et al.* (2011) studied the intermolecular contacts in ^{13}C-labeled *Arabidopsis thaliana* plant cell walls (by two- and three-dimensional MAS NMR). Cellulose showed extensive interaction with pectins but limited entrapment of xyloglucan in the microfibrils rather than extensive surface coating of tethering xyloglucans. Cell walls of triple knockout mutants that were deprived of xyloglucan were less stable compared to the wild type. Dick-perez *et al.* (2012) concluded, that the pectin–cellulose–xyloglucan interactions were responsible for major structural stability of the network. They proposed that pectin might hinder xyloglucan from binding to cellulose and would instead directly interact with xyloglucan (Dick-Perez *et al.* 2012). Pectin was often found to be highly abundant in SBP (§4.2.1.1) and could therefore also play a role in interaction of matrix polysaccharides with cellulose. Nonetheless, xyloglucan was the major matrix polysaccharide found in eC products and therefore considered to have major influence on viscosity by interacting with cellulose microfibrils. This was also strongly suggested by the work of Terenzi *et al.*

(2015) who studied the mobility of water and polymers in a xyloglucan/cellulose composite (in vitro generated from cellulose nanofibrils from softwood pulp mixed with commercial tamarind xyloglucan) hydrated in heavy water. They concluded that xyloglucan was strongly bonded to cellulose and provided stress transfer to preserve mechanical properties, which concurs with the traditional role of xyloglucan (in native cell walls) strengthening and tethering the cellulose network.

4.5 Molecular mass of SBP polysaccharides changes during the production of experimental Curran

Pectic polysaccharides are the dominant species in crude SBP HbP as high levels of Ara, Gal, GalA and Rha residues were found (§3.5 and §3.7). The relative molecular mass of SBP pectins (Ara, Gal, GalA and Rha residues eluted together after size-fractionation; §3.7) was approximately 60–80 kDa. An exception was GalA-containing polysaccharides from SBP AIR preparations with a relative molecular mass of only 21 kDa. Similar results were also found by other studies: alkaline extraction from SBP at high temperature (70–98°C for 15–90 min) followed by neutralisation and ultrafiltration yielded a branched arabinose-rich polysaccharide (with a molecular mass of about 50 kDa) containing around 80% Ara (McCleary *et al.* 1989). Some smaller polysaccharides from SBP were also extracted by Wen *et al.* (1988) (down to ~30 kDa for e.g. GalA containing polysaccharides) which showed fragmentation of polysaccharides like homogalacturonan (possibly due to 6 M NaOH).

Hemicellulosic polysaccharides in SBP, such as xyloglucan or xylan, had a relative molecular mass of approximately 45–50 kDa.

For the extraction of hemicelluloses and cellulose, Wen *et al.* (1988) developed a procedure using fine SBP particles, 85°C EDTA-extraction of pectins (in 0.1 M sodium phosphate buffer), 2.5 M NaOH extraction at 25°C followed by delignification (for more details see §4.2.1.2). Two molecular mass populations were found in each of the two fractions: Ha (separated on a Sepharose CL-6B column) was made of 150-kDa and 40-kDa molecules; Hb (separated on Sephadex G-200) of 150-kDa and 10-kDa. 2.5 M NaOH caused slight fragmentation of Hb (Wen *et al.* 1988), hence 6 M NaOH used in this work may have caused even greater fragmentation of pectins and hemicelluloses and led to smaller polysaccharides. The composition reported by Wen *et al.* did not correspond with the composition of Ha and HbP fractionated in this work

as the methods of extraction were very different. Hemicellulose and pectins from SBP in this work were generally smaller, between 10 and 80 kDa. Xyl, IP and Glc residues (in HbP fractions) were present in smaller polysaccharides between 20 and 45 kDa.

Fishman *et al.* (2009) extracted polysaccharides (mainly containing pectic components) with 12.5 M NaOH in MAE (details in § 4.2.1.2) and discovered a wide range of polysaccharides of 62–324 kDa.

In his thesis, Oosterveld (1997) performed two subsequent autoclave extractions at pH 5.2 (121°C, 40 min) followed by 4 M NaOH extraction (80°C, 2h) on SBP (hence yielding three fractions). The two autoclave fractions contained feruloylated RG-I with highly branched arabinose-rich side-chains and mean molecular masses of 1300 and 129 kDa respectively; these molecular masses were found to be higher than previously reported for hairy regions from beet, which may have been due to diferulate cross-links. Homogalacturonan, which was subjected to degradative conditions during extraction, was only 21 kDa in size. Furthermore, feruloylated arabinose-rich side-chains' molecular mass was 10–15 kDa.

After analysis of the published molecular mass compositions of polysaccharides extracted from SBP, it becomes clear that the method of choice for extraction has a major influence on the size of the extracted polysaccharides (also noticed by Park & Cosgrove (2015)). I therefore expect, that the choice of a different extraction method (instead of 6 M NaOH used for extraction in this work) would have resulted in different relative molecular masses of polysaccharides in eC preparations. Still, the chosen method led to results that can be compared between the eC and SBP fractions.

The relative molecular mass of 8–16 kDa for polysaccharides in HbP (three successive extractions in 6 M NaOH, 24 h at 37°C; §2.9) from eC preparations M–S (§3.7.1) was determined on a Sepharose CL-6B column with the fractionation range of 8–1000 kDa. This fractionation range was therefore considered to be unsuitable for estimating the size of hemicelluloses and pectins in HbP from eC preparations. It was therefore not possible on Sepharose CL-6B to identify differences in the molecular mass of eC products that were created through variations in the production process (§2.1). Consequently, a new column with a fractionation range for dextrans of 1–80 kDa was chosen to analyse normally produced eC B–F (viscosity 1520–1770 cP) and hveC H–J (5400–8620 cP).

Pectins in eC E and F (slightly higher in viscosity than eC B–D) contained higher concentrations of pectic components as well as bigger relative molecular mass polysaccharides than B–D. Pectins in HbP from eC B–D were between 6 and 17 kDa in size and approximately 20–50 kDa in HbP from eC E and F. It is likely that this difference was caused by small variations in the production process (not investigated further). In HbP from normally produced eC B–F, Glc-containing polysaccharides' relative molecular mass was 5–10 kDa but 7–20 kDa for Xyl- and IP- containing polysaccharides (such as xylan and xyloglucan). hveC pectins and hemicelluloses were of 3–10 kDa relative molecular mass and hence the smallest polysaccharides extracted from eC preparations. Xyloglucan in hveC HbP was significantly minor in relative molecular mass compared to xyloglucan from normally produced eC.

Consequently, all matrix polysaccharides identified in SBP were fragmented into smaller molecules during the production of eC. A trend of increasing viscosity with decreasing molecular mass was deduced from the molecular mass differences observed between normally produced eC and hveC matrix polysaccharides. I suspect that the formerly comparably tight primary cell-wall-network in SBP was transformed into a newly arranged polysaccharide network. Crosslinks between polysaccharides were kept or newly formed, building a (pectin-deprived) pectin–hemicellulose–cellulose network. This network was able to form stable viscous suspensions in water by allowing more interaction with water molecules (more details on the interaction with water in §4.7).

4.6 Missing carbohydrate material

From AIR (preparations K–S), 48–92% of the initial dry weight was recovered in fractions (§3.2), whereas from washed preparations (A–J) only 37–61% dry weight could be recovered. Explanations for the unaccountable missing material could be:

- imprecise values of starting solids
    - the AIR used was not completely dry
    - imprecise solid content measurements from washed preparations (although freeze-drying was shown to lead to reliable solid contents (§3.8.6.4)
- material loss during handling (especially when washing and sedimenting the sample solids)

- generation of soluble components which were lost after washing or dialysis (§4.6.1)
- inadequate quantification or TFA hydrolysis (§4.6.2)

The expected carbohydrate content of AIR from SBP and eC was close to 100% as most other components (such as protein, lipids and soil) were removed and lignin content of SBP was shown to be low, between 1 and 2% (Michel *et al.* 1988; Dinand *et al.* 1999) up to 6% (Wen *et al.* 1988). The latter research group delignified crude cellulose by a 1-h incubation in sodium chlorite which was enough to remove most lignin (down to 0.8% dry weight). Lignin could potentially hinder the solubility of the other plant cell wall polysaccharides (known as recalcitrance (Himmel *et al.* 2007)) but due to the low content it was not studied or removed further in this work. Lipids, lignin and protein (some protein might have been removed from SBP G during cooking at CelluComp Ltd.; §2.1) were not removed from SBP A and G preparations, as they were only prepared by washing in water (called washed preparation; §2.2). Dinand *et al.* (1996), when preparing PCC, found that bleaching with sodium chlorite and washing removed most residual lignin and proteins from SBP. I therefore assume that eC preparations (either AIR or washed preparations) were almost free of lignin and proteins. These constituents make about 20% of the total dry weight (§4.2.1) of SBP (Wen *et al.* 1988). During analysis of the carbohydrates present in total SBP and eC preparations (as was done after hydrolysis of all polysaccharides; §3.5) residual lipids, lignin and protein would not be accounted for and hence would be recorded as missing weight. Indeed, TFA hydrolysis (plus quantification) combined with the anthrone assay (§3.5.2.2) of total washed preparations resulted in missing weight of 0–83 µg/ 100 µg washed preparation. This result was much higher and more varied than expected.

During this work, different routes of dry weight loss were discovered (such as loss after gel-permeation chromatography of HbP (Figure 81), after extraction of the different fractions (Figure 7) or dialysis and washing of the fractions (Figure 8)) but did not fully explain the missing weight.

4.6.1 Material was missing after the extraction of fractions from preparations

Different experiments discussed in this chapter led to the discovery of loss or unaccountable material: first, measurement of the dry weight of the fractions extracted from the preparations (§3.2; Figure 7); second, carbohydrate analysis of total washed preparations (§3.5.2.2; Figure 20); third, carbohydrate analysis of extracted fractions

from AIR or washed preparations (§3.5.1; Figure 14) and fourth, carbohydrate analysis of dialysate and washes from fractions (§3.3).

Major weight loss was observed for preparations that had been split into the fractions HbP, Ha, α-cellulose and washings (§2.9). TFA-resistant α-cellulose presented the biggest difference between AIR and washed preparations: 2–29% recovery of the initial dry weight in A–J (AIR) but 32–61% for washed preparations K–S) (§3.2; Figure 7). α-Cellulose was mostly resistant to TFA hydrolysis but the ratio of TFA-hydrolysed to TFA-resistant α-cellulose among all preparations differed greatly. This might have been connected to the different production processes that were used to prepare eC products, but a connection to a specific treatment during production could not be identified. Compared with the other normally produced eC B–F (with similar viscosities), the normally produced eC C preparation showed a very high and unexpected percentage of TFA-hydrolysed α-cellulose.

Carbohydrate analysis of fractions from the preparations (α-cellulose, Ha and HbP) (Figure 14 and Figure 21) could not account for the total weight of the starting preparation. Moreover, the quantities of missing material did not show a correlation with the material missing from carbohydrate analysis of unfractionated preparations (Figure 20). Instead, 50–70 µg/ 100 µg AIR and 0-55 µg/ 100 µg washed preparation could not be accounted for by carbohydrate analysis of the fractions. This again showed a big difference between analysed AIR and washed preparations.

α-Cellulose and Ha fractions (from washed preparations A–J) were analysed by two total carbohydrate methods. The anthrone and the Saeman method both proved suitable to estimate Glc in the cellulose control (§3.5.2.1) but demonstrated difficulty in estimating correct quantities of Glc from α-cellulose and Ha fractions. Glc in the Ha fractions (and paper control) was underestimated by the Saeman method due to the production of intermediate cellulose products that could not be identified. As this proved to be an irreproducible artefact the Saeman method demonstrates sensitivity to small changes (probably small temperature differences) and needs to be improved to reproducibly quantify Glc in Ha fractions from SBP and eC preparations. Considering that Glc in Ha was underestimated, the difference in cellulosic Glc quantified from total preparations compared to Ha and α-cellulose fractions (discussed for SBP in §4.2.1) becomes even greater and less understandable.

Sulfuric acid hydrolysis of α-cellulose and Ha fractions produced brown coloured solutions (with different intensities for the different fractions) (§3.5.2.1). The anthrone reagent was added without determining the absorbance of these blanks. This influenced the absorbance that was measured for each sample and makes them less comparable. To optimise the anthrone method for α-cellulose and Ha fractions the absorbance of these coloured sulfuric acid solutions needs to be measured as a blank before addition of the anthrone reagent (this increases the manual labour for the assay significantly). Overall, Glc quantified after Saeman hydrolysis (in the α-cellulose and Ha fractions of preparations A–J) showed lower SEM and was preferred over the variable anthrone assay results (although it lead to underestimated Glc in Ha).

Comparatively low quantities of components were identified in HbP fractions from eC H, J and D (§3.5.2.2). This might have resulted from loss of material during dialysis of the fraction (§3.3). Carbohydrate material was indeed detected in the washes (mainly Ha washes) and dialysates (of HbP) of the fractions but this was estimated to be a negligible part of the total preparation. The amounts detected by the anthrone assay were variable and showed high SEM (as discussed above for residual carbohydrate quantification of the fractions). The detection of carbohydrates in salt-rich solutions should be optimised to generate reliable results. To further elucidate which carbohydrates were detected and how this material loss during the NaOH treatment could be avoided, these washings and dialysates need to be studied further and great care must be taken when handling and washing eC preparations. The detected carbohydrates could have resulted from the partial breakdown of hemicelluloses and pectins into soluble components or smaller than 12,000 kDa (dialysis tubing cut-off). This could have happened during storage of the eC products or NaOH extraction of the fractions (as discussed in §4.5).

4.6.2 The hydrolysis and quantification of components was insufficient

As was discussed in §4.2.1 the analysis of SBP described in this work might have underestimated the quantities of matrix polysaccharides but overestimated the quantity of cellulose. These conclusions must then also be applied to the eC preparations which were analysed in parallel. Hence, the methodology (TFA hydrolysis of the total preparations or TFA hydrolysis of the Ha, HbP and α-cellulose fractions with subsequent Photoshop quantification) was not adequate to quantify the total composition of hemicelluloses and pectins. After incomplete TFA hydrolysis, mainly hexoses (such as Glc and Gal) would be quantified by the subsequent

anthrone assay on the TFA-resistant residue (performed on total washed preparations (§3.5.2.2) as well as on α-cellulose and Ha from AIR; §3.5.1). This theory does not suffice to explain the results in this work as almost no TFA-resistant residue was left after TFA hydrolysis of HbP (richest in pectic and hemicellulosic components) (§3.2; Figure 7).

TFA hydrolysis products (dried in a SpeedVac and re-dissolved) were quantified from thymol-stained scanned TLC plates by Photoshop (§2.5). The quantity of each component was based on the quantification of marker gradients with known amounts. A good fit was achieved by applying a hyperbola with two or four parameters to the gradient data points (Figure 84); the equations were then used to calculate the quantity of components in the TFA hydrolysis products from the measured Photoshop mean. Several flaws to the method can be identified: quantification by Photoshop is a semi-quantitative method as it depends on the intensity of the bands in the marker gradients. Marker monosaccharides were partially degraded by hot TFA (5–17% degradation) which led to a reduction of the expected yield (§3.4). Furthermore, even and consistent staining with the thymol stain and consistent scanning quality are important for reproducible and comparable results. Drying TFA-hydrolysis products in the SpeedVac did not yield dry material but a partially caramelised syrup which was re-dissolved in a known volume of water, so the concentration of hydrolysed components/ initial dry weight might not have been exact.

2 M TFA had already been used by Dinand *et al.* (1999) for hydrolysis of non-cellulosic polysaccharides in SBP. They did not report incomplete hydrolysis, so I assume that the matrix polysaccharides were fully hydrolysed by 2 M TFA in this work too. This still leaves the possibility that components may have been partially degraded by TFA and not fully quantified by Photoshop. If that was the case, it should lead to a consistent calculatable difference between the true composition of SBP (and eC) preparations and the quantified composition. Hence, presenting the average quantified components in SBP preparations as a percentage of the published mean composition of SBP (§4.2.1; Figure 43) may result in similar percentages. Indeed, the following estimates (at least partly) support this argument: Xyl and Man each make 24–32% of the published composition, Gal and Ara each make 28–49%. These similar numbers led to the hypothesis that maximally half of the hydrolysis products (and minimally 24%) could be successfully quantified by the Photoshop method. Rha/unknown$_{red}$ made 44–46% of the published composition, this higher percentage

was probably due to the additional component $unknown_{red}$ (quantified together with Rha) in some TFA hydrolysed preparations (Figure 12). GalA was only quantified as 7–9% of the published compositions, this great difference cannot be explained momentarily unless most GalA (a major component in published compositions of SBP) was not present in SBP analysed in this work.

In conclusion, the source for the material loss and dry weight loss from eC and SBP preparations could not be fully determined in this work. All the introduced factors may have led to decreased quantification of the weight and carbohydrates present:

- the presence of lignin (hindering carbohydrate hydrolysis)
- underestimated Glc in Saeman hydrolysed Ha
- degradation of monosaccharides by hot TFA hydrolysis
- incomplete TFA hydrolysis of matrix polysaccharides and/or quantification by Photoshop
- imprecise solid content measurements
- material lost in the washing and dialysis steps

Alternative methods for hydrolysis (and quantification) of the carbohydrates are sulfuric acid (12 M, 35°C, 3 h) (Spagnuolo *et al.* 1997); the colorimetric orcinol assay (Guillon & Thibault 1989; Renard *et al.* 1997; Fares *et al.* 2001) or 1 M H_2SO_4 followed by gas-liquid chromatography (Oosterveld 1997). For specifically quantifying neutral sugars a more adequate method could be HPLC (Guillon & Thibault 1989; Spagnuolo *et al.* 1997). GalA in the published studies was most often quantified by an automated *m*-hydroxybiphenyl method (Renard *et al.* 1997; Oosterveld 1997; Fares *et al.* 2001; Reddad *et al.* 2002).

To verify or disprove the methods used in this work and the compositions that were obtained, some of the published methods should be applied to yield further information about the carbohydrate composition of SBP and eC preparations.

Material loss was rarely reported in published articles and it is therefore difficult to compare my results with published data. Agoda-Tandjawa *et al.* (2010) reported a less significant but similar problem when hydrolysing the cellulose residue from SBP, as the sum of all components did not reach 100%. They explained this by limited accessibility of glucosidic bonds in the glucan chains of cellulose to the 2 M H_2SO_4 (at 100°C for 2 h) used for pre-hydrolysis and hydrolysis (discussed in §4.3.1.2).

4.7 –OH group availability in carbohydrates

This work aimed to establish an easy method to semi-quantify –OH groups available for exchange with H_2O in eC and other carbohydrate materials. The proposed method is based on quantification of radioactivity (^3H) remaining bound to carbohydrate samples after removal of ^3H_2O by desiccation. The method that was established (§2.10) is very sensitive, and small changes may result in big differences in retained radioactivity.

Cellulose is known to have a high affinity to other OH group containing compounds, especially to small molecules like water. Site-specific reactivity of –OH groups on the surface as well as cellulose crystalline and amorphous regions increases the challenges to the question of how water molecules adsorb onto cellulose microfibrils (Lindh *et al.* 2017). The possibility of immobile water molecules present (or trapped) inside polymer samples (Silveira *et al.* 2016) adds further complications in testing the interaction of water and polysaccharides like cellulose. Lindh *et al.* (2017) used ^2H MAS-NMR on dried MCC (crystallinity 58 ±3%) that had been exposed to deuterated water before being re-dried in a heated vacuum chamber (0.3 mbar) under N_2 gas (Lindh *et al.* 2017). The work presented in this thesis aimed to establish a “low-tech” quantification method for ^3H bound to carbohydrate samples. First of all, heating was omitted to better represent the conditions of commercial Curran® after mixing with water-based paints (§1.4.1); second of all, the work with radioactive material, such as tritiated water, is strictly controlled and can only be performed in laboratories with equipment that is connected to an approved fume hood (to my knowledge no approved-heated-vacuum-chamber or oven was available at Edinburgh university). For those reasons, the simple setup in the established method in this work, was a desiccator (inside a fume hood) connected to a strong vacuum pump (<5 mbar).

Lindh *et al.* (2017) observed that only a quantitatively minor fraction of the sample’s weight increase was caused by exchange of ^1H in –OH groups of MCC with ^2H in ^2H_2O. Lindh *et al.* (2017), moreover, found that it was necessary to minimise the contact with atmospheric ^1H_2O as an exposure of only a few tens of seconds caused appreciable effects on the ^1H-^2H exchange. Even under strictly controlled conditions, they acknowledged that a negligible part of ^1H_2O vapour molecules could remain in the vacuum chamber and lead to a re-exchange of deuteroxyls in cellulose (Lindh *et*

al. 2017). The same effect was observed in this work, where ^{3}H was lost from all samples upon elongated drying in the desiccator or after direct exposure to the atmosphere (§3.8.3 and §3.8.5). These re-exchanges of H atoms were time dependent and could only be restricted (but not prevented) to an unknown extent by limiting the exposure to the atmosphere to 45–60 seconds after desiccation and choosing a constant drying period of 8 h. If cellulose re-exchanges ^{3}H at the same rate as ^{2}H, dried cellulosic samples could have lost a major percentage of their ^{3}H retained in these 45–60-second exposures to the atmosphere. Further evidence of almost instant ^{3}H exchange through the atmosphere was the observation that, after drying "cold" (non-tritiated) paper in the same desiccator with "hot" tritiated paper, both papers were almost equally radioactive (Figure 35). This leads to the deduction that every available –OH group (in liquid water, water vapour in the atmosphere, carbohydrate or any other material inside the desiccator) can readily exchange and re-exchange their hydrogen with ^{3}H or ^{1}H.

Lindh *et al.* (2017) achieved an almost complete removal of excess adsorbed water in 24 h drying; this was expected to leave deuterated –OH groups in cellulose unaltered. In this work, I tested if samples were visually dry after desiccation by checking if no water was visually present in the $^{3}H_2O$ control or the carbohydrate samples. All results presented in this work were obtained from samples that were visually fully dry. One major flaw of the method established in this work may be that dried samples were not tested further for residual $^{3}H_2O$ which would be adsorbed to different carbohydrate samples to varying extents (which may not be detected by eye). This would have led to higher radioactivity due to residual $^{3}H_2O$ plus the ^{3}H of –OH groups in tritiated carbohydrates. It would require major modifications of the current method to establish a method that guarantees complete removal of water. As Silveira *et al.* (2016) pointed out: when non-cellulosic components (such as hemicellulose, pectins or even water) are removed, cellulose fibrils collapse onto each other. Combinations of high temperature and low solvent density (commonly used for drying) favour this aggregation of cellulose fibrils and might also trap water molecules which then form hydration layers between cellulose microfibrils (Silveira *et al.* 2016). It was furthermore proven that it is impossible to return these cellulose aggregates to their original state (owing to hornification) (Laivins & Scallan 1993). The trapped $^{3}H_2O$ would have been (at least partially) released into the sodium acetate–scintillation fluid mixture and hence contributed to the samples measured radioactivity.

Pönni *et al.* (2014) exposed birch kraft pulp to D_2O vapour and found that the quantity of accessible –OH groups was dependent on the time exposed to D_2O vapour. This was not observed in my work, where liquid ^3H_2O was used instead of D_2O vapour and incubated with different carbohydrate samples. Exchange of H between carbohydrates and ^3H_2O occurred almost instantly (§3.8.2) and longer incubation (for hours not days as was done by Pönni *et al*.) did not change the results.

The higher the relative humidity in the system and the larger the measure of cell wall bound water, the larger the number of exchanged –OH groups (demonstrated by Taniguchi *et al.* (1978), Pönni *et al.* (2014) and Lindh *et al.* (2017)). Water molecules adsorb directly onto –OH groups of external and internal surfaces as well as to amorphous cellulose regions — at high relative humidity, predominantly on external and amorphous regions (Okubayashi *et al.* 2004). My experiments may correlate with these models: drying with a ^3H_2O trap that included the desiccant molecular sieve rods (§3.8.4 and §3.8.6.3) led to increased radioactivity of dried tritiated carbohydrate samples, possibly by providing a reservoir of ^3H_2O that was available for adsorption throughout the drying process. Molecular sieve rods may have released ^3H_2O, even against the vacuum flow of the pump. Hence carbohydrate samples dried with a ^3H_2O trap may have had more ^3H_2O adsorbed than the ones dried without a trap, which led to an increased apparent –OH group exchange and higher radioactivity of the samples.

SBP (after drying without a ^3H_2O trap; Figure 38) showed percentages ^3H retained close to the expected percentage of exchanged ^3H (calculated on the assumption that cellulose, and/or polymers with the same H-exchange capacity, are responsible for most of the ^3H retention by SBP), while drying without a trap led to higher percentages than expected (141–158%). Wen *et al.* (1988) suggested that pectin was mostly responsible for the water-holding capacity of SBP, which might have influenced the complete or incomplete drying of SBP in this work (visually checked to be fully dry but not by any other methods).

All SBP samples showed a percentage of ^3H retained similar to that of plain dry paper (Figure 38) or ‘dried cellulose’ controls. The percentage ^3H retained for ‘changed production process eC’ was significantly lower than for SBP. Normally produced eC products resulted in values close to those of SBP while hveC products gave higher values (mean 168% ^3H retained after drying without a trap and 252% after drying with a trap). This led to the conclusion that confirmed the hypothesis for this experiment:

availability of –OH groups and hence exchange of H between ^3H_2O and carbohydrate samples increases with increasing viscosity of eC products. It also shows, that the availability of –OH groups is not simply increased due to the action of oxidising chemicals on SBP during the production of eC. In fact, it requires elevated concentrations (§2.1) of oxidising chemicals to achieve higher availability of –OH groups and increased viscosity. In addition (or as an alternative) to this conclusion, the water holding capacity or retention of ^3H_2O might have increased with increasing viscosity.

The availability of –OH groups semi-quantified in 'never-dried cellulose' from hardwood pulp (§3.8.6.2, Figure 38) showed higher availability of –OH groups than expected (155% ^3H retained after desiccation without a trap) and was higher than the measured availability for previously 'dried cellulose' (from hardwood pulp) (91% ^3H retained) or paper (105% ^3H retained). These results do not allow for any deductions about which of the three potentially available –OH groups were included in the ^3H exchange (§1.5) as no data about the samples' crystallinity were given. Never-dried cellulose was confirmed to be highly crystalline in structure after the O(3)H was measured to be nearly unavailable when compared to O(2)H (Rowland & Howley 1988). The same research by Rowland & Howley showed that drying led to the distortion of some crystalline cellulose structures into disordered amorphous structures and to an increase in the exchangeability of the O(3)H. At the same time however, dried cellulose also undergoes hornification and does not return to its original structure after rewetting owing to the formation of additional stable H-bonds (Laivins & Scallan 1993). Hornification therefore leads to cellulose with fewer accessible –OH groups which could be further reduced by multiple drying and wetting cycles. Alkaline treatment of birchwood cellulose helped to increase –OH group accessibility (Pönni *et al.* 2014). NaOH was therefore a suitable agent for re-swelling dried carbohydrate samples before quantification of ^3H in this work.

Xyloglucan showed the highest availability of –OH groups after drying without or with a ^3H_2O trap (180% and 239% ^3H retained respectively, relative to the predicted value; Figure 38). It was higher than 100% which probably resulted from the simplified calculations that were done to estimate the expected percentage of ^3H retained (§3.8.6.2) and xyloglucan samples may still have contained ^3H_2O after drying (§3.8.6); visual testing for dryness was difficult as these samples looked like empty vials after drying. Xyloglucan and eC products (§1.4.1) in water are viscous and show good

water holding capacity. Tamarind xyloglucan is known to form a viscous solution in water and is used as a viscosifier in food production (Glicksman 1986).

Glc has a very high solubility in water due to hydrogen bonding (five available –OH groups per Glc; §3.8.6.1; Box 1). Also dextran is soluble in water and can exchange O-bonded H atoms (Lindman *et al.* 2010). Both Glc and dextran were expected to exchange all potentially exchangeable H atoms with ^3H_2O as there was no spatial hindrance through aggregates; in my experiments, they retained 81% and 76% ^3H, relative to the theoretical value, respectively (it needs to be kept in mind that Glc dried as a ^3H_2O containing syrup).

Several simplifications and assumptions had to be made in this work to calculate the expected H exchange and compare it to the measured H exchange (§3.8.6.1). It was assumed that the total dry weight of each sample represented 100% dry carbohydrate and was only composed of Glc residues (except for xyloglucan, assumed to be composed of four Glc, three Xyl and one Gal residue). For cellulosic samples, two out of three –OH groups per Glc residue were expected to exchange H with ^3H_2O, for dextran this number was three, for xyloglucan 2.625, and five for Glc. To simplify comparison of all samples, the contribution of terminal –OH groups (except for the monomeric Glc with no “termini”) as well as the difference between crystalline and amorphous structures was regarded as negligible. Furthermore, a balanced distribution of ^3H between water and carbohydrate sample was expected. All following samples were considered cellulosic: ‘never-dried cellulose’, ‘dried cellulose’, paper, Avicel, MCC, SBP and eC products. This did not take into account the presence of other polysaccharides composed of different monomeric residues (such as the major non-cellulosic residues Ara or Xyl in eC products and SBP). All these assumptions and simplifications enabled a relative comparison of the percentage ^3H retained, representing the percentage of ^3H retained relative to the ^3H expected to be retained through the exchanged H atoms of –OH groups in carbohydrate samples.

In conclusion, the results in this work represented the exchanged –OH groups as well as the residual ^3H_2O (if any; in unknown quantities) and hence overestimated the real number of available –OH groups. This is supported by the high improbability that all expected available –OH groups were accessible in cellulosic samples due to intra- and inter-molecular H-bonds (§1.3.2.1) in the cellulose network or shielded microfibril surfaces.

In summary, this work reports an easy, but sensitive, relative quantification method for measuring available –OH groups in different carbohydrate materials such as paper, xyloglucan, SBP or eC products. It is based on the quantification of ^{3}H remaining bound to carbohydrate samples after removal of $^{3}H_2O$ by desiccation. Because of the generalised assumptions, simplified calculations and possibly insufficient removal of water, the results obtained can only be used for relative comparison of the samples with each other and represent ^{3}H in accessible –OH groups plus any residual $^{3}H_2O$. Among the experts, it is a well-established fact that the O(3)H in highly crystalline cellulose is not exchanged, but becomes available after structural changes (e.g. introduced by drying) into amorphous cellulose (Rowland *et al.* 1969). 'Never-dried cellulose' (highly crystalline) in this work showed higher availability of –OH groups than 'dried cellulose' (likely to have decreased crystallinity (Rowland *et al.* 1969)) due to hornification of cellulose microfibrils. Exchange between –OH groups and $^{3}H_2O$ probably took place on the surface of microfibrils accessible to water; it occurs instantaneously and the number of accessible OH groups correlates with the measure of cell wall bound water (Taniguchi *et al.* 1978; Pönni *et al.* 2014). Contact with atmospheric $^{1}H_2O$ should ideally be excluded as it results in further exchange of retained ^{3}H. The percentage of ^{3}H retained and hence availability of –OH groups in eC increases with increasing viscosity. This was true for the hveC samples produced with elevated concentrations of oxidising chemicals (normally produced eC were not generally higher in ^{3}H retained than the SBP controls). In conclusion, viscosity of eC (and Curran®) products probably benefits from increasing the availability of –OH groups as these may lead to the formation of more H-bonds between polysaccharide-particles as well as between polysaccharide-particles and water molecules (meaning greater stability of the polysaccharide-water-network to flocculation of eC or Curran® suspensions). More –OH groups in Curran®, as an additive in paints, may moreover result in enhanced viscosity and cracking resistance (in cold and hot environments) as they bind polysaccharide-particles to paint ingredients such as paint particles.

4.8 Future experiments

This work showed that the SBP derived eC was enriched in cellulose and contained fragmented hemicelluloses (such as xyloglucan) and residual pectins (like RG-I). As many previous studies (e.g. Wen *et al.* (1988), Dinand *et al.* (1996, 1999) and Agoda-

Tandjawa *et al.* (2010)) on comparable products showed that these residual matrix polysaccharides are crucial for viscosity and stability of the cellulose-rich suspensions, it would be interesting to confirm if that is also true for eC products. This could be achieved by analysing a never-dried cellulose fraction of eC preparations (after careful removal of matrix polysaccharides so to not fragment the cellulose further) for molecular mass of cellulose chains (gel-permeation chromatography), viscosity (with a viscometer) and –OH-group availability. The cellulose sample should ideally also include the cellulose that was extracted in the 'Ha' fraction from eC (especially hveC) preparations. It can help to further explain the reasons for the high viscosity of hveC compared with eC products.

The investigation of the composition of eC and SBP was difficult as material weight loss led to incompletely determined compositions. Future experiments on SBP and eC could include alternative methods to extract and quantify carbohydrates and monomers. A plausible quantification method could be the colorimetric orcinol assay (for assaying pentose residues), the *m*-hydroxybiphenyl method (for uronic acid residues) or HPLC besides TFA hydrolysis, the anthrone assay and the Saeman hydrolysis. The alternative methods might aid in identifying the routes for material loss or avoid these losses completely. Furthermore, lignin should be quantified and separated from the other cell wall components in eC products. This could then help to determine lignin's potential contribution to the samples' recalcitrance towards hydrolysis.

The method for quantification of –OH-group accessibility established in this work should be optimised to exclude some of the identified factors that could interfere with the results and the true number of available –OH groups in the samples. Exposure to atmospheric water vapour should ideally be omitted, possibly by passing a gas (heavier than atmospheric air) into the desiccator when releasing the vacuum. As however, the samples' radioactivities were mostly found to be higher than expected, it is most important to ensure that all samples are completely dry, which could be realised by pre-experiments that measure the residual moisture in the desiccated samples (especially in eC and xyloglucan, which show good water holding capacity).

5 References

Agoda-Tandjawa G., Durand S., Berot S., Blassel C., Gaillard C., Garnier C., Doublier J. (2010) Rheological characterization of microfibrillated cellulose suspensions after freezing. *Carbohydrate Polymers* **80**:677–686.

Agoda-Tandjawa G., Durand S., Gaillard C., Garnier C., Doublier J.L. (2012) Properties of cellulose/pectins composites : Implication for structural and mechanical properties of cell wall. *Carbohydrate Polymers* **90**:1081–1091.

Aksu Z., Işoğlu I.A. (2005) Removal of copper(II) ions from aqueous solution by biosorption onto agricultural waste sugar beet pulp. *Process Biochemistry* **40**:3031–3044.

Albersheim P., Darvill A., Roberts K., Sederoff R., Staehelin A. (2010) The structural polysaccharides of the cell wall and how they are studied. In: Plant Cell Walls. From Chemistry to Biology, 1st edn. Garland Science, New York, p 430.

Atalla R.H., VanderHart D.L. (1984) Native cellulose: a composite of two distinct crystalline forms. *Science* **223**:283–285.

Bauer W.D., Talmadge K.W., Keegstra K., Albersheim P. (1973) The structure of plant cell walls. The hemicellulose of the walls of suspension-cultured sycamore cells. *Plant Physiology* **51**:174–187.

Beale R.J., Bradbury A.G.W., Medcalf D.G., Romig W.R. (1984) Sugar beet Pulp bulking agent and process. :1–5.

Bootten T.J., Harris P.J., Melton L.D., Newman R.H. (2004) Solid-state 13 C-NMR spectroscopy shows that the xyloglucans in the primary cell walls of mung bean (Vigna radiata L.) occur in different domains: a new model for xyloglucan-cellulose interactions in the cell wall. *Journal of Experimental Botany* **55**:571–583.

Bridge M. (2018) Carrots give extra strength to concrete. *The Times*:14.

Buchholt H.C., Christensen T.M.I.E., Fallesen B., Ralet M.C., Thibault J.F. (2004) Preparation and properties of enzymatically and chemically modified sugar beet pectins. *Carbohydrate Polymers* **58**:149–161.

Cárdenas-Fernández M., Bawn M., Hamley-Bennett C., Bharat P.K. V., Subrizi F., Suhaili N., Ward D.P., Bourdin S., Dalby P.A., Hailes H.C., Hewitson P., Ignatova S., Kontoravdi C., Leak D.J., Shah N., Sheppard T.D., Ward J.M., Lye G.J. (2017) An integrated biorefinery concept for conversion of sugar beet pulp into value-added chemicals and pharmaceutical intermediates. *Faraday Discussions* **202**:415–431.

CelluComp Ltd. CelluComp, sustainable materials. *CelluComp.com* [online] URL: http://cellucomp.com/ (accessed 20 May 2018).

Centre, F. A. O. I., Europe, E. and States I. (1999) Sugar Beets / White Sugar. *Agribusiness Handbooks* **4**:35–43.

Centre, F. A. O. I., Europe, E. and States I. (2009) Sugar Beet White Sugar. *Agribusiness Handbooks*:1–55.

Chanliaud E., De Silva J., Strongitharm B., Jeronimidis G., Gidley M.J. (2004) Mechanical effects of plant cell wall enzymes on cellulose/xyloglucan composites. *The Plant Journal* **38**:27–37.

Davidson G.F.D.S. (1938) 18—The effect of alkalis on the molecular chain length of chemically modified cotton celluloses, as shown by fluidity measurements on the derived nitrocelluloses. *Journal of the Textile Institute Transactions* **29**:T195–T218.

Diankova S.M., Doneva M.D. (2009) Analysis of oxycellulose obtained by partial oxidation with different reagents. *Bulgarian Chemical Communications* **41**:391–396.

Dick-Perez M., Wang T., Salazar A., Zabotina A., Hong M. (2012) Multidimensional solid-state NMR studies of the structure and dynamics of pectic polysaccharides in uniformly 13 C-labeled Arabidopsis primary cell walls. *Magnetic Resonance in Chemistry* **50**:539–550.

Dick-Pérez M., Zhang Y., Hayes J., Salazar A., Zabotina O.A., Hong M. (2011) Structure and interactions of plant cell-wall polysaccharides by two- and three-dimensional magic-angle-spinning solid-state NMR. *Biochemistry* **50**:989–1000.

Dinand, Chanzy H., Vignon M.R. (1996) Parenchymal cell cellulose from sugar beet pulp: preparation and properties. *Cellulose* **3**:183–188.

Dinand, Chanzy H., Vignon R.M. (1999) Suspensions of cellulose microfibrils from sugar beet pulp. *Food Hydrocolloids* **13**:275–283.

Dinand E., Vignon M.R. (2001) Isolation and NMR characterisation of a (4-O-methyl-D-glucurono)-D-xylan from sugar beet pulp. *Carbohydrate Research* **330**:285–288.

Dohm J.C., Minoche A.E., Holtgräwe D., Capella-Gutiérrez S., Zakrzewski F., Tafer H., Rupp O., Sörensen T.R., Stracke R., Reinhardt R., Goesmann A., Kraft T., Schulz B., Stadler P.F., Schmidt T., Gabaldón T., Lehrach H., Weisshaar B., Himmelbauer H. (2014) The genome of the recently domesticated crop plant sugar beet (Beta vulgaris). *Nature* **505**:546–549.

Dronnet V.M., Renard C.M.G.C., Axelos M.A.V., Thibault J.F. (1997) Binding of divalent metal cations by sugar-beet pulp. *Carbohydrate Polymers* **34**:73–82.

Drusch S. (2007) Sugar beet pectin: A novel emulsifying wall component for microencapsulation of lipophilic food ingredients by spray-drying. *Food Hydrocolloids* **21**:1223–1228.

Edelmann H.G., Fry S.C. (1992) Factors that affect the extraction of xyloglucan from the primary cell walls of suspension-cultured rose cells. *Carbohydrate Research* **228**:423–431.

Encyclopaedia Britannica (2015) Caryophyllales. *Encyclopaedia Britannica Online* [online] URL: http://www.britannica.com/plant/sugar-beet

European Biogas Association (2017) *Monofermentation of industrial by-products: implementation at industrial quality level in the sugar industry; in Success Stories of the Members of the European Biogas Association*. Brussels.

Fares K., Renard C.M.G.C., R'zina Q., Thibault J.F. (2001) Extraction and composition of pectins and hemicelluloses of cell walls of sugar beet roots grown in Morocco. *International Journal of Food Science and Technology* **36**:35–46.

Faruk O., Bledzki A.K., Fink H.P., Sain M. (2012) Biocomposites reinforced with

natural fibers: 2000-2010. *Progress in Polymer Science* **37**:1552–1596.

Finkenstadt V.L., Liu C.-K., Cooke P.H., Liu L.S., Willett J.L. (2008) Mechanical property characterization of plasticized sugar beet pulp and poly(lactic acid) green composites using acoustic emission and confocal microscopy. *Journal of Polymers and the Environment* **16**:19–26.

Fishman M.L., Chau H.K., Cooke P.H., Yadav M.P., Hotchkiss A.T. (2009) Physico-chemical characterization of alkaline soluble polysaccharides from sugar beet pulp. *Food Hydrocolloids* **23**:1554–1562.

Fleming A. (2018) UK sugar beet yields hit record levels - Farmers Weekly. *Farmers Weekly* [online] URL: https://www.fwi.co.uk/arable/sugar-beet/uk-sugar-beet-yields-hit-record-levels (accessed 22 August 2018).

Fowler P.A., Hughes J.M., Elias R.M. (2006) Biocomposites : technology , environmental credentials and market forces. *Journal of the Science of Food and Agriculture* **8**:1781–1789.

Fry S.C. (1989a) Cellulases , hemicelluloses and auxin-stimulated growth: a possible relationship. *Physiologia Plantarum* **75**:532–536.

Fry S.C. (1989b) The structure and functions of xyloglucan. *Journal of Experimental Botany* **40**:1–11.

Fry S.C. (2000) *The growing plant cell wall: Chemical and metabolic analysis*, Reprint. The Blackburn Press, Caldwell.

Fry S.C. (2011) Cell Wall Polysaccharide Composition and covalent crosslinking. In: Ulvskov P (ed) Plant polysaccharides, Biosynthesis and Bioengineering, Annual Pla. Wiley-Blackwell, p 41: 1-42.

Fry S.C., Franková L., Chormova D. (2011) Primary cell wall synthesis and expansion: setting the boundaries. *The Biochemist* **33**:14–19.

Gårdebjer S., Larsson A., Löfgren C., Ström A. (2015) Controlling water permeability of composite films of polylactide acid, cellulose, and xyloglucan. *Journal of Applied Polymer Science* **41219**:1–8.

Gardner K.H., Blackwell J. (1974) The structure of native cellulose. *Biopolymers*

13:1975–2001.

Gérente C., Couespel Du Mesnil P., Andrès Y., Thibault J.F., Le Cloirec P. (2000) Removal of metal ions from aqueous solution on low cost natural polysaccharides. Sorption mechanism approach. *Reactive and Functional Polymers* **46**:135–144.

Gilbert B.C., King D.M., Thomas C.B. (1984) The oxidation of some polysaccharides radical: an e.s.r. investigation. *Carbohydrate Research* **125**:217–235.

Glicksman M. (1986) *Food Hydrocolloids* (M. Glicksman, Ed.), Volume III. CRC-Press, Bocca Raton, Florida.

Guillon F., Auffret A., Robertson J.A., Thibault J.F., Barry J.L. (1998) Relationships between physical characteristics of sugar-beet fibre and its fermentability by human faecal flora. *Carbohydrate Polymers* **37**:185–197.

Guillon F., Thibault J. (1989) Methylation analysis and mild acid hydrolysis of the “hairy” fragments of sugar beet pectins. *Carbohydrate Research* **190**:85–96.

Hayashi T. (1989) Xyloglucans in the primary cell wall. *Annual Review of Plant Physiology and Plant Molecular Biology* **40**:139–168.

Hayashi T., Maclachlan G. (1984) Pea xyloglucan and cellulose: I. Macromolecular organization. *Plant physiology* **75**:596–604.

Hayashi T., Marsden M.P.F., Delmer D.P. (1987) Pea xyloglucan and cellulose: V. xyloglucan-cellulose interactions in vitro and in vivo. *Plant Physiology* **83**:384–389.

Heinze T., El Seoud O.A., Koschella A. (2018) *Cellulose Derivatives: Synthesis, Structure and Properties*. Springer International Publishing, Cham, Switzerland.

Heitner C., Dimmel D., Schmidt J. (2010) Overview. In: Heitner C, Dimmel D, Schmidt J (eds) Lignin and Lignans: Advances in Chemistry, 1st edn. CRC Press, Boca Raton, Florida, pp 1–10.

Hepworth D.G., Bruce D.M. (2004) Relationship between primary plant cell wall architecture and mechanical properties for onion bulb scale epidermal cells.

Journal of Texture Studies **35**:586–602.

Hepworth D., Whale E. (2016) Cellulose particulate material. :1–50.

Himmel M.E., Ding S., Johnson D.K., Adney W.S., Nimlos M.R., Brady J.W., Foust T.D. (2007) Biomass recalcitrance: engineering plants and enzymes for biofuels production. *Nature* **315**:804–807.

Hoffmann C.M., Kenter C., Bloch D. (2005) Marc concentration of sugar beet (Beta vulgaris L) in relation to sucrose storage. *Journal of the Science of Food and Agriculture* **85**:459–465.

Huang X., Dou J. yang, Li D., Wang L. jun (2018) Effects of superfine grinding on properties of sugar beet pulp powders. *LWT - Food Science and Technology* **87**:203–209.

Huang X., Li D., Wang L. jun (2018) Effect of particle size of sugar beet pulp on the extraction and property of pectin. *Journal of Food Engineering* **218**:44–49.

Ishii T., Matsunaga T. (2001) Pectic polysaccharide rhamnogalacturonan II is covalently linked to homogalacturonan. *Phytochemistry* **57**:969–974.

Kar F., Arslan N. (1999) Effect of temperature and concentration on viscosity of orange peel pectin solutions and intrinsic viscosity-molecular weight relationship. *Carbohydrate Polymers* **40**:277–284.

Kawamoto H. (2007) Trends in research and development on plastics of plant origin — from the perspective of nanocomposite polylactic acid for automobile use —. *Science & Technology Trends* **22**:62–75.

Komalavilas P., Mort A. (1986) Identification of acetate groups on the backbone of rhamnogalacturonan I, a pectic polysaccharide of primary walls, obtained from suspension cultured cotton cells. In: Annual meeting of the American Society of Plant Physiologists. Baton Rouge (LA) USA

Kondo T. (2004) Hydrogen bonds in cellulose and cellulose derivatives. In: Dumitriu S (ed) Polysaccharides: Structural Diversity and Functional Versatility, 2nd edn. CRC Press, Boca Raton, Florida, pp 62–98.

Kraemer E.O., Natta F.J. Van (1931) Viscosity and molecular weights of polymeric

materials. *The Journal of Physical Chemistry* **36**:3175–3186.

Kühnel S., Schols H.A., Gruppen H. (2011) Aiming for the complete utilization of sugar-beet pulp: Examination of the effects of mild acid and hydrothermal pretreatment followed by enzymatic digestion. *Biotechnology for biofuels* **4**:1–14.

Laivins G. V., Scallan H.M. (1993) The mechanism of hornification of wood pulps. In: Baker CF (ed) Products of Papermaking, Transactions of the tenth fundamental Research Symposium. Pira International, Leatherhead Surrey, U. K., Oxford, U. K., pp 1235–1260.

Lancaster University (2018) Vegetables could hold the key to stronger buildings and bridges. *Lancaster.ac.uk* [online] URL: http://www.lancaster.ac.uk/news/vegetables-could-hold-the-key-to-stronger-buildings-and-bridges (accessed 22 August 2018).

Leitner J., Hinterstoisser B., Wastyn M., Keckes J., Gindl W. (2007) Sugar beet cellulose nanofibril-reinforced composites. *Cellulose* **14**:419–425.

Levigne S., Ralet M.C., Thibault J.F. (2002) Characterisation of pectins extracted from fresh sugar beet under different conditions using an experimental design. *Carbohydrate Polymers* **49**:145–153.

Lindh E.L., Bergenstråhle-Wohlert M., Terenzi C., Salmén L., Furó I. (2016) Non-exchanging hydroxyl groups on the surface of cellulose fibrils: The role of interaction with water. *Carbohydrate Research* **434**:136–142.

Lindh E.L., Terenzi C., Salmén L., Furó I. (2017) Water in cellulose: evidence and identification of immobile and mobile adsorbed phases by 2H MAS NMR. *Physical Chemistry Chemical Physics* **19**:4360–4369.

Lindman B., Karlström G., Stigsson L. (2010) On the mechanism of dissolution of cellulose. *Journal of Molecular Liquids* **156**:76–81.

Liquid Energy Trading Company Swiss S.A. (2015) Molasses and congeneric products - Sugar beet molasses. [online] URL: http://www.liquid-energy.ch/en/products.html

Ma S., Yu S.J., Zheng X.L., Wang X.X., Bao Q.D., Guo X.M. (2013) Extraction,

characterization and spontaneous emulsifying properties of pectin from sugar beet pulp. *Carbohydrate Polymers* **98**:750–753.

Mathew A.P., Oksman K., Sain M. (2006) The effect of morphology and chemical characteristics of cellulose reinforcements on the crystallinity of polylactic acid. *Journal of Applied Polymer Science* **101**:300–310.

Matthews J.F., Skopec C.E., Mason P.E., Zuccato P., Torget R.W., Sugiyama J., Himmel M.E., Brady J.W. (2006) Computer simulation studies of microcrystalline cellulose Iβ. *Carbohydrate Research* **341**:138–152.

McCleary B. V., Cooper J.M., Williams E.L. (1989) Debranched araban and its use as fat substitute.

McCready R.M. (1966) Polysaccharides of Sugar Beet Pulp, A Review of Their Chemistry. *Journal of the American Society of Sugar Beet Technologists* **14**:260–270.

Michel F., Thibault J., Barry J., de Baynast R. (1988) Preparation and characterization of dietary fibre from sugar beet pulp. *Science of food and agriculture* **42**:77–85.

Michel F., Thibault J.-F., C. M., Heitz F., Pouillaude F. (1985) Extraction and characterization of pectins from sugar beet pulp. *Journal of Food Science* **50**:1499–1500.

Miller A.R. (1986) Oxidation of cell wall polysaccharides by hydrogen peroxide: A potential mechanism for cell wall breakdown in plants. *Biochemical and Biophysical Research Communications* **141**:238–244.

Minor J.L. (1994) Hornification - its origin and meaning. *Progress in paper recycling* **3**:93–95.

Mouelhi R., Abidi F., Galai S., Marzouki M.N. (2014) Immobilized sclerotinia sclerotiorum invertase to produce invert sugar syrup from industrial beet molasses by-product. *World journal of microbiology & biotechnology* **30**:1063–73.

Muller F., Manet S., Jean B., Chambat G., Boué F., Heux L., Cousin F. (2011) SANS Measurements of semiflexible xyloglucan polysaccharide chains in water

reveal their self-avoiding statistics. *Biomacromolecules* **12**:3330–3336.

Nordic Sugar (2011) Fibrex® proves its value in gluten-free ready meals - Nordic Sugar. *Nordic Sugar*

Nordic Sugar (2014) Fibrex: product specification. :1–2.

O'Rourke C., Gregson T., Murray L., Sadler I.H., Fry S.C. (2015) Sugar composition of the pectic polysaccharides of charophytes, the closest algal relatives of land-plants: presence of 3-O-methyl-D-galactose residues. *Annals of Botany*:1–12.

Okubayashi S., Griesser U.J., Bechtold T. (2004) A kinetic study of moisture sorption and desorption on lyocell fibers. *Carbohydrate Polymers* **58**:293–299.

Oosterveld A. (1997) *Pectic substances from sugar beet pulp: structural features, enzymatic modification, and gel formation*. Wageningen University & Research Centre

Oosterveld A., Beldman G., Schols H.A., Voragen A.G.J. (1996) Arabinose and ferulic acid rich pectic polysaccharides extracted from sugar beet pulp. *Carbohydrate Research* **288**:143–153.

Park Y.B., Cosgrove D.J. (2015) Xyloglucan and its interactions with other components of the growing cell wall. *Plant and Cell Physiology* **56**:180–194.

Pauly M., Albersheim P., Darvill A., York W.S. (1999) Molecular domains of the cellulose/xyloglucan network in the cell walls of higher plants. *The Plant Journal* **20**:629–639.

Pehlivan E., Yanik B.H., Ahmetli G., Pehlivan M. (2008) Equilibrium isotherm studies for the uptake of cadmium and lead ions onto sugar beet pulp. *Bioresource Technology* **99**:3520–3527.

Pippen E.L., McCready R.M., Owens H.S. (1950) Gelation properties of partially acetylated pectins. *Journal of the American Chemical Society* **72**:813–816.

Pönni R., Rautkari L., Hill C.A.S., Vuorinen T. (2014) Accessibility of hydroxyl groups in birch kraft pulps quantified by deuterium exchange in D2O vapor. *Cellulose* **21**:1217–1226.

Ralet M., Guillon F., Renard C.M.G.C., Thibault J. (2009) Sugar beet fiber: production, characteristics, food applications and physiological benefits. *Fiber Ingredients: Food Applications and Health Benefits*:365–369.

Reddad Z., Gérente C., Andrès Y., Ralet M.C., Thibault J.-F., Le Cloirec P. (2002) Ni(II) and Cu(II) binding properties of native and modified sugar beet pulp. *Carbohydrate Polymers* **49**:23–31.

Reddy N., Yang Y. (2005) Biofibers from agricultural byproducts for industrial applications. *Trends in biotechnology* **23**:22–7.

Renard C.M.G.C., Jarvis M.C. (1999) A cross-polarization, magic-angle-spinning, 13C-nuclear-magnetic-resonance study of polysaccharides in sugar beet cell walls. *Plant Physiology* **119**:1315–1322.

Renard C.M.G.C., Lahaye M., Mutter M., Voragen F.G.J., Thibault J.F. (1997) Isolation and structural characterisation of rhamnogalacturonan oligomers generated by controlled acid hydrolysis of sugar-beet pulp. *Carbohydrate Research* **305**:271–280.

Roboz E., Van Hook A. (1946) Chemical study of beet pectin. In: American Society of Sugar Beet Technologists.pp 574–583.

Roland J.C., Reis D., Vian B., Roy S. (1989) The helicoidal plant cell wall as a performing cellulose-based composite. *Biology of the Cell* **67**:209–220.

Rowland S.P., Howley P.S. (1988) Structure in “amorphous regions”, accessible segments of fibrils, of the cotton fiber. *Textile Research Journal* **58**:96–101.

Rowland S.P., Roberts E.J. (1972) The nature of accessible surfaces in the microstructure of cotton cellulose. *Polymer chemistry* **10**:2447–2461.

Rowland S.P., Roberts E.J., Wade C.P. (1969) Selective accessibilities of hydroxyl groups in the microstructure of cotton cellulose. *Textile Research Journal* **39**:530–542.

Rutherford H.A., Minor F.W., Martin A.R., Harris M. (1942) Oxidation of cellulose: the reaction of cellulose with periodic acid. *Journal of Research of the national Bureau of Standards* **29**:131–141.

Saeman J.F. (1945) Kinetics of wood saccharification - hydrolysis of cellulose and decomposition of sugars in dilute acid at high temperature. *Industrial & Engineering Chemistry* **37**:43–52.

Sarko A., Muggli R. (1974) Packing analysis of carbohydrates and polysaccharides. III. Valonia cellulose and cellulose II. *Macromolecules* **7**:486–494.

Schramm G. (1994) *A Practical Approach to Rheology and Rheometry*, 2nd edn. Thermo Haake, Karlsruhe.

Sidi Ali L., Cochet N., Ghose T.K., Lebeault J.M. (1984) Enzymatic hydrolysis of sugar beet pulp. *Biotechnology Letters* **6**:723–728.

Silveira R.L., Stoyanov S.R., Kovalenko A., Skaf M.S. (2016) Cellulose Aggregation under Hydrothermal Pretreatment Conditions. *Biomacromolecules* **17**:2582–2590.

Spagnuolo M., Crecchio C., Pizzigallo M.D.R., Ruggiero P. (1997) Synergistic effects of cellulolytic and pectinolytic enzymes in degrading sugar beet pulp. *Bioresource Technology* **60**:215–222.

Staudinger H. (1930) Über hochpolymere Verbindungen: Viscositätsuntersuchungen an Molekül-Kolloiden. *Kolloid Zeitschrift* **51**:71.

Steele N.M., Sulová Z., Campbell P., Braam J., Farkas V., Fry S.C. (2001) Ten isoenzymes of xyloglucan endotransglycosylase from plant cell walls select and cleave the donor substrate stochastically. *The Biochemical Journal* **355**:671–679.

Stipanovic A.J., Sarko A. (1976) Packing analysis of carbohydrates and polysaccharides. 6. Molecular and crystal structure of regenerated cellulose II. *Macromolecules* **9**:851–857.

Takahashi M., Shimazaki M. (1995) Solubility of cellulose IV in sodium hydroxide solution. *Konbunshi Ronbunshu* **52**:60–65.

Taniguchi T., Harada H., Nakato K. (1978) Determination of water adsorption sites in wood by a hydrogen-deuterium exchange. *Nature* **272**:230–231.

Terenzi C., Prakobna K., Berglund L.A., Furó I. (2015) Nanostructural effects on polymer and water dynamics in cellulose biocomposites: 2H and 13C NMR relaxometry. *Biomacromolecules* **16**:1506–1515.

Thibault J.-F., Renard C.M.G.C., Guillon F. (1994) Physical and chemical analysis of dietary fibres in sugar beet and vegetables. In: Linskens HF, Jackson JF (eds) Vegetables and Vegetable Products. Springer Berlin Heidelberg, Berlin, Heidelberg, pp 23–55.

Thibault J.-F., Rouau X. (1990) Studies on enzymic hydrolysis of polysaccharides in sugar Beet pulp. *Carbohydrate Polymers* **13**:1–16.

Toğrul H., Arslan N. (2003a) Flow properties of sugar beet pulp cellulose and intrinsic viscosity – molecular weight relationship. *Carbohydrate Polymers* **54**:63–71.

Toğrul H., Arslan N. (2003b) Production of carboxymethyl cellulose from sugar beet pulp cellulose and rheological behaviour of carboxymethyl cellulose. *Carbohydrate Polymers* **54**:73–82.

Tomaszewska J., Bieliński D., Binczarski M., Berlowska J., Dziugan P., Piotrowski J., Stanishevsky A., Witońska I.A. (2018) Products of sugar beet processing as raw materials for chemicals and biodegradable polymers. *Royal Society of Chemistry Advances* **8**:3161–3177.

Turesson H., Andersson M., Marttila S., Thulin I., Hofvander P. (2014) Starch biosynthetic genes and enzymes are expressed and active in the absence of starch accumulation in sugar beet tap-root. *BMC Plant Biology* **14**:1–12.

Vincken J.P., Beldman G., Niessen W.M.A., Voragen A.G.J. (1996) Degradation of apple fruit xyloglucan by endoglucanase. *Carbohydrate Polymers* **29**:75–85.

Viswanath D.S., Ghosh T.K., Prasad D.H.L., Dutt N.V.K., Rani K.Y. (2007) *Viscosity of Liquids: Theory, Estimation, Experiment, and Data*, 1st edn. Springer Netherlands, Dordrecht.

Vučurović V.M., Razmovski R.N. (2012) Sugar beet pulp as support for Saccharomyces cerivisiae immobilization in bioethanol production. *Industrial Crops and Products* **39**:128–134.

Wada M., Heux L., Sugiyama J. (2004) Polymorphism of cellulose I family: Reinvestigation of cellulose IVl. *Biomacromolecules* **5**:1385–1391.

Wang D., Yeats T.H., Uluisik S., Rose J.K.C., Seymour G.B. (2018) Fruit Softening: Revisiting the Role of Pectin. *Trends in Plant Science* **23**:302–310.

Weibel M.K. (1986) Well drilling and production fluids employing parenchymal cell cellulose. :1–21.

Weibel M.K. (1989) Parenchymal cell cellulose and related materials. :1–14.

Weibel M.K., Myers C.D. (1990) Use of parenchymal cell cellulose to improve comestibles.

Wen L.F., Chang K.C., Brown G., Gallaher D.D. (1988) Isolation and characterization of hemicellulose and cellulose from sugar beet pulp. *Journal of food Science* **53**:826–829.

Whitney S.E.C., Gothard M.G.E., Mitchell J.T., Gidley M.J. (1999) Roles of cellulose and xyloglucan in determining the mechanical properties of primary plant cell walls. *Plant Physiology* **121**:657–663.

Zeronian S.H., Inglesby M.K. (1995) Bleaching of cellulose by hydrogen peroxide. *Cellulose* **2**:265–272.

Zhang Z., Gibson P., Clark S.B., Tian G., Zanonato P.L., Rao L. (2007) Lactonization and protonation of gluconic acid: a thermodynamic and kinetic study by potentiometry, NMR and ESI-MS. *Journal of Solution Chemistry* **36**:1187–1200.

Zhao X., Liang X., Han S., Uryu T., Yoshida T. (2014) Successive saccharification and fermentation of cellulosic agricultural residues using a combination of cellulase and recombinant yeast. *Sen'i Gakkaishi* **70**:191–196.

6 Appendix

6.1 Appendix to §3.5.2.1

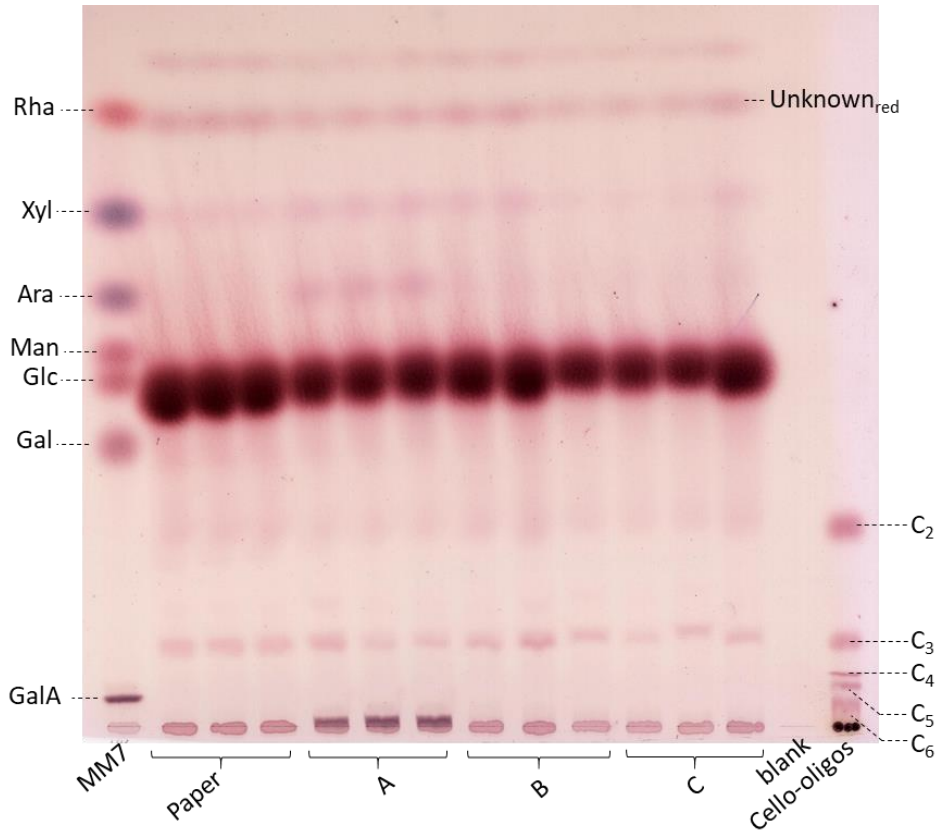

Figure 44: Saeman hydrolysis of α-cellulose fractions and paper into glucose and unknowns. Paper, α-cellulose fractions from SBP A, eC B, eC C preparations were hydrolysed by the Saeman method into Glc, Xyl, Ara and unknown components. All Saeman hydrolysis products were applied to TLC plates, run in the solvent EPyAW (6:3:1:1) for 2 × 2.5 h, stained with thymol and quantified by Photoshop. Cello-oligos (C_2 to C_6) were applied as a marker mixture of different degrees of polymerization of Glc (dimer to hexamer).

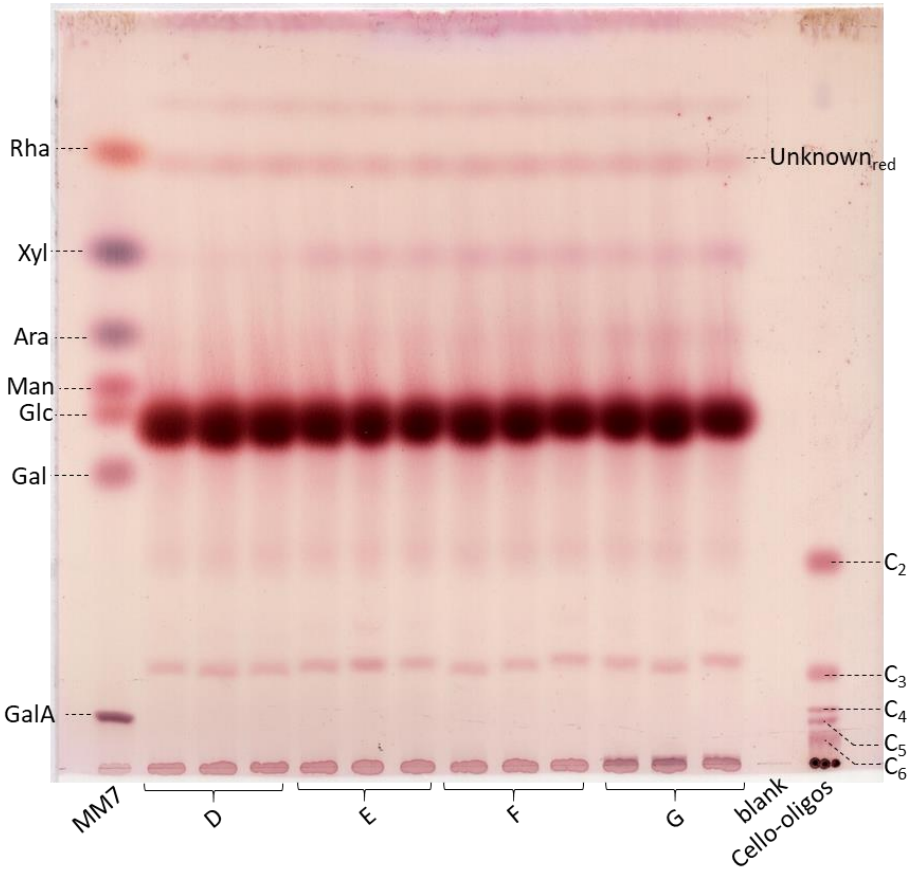

Figure 45: Saeman hydrolysis of α-cellulose fractions into glucose and unknowns. α-cellulose fractions from eC D–F and SBP G preparations were hydrolysed by the Saeman method into Glc, Ara, Xyl and unknown components. Further details as in Figure 44.

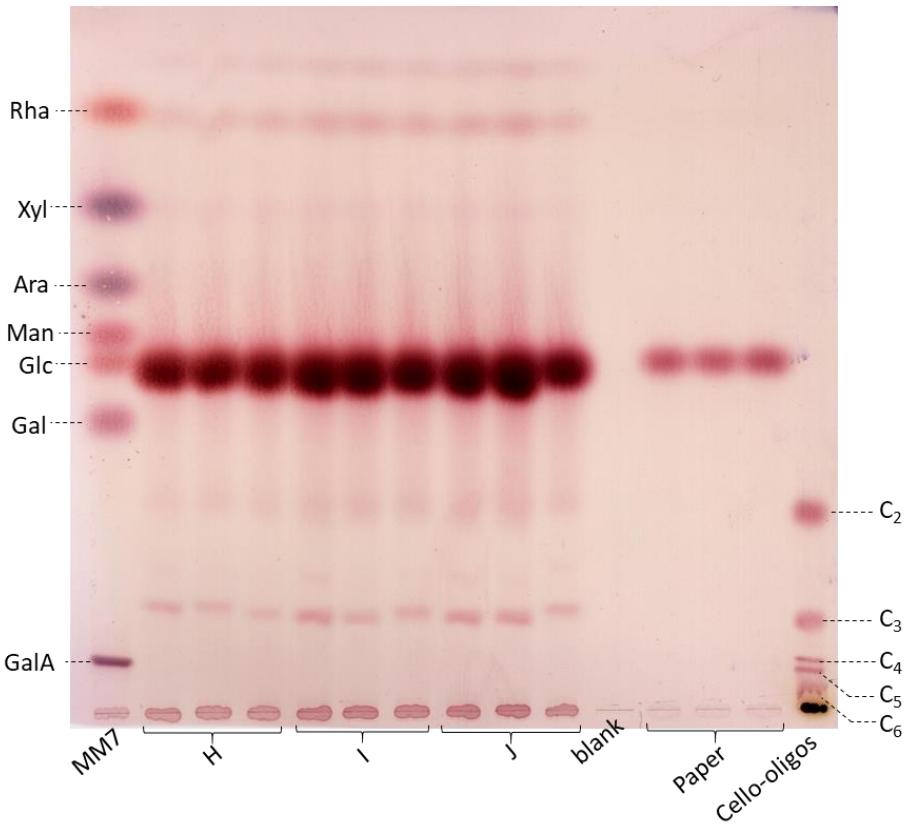

Figure 46: Saeman hydrolysis of α-cellulose fractions and paper into glucose and unknowns. α-cellulose fractions from hveC H–J preparations were hydrolysed by the Saeman method into Glc, Xyl and unknown components. The paper sample was diluted 1:25. Further details as in Figure 44.

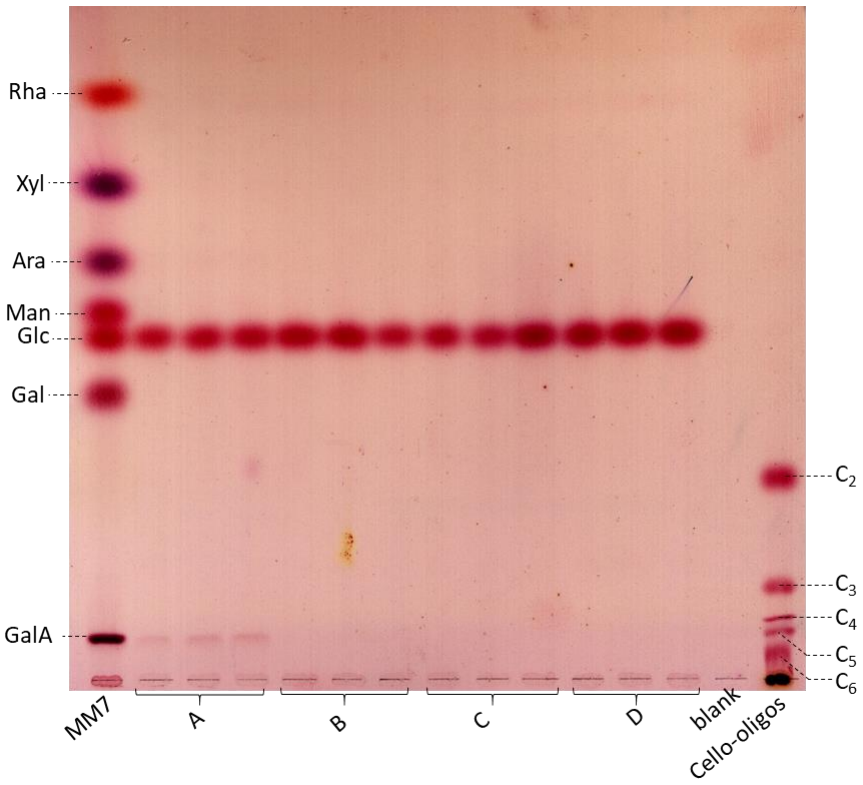

Figure 47: Saeman hydrolysis of α-cellulose fractions into glucose.
α-cellulose fractions from SBP A and eC B–D preparations were hydrolysed by the Saeman method and diluted 1:25. The hydrolysis products visible for SBP A are Glc and GalA. Further details as in Figure 44.

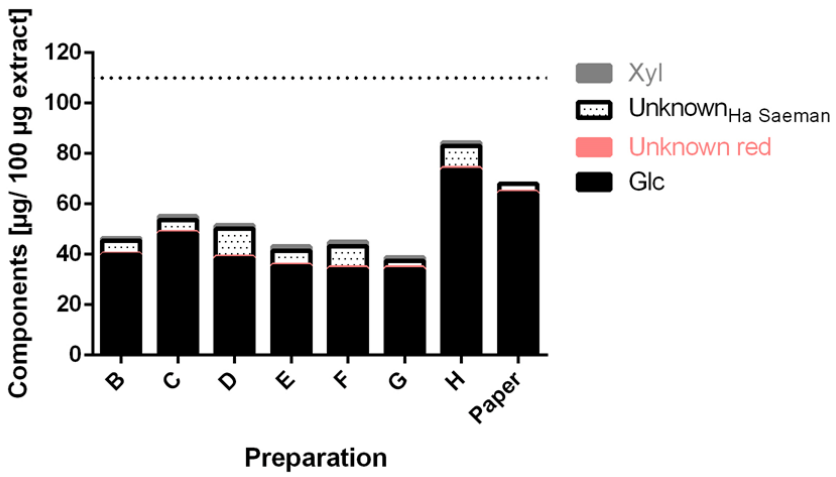

Figure 48: Saeman hydrolysis of paper as well as Ha fractions from experimental Curran and SBP G preparations.
Components were quantified from the TLC plate in Figure 18. A dotted line represents the expected value for the hydrolysis of 100 µg cellulose. Paper was the hydrolysed cellulose control.

6.2 Appendix to §3.5.2.2

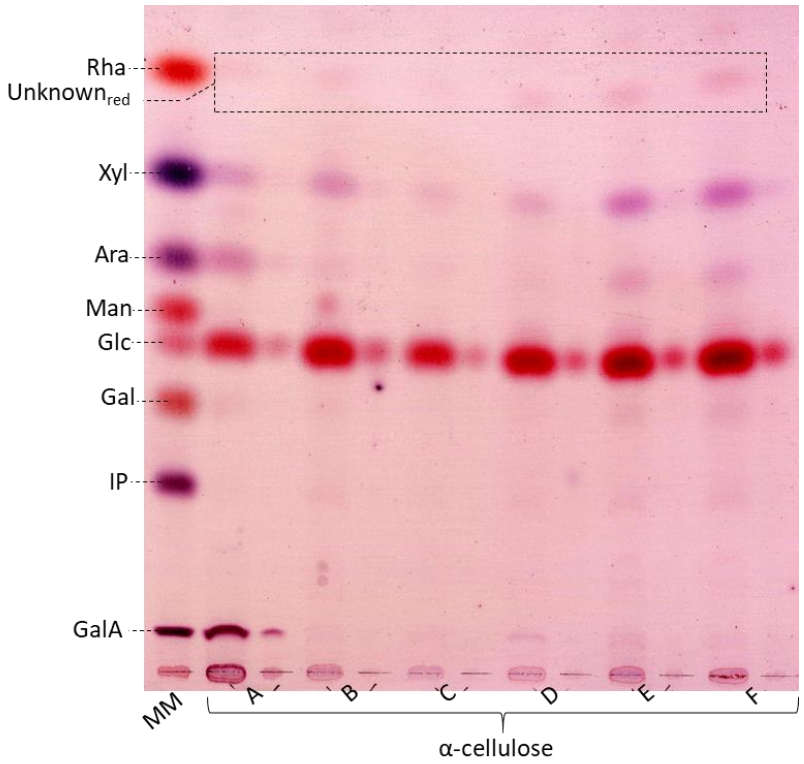

Figure 49: Composition of α-cellulose fractions from SBP and experimental Curran preparations hydrolysed by TFA.
The α-cellulose fractions from SBP A and eC B–F preparations were hydrolysed in 2 M TFA for 1 h at 120°C. All supernatants were applied to TLC plates, per 100 µg and 10 µg starting dry weight (next to each other on the TLC plates respectively), run in the solvent EPyAW (6:3:1:1) for 2 × 2.5 h, stained with thymol and quantified by Photoshop. MM: marker mixture.

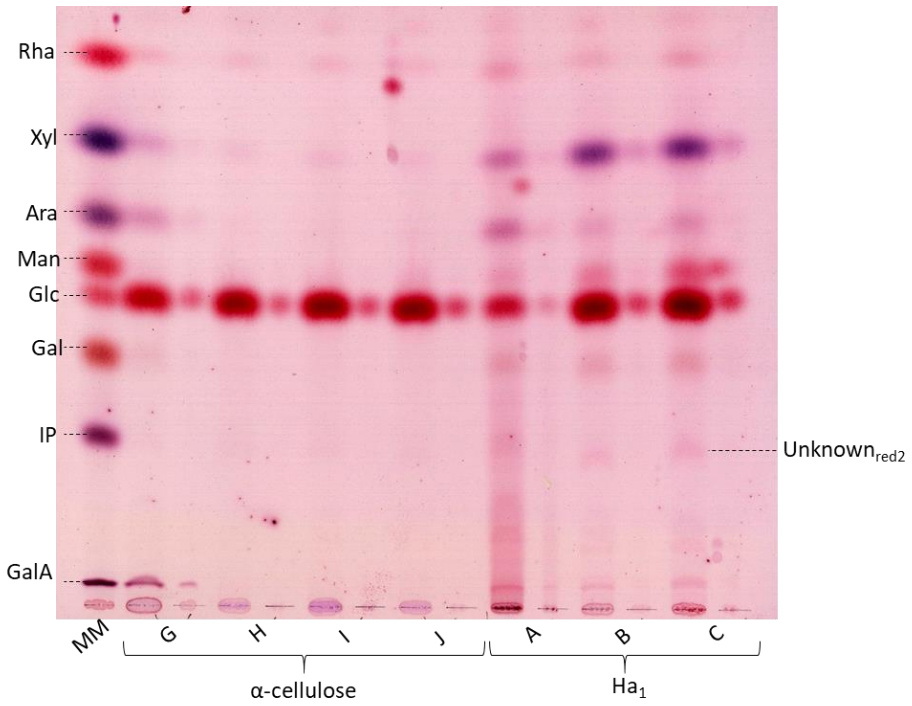

Figure 50: Composition of α-cellulose and Ha fractions from SBP and experimental Curran preparations hydrolysed by TFA.
The α-cellulose fractions, from SBP G and hveC H–J preparations, and Ha_1 fractions from SBP A, eC B and eC C preparations, were hydrolysed in 2 M TFA for 1 h at 120°C. Further details as in Figure 49.

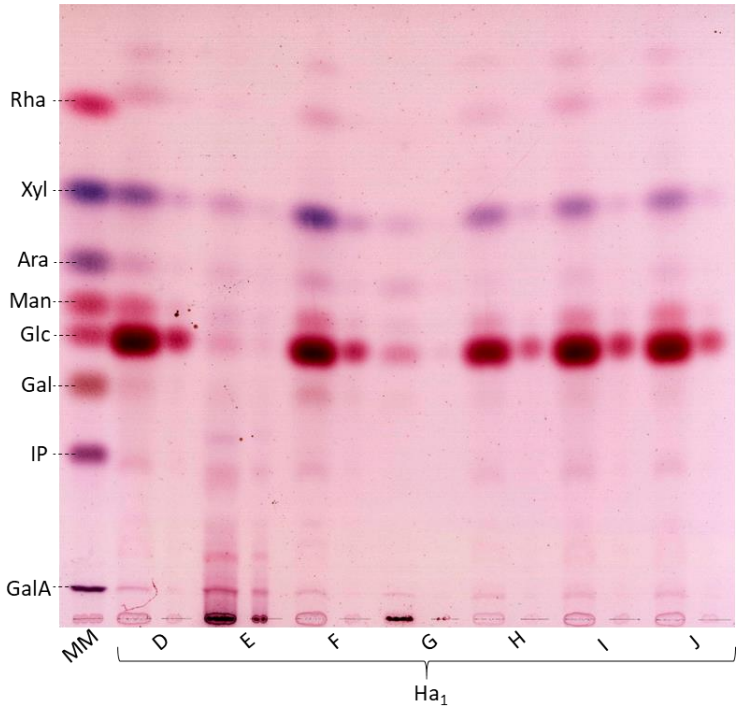

Figure 51: Composition of Ha fractions from SBP and experimental Curran preparations hydrolysed by TFA.
Ha_1 fractions, from SBP G and eC D–F and H–J preparations, were hydrolysed in 2 M TFA for 1 h at 120°C. Further details as in Figure 49.

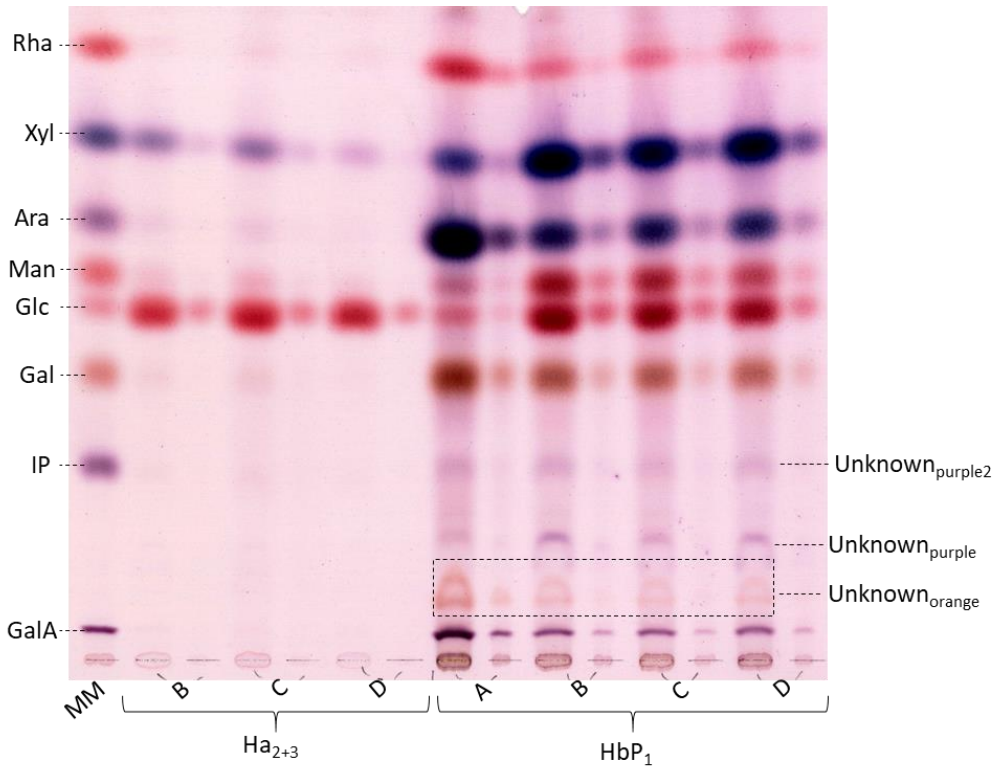

Figure 52: Composition of Ha and HbP fractions from SBP and experimental Curran preparations hydrolysed by TFA.
Ha_{2+3} fractions (from eC B–D preparations) and HbP_1 fractions, from SBP A and eC B–D preparations, were hydrolysed in 2 M TFA for 1 h at 120°C. Further details as in Figure 49.

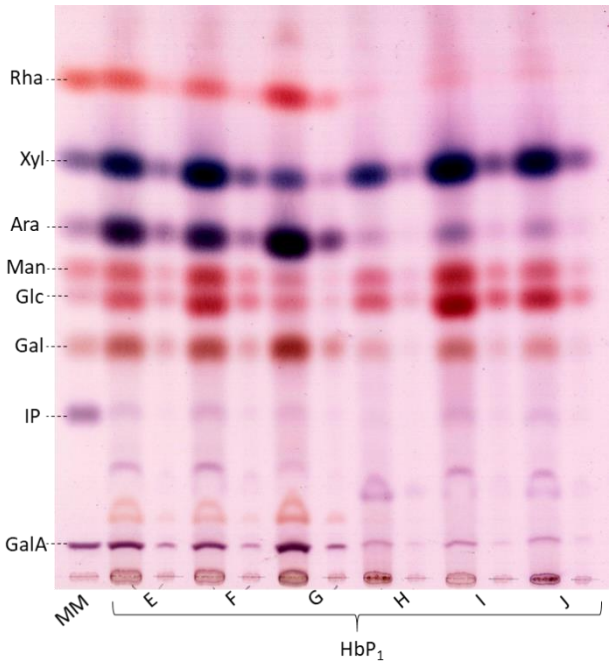

Figure 53: Composition of HbP fractions from SBP and experimental Curran preparations hydrolysed by TFA.
HbP_1 fractions, from SBP G and eC E–J preparations, were hydrolysed in 2 M TFA for 1 h at 120°C. Further details as in Figure 49.

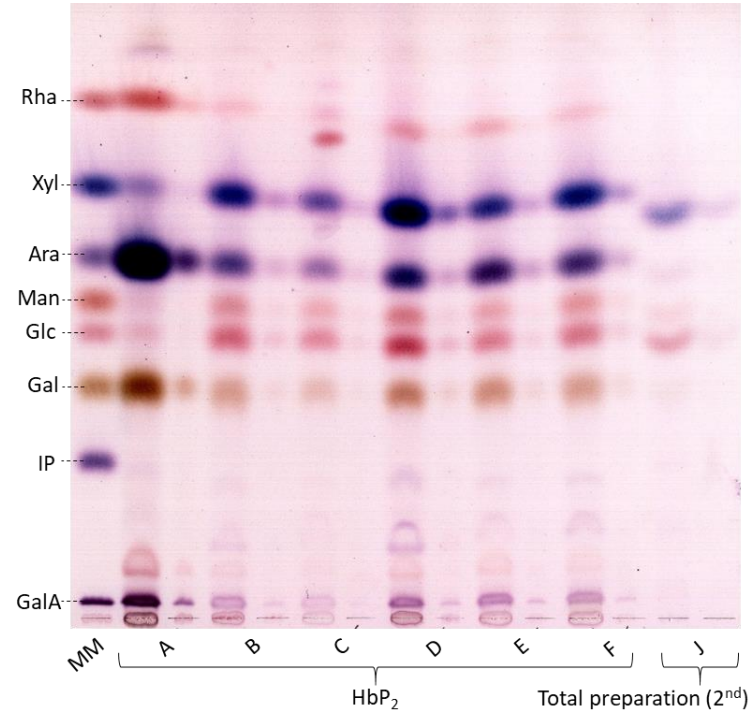

Figure 54: Composition of total preparations and HbP fractions from SBP and experimental Curran preparations hydrolysed by TFA.
HbP_2 fractions, from SBP A and eC B–F preparations, and total preparation (2^{nd} replicate) of eC J were hydrolysed in 2 M TFA for 1 h at 120°C. Further details as in Figure 49.

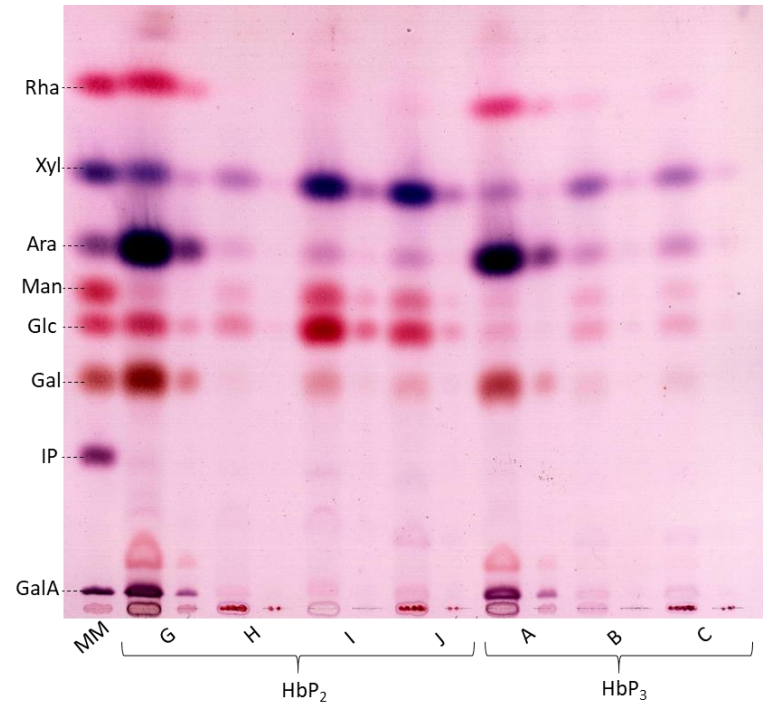

Figure 55: Composition of HbP fractions from SBP and experimental Curran preparations, hydrolysed by TFA.
HbP_2 fractions, from SBP G and eC H–J preparations, and HbP_3, from SBP A and eC B–C preparations, were hydrolysed in 2 M TFA for 1 h at 120°C. Further details as in Figure 49.

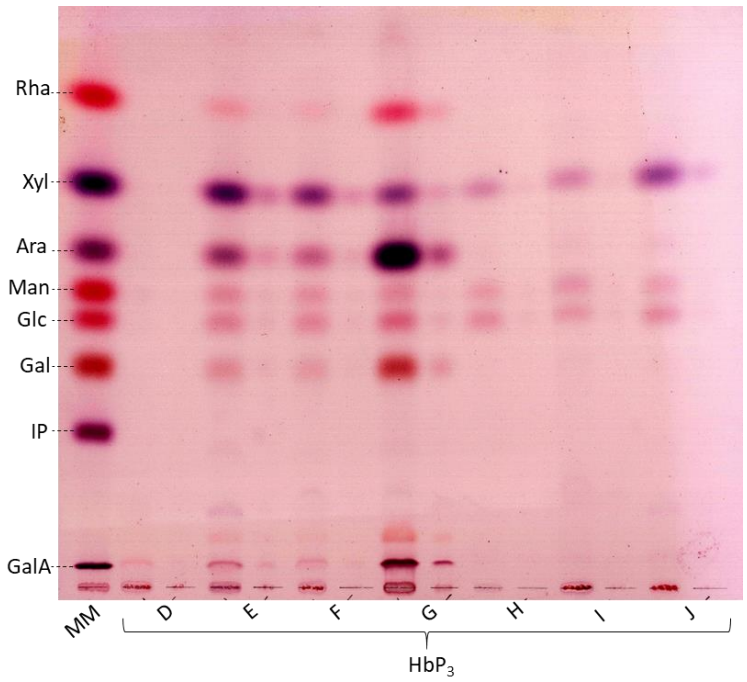

Figure 56: Composition of HbP fractions from SBP and experimental Curran preparations hydrolysed by TFA.
HbP_3 fractions, from SBP G and eC D–F and H–J preparations, were hydrolysed in 2 M TFA for 1 h at 120°C. Further details as in Figure 49.

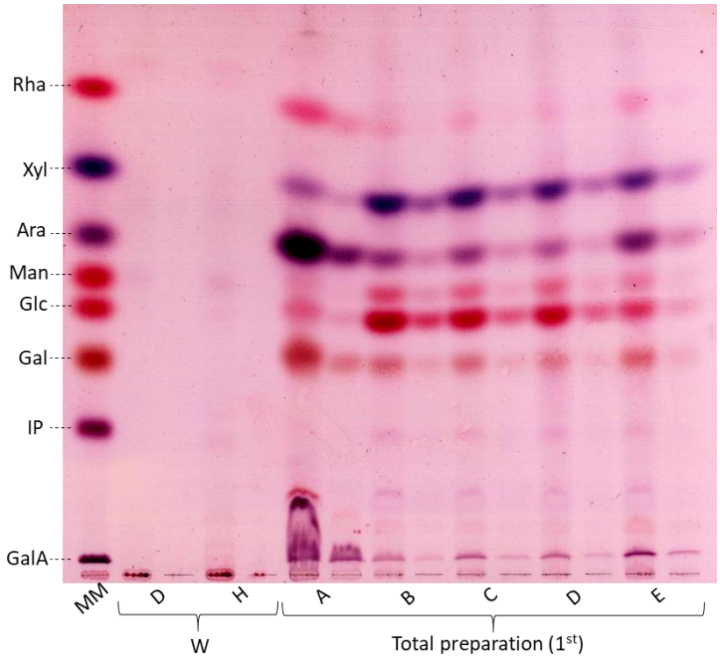

Figure 57: Composition of total preparation and the acetic acid wash from SBP and experimental Curran preparations hydrolysed by TFA.
Total preparation (1st replicate) from SBP A and eC B–E were hydrolysed in 2 M TFA for 1 h at 120°C. α-Cellulose was washed with 1% acetic acid, which was then dialysed and freeze-dried (W). W from eC D and H preparations were big enough for the hydrolysis by TFA and the following analysis by TLC. Further details as in Figure 49.

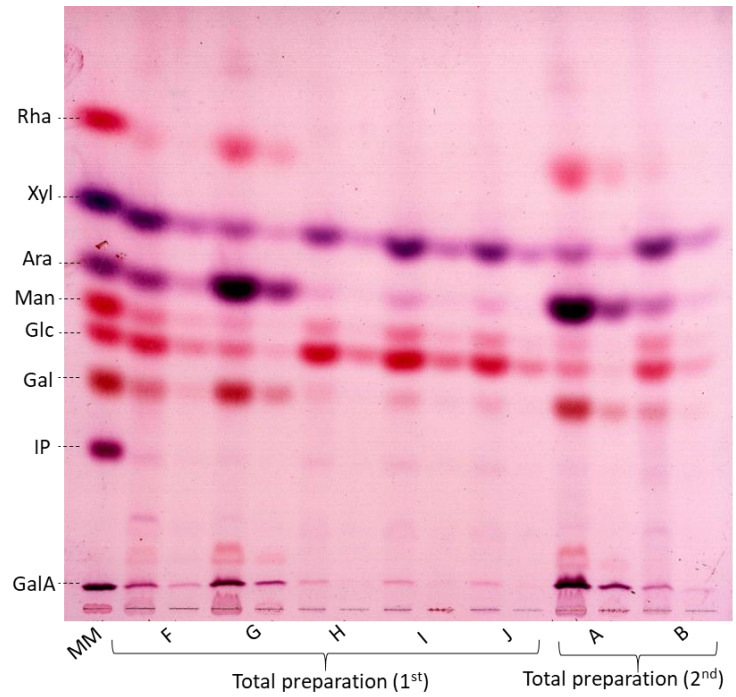

Figure 58: Composition of total preparations from SBP and experimental Curran hydrolysed by TFA.
Total preparations from SBP A and G and eC B, F and H–J, were hydrolysed in 2 M TFA for 1 h at 120°C (in duplicate, 1st and 2nd). Further details as in Figure 49.

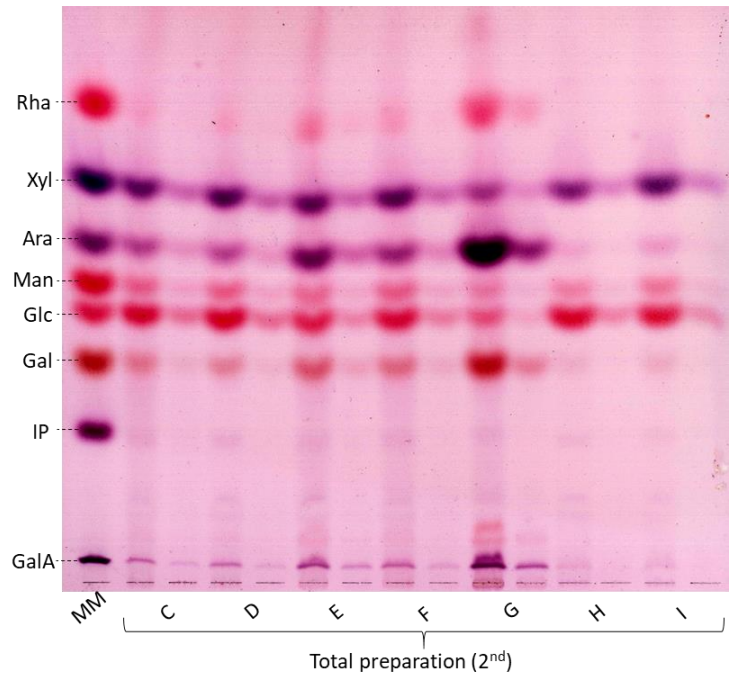

Figure 59: Composition of total preparations from SBP and experimental Curran hydrolysed by TFA.
Total preparations from SBP G and eC C–F and H–I, were hydrolysed in 2 M TFA for 1 h at 120°C (2nd duplicate). Further details as in Figure 49

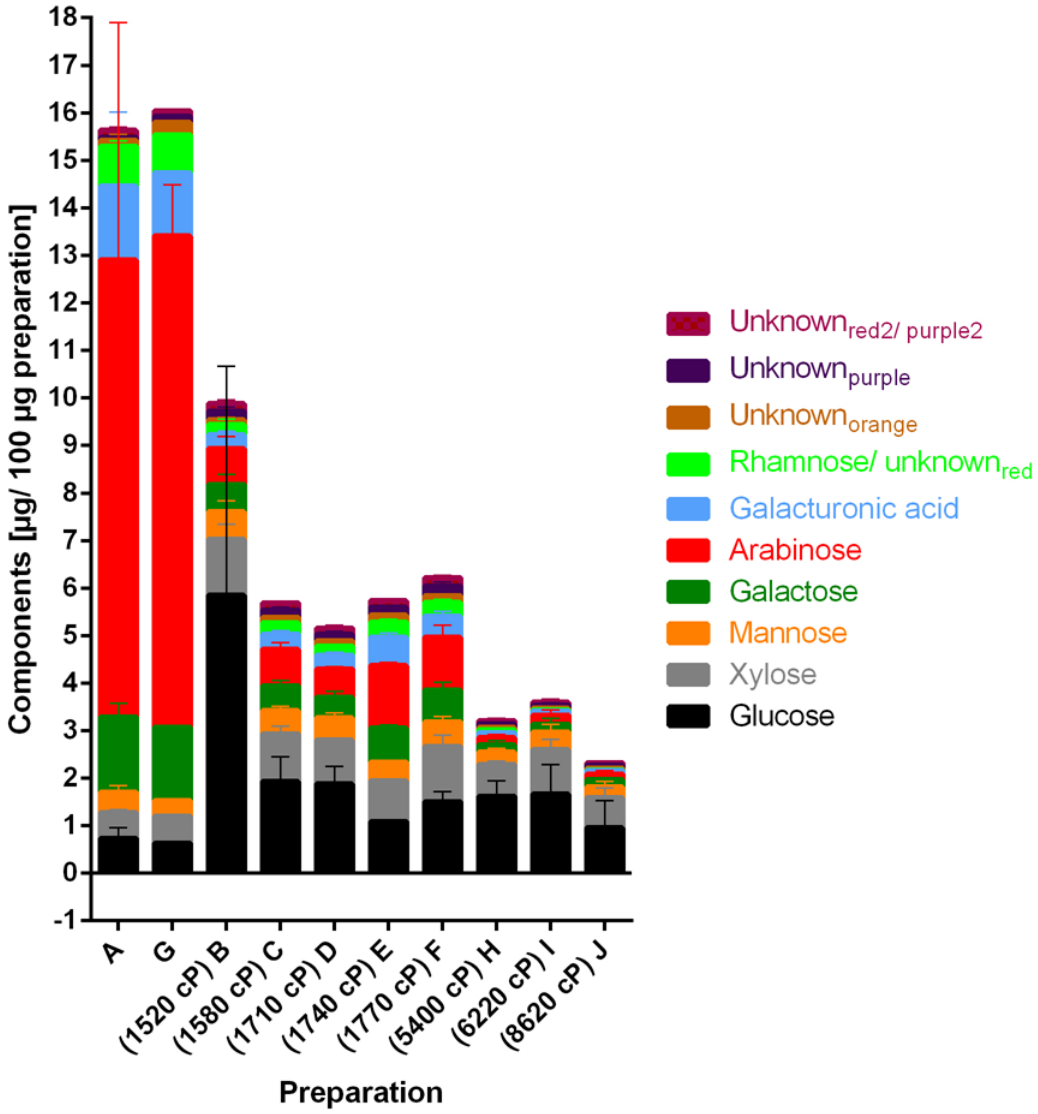

Figure 60: Quantified components in hot TFA-hydrolysed total SBP and experimental Curran (including high viscosity experimental Curran) preparations.
The TLC plates (Figure 53, Figure 56–Figure 58), with TFA-hydrolysed preparations from SBP (A and G) and eC B–J, were quantified by Photoshop (error bars represent SEM, N=2). eC B–J are in order of increasing viscosity (1520–8620 cP).

6.3 Appendix to §3.7.1

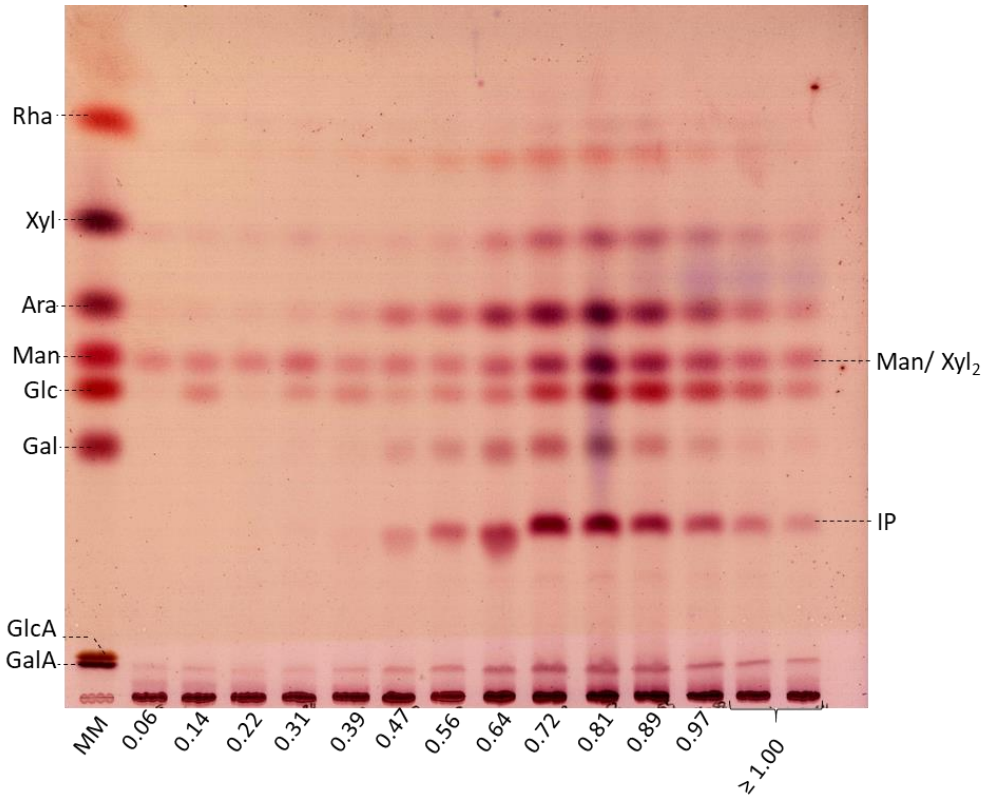

Figure 61: Composition of HbP from experimental Curran M separated by molecular mass and Driselase-digested.
eC M HbP was run on Sepharose CL-6B, three column fractions were pooled for Driselase digestion and the supernatants applied to a TLC plate. This plate was run in the solvent EPyAW (6:3:1:1) for 2 × 2.5 h and stained with thymol. Each lane was labelled with the pool's respective median K_{av} value. MM: marker mixture.

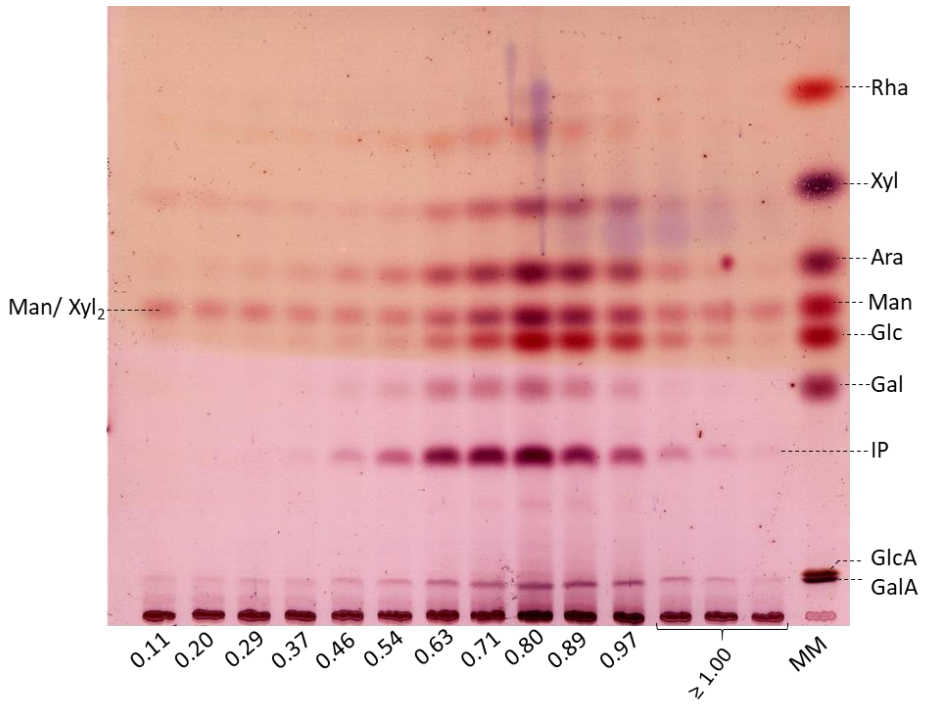

Figure 62: Composition of HbP from experimental Curran S separated by molecular mass and Driselase-digested.
eC S HbP was run on Sepharose CL-6B. Further details as in Figure 61.

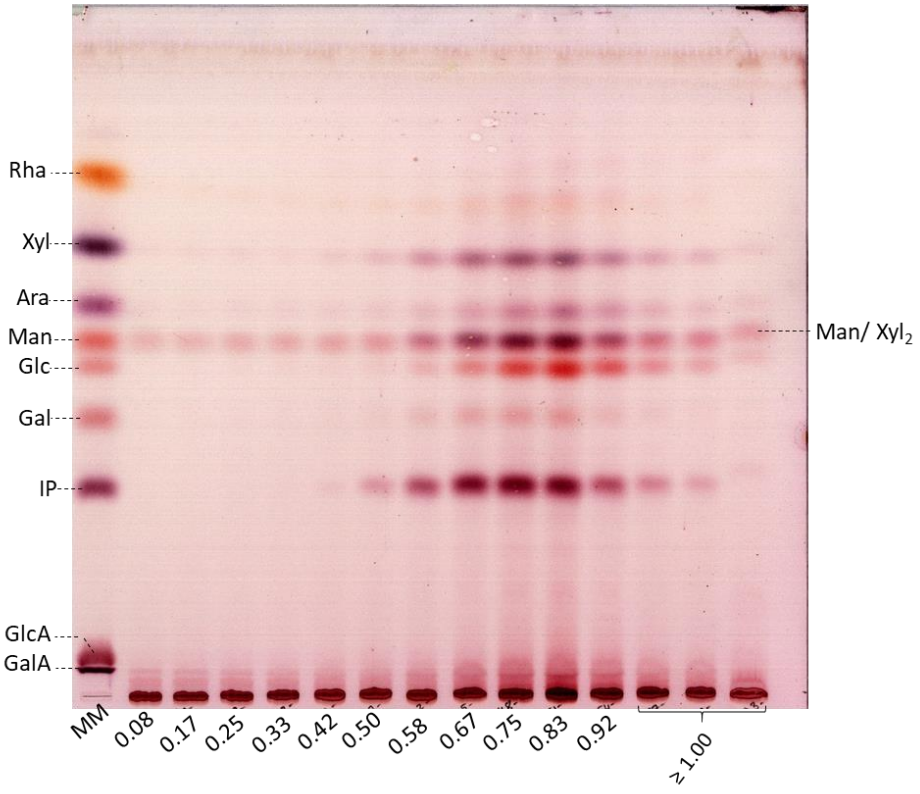

Figure 63: Composition of HbP from experimental Curran R separated by molecular mass and Driselase-digested.
eC R HbP was run on Sepharose CL-6B. Further details as in Figure 61.

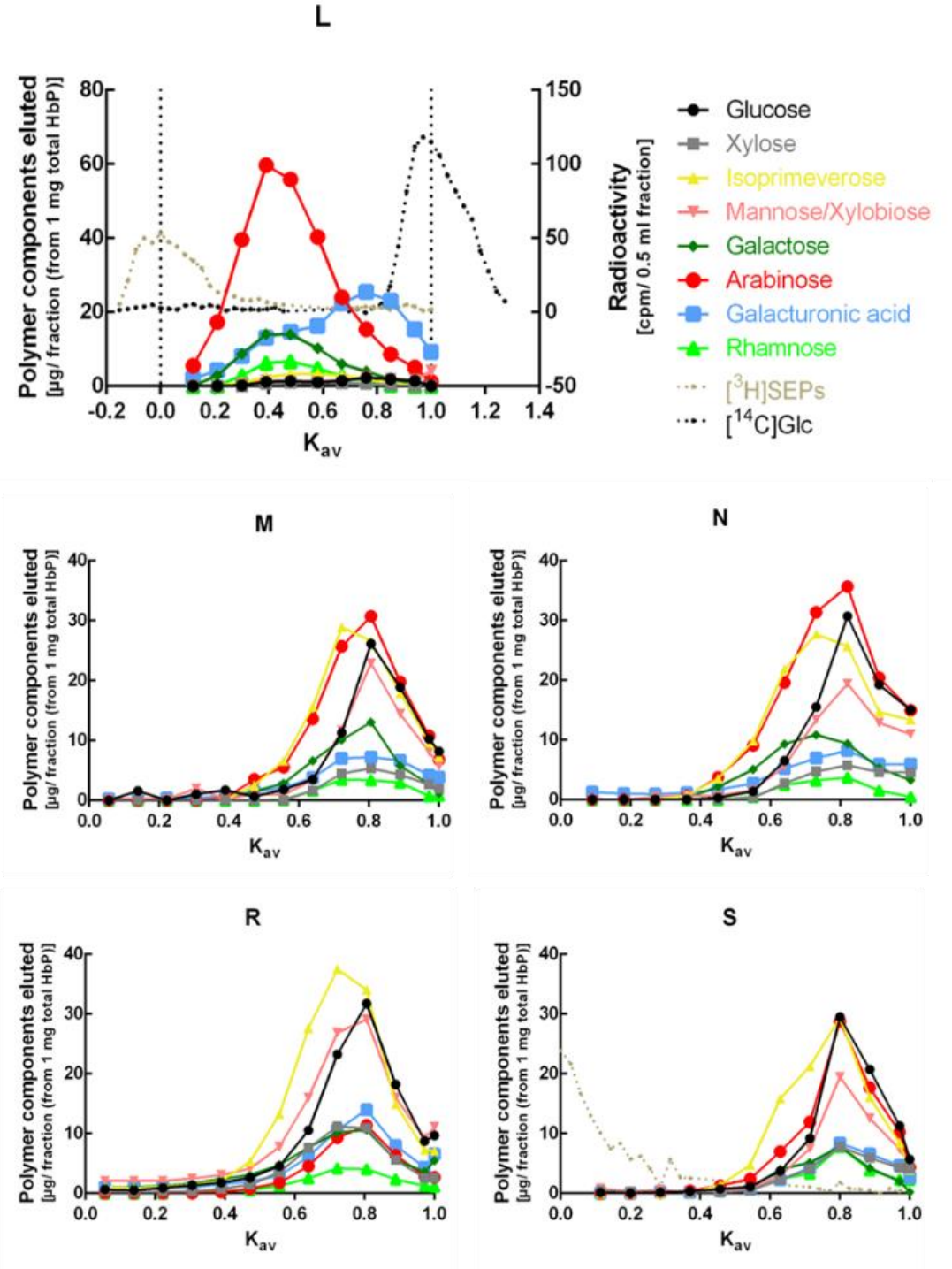

Figure 64: Quantified components in size-fractionated, Driselase-digested HbP from experimental Currans and SBP L.
The TLC plates (Figure 23, Figure 25 and Figure 61–Figure 63) with the Driselase-digested HbP column fractions (after the run on Sepharose CL-6B) were quantified by Photoshop. Nine polymer components were identified and their elution profiles are shown according to the pools' respective median Kav value. Man and Xyl_2 were quantified together. In SBP L preparation radioactive markers—[^{3}H]SEPs and [^{14}C]Glc—mark the V_0 (K_{av} 0) and the V_i (K_{av} 1) respectively.

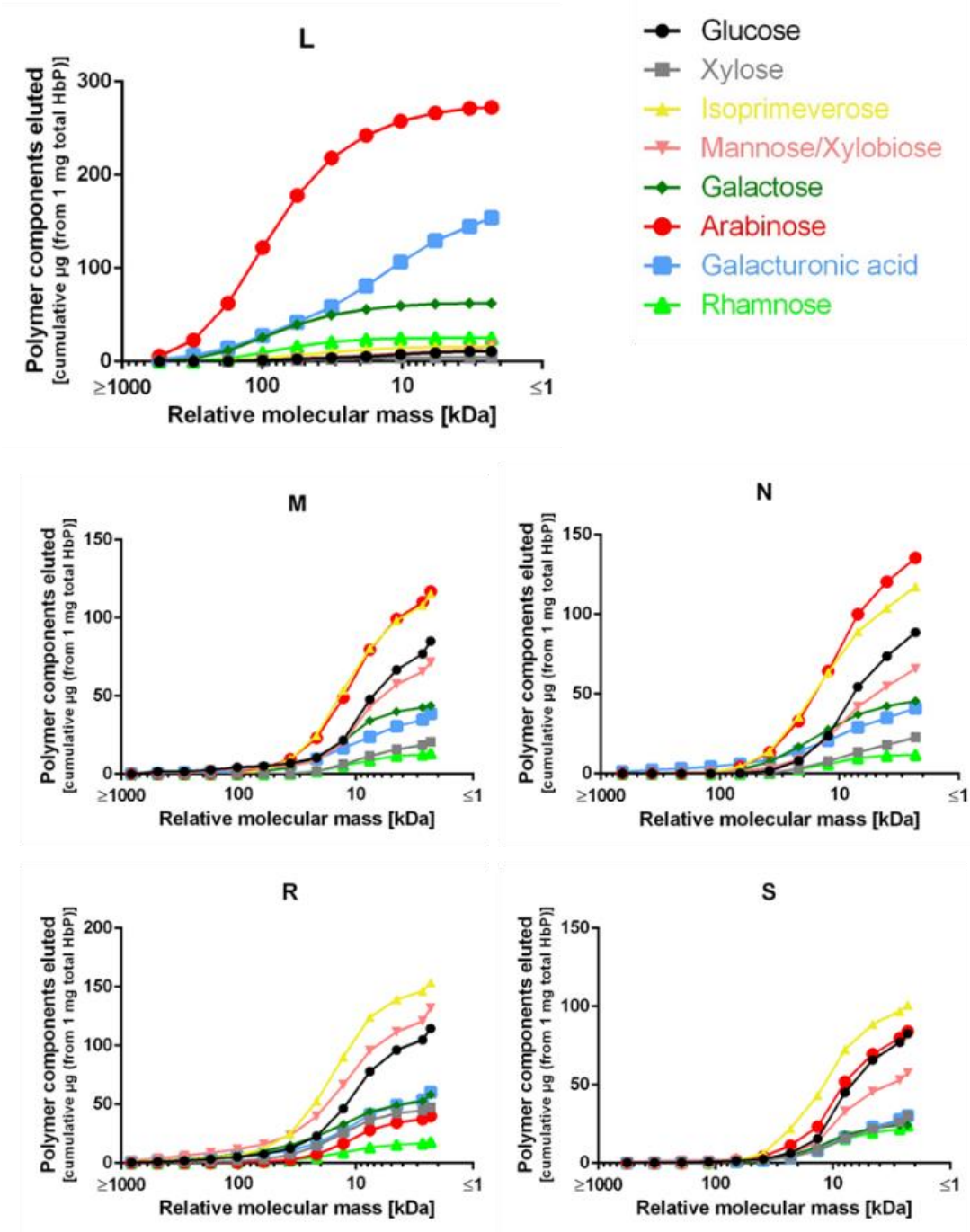

Figure 65: Cumulative components eluted from Sepharose CL-6B size fractionated, Driselase digested HbP from SBP L and experimental Curran preparations.
The results displayed in Figure 64 were converted into cumulative components eluted. The K_{av} was converted into the relative molecular mass.

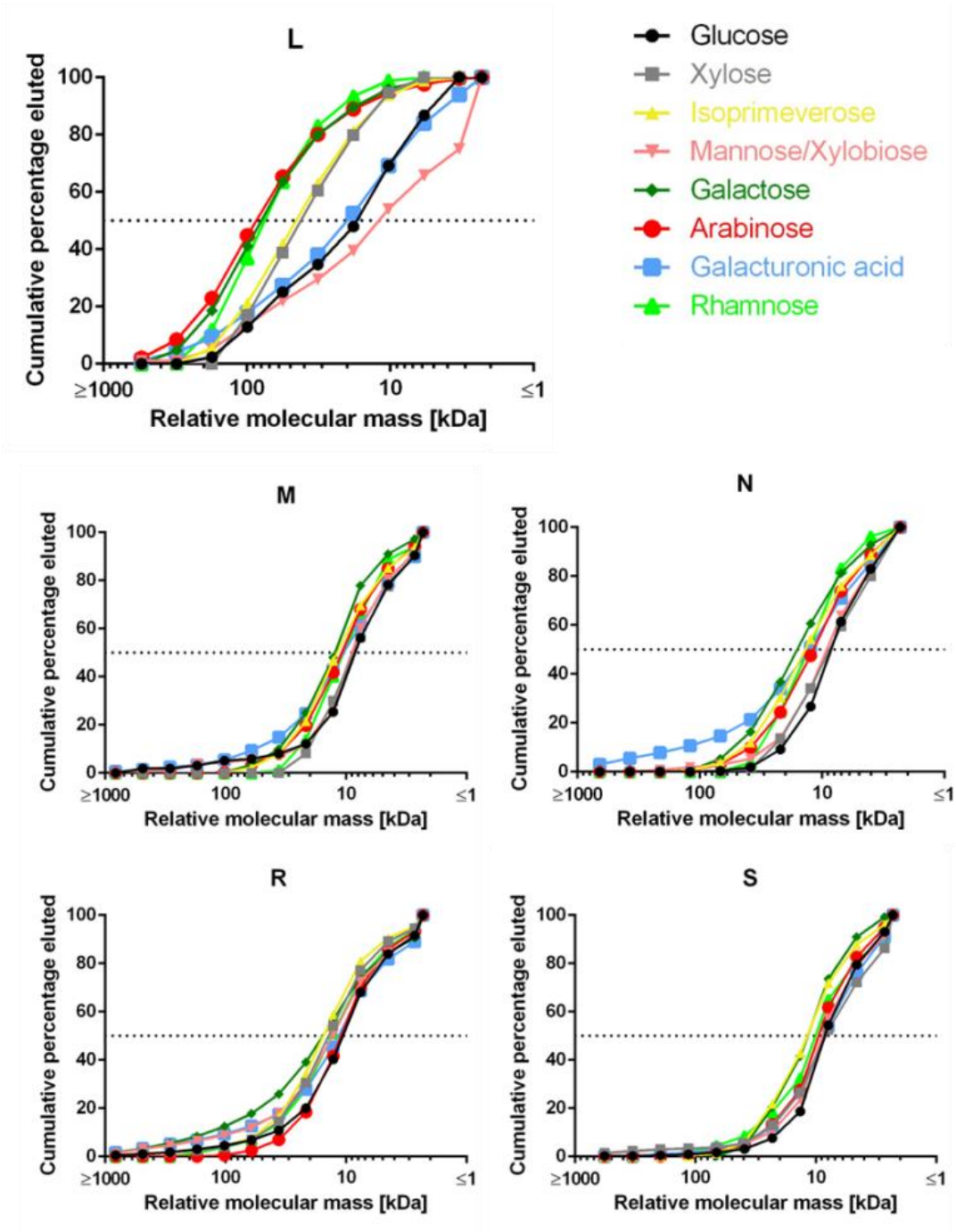

Figure 66: Cumulative percentages eluted from Sepharose CL-6B size fractionated, Driselase digested HbP for SBP L and experimental Curran preparations.
The results displayed in Figure 64 were converted into cumulative percentage eluted. The K_{av} was converted into the relative molecular mass. A dotted line indicates where 50% eluted.

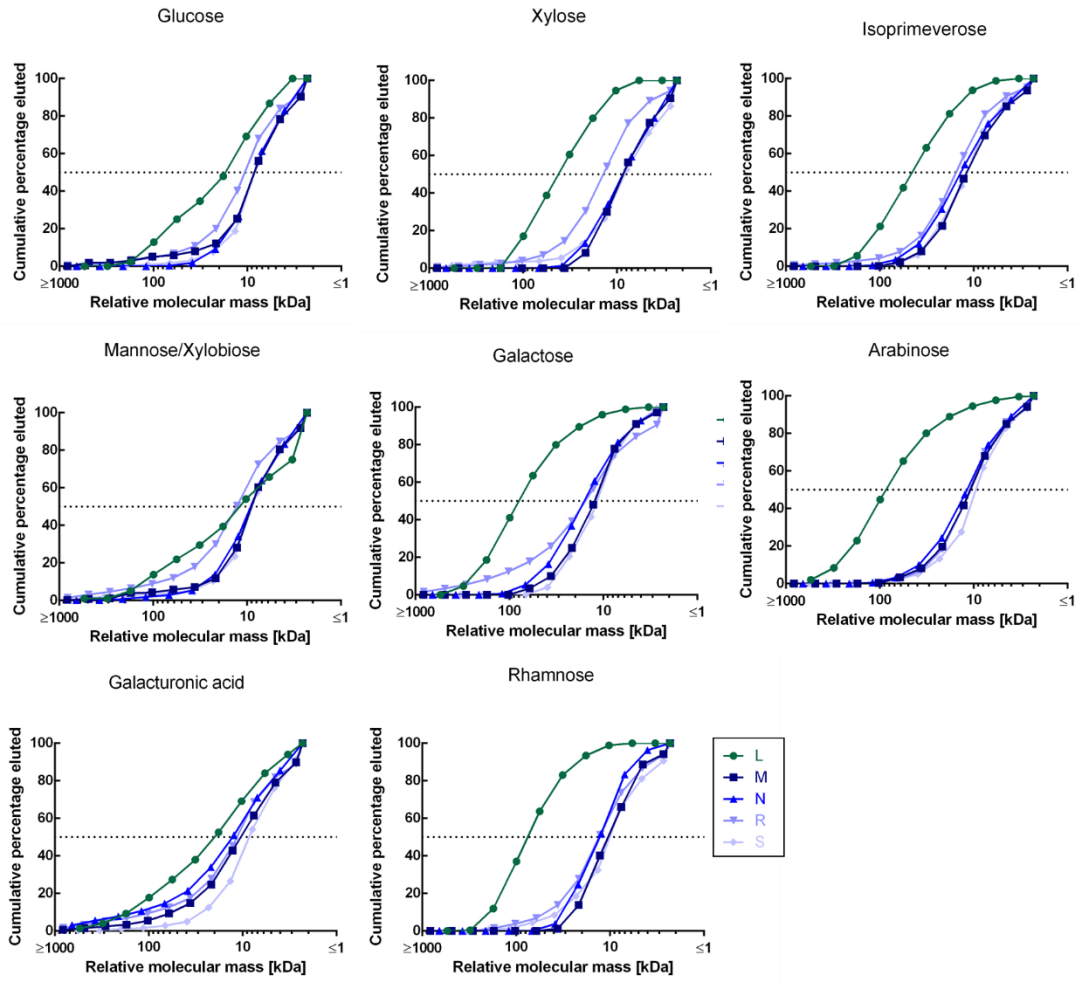

Figure 67: Cumulative percentages eluted from Sepharose CL-6B size fractionated, Driselase digested HbP from SBP L and experimental Curran preparations, grouped for their components.
The results displayed in Figure 66 were re-grouped to present the results for each component amongst all five HbP fractions tested. Further details as in Figure 66.

6.4 Appendix to §3.7.2

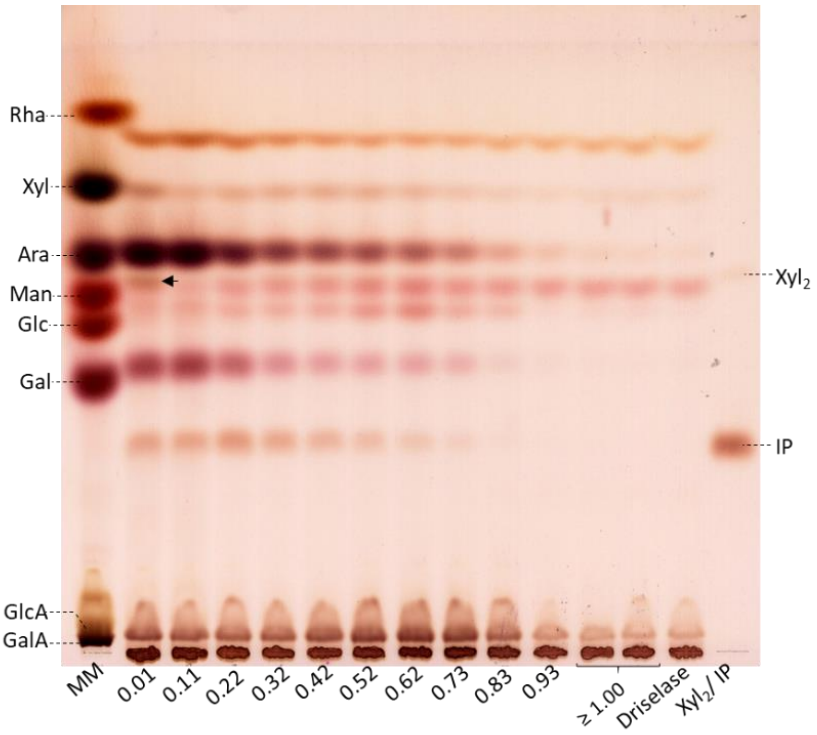

Figure 68: Composition of HbP column fractions from SBP K separated by molecular mass on Sephacryl S-200 and Driselase digested.
The ← marks the overlapping components Man and Xyl_2. SBP K HbP was size-fractionated on Sephacryl S-200, three fractions were pooled for Driselase digestion and the supernatants applied to a TLC plate. This plate was run in the solvent EPyAW (6:3:1:1) for 2 × 2.5 h and stained with thymol. Each lane was labelled with the pool's respective median K_{av} value. MM: marker mixture. Driselase: Driselase without substrate (background).

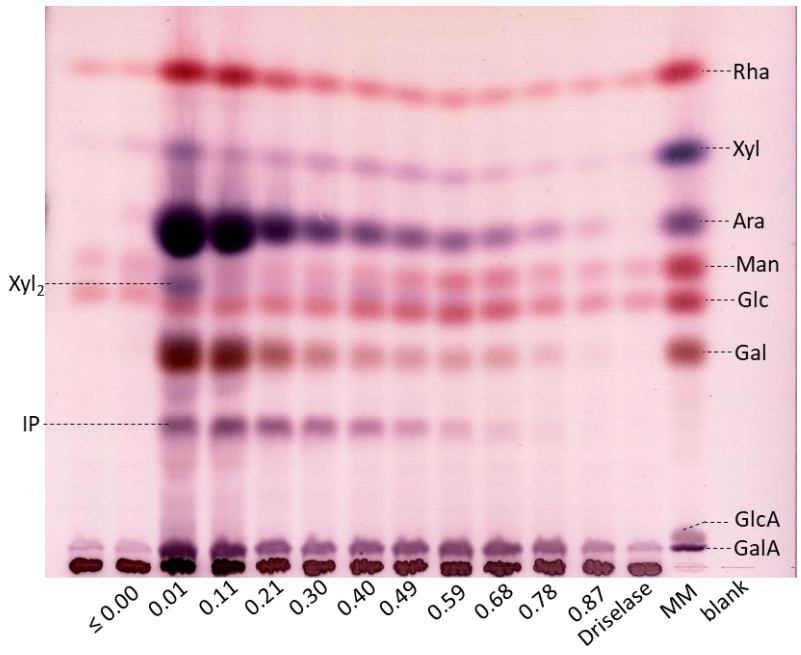

Figure 69: Composition of HbP column fractions from SBP A separated by molecular mass on Sephacryl S-200 and Driselase-digested.
SBP A HbP was run on Sephacryl S-200. The biggest polysaccharides are ≤ 0.00 K_{av} (first and second lane left of ≤ 0.00). Further details as in Figure 68.

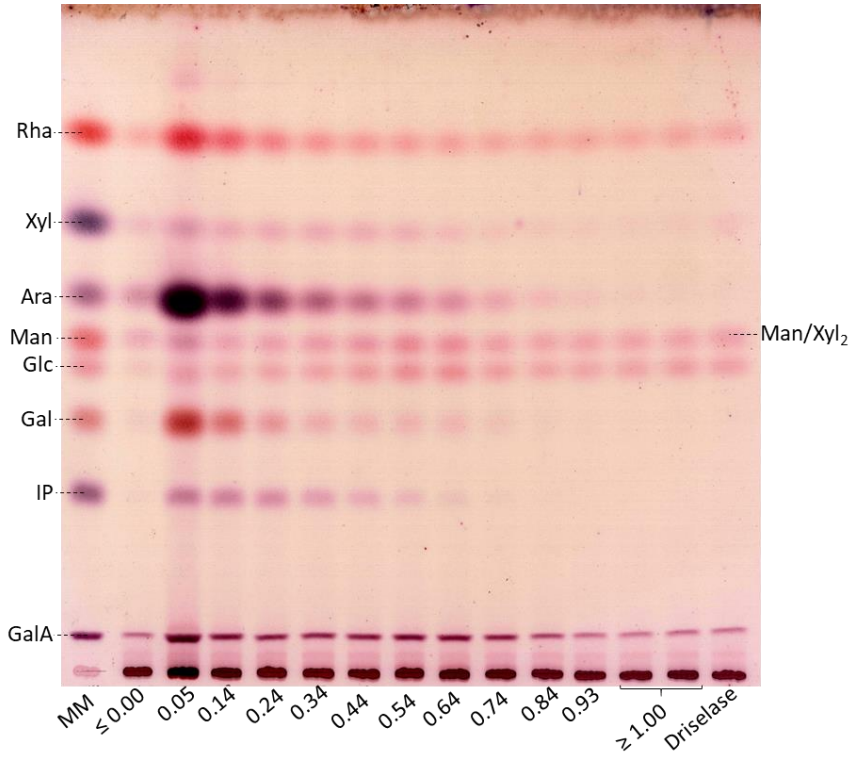

Figure 70: Composition of HbP column fractions from SBP A.2 separated by molecular mass on Sephacryl S-200 and Driselase-digested.
SBP A.2 HbP was run on Sephacryl S-200. Further details as in Figure 68.

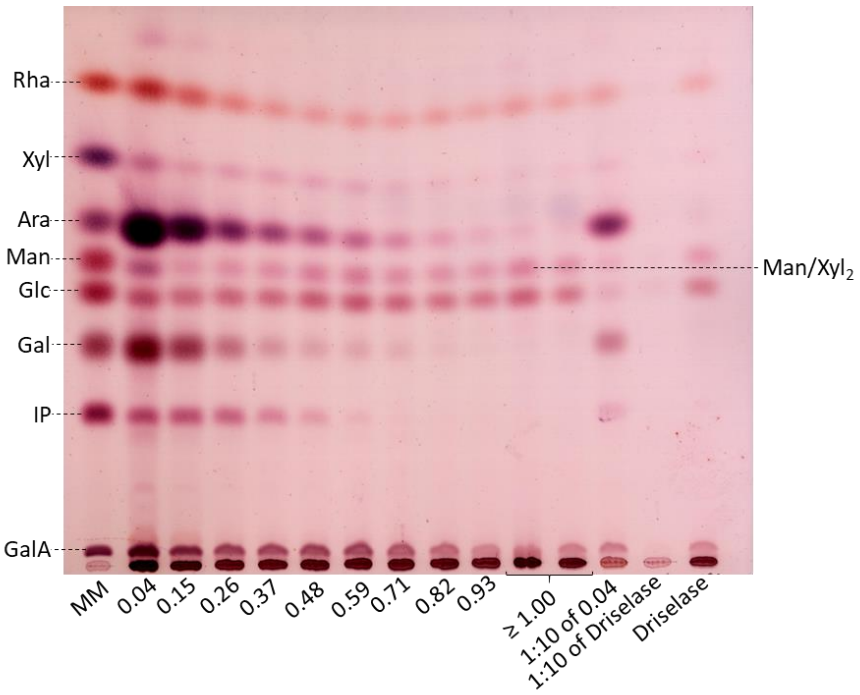

Figure 71: Composition of HbP column fractions from SBP G separated by molecular mass on Sephacryl S-200 and Driselase-digested.
SBP G HbP was run on Sephacryl S-200. The Driselase supernatant for median K_{av} 0.04 (the original concentration was likely to be overloaded for quantification) and the Driselase without substrate were also applied in a 1:10 dilution. Further details as in Figure 68.

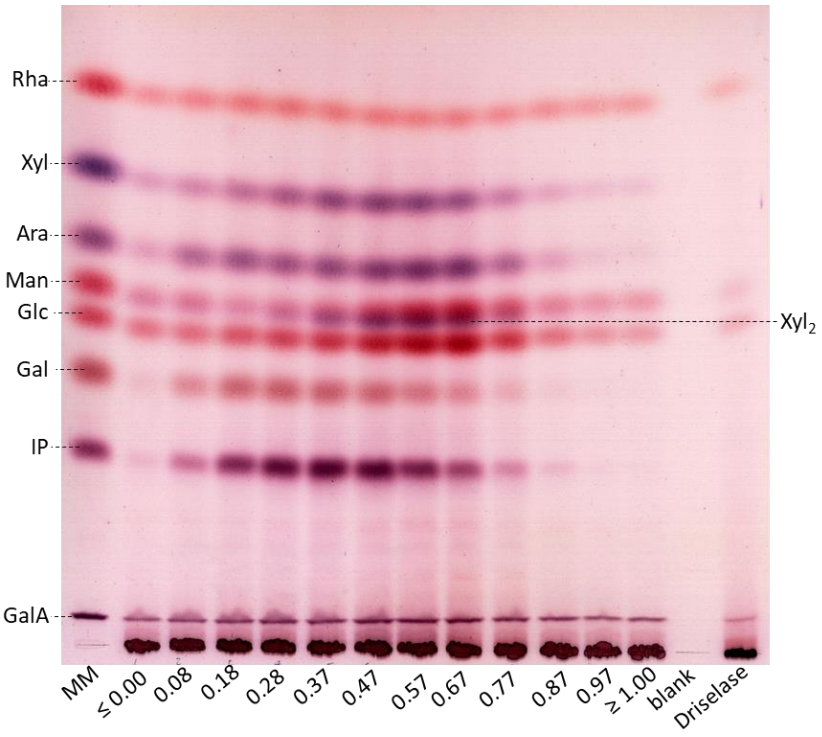

Figure 72: Composition of HbP column fractions from experimental Curran separated by molecular mass on Sephacryl S-200 and Driselase-digested.
eC B HbP was run on Sephacryl S-200. Further details as in Figure 68.

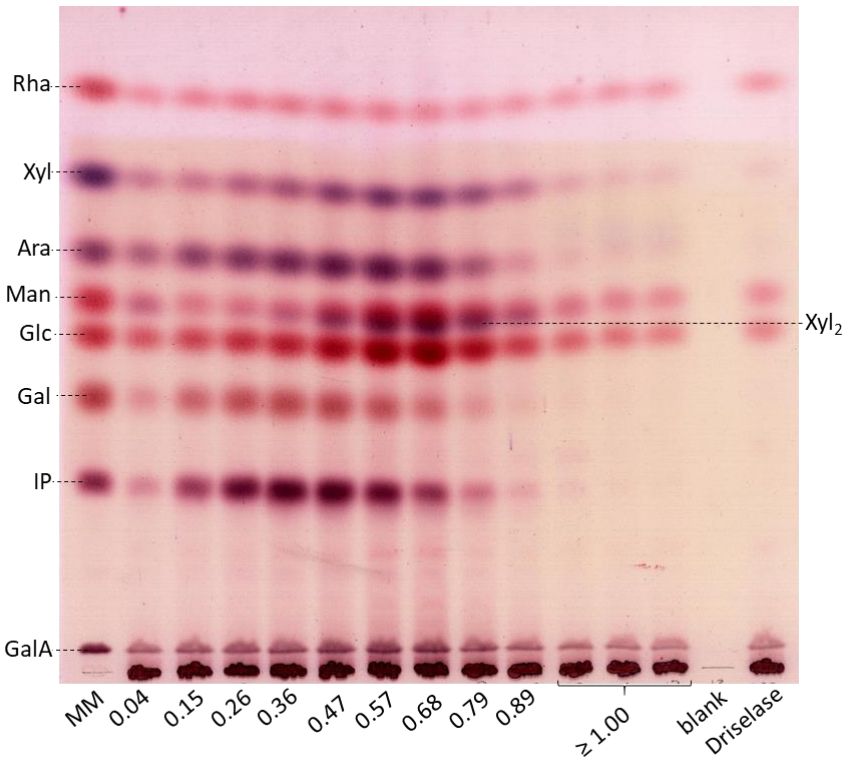

Figure 73: Composition of HbP column fractions from experimental Curran C separated by molecular mass on Sephacryl S-200 and Driselase-digested.
eC C HbP was run on Sephacryl S-200. Further details as in Figure 68.

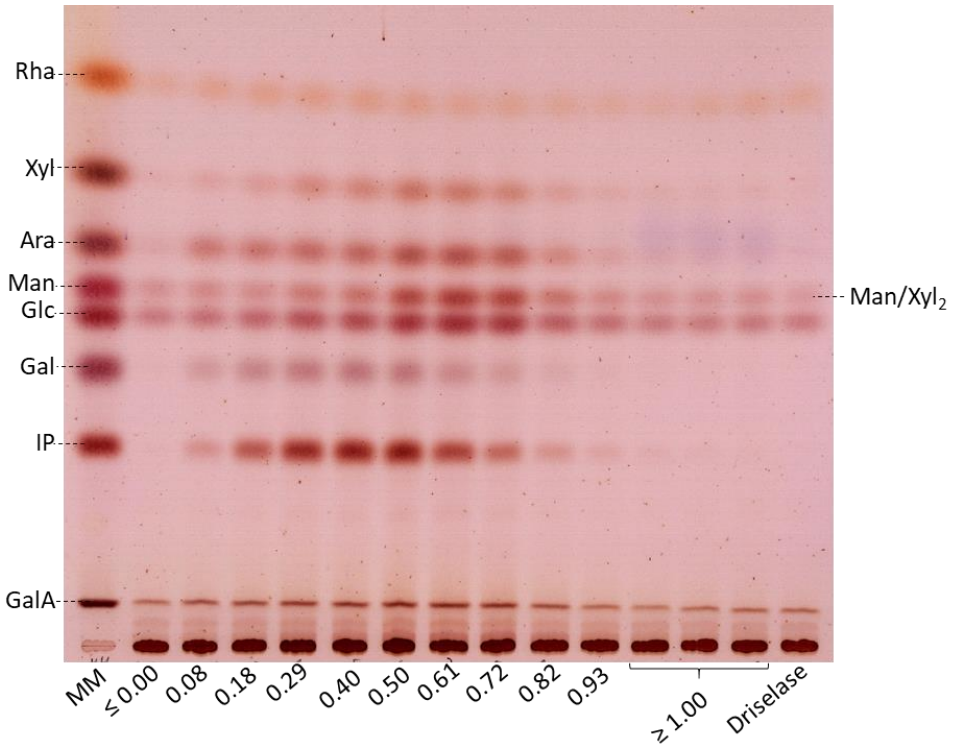

Figure 74: Composition of HbP column fractions from experimental Curran D separated by molecular mass on Sephacryl S-200 and Driselase-digested.
eC D HbP was run on Sephacryl S-200. Further details as in Figure 68.

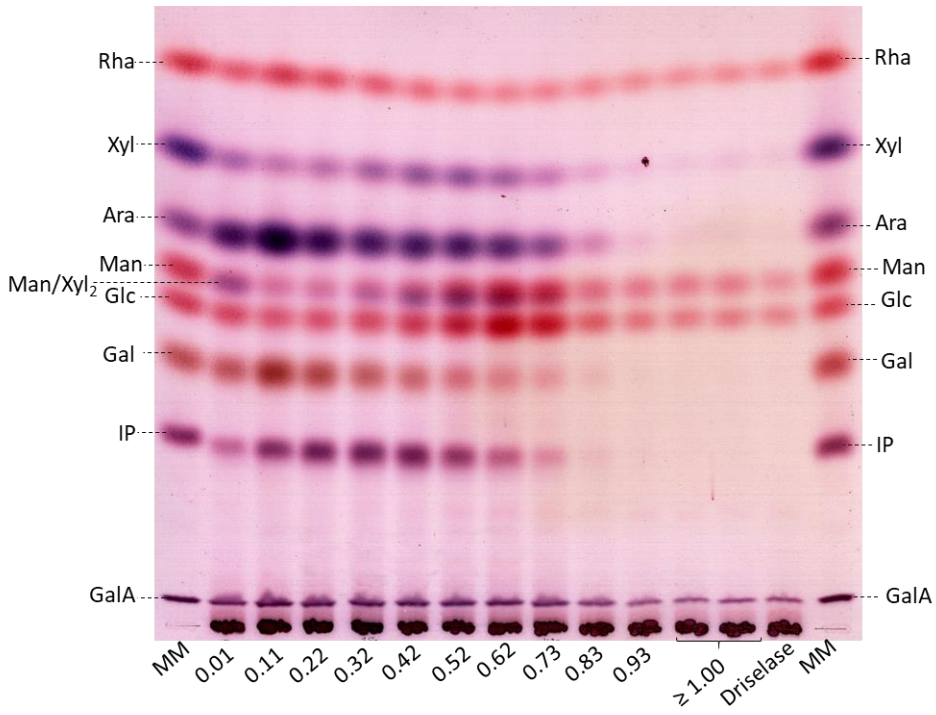

Figure 75: Composition of HbP column fractions from experimental Curran E separated by molecular mass on Sephacryl S-200 and Driselase-digested.
eC E HbP was run on Sephacryl S-200. Further details as in Figure 68.

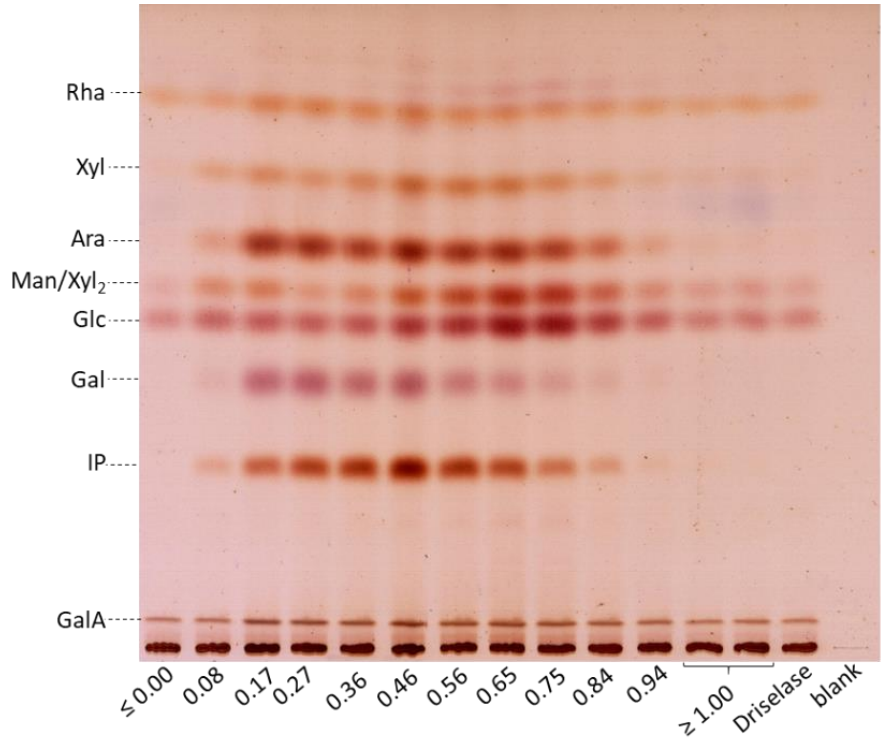

Figure 76: Composition of HbP column fractions from experimental Curran F separated by molecular mass on Sephacryl S-200 and Driselase-digested.
eC F HbP was run on Sephacryl S-200. Further details as in Figure 68.

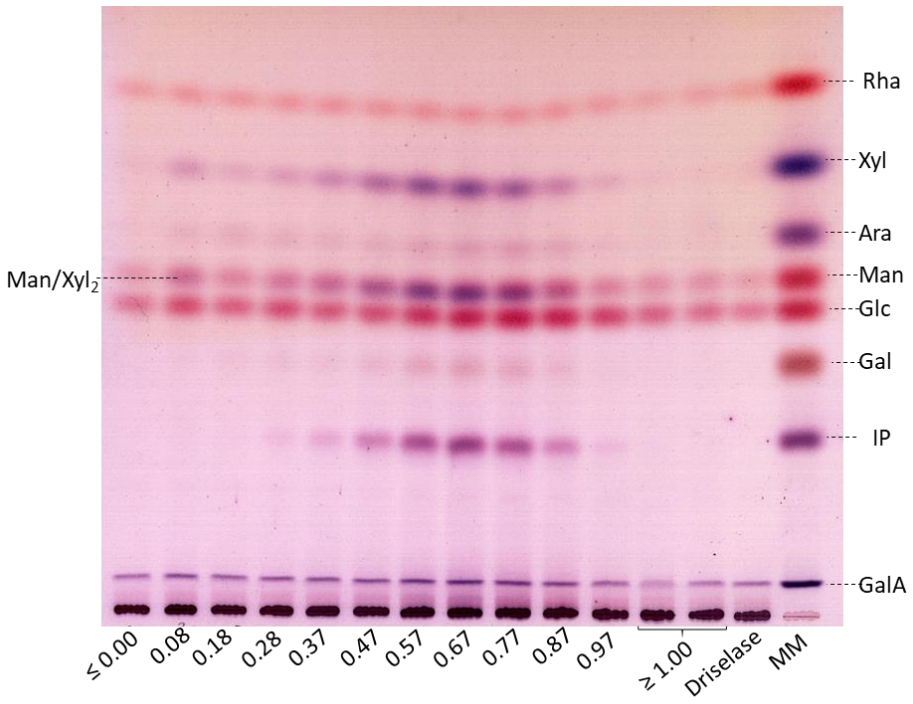

Figure 77: Composition of HbP column fractions from high viscosity experimental Curran H separated by molecular mass on Sephacryl S-200 and Driselase-digested.
hveC H HbP was run on Sephacryl S-200. Further details as in Figure 68.

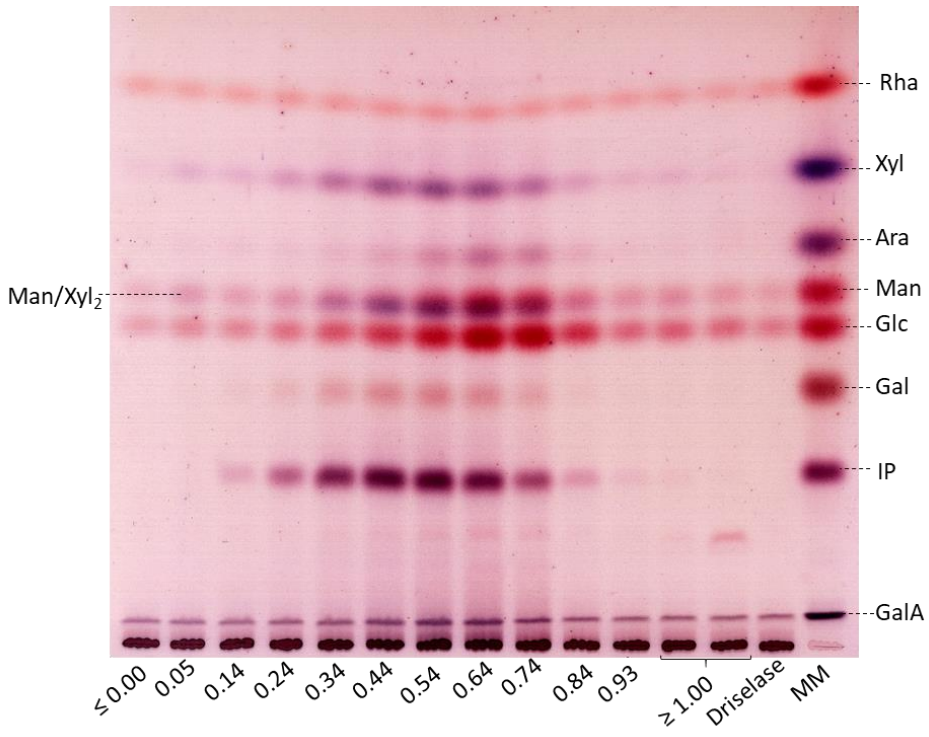

Figure 78: Composition of HbP column fractions from high viscosity experimental Curran I separated by molecular mass on Sephacryl S-200 and Driselase-digested.
hveC I HbP was run on Sephacryl S-200. Further details as in Figure 68.

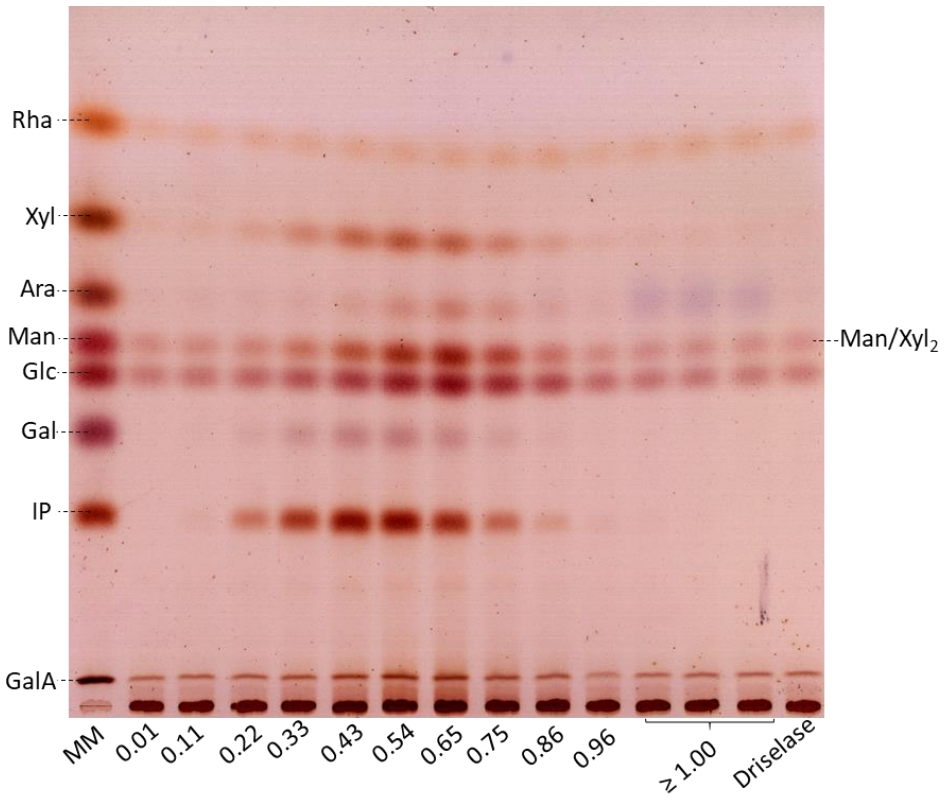

Figure 79: Composition of HbP column fractions from high viscosity experimental Curran J separated by molecular mass on Sephacryl S-200 and Driselase-digested.
hveC J HbP was run on Sephacryl S-200. Further details as in Figure 68.

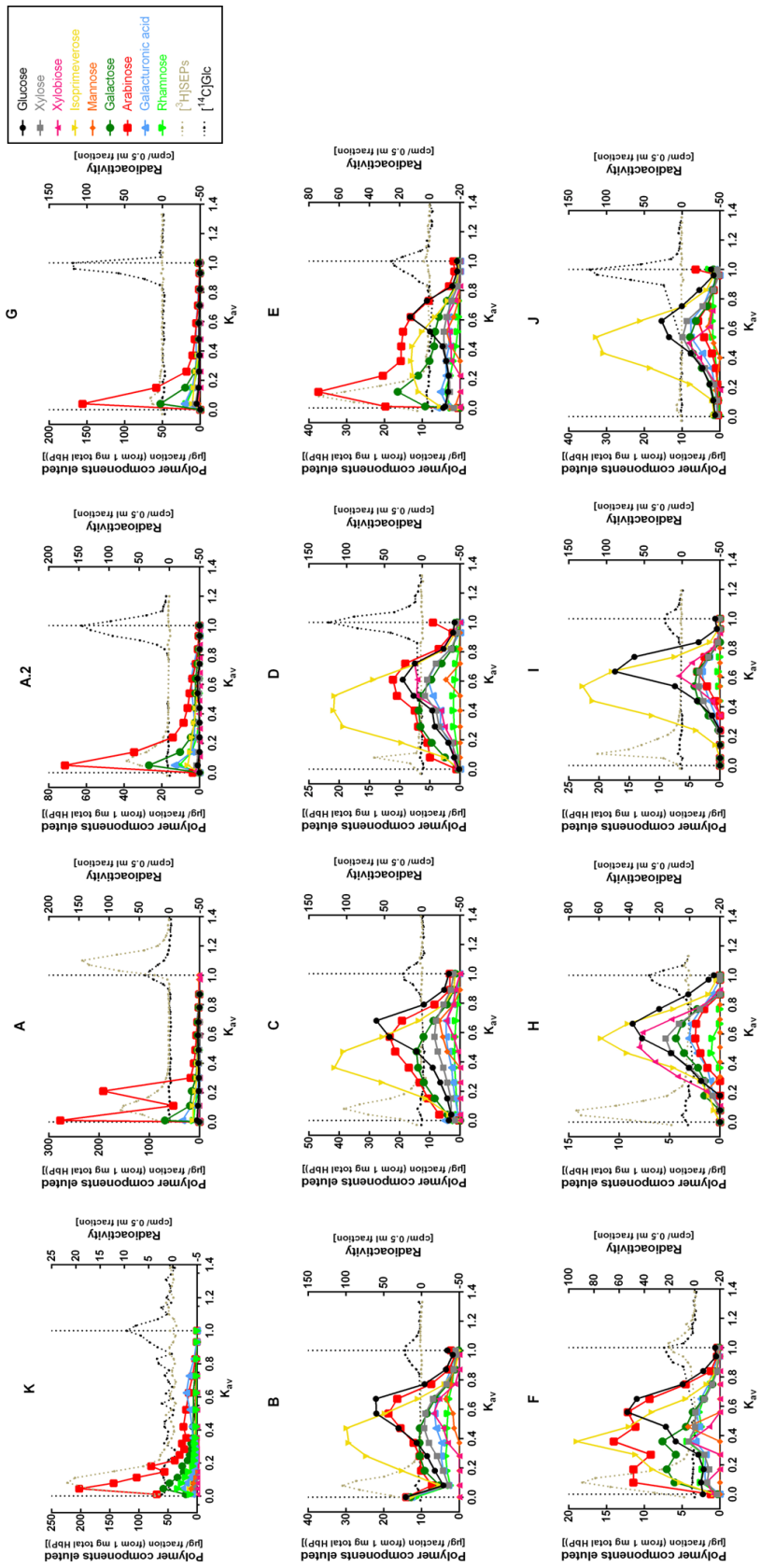

Figure 80: Quantified components in size-fractionated, Driselase-digested HbP from experimental Curran and SBP preparations. The TLC plates (Figure 68–Figure 79) with the Driselase-digested HbP column fractions from preparations A–K (after the run on Sephacryl S-200) were quantified by Photoshop. Preparations K, A, A.2 and G are from SBP; B–F are normally produced eC and H–J are hveC preparations. Nine polymer components were identified and their elution profiles are shown according to the pools' respective median K_{av} value. Man and Xyl_2 were quantified together. Radioactive markers—[^{3}H]SEPs and [^{14}C]Glc—mark the K_{av} 0.08 and the V_t (K_{av} 1) respectively.

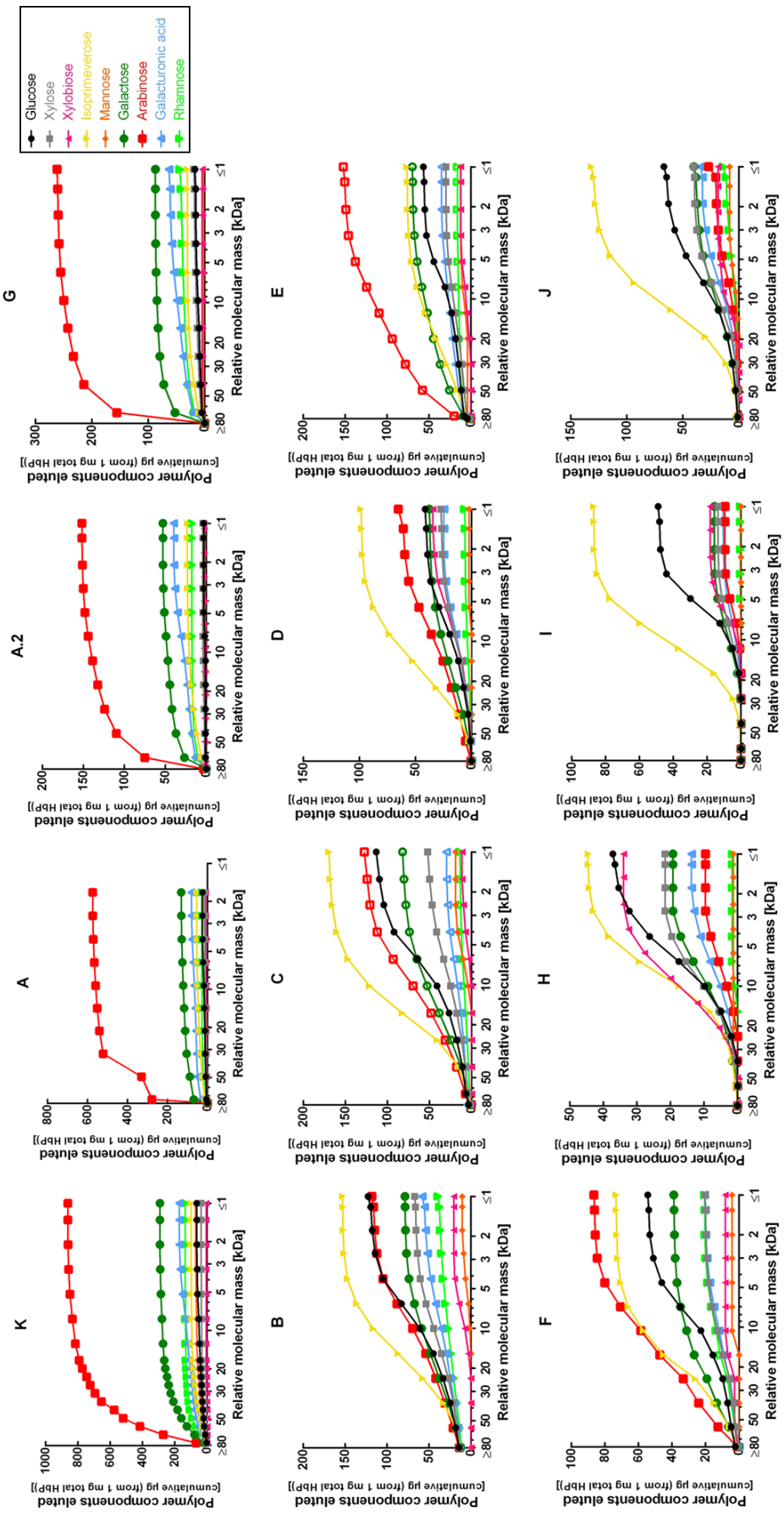

Figure 81: Cumulative amounts eluted from Sephacryl S-200 size-fractionated, Driselase-digested HbP from SBP and experimental Curran preparations.
The results displayed in Figure 80 were converted into cumulative components eluted. Preparations K, A, A.2 and G are SBP , B–F are eC and H–J are hveC preparations. The K_{av} was converted into the relative molecular mass.

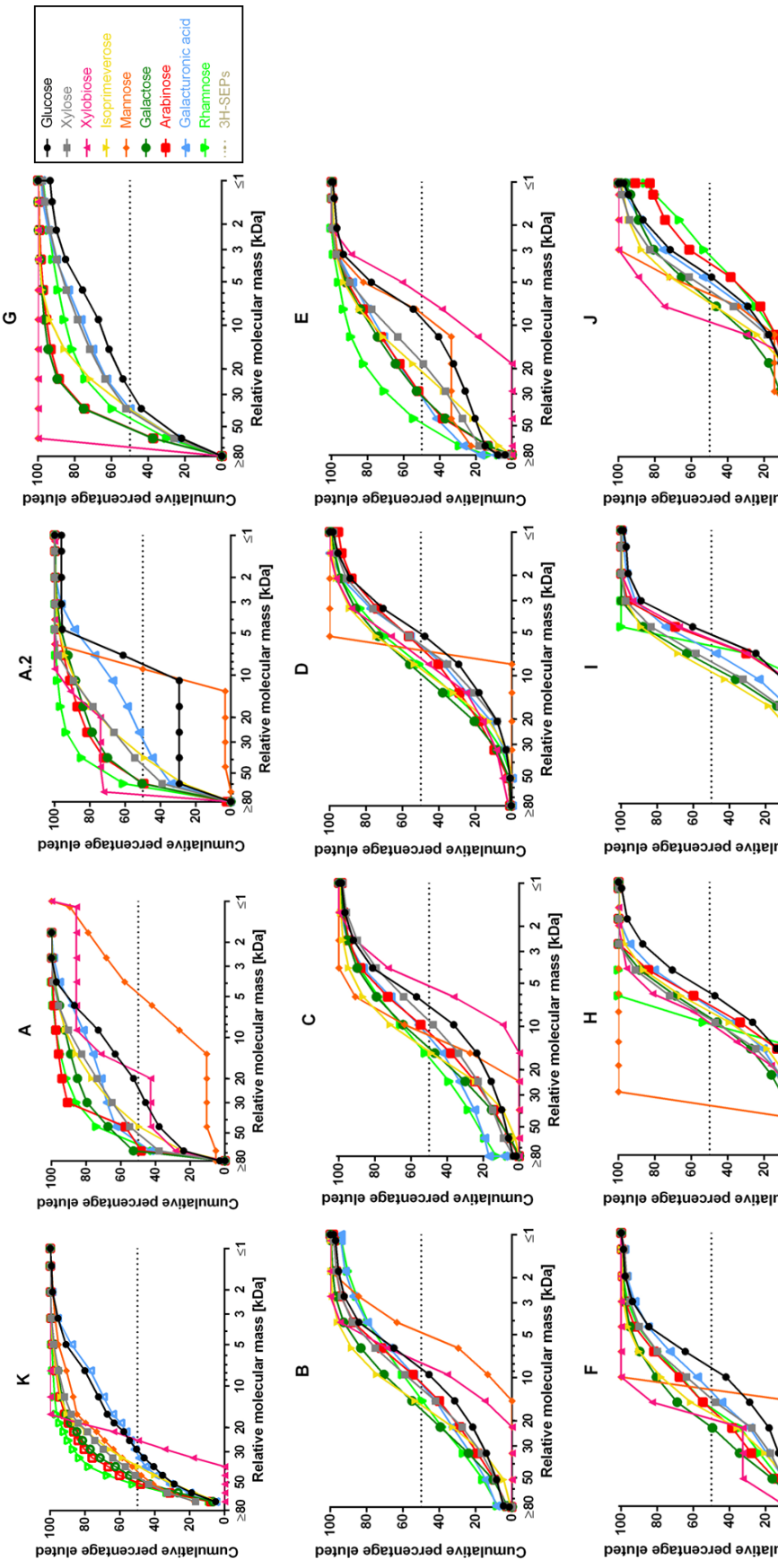

Figure 82: Cumulative percentages eluted for components in HbP from SBP and experimental Curran preparations size-fractionated on Sephacryl S-200 and Driselase-digested.
The results displayed in Figure 80 were converted into cumulative percentage eluted. Preparations K, A, A.2 and G are from SBP; B–F are normally produced eC and H–J are hveC preparations. The K_{av} was converted into the relative molecular mass. A dotted line indicates where 50% eluted.

6.5 Appendix to §3.8

Table 6: Tritiated water experiment with a ^3H_2O trap on experimental Currans and controls. The table (on the next page) shows some important parameters used to calculate the percentage of ^3H retained per sample ('% ^3H retained) that are presented in §3.8.6. eC samples were: normally produced eC (samples B–F'), hveC (samples H–V') and changed production process eC (samples T–Z) (for details see Table 2). Viscosity was measured for all eC products (in cP). All samples, except for Glc, xyloglucan and dextran, were estimated to have two H available for exchange per monomeric residue (equivalent to cellulose); Glc had 5, xyloglucan 2.625 and dextran 3 ('H available'). Approximately 0.01 g dry weight of eC and controls was incubated with ^3H_2O (containing 15.9 or 16 kBq each) and dried for 8 h. The desiccator was attached to the pump via a ^3H_2O trap. The H# measured for each sample (with the scintillation counter) was used to calculate the efficiency factor (linear relationship between 60–100 H#; Figure 83). With help of the estimated number of H atoms available for exchange per residue in the dry sample, the number of H atoms added in ^3H_2O and the radioactivity supplied to the sample, the expected maximal number of H that could be exchanged ('expected H exchange' in kBq) was calculated. By using the measured radioactivity of each dried sample and the efficiency factor, the measured number of H exchange was calculated. Finally, 'H exchanged' represents the percentage of ^3H that were retained over the expected maximal number of H atoms that could be exchanged. Mean, SEM and N for each sample are listed.

			^3H_2O [g]			dry weight [g]		cpm minus blank		efficiency factor	expected H exchange [kBq]		measured H exchanged [kBq]		H exchanged [%]	
Sample	Viscosity [cP]	H atoms available	Mean	SEM	N	Mean	SEM	Mean	SEM	Mean	Mean	SEM	Mean	SEM	Mean	SEM
B	1520	2	0.549	0.050	3	0.0087	0.0008	931	119.2	0.33	0.0281	0.0001	0.0470	0.0062	167	22
B'	720	2	0.853	0.084	3	0.0089	0.0009	801	44.5	0.33	0.0185	0.0001	0.0402	0.0026	216	13
B.B	1520	2	0.499	0.039	3	0.0106	0.0009	1021	1.4	0.33	0.0376	0.0001	0.0522	0.0005	139	1
C	1580	2	0.699	0.032	3	0.0120	0.0006	1280	104.0	0.32	0.0305	0.0000	0.0662	0.0054	217	18
C.C	1580	2	0.600	0.064	3	0.0135	0.0015	1449	221.2	0.31	0.0397	0.0001	0.0778	0.0113	196	28
D	1710	2	0.603	0.016	3	0.0094	0.0003	976	72.6	0.34	0.0275	0.0001	0.0484	0.0037	176	14
E	1740	2	0.634	0.021	3	0.0105	0.0004	1307	133.7	0.33	0.0293	0.0000	0.0655	0.0065	224	22
E'	640	2	0.639	0.007	3	0.0057	0.0001	562	110.7	0.34	0.0158	0.0000	0.0273	0.0056	173	35
F	1770	2	0.492	0.063	3	0.0091	0.0012	925	69.3	0.34	0.0328	0.0002	0.0459	0.0039	140	11
F'	1080	2	0.755	0.028	3	0.0075	0.0003	668	50.8	0.34	0.0176	0.0000	0.0329	0.0025	186	14
H	5400	2	0.712	0.022	4	0.0089	0.0003	1196	121.3	0.35	0.0221	0.0000	0.0578	0.0060	261	27
I	6220	2	0.724	0.051	4	0.0093	0.0007	1321	128.7	0.35	0.0227	0.0001	0.0636	0.0061	280	26
J	8620	2	0.752	0.100	5	0.0096	0.0013	1138	207.5	0.34	0.0226	0.0001	0.0555	0.0103	244	45
T	116	2	0.468	0.089	3	0.0071	0.0014	438	89.9	0.34	0.0267	0.0002	0.0216	0.0045	81	17
U	1310	2	0.559	0.033	3	0.0143	0.0009	716	50.9	0.28	0.0453	0.0001	0.0421	0.0028	93	6
V	4020	2	0.551	0.065	4	0.0086	0.0011	1038	186.5	0.34	0.0278	0.0001	0.0504	0.0093	181	33
V'	4020	2	0.772	0.030	3	0.0068	0.0003	954	195.5	0.35	0.0157	0.0000	0.0461	0.0098	294	62
W	1280	2	0.583	0.024	3	0.0462	0.0020	1027	50.4	0.32	0.1405	0.0002	0.0537	0.0028	38	2
X	1250	2	0.459	0.055	3	0.0133	0.0017	1193	140.9	0.32	0.0513	0.0003	0.0624	0.0083	121	15
Y	460	2	0.485	0.061	3	0.0083	0.0011	564	85.5	0.30	0.0301	0.0002	0.0313	0.0051	104	17
Z	148	2	0.525	0.058	3	0.0107	0.0012	449	48.1	0.32	0.0362	0.0002	0.0235	0.0026	65	7
SBP G		2	0.461	0.022	3	0.0107	0.0005	1197	156.2	0.30	0.0414	0.0000	0.0655	0.0086	158	21
SBP A		2	0.670	0.000	3	0.0099	0.0006	666	10.7	0.30	0.0263	0.0015	0.0371	0.0007	142	7
Glucose		5	0.122	0.005	3	0.0113	0.0005	16331	597.4	0.36	0.4116	0.0034	0.7547	0.0273	183	8
MCC		2	0.320	0.109	3	0.0333	0.0121	7399	3196.3	0.37	0.1777	0.0095	0.3330	0.1439	179	75
Avicel		2	0.135	0.015	3	0.0127	0.0017	1362	147.8	0.35	0.1674	0.0032	0.0649	0.0070	39	3
Dextran		3	0.413	0.122	3	0.0437	0.0136	12936	2915.6	0.36	0.2774	0.0055	0.6001	0.1357	215	45
Paper		2	0.670	0.000	3	0.0110	0.0004	846	13.8	0.36	0.0293	0.0010	0.0396	0.0006	135	3
Xyloglucan		2.625	0.785	0.065	3	0.0077	0.0007	1279	234.5	0.36	0.0247	0.0001	0.0589	0.0109	239	44

Table 7: Tritiated water experiment <u>without</u> a ^3H_2O trap on experimental Currans and controls.
The table (on the next page) shows some important parameters used to calculate the percentage of ^3H retained per sample ('% ^3H retained') that are presented in §3.8.6. Approximately 0.01 g of eC and controls dry weight was incubated with ^3H_2O (containing 14.1, 16.0, 23.0 or 103.8 kBq each) and dried for 8 h. The desiccator was attached directly to the pump. Further details in Table 6.

			^3H_2O [g]			Dry weight [g]		cpm minus blank		Efficiency factor	Expected H exchange [kBq]		Measured H exchange [kBq]		H exchanged [%]	
Sample	**Viscosity [cP]**	**H atoms available**	**Mean**	**SEM**	**N**	**Mean**	**SEM**	**Mean**	**SEM**	**Mean**	**Mean**	**SEM**	**Mean**	**SEM**	**Mean**	**SEM**
B'	720	2	0.849	0.045	3	0.0089	0.0005	402	78	0.32	0.0163	0.0000	0.0207	0.0041	127	25
B.B	1520	2	0.456	0.047	4	0.0087	0.0009	631	153	0.32	0.0317	0.0012	0.0331	0.0080	102	23
C	1580	2	0.527	0.028	3	0.0089	0.0005	2486	1682	0.33	0.0849	0.0550	0.1287	0.0880	143	7
C.C	1580	2	0.373	0.032	2	0.0076	0.0007	1117	252	0.32	0.0442	0.0082	0.0576	0.0137	129	7
D	1710	2	0.573	0.053	3	0.0079	0.0008	322	44	0.33	0.0225	0.0010	0.0165	0.0022	74	11
E	1740	2	0.580	0.006	4	0.0102	0.0001	831	213	0.33	0.0303	0.0009	0.0421	0.0106	136	33
E'	640	2	0.921	0.107	3	0.0083	0.0010	1465	1282	0.33	0.0439	0.0299	0.0740	0.0645	110	43
F	1770	2	0.356	0.128	2	0.0043	0.0016	2194	2057	0.33	0.0803	0.0619	0.1140	0.1073	96	60
F'	1080	2	0.889	0.085	3	0.0089	0.0009	1587	1051	0.33	0.0486	0.0330	0.0801	0.0529	170	4
H	5400	2	0.656	0.069	4	0.0148	0.0016	537	179	0.33	0.0409	0.0054	0.0268	0.0088	64	20
I	6220	2	0.735	0.029	3	0.0133	0.0005	4340	2726	0.34	0.0911	0.0588	0.2143	0.1348	242	5
J	8620	2	0.679	0.069	3	0.0106	0.0011	1076	127	0.34	0.0277	0.0001	0.0533	0.0067	193	24
V	4020	2	0.642	0.057	4	0.0089	0.0008	1247	699	0.33	0.0570	0.0343	0.0625	0.0349	117	30
V'	4020	2	0.723	0.023	3	0.0064	0.0002	724	42	0.35	0.0157	0.0000	0.0350	0.0024	223	15
SBP G		2	0.598	0.035	5	0.0159	0.0010	1641	509	0.29	0.1025	0.0503	0.0952	0.0291	116	12
SBP A		2	0.670	0.000	3	0.0097	0.0005	1803	863	0.30	0.1218	0.0507	0.0996	0.0474	91	19
Glucose		5	0.134	0.010	4	0.0126	0.0011	5757	1954	0.35	0.3679	0.0048	0.2774	0.0943	76	26
MCC		2	0.221	0.031	3	0.0223	0.0034	7765	2953	0.36	0.8277	0.3236	0.3652	0.1401	48	7
Avicel		2	0.215	0.018	3	0.0217	0.0020	4529	2767	0.35	0.4934	0.3242	0.2146	0.1308	47	6
Dextran		3	0.199	0.020	4	0.0199	0.0022	4036	1522	0.35	0.2335	0.0023	0.1932	0.0727	82	30
Paper		2	0.670	0.000	3	0.0073	0.0005	430	26	0.36	0.0194	0.0014	0.0201	0.0013	105	7
Xyloglucan		2.625	0.663	0.049	3	0.0065	0.0005	6053	559	0.35	0.1593	0.0004	0.2860	0.0272	179	17
dried cellulose		2	0.670	0.000	3	0.0125	0.0025	631	344	0.35	0.0291	0.0059	0.0300	0.0162	91	33
never-dried		2	0.716	0.013	3	0.0173	0.0049	1410	645	0.34	0.0375	0.0102	0.0672	0.0303	155	53

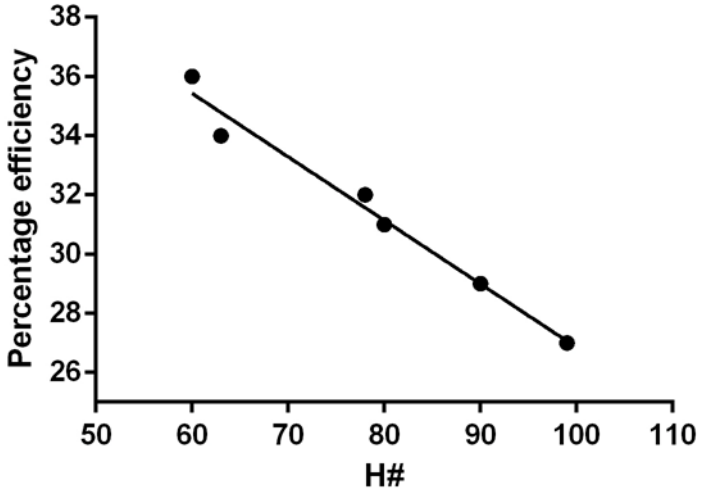

Figure 83: ^{3}H Quench relationship created by using 10 ml Optiphase scintillation fluid in a Beckman LS5000 CE scintillation counter.
The relationship between efficiency and H# (measured by the scintillation counter) can be described in a linear relationship between 60 and 100 H#:
Percentage efficiency = -0.2145 × H# + 48.31; R^2 0.98.

6.6 Appendix to §4.2.1

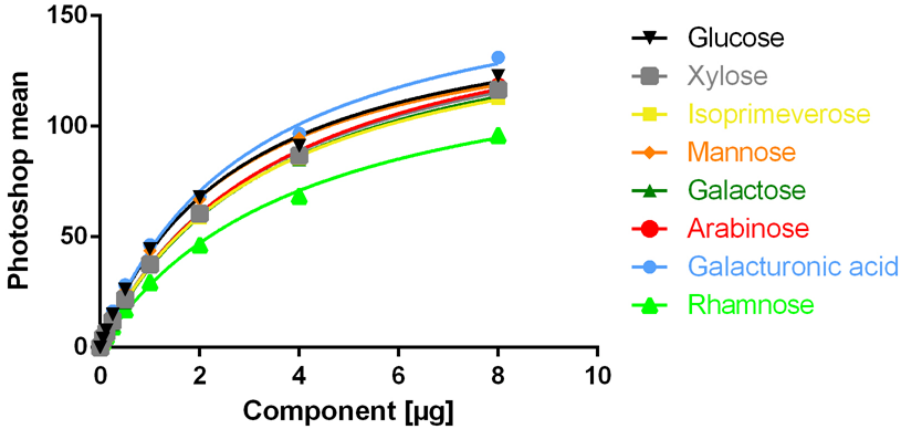

Figure 84: Typical gradient of marker components with fitted hyperbola.
Different amounts of marker mixture (0.06–8µg) were applied to a TLC plate, this plate was run in the solvent EPyAW (6:3:1:1) for 2 × 2.5 h, stained with thymol and the mean Photoshop value was measured. The quantities of components in preparations tested in this work were calculated with help of the hyperbolic function from these component gradients:
Photoshop mean = (a × component [µg]) / (b + component [µg])